

UNIVERSITY OF MODENA AND REGGIO EMILIA

**International Doctoral Program in
CLINICAL AND EXPERIMENTAL MEDICINE (CEM)
Curriculum: Nanomedicine, Medicinal and Pharmaceutical Sciences
Cycle XXXVI**

**DEVELOPMENT OF SYNTHETIC STRATEGIES AND
ANALYTICAL METHODS BASED ON LIQUID
CHROMATOGRAPHY COUPLED TO HIGH-
RESOLUTION MASS SPECTROMETRY (HPLC-HRMS)
FOR A CHEMICAL-PHARMACEUTICAL
CHARACTERIZATION OF ACTIVE INGREDIENTS OF
CANNABIS SATIVA L. EXTRACTS AND NEW
PSYCHOTROPIC SUBSTANCES (NPS)**

Sviluppo di strategie sintetiche e di metodi analitici basati su cromatografia liquida accoppiata a spettrometria di massa ad alta risoluzione (HPLC-HRMS) per la caratterizzazione chimico-farmaceutica di principi attivi degli estratti di *Cannabis Sativa* L. e di nuove sostanze psicotrope (NPS)

PhD Candidate: Fabiana Russo

Supervisor: Prof. Giuseppe Cannazza

PhD program coordinator: Prof. Marco Vinceti

Abstract

Cannabis sativa L., a plant known for a long time for its pharmacological properties, is currently approved for various therapeutic indications, such as the treatment of muscular and neuropathic pain, epilepsy, and multiple sclerosis. However, still very little is known about the complex chemical composition of cannabis extracts. Over 150 active terpenophenolic components called phytocannabinoids are known to be present in the plant, but only a few of them have been isolated and characterized. It is important to characterize the phytocannabinoid composition of cannabis extracts as it influences the pharmacological profile. In light of this, my doctoral project aims to identify and quantify new phytocannabinoids and evaluate their pharmacological activity. In the first part of my PhD program, an analytical method based on high-performance liquid chromatography coupled to high-resolution mass spectrometry (HPLC-HRMS) was developed in an *untargeted* metabolomics fashion. This allowed for the putative identification of numerous carboxylated and decarboxylated phytocannabinoids, including cannabidihexol (CBDH), tetrahydrocannabihexol (Δ^9 -THCH), cannabigerobutol (CBGB), *cis*- Δ^9 -tetrahydrocannabinolic acid (*cis*- Δ^9 -THCA), Δ^9 -tetrahydrocannabiphorolic acid (Δ^9 -THCPA), cannabidiphorolic acid (CBDPA). To confirm their identity, these compounds were isolated, characterized, and their chemical properties were compared to those of the corresponding synthetic species obtained through stereoselective synthesis developed *ad hoc*. The latter were used as reference standards for the development of sensitive and selective HPLC-UV-HRMS methods under a *targeted* metabolomics fashion in order to quantify the new phytocannabinoids in different cannabis varieties. Such new compounds were further subjected to *in vitro* and *in vivo* tests to assess their pharmacological profile. In the second part, the stereoisomeric composition of the two major phytocannabinoids, Δ^9 -tetrahydrocannabinol (Δ^9 -THC) and cannabidiol (CBD), as well as of their carboxylated precursors, Δ^9 -tetrahydrocannabinolic acid (Δ^9 -THCA) and cannabidiolic acid (CBDA), was investigated in the Italian medicinal cannabis variety FM2. Bidimensional achiral-chiral HPLC methods coupled to UV and HRMS were developed and optimized for this purpose. Ultimately, the project focused on the study of new psychoactive substances (NPS), psychoactive drugs not controlled by the Single Convention on Narcotic Drugs (1961) or the Convention on Psychotropic Substances (1971), but which may pose a public health threat. Specifically, two NPS derived from CBD, a non-psychoactive component of cannabis, were investigated: hexahydrocannabinol (HHC) and tetrahydrocannabinol (H4-CBD). Synthetic strategies were developed to obtain epimers of both HHC and H4-CBD which were used as reference standards for the development of quantitative analytical methods to be applied to commercial samples. For HHC epimers, an HPLC-HRMS method was developed, while for H4-CBD epimers, known to have cannabinomimetic activity, a qualitative-quantitative gas chromatography-mass spectrometry (GC-

MS) method was developed. Furthermore, HHC epimers were purified and individually tested for their cannabinomimetic activity. As a result of the present PhD study, new cannabinoids have been added to the inventory, providing an increasingly comprehensive overview of the phytocannabinome. The project also supplied sensitive and specific HPLC-UV-HRMS methods for the qualitative-quantitative and stereoisomeric evaluation of phytocannabinoids in *Cannabis sativa* L. extracts. Additionally, HPLC-HRMS and GC-MS methods were provided for the qualitative and quantitative analysis of semisynthetic CBD derivatives in real samples.

La *Cannabis sativa* L., pianta conosciuta da tempo per le sue proprietà farmacologiche, è attualmente approvata per diverse applicazioni terapeutiche come il trattamento del dolore muscolare e neuropatico, epilessia e sclerosi multipla. Tuttavia, si sa molto poco sulla complessa composizione chimica dell'estratto di cannabis. Più di 150 componenti attivi a struttura terpenofenolica, chiamati fitocannabinoidi, sono stati individuati nella pianta, ma solo pochi di essi sono stati isolati e caratterizzati. È importante caratterizzare la composizione in fitocannabinoidi negli estratti in quanto essa influenza l'effetto farmacologico. Alla luce di ciò, il mio progetto di dottorato ha lo scopo di identificare e quantificare nuovi fitocannabinoidi per poi valutarne l'attività farmacologica. Nella prima fase del progetto, ho sviluppato un metodo di cromatografia liquida accoppiata a spettrometria di massa ad alta risoluzione (HPLC-HRMS) con approccio metabolomico *untargeted*. Ciò ha permesso di identificare putativamente numerosi fitocannabinoidi carbossilati e decarbossilati come: cannabidiexolo, tetraidrocannabiexolo, cannabigerobutolo, acido *cis*- Δ^9 -tetraidrocannabinolico, acido Δ^9 -tetraidrocannabiforolico, acido cannabidiforolico. Per confermarne l'identità, i fitocannabinoidi identificati sono stati isolati dall'estratto e caratterizzati e le loro proprietà chimiche sono state confrontate con quelle degli analoghi sintetici ottenuti mediante sintesi stereoselettive sviluppate *ad hoc*. Questi ultimi sono stati utilizzati come standard analitici nello sviluppo di metodi HPLC-HRMS basati su un approccio metabolomico *targeted* al fine di quantificare i nuovi fitocannabinoidi in diverse varietà di cannabis. Inoltre, tali nuovi composti sono stati impiegati in test *in vitro* e *in vivo* per studiarne il profilo farmacologico. Nella seconda fase del progetto di dottorato, ho indagato la composizione stereochimica dei due principali fitocannabinoidi, Δ^9 -tetraidrocannabinolo (Δ^9 -THC) e cannabidiolo (CBD), nonché dei rispettivi precursori carbossilati, acido Δ^9 -tetraidrocannabinolico (Δ^9 -THCA) e acido cannabidiolico (CBDA) nell'estratto di cannabis medicinale italiana FM2. A tale scopo sono stati sviluppati e ottimizzati metodi HPLC bidimensionale achirale-chirale accoppiati ad UV e HRMS. In ultima analisi, il progetto ha riguardato lo studio di nuove sostanze psicoattive (NPS), nuove droghe psicotrope non controllate dalla Single Convention on Narcotic Drugs (1961) o dalla Convention on Psychotropic Substances (1971), ma

che possono rappresentare una minaccia per la salute pubblica. In particolare, sono stati investigati due NPS derivanti dal CBD, componente non psicoattivo della cannabis: esaidrocannabinolo (HHC) e tetraidrocannabinolo (H4-CBD). Sono quindi state messe a punto strategie sintetiche per ottenere gli epimeri di entrambi i derivati, i quali sono stati poi impiegati come standard per lo sviluppo di metodi analitici quantitativi da applicare a campioni commerciali. Per l'HHC è stato sviluppato un metodo HPLC-HRMS, mentre per gli epimeri dell'H4-CBD è stato messo a punto un metodo basato su gas cromatografia accoppiata a spettrometria di massa (GC-MS). Inoltre, i due epimeri dell'HHC sono stati purificati e testati singolarmente per valutarne l'attività cannabinomimetica. Attraverso tale studio nuovi cannabinoidi sono stati aggiunti all'inventario fornendo una panoramica sempre più completa del fitocannabinoma. Inoltre, questo lavoro di tesi ha fornito nuovi metodi HPLC-UV-HRMS sensibili e specifici per la valutazione della composizione quali-quantitativa e stereoisomerica di fitocannabinoidi in estratti di *C. sativa* L. Questo studio ha infine fornito metodi HPLC-HRMS e GC-MS per analisi quali-quantitative di derivati semisintetici del CBD in campioni reali.

TABLE OF CONTENTS

ABSTRACT	p. I
TABLE OF CONTENTS	p. IV
GENERAL INTRODUCTION	p.1
AIM	p.8
CHAPTER 1	p.9
<i>IDENTIFICATION OF ACTIVE INGREDIENTS IN CANNABIS SATIVA L. EXTRACTS: SYNTHESIS AND DEVELOPMENT OF ANALYTICAL METHODS IN UNTARGETED AND TARGETED METABOLOMIC APPROACHES</i>	
<i>Section 1</i>	p.10
<i>HPLC-UV-HRMS ANALYSIS OF CANNABIGEROVARIN AND CANNABIGEROBUTOL, THE TWO IMPURITIES OF CANNABIGEROL EXTRACTED FROM HEMP</i>	
<i>References</i>	p.26
<i>Supplementary material</i>	p.28
<i>Section 2</i>	p.51
<i>IDENTIFICATION OF A NEW CANNABIDIOL N-HEXYL HOMOLOG IN A MEDICINAL CANNABIS VARIETY WITH ANTINOCICEPTIVE ACTIVITY IN MICE: CANNABIDIHEXOL</i>	
<i>References</i>	p.69
<i>Supplementary material</i>	p.71
<i>Section 3</i>	p.82
<i>THE NOVEL HEPTYL PHOROLIC ACID CANNABINOIDS CONTENT IN DIFFERENT CANNABIS SATIVA L. ACCESSIONS</i>	
<i>References</i>	p.97
<i>Supplementary material</i>	p.99
CHAPTER 2	p.116
<i>DEVELOPMENT OF ANALYTICAL METHODS TO ASSESS THE STEREOISOMERIC COMPOSITION OF THE MAIN PHYTOCANNABINOIDS IN CANNABIS SATIVA L.</i>	
<i>Section 1</i>	p.117
<i>CIS-Δ^9-TETRAHYDROCANNABINOLIC ACID OCCURRENCE IN CANNABIS SATIVA L.</i>	
<i>References</i>	p.133
<i>Supplementary material</i>	p.136

Section 2	p.146
ENANTIOSEPARATION OF CHIRAL PHYTOCANNABINOIDS IN MEDICINAL CANNABIS	
<i>References</i>	p.162
<i>Supplementary material</i>	p.166
Section 3	p.172
BIDIMENSIONAL HEART-CUT ACHIRAL-CHIRAL LIQUID CHROMATOGRAPHY COUPLED TO HIGH-RESOLUTION MASS SPECTROMETRY FOR THE SEPARATION OF THE MAIN CHIRAL PHYTOCANNABINOIDS AND ENANTIOMERIZATION STUDIES OF CANNABICHROMENE AND CANNABICHROMENIC ACID	
<i>References</i>	p.190
<i>Supplementary material</i>	p.192
CHAPTER 3	p.198
IDENTIFICATION OF PHYTOCANNABINOID DERIVATIVES AS NEW PSYCHOACTIVE SUBSTANCES (NPS)	
Section 1	p.199
SYNTHESIS AND PHARMACOLOGICAL ACTIVITY OF THE EPIMERS OF HEXAHYDROCANNABINOL (HHC)	
<i>References</i>	p.215
<i>Supplementary material</i>	p.218
Section 2	p.225
SYNTHESIS AND GAS-CHROMATOGRAPHY COUPLED TO MASS SPECTROMETRY ANALYSIS OF HEXAHYDROCANNABIDIOL (H4-CBD)	
<i>References</i>	p.227
<i>Supplementary material</i>	p.228
GENERAL CONCLUSIONS	p.232
REFERENCES	p.233

GENERAL INTRODUCTION

Cannabis sativa L. is a plant belonging to the *Cannabaceae* family and native to Central Asia. It has been used in folk medicine and as a source of textile fibre since ancient times. This plant has recently seen an increase in interest due to its versatile applications: from the pharmaceutical, nutraceutical, and cosmeceutical to the industrial sector. That is because its metabolites show potent bioactivities on human health and its outer and inner stem tissues can be used to make bioplastics and concrete-like material, respectively.

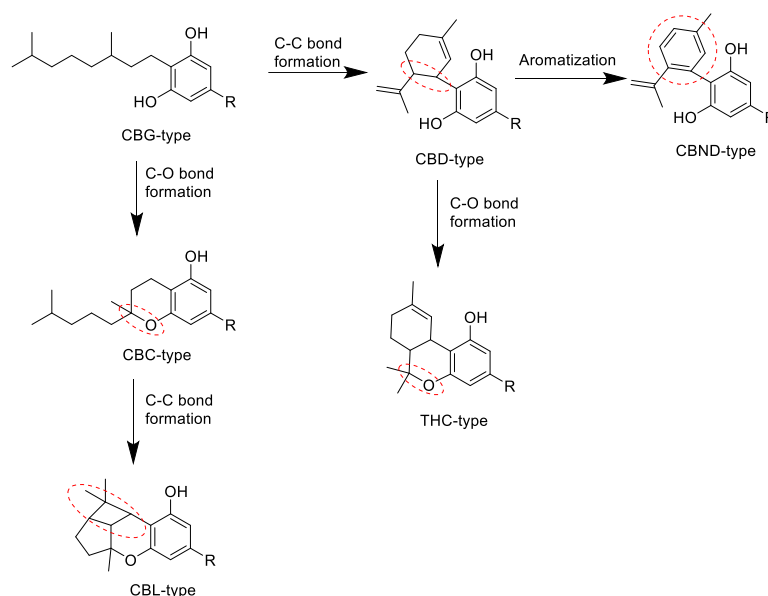
Cannabis sativa L. can be considered a pharmaceutical industry due to its ability to produce a plethora of bioactive chemical compounds. Notably, the chief chemical constituents of pharmaceutical significance are phytocannabinoids and terpenes. These active chemicals of Cannabis are produced in specialized tiny secretory trichomes called “glandular trichomes”. The core of the gland is primarily a hemispherical head. Within the base of the head are specialized secretory 'disk cells,' while above them exists a noncellular cavity where the secreted resin accumulates, causing the covering sheath (a waxy cuticle) of the head to expand into a spherical blister. This resin is a sticky mixture comprising cannabinoids and a variety of terpenes.^{1,2}

Terpenes consist of units of isoprene ($\text{CH}_2=\text{C}(\text{-CH}_3)\text{-CH}=\text{CH}_2$) and they are divided into eight main subclasses based on carbon numbers and isoprene units: hemiterpene (C = 5, 1 isoprene unit), monoterpene (C = 10, 2 isoprene units), sesquiterpene (C = 15, 3 isoprene units), sesterterpenes (C = 20, 4 isoprene units), diterpenes (C = 25, 5 isoprene units), triterpenes (C = 30, 6 isoprene units), tetraterpenes (C = 35 – 7 isoprene units), politerpenes (C = >40, >8 isoprene units). Many terpenes are detectable by smell at very low concentrations because they are extremely odoriferous.³ Terpenes are known to have a variety of medicinal effects: several are anti-inflammatory (e.g. alpha-pinene, beta-caryophyllene, and beta-myrcene) or psychologically soothing (Linalool, Nerolidol, and Phytol), and some have specific therapeutic applications for human illnesses and disorders (e.g. Beta-caryophyllene and Nerolidol have antimalarial activity, Limonene is an antidepressant agent, Caryophyllene oxide is able to treat nail infection, Linalool is a local anaesthetic, anticonvulsant and sedative agent).⁴ However, most of terpenes are potentially cytotoxic, except for some of them, such as β -caryophyllene, which has shown cytoprotective effects. The cytotoxic effect it seems to be primarily mediated by plasma membrane disruption, lipid peroxidation, ROS production and mitochondrial impairment.⁵ Moreover, it is important to note that UV light or heat can cause terpenes oxidation and determine the formation of oxygen-containing products as terpenoids (terpenes containing heteroatoms like oxygen) and ketones.^{6,7} Unstable allylic hydroperoxides can be formed during secondary photo-oxidation, whose reduction and subsequent oxidation can lead to the

formation of alcohols and then aldehydes or ketones.⁸ These compounds are reported to have potential toxicity, inherent to the promotion of oxidative stress.^{9,10}

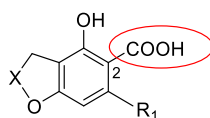
Phytocannabinoids represent the most studied group of compounds, mainly due to their wide range of pharmaceutical effects in humans. The plant produces over 150 phytocannabinoids. They are a group of isoprenylated resorcinyl polyketides. They consist of three moieties namely the isoprenyl residue, the resorcinyl core, and the side-chain.¹¹

The *isoprenyl moiety* of phytocannabinoids can occur in different topological arrangements (Scheme 1), according to: carbon-carbon or carbon-oxygen connectivity; aromatization; additional carbon-bonds (as exemplified by cannabicyclol derivatives).



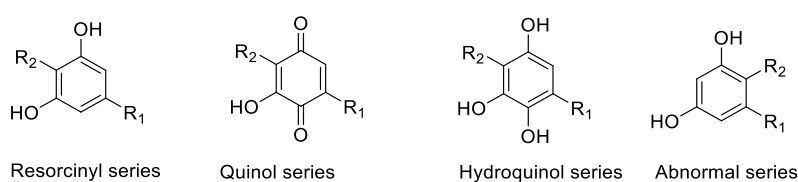
Scheme I. Topological arrangements of the main phytocannabinoids (cannabigerol (CBG), cannabidiol (CBD), cannabinodiol (CBND), cannabichromene (CBC), tetrahydrocannabinol (THC), cannabicyclol (CBL))

The *resorcinyl core* of native phytocannabinoids is carboxylated in position 2, and these compounds are also known as pre-cannabinoids or acidic phytocannabinoids. To date, pre-cannabinoids have been little investigated but interest in them is increasing. Pre-THC has been found to maintain activity on both CB1 and CB2 but is not narcotic due to its very poor brain penetration.¹² Moreover, pre-cannabinoids show strong anti-bacterial activity similar to the one of their corresponding decarboxylated derivatives.¹³



Pre-cannabinoids

O-Alkylation, generally with a methyl group, or oxidation to quinol or hydroquinol can also be found in the resorcinyl moiety. The carbon-substitution pattern of the resorcinyl core is generally 1,4, with the isoprenyl and the side-chain *para*-related. However, few phytocannabinoids show the two substituents in an *ortho*-relationship, thus falling into the "abnormal series".



The *alkyl residue* of the resorcinyl moiety can have a different number of carbon atoms resulting in different potency.¹⁴ The most frequent alkyl residue consists of five carbons (olivetoids), however less frequently three (viridinoids) and one (orcinoids) carbons have been found. Through the present work and previous studies conducted by Prof. G. Cannazza's team, alkyl residue of four (butoids), six (hexoids) and seven (phoroids) carbons have been discovered. The names refer to their corresponding non-prenylated resorcinyl derivatives (olivetol, divarinol, orcinol, butol, hexol and phorol).

All subclasses of phytocannabinoids originally derive from cannabigerolic acid (CBGA), which is converted into Δ^9 -tetrahydrocannabinolic acid (Δ^9 -THCA), cannabidiolic acid (CBDA) or cannabichromenic acid (CBCA) depending on the specific synthase enzymes present in the plant (THCA, CBDA, and CBCA synthase). Then, these phytocannabinoids can be converted into other phytocannabinoids through oxidation, isomerization or photochemical reaction (Scheme II).¹⁵

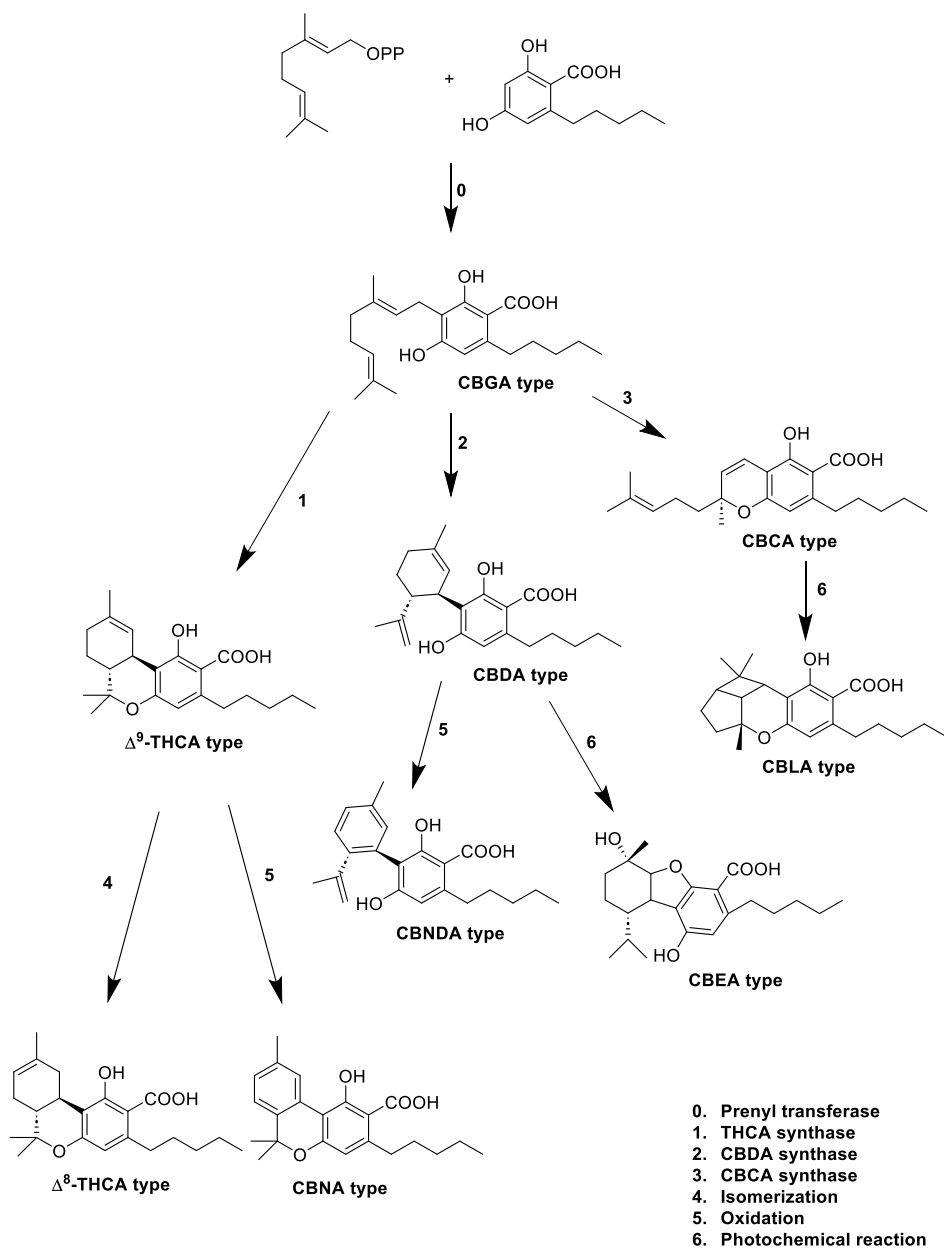
Here some examples:

Oxidation. Cannabinolic acid (CBNA) and cannabinodiolic acid (CBNDA) are the fully aromatized forms of Δ^9 -THCA and CBDA, respectively.

Isomerization. (-)-*trans*- Δ^8 -tetrahydrocannabinolic acid (Δ^8 -THCA) presents the double bond at the position C-8 instead of C-9.

Photochemical reaction. Cannabicyclolic acid (CBLA) is formed by the creation of two additional rings to cannabichromenic acid (CBCA). Cannabielsoic acid (CBEA) is the result of hydroxylation

and attachment of one of the two phenolic oxygen atoms at the endocyclic double bond of the monoterpene unit of CBDA.



Scheme II. Biosynthesis of phytocannabinoids

Through the decarboxylation, all these carboxylated phytocannabinoids can lose a molecule of CO₂ and be converted into the corresponding decarboxylated compounds. The decarboxylation can occur spontaneously in the plant material (over time and under specific climatic conditions) or it can be induced (e.g. 130 °C, 2 hours).¹⁶

The effects of phytocannabinoids (e.g. Δ⁹-THC), as well as endocannabinoids (endogenous cannabinoids, e.g. anandamide), are primarily mediated by the CB1 and CB2 cannabinoid receptors. These receptors are part of the endocannabinoid system (ECS) as endogenous cannabinoids and the

enzymes responsible for the synthesis and degradation of the endocannabinoids. CB1 receptors are abundant in the central nervous system (CNS)¹⁷, while CB2 receptors are primarily present in microglia and vascular elements and are expressed at very low levels in the CNS.^{18,19}

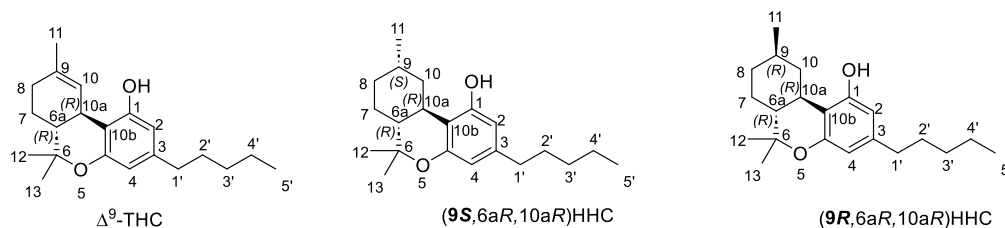
The two major pharmacologically relevant compounds of Cannabis are Δ^9 -THC and CBD. Δ^9 -THC is the well-known psychotropic component of cannabis. It exerts its psychoactive action (hypolocomotion, hypothermia, catalepsy, and analgesia) by activating the CB1 receptor. On the other hand, THC has antispasmodic, anti-inflammatory, and neuroprotective actions, which are mediated by different receptors, such as CB2 and peroxisome proliferator-activated receptors (PPAR).²⁰ In contrast, CBD, which has no psychotropic effects, displays no activity for either CB1 or CB2 receptors. Its molecular mechanisms are not yet clear. However, several studies describe CBD as an interesting therapeutic drug for cancer, diabetes, neurodegenerative disorders, and inflammation.²¹ Moreover, CBD acts as an entourage molecule, reducing the psychotic effects of THC, such as tachycardia, anxiety, and hunger.²² Considering that, different cannabis-derived drugs have been approved by the FDA and they are employed in therapy. Among these, EPIDIOLEX® (oral solution of CBD at concentration of 100 mg/mL) is used to treat two rare childhood epilepsy syndromes, namely Dravet syndrome (DS) and Lennox-Gastaut syndrome (LGS); SATIVEX® (2.5 mg of CBD and 2.7 mg of Δ^9 -THC for a single application of 100 μ L) is an oral spray used to alleviate pain and spasticity in multiple sclerosis refractory to conventional anti-spasticity treatments; MARINOL® (2.5, 5 or 10 mg of synthetic Δ^9 -THC also called Nabilone) are capsules for oral administration used for the treatment of chemotherapy-induced nausea and vomiting in cancer patients. In Italy, galenic preparations made from certified cannabis varieties are also prescribable. The varieties of prescribable therapeutic cannabis are of pharmaceutical grade. In Italy, part of the entire supply is imported from Holland after authorization by the Ministry of Health and part is produced in Italy by Military Chemical Pharmaceutical Plant in Florence. The former includes Bedrocan containing 22% of Δ^9 -THC and less than 1% of CBD, Bediol with 6% of Δ^9 -THC and 8% of CBD and Bedrolite with less than 0.4% of Δ^9 -THC and 9% of CBD. The latter, instead, are Italian medicinal cannabis varieties FM1 (<1% CBD, 13-19% Δ^9 -THC) and FM2 (5-8% Δ^9 -THC, 7.5-12% CBD). Beyond CBD and Δ^9 -THC, other phytocannabinoids have been reported to have therapeutic potential. CBC has shown promising anti-inflammatory²³, anticonvulsant²⁴, anticancer²⁵, and antidepressant activities.²⁶ CBG is known for its antioxidant, anti-inflammatory, neuroprotective,²⁷ antiproliferative and anti-glaucoma actions.²⁸ Additionally, CBG exerts protective and curative effects in the model of murine colitis.²⁹ Unlike decarboxylated phytocannabinoids which have been widely investigated, the information regarding the biological activity of native carboxylated phytocannabinoids are currently scarce. Recently, CBGA has been reported as a promising protective agent against kidney damage for its anti-

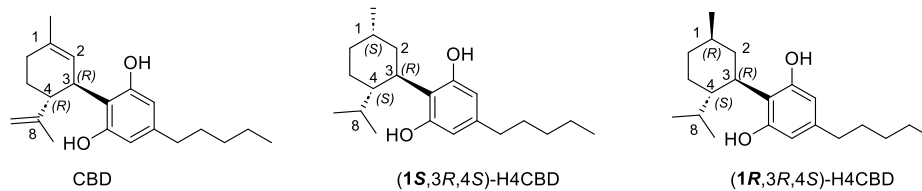
inflammatory and anti-fibrotic effects.³⁰ About a decade ago CBDA bioactivity began to be investigated and anti-microbial³¹, anti-inflammatory, anti-emetic, anti-convulsant, and anti-cancerogenic³² properties have been ascribed to this phytocannabinoid. Probably, THCA has been the most investigated compound among carboxylated phytocannabinoids and has been reported to produce anti-inflammatory effects via antagonism of tumour necrosis factor-alpha (TNF- α).³³ It has also been proved to act as a strong anti-emetic³⁴ and an agonist of the PPAR- γ nuclear receptor with neuroprotective³⁵ as well as anticonvulsant effects.³⁶ Lastly, CBCA has been recently reported to possess anticonvulsant properties²⁴ and exhibit significant antibacterial effects against methicillin-resistant *Staphylococcus aureus* (MRSA), surpassing the potency of vancomycin.³⁷ It is known that over 150 phytocannabinoids are present in the plant, but only a few of them have been isolated and characterized. Since the pharmaceutical properties of *Cannabis sativa* L. extracts depend on their chemical profile, it is important to provide an increasingly comprehensive overview of the phytocannabinome. In light of this, my PhD project aimed to identify and quantify new phytocannabinoids and evaluate their pharmacological activity. **(Chapter 1)** From pharmacological point of view, the stereochemistry of phytocannabinoids also plays an important role. Phytocannabinoids can present one or more chirality centers which generate different stereoisomeric forms. In the case of the two main phytocannabinoids CBD and Δ^9 -THC, the presence of two chirality centers potentially leads to the existence of four stereoisomers for each one: (-)-*trans* - Δ^9 -THC, (+)-*trans* - Δ^9 -THC, (-)-*cis* - Δ^9 -THC, (+)-*cis* - Δ^9 -THC and (-)-*trans* -CBD, (+)-*trans* -CBD, (-)-*cis* -CBD, (+)-*cis*-CBD. The most abundant in nature are (-)-*trans* enantiomers. The stereoisomers of a chiral compound are not equivalent and often show completely different activities^{38,39} and the (+)- and (-)-isomers *trans*-CBD and *trans*- Δ^9 -THC are no exception. They showed to have contrasting biological activities. Indeed, for example, unlike (-)-*trans*-CBD which has no affinity for either CB1 or CB2 receptors, (+)-*trans*-CBD is reported to have a strong binding for CB2 and enhanced affinity for CB1 receptors⁴⁰, though not as high as (-)-*trans*- Δ^9 -THC.¹⁷ Given that, the evaluation of the stereoisomeric composition of the phytocannabinoids is extremely important, especially in medicinal cannabis extracts. Therefore, in the present project, the isomers of the major chiral phytocannabinoids Δ^9 -THC, CBD and CBC, as well as of their carboxylated precursors Δ^9 -THCA, CBDA and CBCA, have been investigated in the Italian medicinal cannabis variety FM2. **(Chapter 2)**

CBD-derived NPS

New psychoactive substances (NPS) are defined by the United Nations Office on Drugs and Crime (UNODC) as “substances of abuse, either in a pure form or a preparation, that are not controlled by the 1961 Single Convention on Narcotic Drugs or the 1971 Convention on Psychotropic substances,

but which may pose a public health threat". The term "new" does not necessarily refer to new inventions, several NPS were first synthesized decades ago, but to substances that have recently become available on the market. Semi-synthetic derivatives of CBD are included in this category. CBD, the non-psychoactive component, is largely employed for pharmaceutical and cosmetic purposes and is predominantly present in cannabis cultivated for industrial intent (hemp varieties). Due to its reported beneficial effects, pure extracted CBD and CBD-rich cannabis varieties have spread worldwide and are openly sold in shops and online. In order to overcome the legal issues, the new-born trend is to add semi-synthetic derivatives of the legal CBD to cannabis products with "high" effects similar to those given by Δ^9 -THC. Considering this, in the present project two NPS derived from CBD were investigated: hexahydrocannabinol (HHC) and hexahydrocannabidiol (H4-CBD). The former, which comes from cyclization and hydrogenation of CBD, was first described in 1940 by Adams⁴¹ but it has only recently gained attention from toxicologists and analysts.⁴² It is reported in the EU and monitored as a NPS by the EU Early Warning System since October 21, 2022.⁴³ On the other hand, the latter is the hydrogenated derivative of CBD and since both double bonds in position 1 and 8 of CBD are hydrogenated, it is also called tetrahydrocannabidiol (THD). H4-CBD is reported in the literature to have cannabinomimetic activity as it is able to bind the central cannabinoid receptor CB1 with a K_i of 145 ± 5 nM.⁴⁴ The lack of reference standards of such compounds prevents the development of analytical methods to apply to commercial samples. To this aim, in the present project, synthetic strategies were developed to obtain epimers of both HHC and H4-CBD. HHC is an analogous of Δ^9 -THC. The double bond in position C-9 is absent and generates a new stereogenic centre. Keeping the configuration at C10a (*R*) and C6a (*R*) unchanged, HHC can exist as two epimers, *9R* and *9S*. The same applies for H4CBD which is an analogous of CBD without the double bond in position C-1 and C-8. The hydrogenation of double bond in position C-1 generates two epimers (**1R,3R,4S**)H4-CBD and (**1S,3R,4S**)H4-CBD. (*9S,6aR,10aR*)HHC, (*9R,6aR,10aR*)HHC, (**1S,3R,4S**)H4CBD and (**1R,3R,4S**)H4CBD were synthesized and used as analytical standards to develop analytical methods. In particular, HPLC-HRMS method and a qualitative gas chromatography-mass spectrometry (GC-MS) method were developed for HHC and H4-CBD epimers, respectively. Moreover, since experimental studies on HHC effects are scarce, HHC epimers were purified and individually tested for their cannabinomimetic activity. (**Chapter 3**)





AIM

The aim of my PhD program is to identify new active ingredients of *Cannabis sativa* L. extracts and provide a complete chemical-pharmaceutical characterization of such compounds and of two CBD-derived NPS, through the development of synthetic strategies and analytical methods based on liquid chromatography coupled to high-resolution tandem mass spectrometry (HPLC-HRMS/MS). The project also aims to evaluate the pharmacological activity of these compounds and develop sensitive and selective analytical methods for their quantification.

CHAPTER 1

***IDENTIFICATION OF ACTIVE INGREDIENTS IN CANNABIS SATIVA L.
EXTRACTS: SYNTHESIS AND DEVELOPMENT OF ANALYTICAL METHODS IN
UNTARGETED AND TARGETED METABOLOMIC APPROACHES.***

HPLC-UV-HRMS ANALYSIS OF CANNABIGEROVARIN AND CANNABIGEROBUTOL, THE TWO IMPURITIES OF CANNABIGEROL EXTRACTED FROM HEMP

Francesco Tolomeo^{a,1}, **Fabiana Russo**^{b,c,1}, **Maria Angela Vandelli**^b, **Giuseppe Biagini**^d, **Anna Laura Capriotti**^e, **Aldo Laganà**^{a,e}, **Luigi Carbone**^a, **Giuseppe Gigli**^a, **Giuseppe Cannazza**^{a,b,*}, **Cinzia Citti**^{a,b,*}

a Institute of Nanotechnology – CNR NANOTEC, Campus Ecotekne, Via Monteroni, 73100, Lecce, Italy

b Department of Life Sciences, University of Modena and Reggio Emilia, Via Campi 103, 41125, Modena, Italy

c Clinical and Experimental Medicine PhD Program, University of Modena and Reggio Emilia, 41125, Modena, Italy

d Department of Biomedical, Metabolic and Neural Sciences, University of Modena and Reggio Emilia, 41125, Modena, Italy

e Department of Chemistry, Sapienza University of Rome, Piazzale Aldo Moro 5, 00185, Rome, Italy

Published in: *J. Pharm. Biomed. Anal.* 203 (2021).
doi.org/10.1016/j.jpba.2021.114215

* Corresponding authors at: Institute of Nanotechnology – CNR NANOTEC, Campus Ecotekne, Via Monteroni, 73100, Lecce, Italy.

E-mail addresses: giuseppe.cannazza@unimore.it (G. Cannazza), cinzia.citti@unimore.it (C. Citti).

¹ These authors contributed equally to the work

Abstract

A sensitive and straightforward HPLC-UV method was developed for the simultaneous quantification of the two main impurities in “pure” commercial cannabigerol (CBG) samples. The identification of such impurities, namely cannabigerovarin (CBGV) and cannabigerobutol (CBGB), the propyl and butyl homologs of CBG, respectively, was accomplished employing the high-resolution mass spectrometry (HRMS) technique, and subsequently confirmed by comparison with the same compounds obtained by chemical synthesis. Complete spectroscopic characterization (NMR, FT-IR, UV, and HRMS) of both impurities is reported in the present work. The method was validated in terms of linearity, which was assessed in the range 0.01–1.00 g/mL, sensitivity, selectivity, intra- and inter-day accuracy and precision, and short-term stability, which all satisfied the acceptance criteria of the ICH guidelines. Application of the method to the analysis of four commercial CBG samples highlighted a certain variability in the impurity profile that might be ascribed to the hemp variety of the starting plant material. With these new analytical standards in hand, it would be interesting to investigate their concentrations in different hemp varieties and expand the scope of a phytocannabinomics approach for a comprehensive profiling of this remarkable class of natural compounds.

1. Introduction

Cannabis sativa L. is a plant producing over 150 different phytocannabinoids, of which only a few have been isolated and fully characterized to date. Considerable efforts have been devoted to the investigation of the chemistry of the main psychotropic compound of cannabis, Δ^9 - tetrahydrocannabinol (Δ^9 -THC), and its pharmacology; in comparison, very little has been done on the front of the non-psychotropic phytocannabinoids, such as cannabidiol (CBD), cannabigerol (CBG), cannabichromene (CBC), and so forth. CBD has certainly gained much more attention in the last five years due to the discovery of a plethora of pharmacological properties that have prompted industrial companies to start a business on the extration of CBD from the plant to market it as a pure active ingredient of pharmaceutical grade. Since its approval as a drug for the treatment of severe forms of infant epilepsy under the commercial name of Epidiolex (GW Pharmaceuticals, UK), CBD has been extensively extracted from cannabis/hemp for pharmaceutical purposes and marketed as a pure substance. However, recent studies revealed two main impurities in such commercial products with chemical structures similar to that of CBD but with a different length of the side alkyl chain [1,2]. The most abundant impurity, cannabidivarin (CBDV), has a three-term

linear side chain. In contrast, the second impurity, cannabidibutol (CBDB), has a four-term chain and was characterized for the first time by our research group [1,2].

Similarly, CBG has recently attracted the interest of both the industrial and scientific community, as shown by the increase in the number of publications per year on PubMed [3]. Although CBG is generally present as a minor component (<10% of the total cannabinoid fraction) compared to either the dominant CBD in the most common fiber-type cannabis varieties or to THC in drug-type cannabis, CBG-predominant cultivars (with >85 % CBG) have also been reported in the literature [4]. Such a very attractive chemotype has started to be bred [4] due to the remarkable pharmacological properties of this phytocannabinoid especially as antimicrobial, anti-inflammatory, cytotoxic, and antidepressant agent, besides its non-psychoactive nature [5]. CBG-rich cannabis varieties are therefore genetically selected for the extraction of CBG to make a pure marketable substance.

Commercial CBG is generally labelled as ≥ 98 % pure, bearing two main impurities, one of which is cannabigerovarin (CBGV) and another compound with the hypothetical structure of a cannabigerol with a butyl side chain, commonly named CBG-C4. Some companies do not even mention the chemical nature of the impurities in their certificate of analysis. However, to the best of the authors' knowledge, the butyl homolog of CBG has been neither identified nor characterized up to now. The aim of the present work was to characterize the impurities of commercial CBG and provide a simple method for their qualitative and quantitative determination. Such impurities were first putatively identified by high-performance liquid chromatography coupled to high-resolution mass spectrometry (HPLC-HRMS) as the propyl and butyl homologs of CBG, namely CBGV and cannabigerobutol (CBGB) in line with the common nomenclature given to this type of variants with respect to olivetol-derived phytocannabinoids [1,2,6]. The former was first reported in 1975 [7], and its chemical and pharmacological properties have been investigated [8–10], although not extensively, whereas the latter has never been characterized to date. Only two records from Berman et al. mention the presence of a minor peak putatively identified as CBG-C4 in the same cannabis extracts, but it was not chemically characterized [11,12]. An ad hoc stereoselective synthesis of the pure E-isomers of both CBGV and CBGB and their complete chemical, physical characterization by spectroscopic techniques (HRMS, NMR, FT-IR, and UV spectroscopy) allowed for the identification of the two main impurities in “pure” CBG samples. In particular, the present work represents the first reported full chemical characterization of the butyl homolog of CBG, which will enable to determine such compound in different hemp varieties and perhaps study a potential correlation among the several cannabinoid homologs with different length of the alkyl chain [6,13,14]. Lastly, a straightforward and fast HPLC method coupled to UV detection was developed

and validated according to ICH guidelines (Q3A) in terms of selectivity, linearity, sensitivity, intra- and inter-day accuracy and precision, carry-over, and stability [15].

2. Materials and methods

2.1. Chemicals and reagents

Ethanol 96 % analytical grade was bought from Carlo Erba (Milan, Italy). Acetonitrile, water and formic acid were all LC–MS grade and purchased from Carlo Erba. Samples of pure CBG extracted from hemp were kindly donated by three private companies, KannaStar (Pruszkow, Poland), Mile High Labs (Broomfield, United States), and CBDepot (Teplice, Czech Republic). Chemicals and solvents employed in the synthetic process were reagent grade and used without further purification. The following abbreviations for common organic solvents were adopted: dichloromethane (DCM); cyclohexane (CE). Air- or moisture-sensitive reactions were performed under nitrogen atmosphere. Flash column liquid chromatography purifications were carried out using Merck silica gel 60 (230–400 mesh, ASTM).

2.2. HPLC-UV-HRMS method for the identification and quantification of CBG impurities

The HPLC technique coupled to both UV and HRMS detection was employed for the analysis of commercial CBG powder and identification of its impurities. The chromatographic apparatus used was a Thermo Fisher Scientific Vanquish Core (Thermo Fisher Scientific, Waltham, Massachusetts, United States) equipped with a vacuum degasser, a binary pump, a thermostated autosampler set at 4°C, a thermostated column compartment set at 30°C, and a diode array detector (DAD). The column employed for the separation was a Poroshell 120 EC-C18 (100 × 3 mm I.D., 2.7 m) used with a guard (50 × 3 mm I.D., 2.7 m) (both from Agilent Technologies, Milan, Italy) and the mobile phase consisted of a mixture of water (solvent A) and acetonitrile (solvent B) in a 25:75 ratio (v/v) both with 0.1% of formic acid (v/v). The elution program included an isocratic step with 75% B for 6 min, which allowed for the elution of all analytes including the main ingredient CBG, a washing step with 98 % B from 6.1–8 min, and a final re-equilibration step at 75 % B from 8.1 to 13 min (total run time). The flow rate was maintained constant at 0.5 mL/min throughout the analysis. The DAD recorded all wavelengths from 190 to 900 nm, but the integration of the analytes peaks was performed at the wavelength of 210 nm, which provided the best detector response.

The liquid chromatography apparatus was interfaced to a heated electrospray ionization source

(HESI) of an Orbitrap Exploris 120 mass spectrometer. The HESI source parameters were optimized by direct infusion of a real sample of CBG in acetonitrile (5g/L) with a syringe pump: the spray voltage was maintained static at 4200 V for the positive ionization mode and at 3800 V for the negative mode; sheath gas, auxiliary gas and sweep gas were set in the static mode at 60, 25, and 1 au respectively; the ion transfer tube temperature was set at 400 °C and the vaporizer temperature at 150 °C. A resolution of 60,000 FWHM (full-width at half-maximum) was applied to the mass spectrometer operating in full scan (FS) mode in the range 75–750 (m/z) in both positive and negative polarity mode. The radio frequency (RF) of the S lens was set at 70 % and the expected LC peak width at 6 s. Also, the mild trapping mode was activated in order to improve selectivity, while the source fragmentation was disabled to avoid misleading results. For identification purposes a data-dependent acquisition (DDA) scan was added to the method applying the following parameters: resolution 15,000 FWHM, collision energy for the fragmentation of the precursor ions 17.9 eV (NCE 30), maximum injection time 22 ms, isolation window of the precursor ion 1.2 m/z. The injection volume was 10 μ L. The analytes mass range was extracted with a 5 ppm mass tolerance from the total ion current.

HPLC-UV-HRMS analyses were acquired with Chromeleon 7.3 Data System (Thermo Fisher Scientific), which was also used for UV peak automatic integration (manually checked for software random errors). HRMS spectra were handled with FreeStyle software v.1.3 (Thermo Fisher Scientific).

2.3. General synthetic procedure

A solution of resorcinol with the appropriate length chain (1eq.) and geraniol (1eq.) in dry toluene (1M for resorcinol) was stirred at room temperature and under nitrogen atmosphere. Then, p-toluenesulfonic acid (0.08 eq.) was added and the solution was stirred at 70°C in the absence of light for 1 h. The reaction was quenched with a saturated solution of sodium bicarbonate. The organic phase was washed with brine, dried over anhydrous Na₂SO₄, and concentrated under vacuum. The crude was purified over silica gel.

The reaction and purification conditions for (E)-2-(3,7-dimethylocta-2,6-dien-1-yl)-5-propylbenzene-1,3-diol (CBGV) and (E)-5-butyl-2-(3,7-dimethylocta-2,6-dien-1-yl)benzene-1,3-diol (CBGB) are reported in the Supplementary material.

2.4. Chemical and spectroscopic characterization of CBGB and CBGV

The structures of all isolated compounds were ensured by HRMS, nuclear magnetic resonance (NMR), UV, and FT-IR spectroscopy. A DPX-400 Avance (Bruker) spectrometer was employed to acquire one-dimensional ^1H and ^{13}C NMR and two-dimensional NMR (COSY, HSQC and HMBC) spectra (400.134 MHz for ^1H NMR and 100.62 MHz for ^{13}C NMR). In order to get a reasonable resolution of the NMR spectra, a 10 mg aliquot of the synthetic compound was solubilized with 700 μL of CDCl_3 (99.96 % deuteration) in a 5 mm NMR tube. All NMR spectra were recorded at 300 K. ^1H -NMR signals were acquired with a spectral width of 8278.146 Hz, a relaxation delay of 1 s and 16 transients. Proton and carbon chemical shifts were reported in parts per million (ppm, units) and referenced to the solvent residual peaks ($\text{CDCl}_3 = 7.26$ ppm and 77.05 ppm for proton and carbon respectively). Coupling constants (J) are reported in Hz. ^{13}C -NMR spectra were acquired with a spectral width of 23.9 kHz, a relaxation delay of 1s and 1024 number of transients for both synthetic CBGB and CBGV. NMR data are reported as follows: chemical shift, multiplicity (s, singlet; d, doublet; t, triplet; q, quartet; qnt, quintet; sxt, sextet; m, multiplet; br, broad), coupling constants (Hz) and number of protons/carbons (Supplementary material). ^1H - ^1H correlation spectroscopy (COSY), ^1H - ^{13}C heteronuclear multiple quantum coherence (HMQC) and heteronuclear multiple bond connectivity (HMBC) experiments were recorded for determination of ^1H - ^1H and ^1H - ^{13}C correlations, respectively. The COSY experiments were recorded as a 2048×256 matrix with 2 transients per t1 increment. The HSQC spectra were collected as a 2048×256 matrix with 4 transients per t1 increment and the one-bond heteronuclear coupling value was set at 145 Hz. The HMBC spectra were collected as a 2048×220 matrix with 8 transients per t1 increment and processed as a 4096×256 matrix, and the long-range coupling value was set at 8 Hz.

FT-IR spectra were recorded at 25 ° C on a Bruker Spectrum FTIR Vertex, scanning from 600 to 8000 cm^{-1} . After a background sub-traction, about 2 mg of the compound was placed on the diamond platform and scanned to acquire the spectrum.

2.5. Standard solution and sample preparation

Individually prepared standard stock solutions of CBGV and CBGB in acetonitrile (1 mg/mL) were properly diluted to obtain five non-zero calibration standards at the concentration of 0.01, 0.05, 0.10, 0.50, and 1.00 g/mL. Three quality control levels were also prepared for method validation: low concentration quality control (LQC), medium concentration quality control (MQC), and high concentration quality control (HQC), being respectively 0.02, 0.25, and 0.75 g/mL for both CBGV and CBGB. Authentic samples of CBG powder were analyzed at the concentration of 100 g/mL prepared as for the standard solutions to reveal potential impurities.

2.6. Method validation

Method validation was carried out following the international guidelines for analytical techniques for the quality control of pharmaceuticals (ICH guidelines) [15]. Selectivity of the method, linearity, sensitivity (limit of detection and limit of quantification), intra- and inter-day accuracy, intra- and inter-day precision, autosampler carry-over, and stability were assessed in order to prove the reliability and robustness of the developed method. Neither matrix effect nor recovery was evaluated as the solvent used for sample preparation and dilutions (acetonitrile) is also present in the mobile phase, thus it is void of such issues.

2.6.1. Selectivity and peak purity

The selectivity of the method towards CBGV and CBGB was assessed by comparing the retention times of the analytes in pure standard solutions and of potential interfering compounds contained in authentic CBG samples. To this end, blank samples, authentic CBG samples containing the analytes, and pure standards of CBGV and CBGB were used.

The peak purity test was performed by comparing the UV spectrum of the analyte at the beginning, the apex, and the end of the peak.

2.6.2. Linearity

Peak areas of the analytes (y) were plotted vs actual concentrations (x). A calibration curve was built for each analyte every day for five consecutive days (n = 5). A coefficient of determination (R²) greater than 0.99 was considered acceptable for a linear correlation. The back-calculated concentration was used to determine the concentration of each analyte in each individual calibration standard and considered acceptable if the mean precision (CV%) was within ±15 % of the nominal concentrations for all calibration points and ±20 % of the lower limit of quantification (LLOQ).

2.6.3. Sensitivity

Stock solutions of the analytes were properly diluted at the limit of detection (LOD) value, which was estimated at a 3:1 signal-to-noise (S/N) ratio. LOD was then calculated as three times the standard deviation obtained by analyzing five replicates of the prepared dilutions. The lower limit of quantification (LLOQ) was estimated at a 10:1 S/N ratio and calculated as ten times the SD of five injections of the appropriately diluted standards. The upper limit of quantification (ULOQ) was set at 1 g/mL.

2.6.4. Autosampler carry-over

Autosampler carry-over was evaluated by running two blank samples after a calibration standard at the ULOQ and after an authentic sample containing the analytes (CBG 100 g/mL). The carry-over was considered acceptable if the detector response for the analytes was within ±20 % of the LLOQ.

2.6.5. Accuracy and precision

Precision and accuracy were evaluated at four levels, LLOQ (0.01 g/mL), LQC (0.02 g/mL), MQC (0.25 g/mL), and HQC (0.75 g/mL). Each level was analyzed three times ($n = 3$) within a single day to determine the intra-day precision and accuracy and repeated for five consecutive days ($n = 15$) preparing fresh standard solutions. The precision was expressed as coefficient of variation (%CV), and the accuracy was expressed as the percentage of the mean calculated against nominal concentration.

2.6.6. Stability

The short-term stability of the standard analytes was determined at four levels (LLOQ, LQC, MQC, and HQC) in a 24 -h interval (bench-top stability) and under refrigeration (2-8°C). The analytes were considered stable if the mean concentration ($n = 3$ for each sample) was within $\pm 15\%$ of the nominal concentration of a freshly prepared calibration curve.

3. Results and discussion

3.1. Identification of CBG impurities by HRMS

Analysis of hemp products is important to ensure quality and safety. LC-UV and LC-MS based methods have been developed in the last years for the detection and quantitative determination of the cannabinoid profile of hemp-derived products [16,17]. Assessment of the impurity profile of a new drug substance is recommended in pharmaceutical research when impurities are above 0.05% [15].

Analysis of commercial CBG powder by HPLC-UV showed the presence of two peaks eluting before that of the main ingredient (3.30 min), specifically at 2.26 min and 2.70 min (Fig. 1). However, the UV trace of the sample does not provide information on the chemical structure of unknown compounds unless the corresponding pure standards are available. For this reason, HRMS is amongst the techniques of choice for the identification of unknown chromatographic peaks [18]. Taking advantage of the high sensitivity, accuracy, and precision performances offered by the latest Orbitrap technology (Exploris 120), commercial CBG samples were analyzed, and the HRMS trace showed the presence of the same two peaks eluting before the main ingredient (2.28 and 2.72 min respectively, which were compatible with the delay after detection in the UV cell) (Fig. 1).

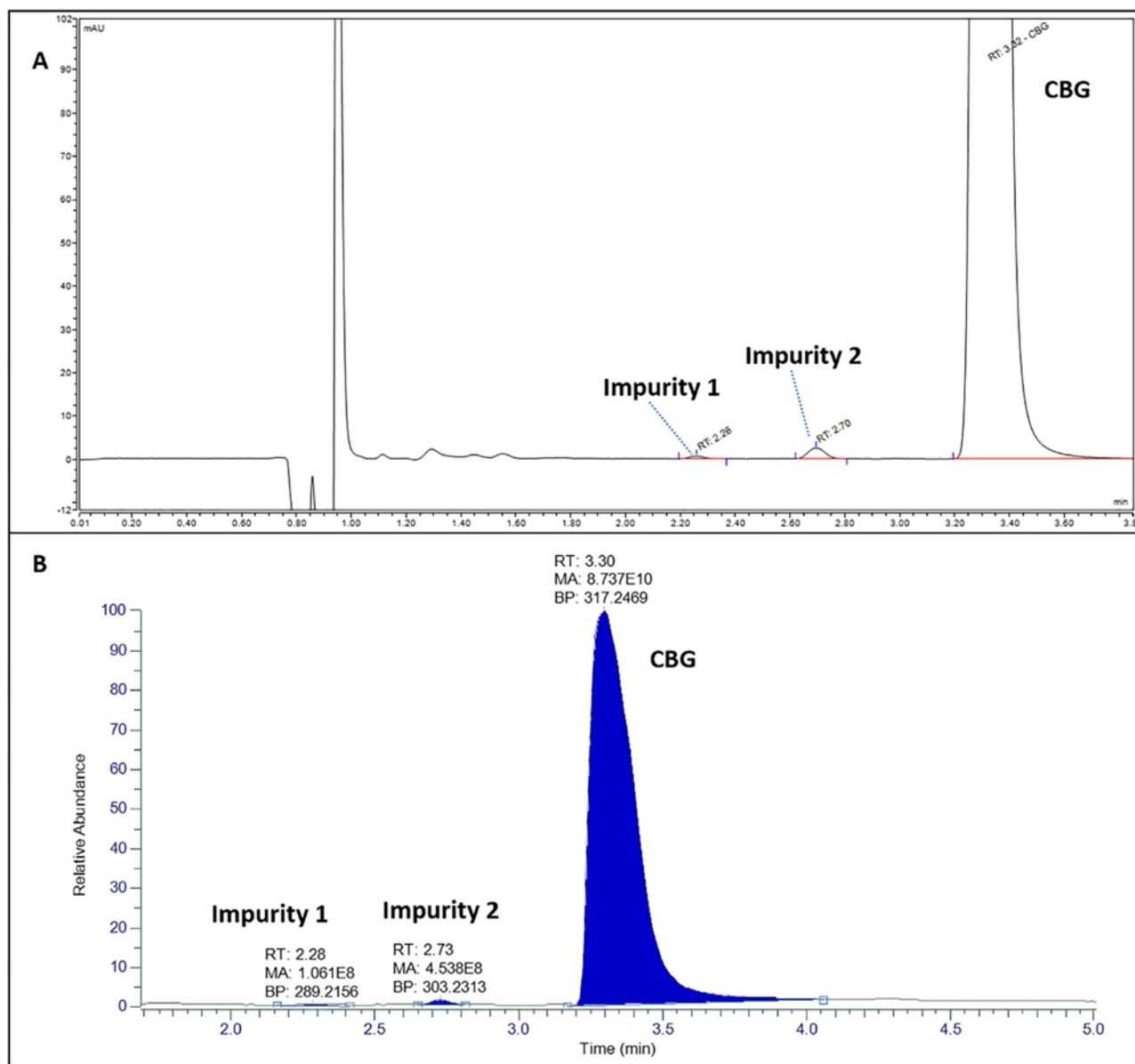


Fig. 1. HPLC-UV-HRMS traces of a commercial CBG sample. A) HPLC-UV chromatogram acquired at 210 nm of a commercial sample of CBG (100 g/mL); the retention time of the impurities and CBG are reported. B) HPLC-HRMS total ion chromatogram of a commercial sample of CBG (100 g/mL); retention time, peak area and precursor ion in HESI⁺ are reported.

With the aim of identifying the two impurities in the CBG powder, the corresponding precursor ions $[M+H]^+$ and $[M-H]^-$ were subject to HRMS fragmentation. The HRMS spectrum of the peak eluting at 3.3 min corresponding to CBG was also analyzed in both HESI⁺ and HESI⁻ mode to confirm its identity. The fragmentation pattern of CBG (C₂₁H₃₂O₂) is characteristic for the presence of a single fragment in both polarities: the base peak at m/z 193.1212 in HESI⁺ mode corresponds to a methyl and pentyl disubstituted resorcinol in para position, while the precursor ion at m/z 317.2475 is barely visible (Fig. 2); the HESI⁻ fragmentation spectrum shows only the precursor ion at m/z 315.2332,

while the other main fragment at m/z 191.1071 has a relative abundance (RA) below 5% (Fig. 3). The latter is a characteristic feature of CBG-type cannabinoids made of three fragments bearing the difference of a hydrogen atom with the first two fragments having similar RA and the third one with a very low abundance (<1%). Both peaks corresponding to the two CBG impurities showed the same HRMS fragmentation patterns. Specifically, the base peaks showed m/z 165.0909 and 179.1065 and the precursor ions at m/z 289.2159 and 303.2313 in the HESI⁺ spectra of the first and second impurity, respectively (Fig. 2). The HESI⁻ spectra presented the precursor ions at m/z 287.2020 and 301.2175 corresponding to the molecular formulas C₁₉H₂₈O₂ and C₂₀H₃₀O₂, respectively, and the characteristic triple fragment at m/z 163.0770 and 177.0927 for the first and second impurity, respectively (Fig. 3). It was not surprising to note the exact difference of 14.0157 amu between the first and second impurity fragments and between the second impurity and CBG. Therefore, the first impurity was putatively identified as cannabigerovarín (CBGV), the propyl homolog of CBG, while the second impurity was putatively identified as cannabigerobutol (CBGB), the butyl homolog of CBG. Injection of the corresponding synthesized analytical standards confirmed such hypothesis.

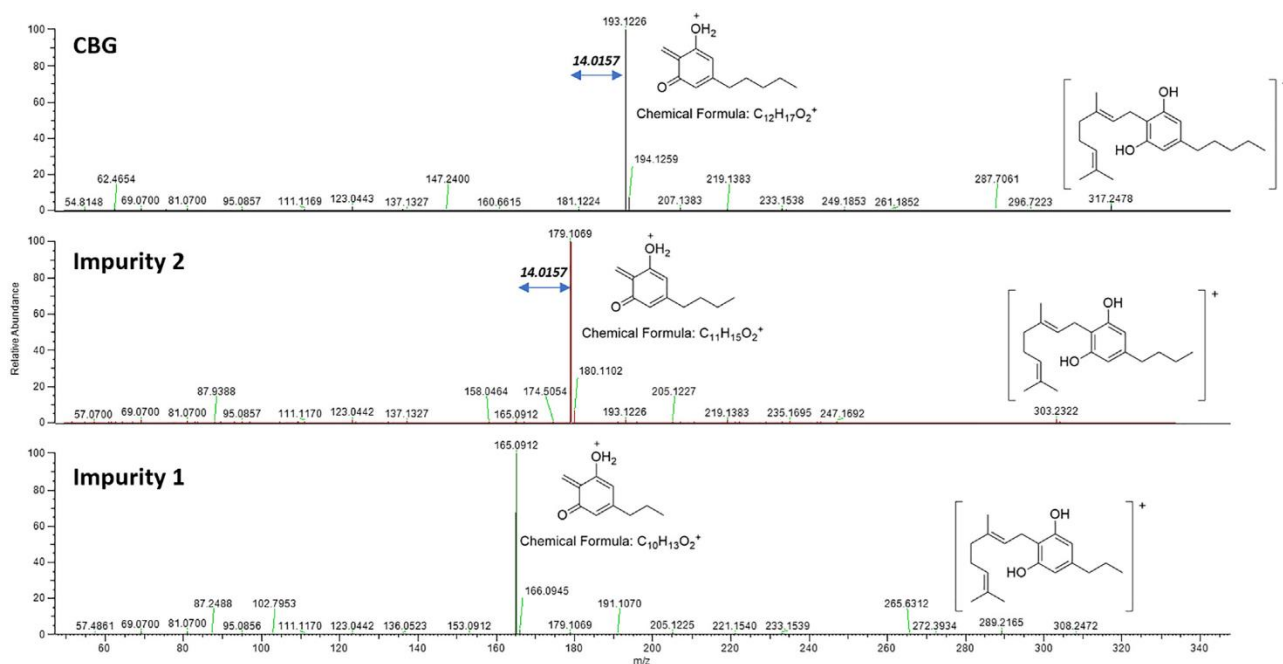


Fig. 2. HRMS spectra of CBG, impurity 2 and impurity 1. Stacked HRMS spectra of CBG, impurity 2 and impurity 1 (from the top to the bottom) obtained in HESI⁺ mode with a NCE of 30. For the precursor ion and the base peak, the hypothetical chemical structure is proposed.

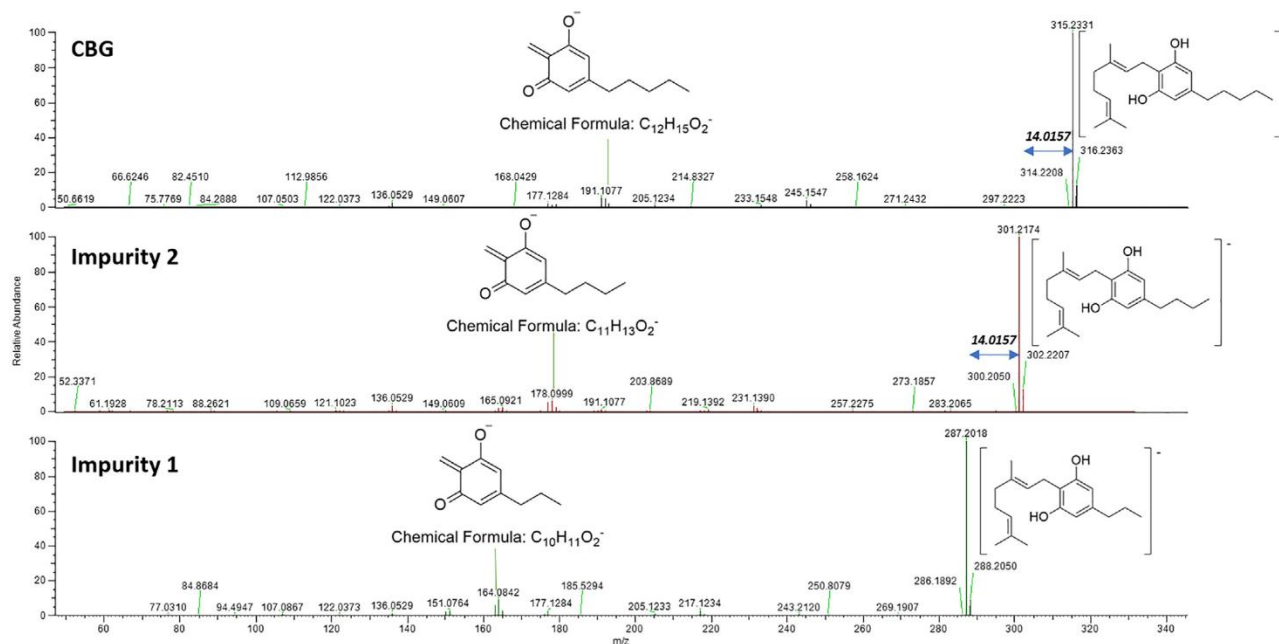
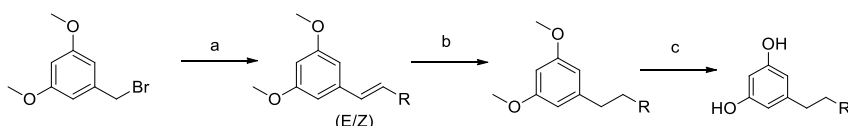


Fig. 3. HRMS spectra of CBG, impurity 2 and impurity 1. Stacked HRMS spectra of CBG, impurity 2 and impurity 1 (from the top to the bottom) obtained in HESI- mode with a NCE of 30. For the precursor ion (base peak) and the main fragment the hypothetical chemical structure is proposed.

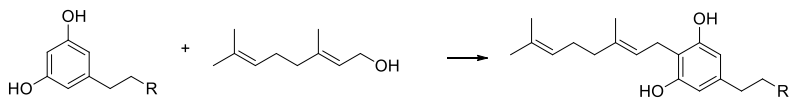
3.2. Synthesis and spectroscopic characterization of CBGV and CBGB

Isolation of unknown compounds and comparison of their chemical properties with those of authentic standards gives the highest confidence level for compound identification, although the isolation step often results tricky, especially in the case of trace compounds or very complex mixtures. When isolation is not a viable option, the chemical synthesis of the analytes under investigation and comparison of their MS features with those of the analytes in a real sample seems the most suitable way to achieve their unambiguous identification. Due to the difficulty in isolating a sufficient amount of the CBGV and CBGB from CBG samples, an ad hoc synthesis was set up in order to obtain the two compounds under investigation.

The precursors 5-butylbenzene-1,3-diol and 5-propylbenzene-1,3-diol were synthesized as reported by our group for the 5-hexylbenzene-1,3-diol synthesis (Ref. CBDH) (Scheme1). In particular, 1-(bromomethyl)-3,5-dimethoxybenzene was converted into the corresponding alkenes by performing the Wittig reaction using propionaldehyde and acetaldehyde respectively. Subsequently, the alkenes were reduced and deprotected. The precursors obtained were converted into the products of interest (CBGV and CBGB) by reacting with geraniol and catalytic amount of p-toluenesulfonic acid (pTSA) as reported in Scheme 2.



Scheme 1. General synthetic approach to obtain 5-butylbenzene-1,3-diol (R= -CH₂CH₃) and 5-propylbenzene-1,3-diol (R= -CH₃). Reagents and conditions: a) Step 1. Triphenylphosphine (1.1eq), Toluene, reflux, 6 h, yield 96%. Step 2. Aldehyde (1.5 eq), aqueous 0.1 M K₂CO₃ (20mL), reflux overnight. b) H₂ Pd/C flux reactor H-Cube Mini Plus ThalesNano, 30°C, 1 mL/min, EtOH. c) BBr₃ 1 M in dry DCM (2.2eq.), -15°C → room temperature.



Scheme 2. General synthetic approach to obtain CBGB (R= -CH₂CH₃) and CBGV (R= -CH₃). Reagents and conditions: geraniol (1eq.), pTSA (0.08 eq.), 70 °C, 1h, in the dark.

The compounds obtained by chemical synthesis were used as analytical standards and injected into the HPLC-HRMS system as a 1g/mL solution mix to confirm their putative identification. The precursor ions of the impurities and the standards extracted in both HESI+ (Fig. 4) and HESI- mode (Fig. 5) showed a perfect match of exact mass, retention time, isotopic pattern, and HRMS fragmentation spectra.

Synthetic CBGV and CBGB were also characterized by other spectroscopic techniques like UV, NMR, and FT-IR. UV spectra of both synthetic compounds showed a perfect match with those of the two CBG impurities and were identical to that of CBG with maximum absorption peaks at 206 and 274 nm (Fig. S4).

CBG spectroscopic characterization has already been reported [19], but it was surprising that the literature reports only the ¹H-NMR and FT-IR signals of CBGV. ¹H-NMR, ¹³C-NMR, and COSY experiments allowed to assign all chemical shifts of protons and carbons and eventually the correct chemical structure of both CBGV and CBGB. Table 1 shows ¹H-NMR and ¹³C-NMR signals assigned to the corresponding atom position. NMR data and comparison with the CBG reported signals were crucial to understand that carbons 2 and 3 forming the double bond were in the correct E-configuration, thus confirming that the terpene retained its geometric configuration in the final product. Since CBGV and CBGB differ only for a methylene group, identical NMR signals were expected for the resorcinyl and terpene moieties, while a slight difference was registered for the alkyl chain. In particular, CBGV shows one single multiplet for 3H in 10 and 2H in 2 slightly deshielded compared to CBGB (1.62–1.57), which presented a clear singlet for 3H in 10 and a multiplet for 2H in 2 (1.57–1.53). The sextet for the 2H in 3 of the CBGB molecule was diagnostic of the additional methylene unit in the butyl homolog. Carbon signals were also significantly different for the alkyl chain, primarily because of a shielding effect in the CBGB molecule for positions 1 and 2.

FT-IR of the three molecules (standard CBG, synthetic CBGV, and synthetic CBGB) were also compared and reported (Figs. S1–S3, Supplementary material).

Table 1. ^1H and ^{13}C NMR assignments (δ) of CBGB.

Position	$^1\text{H-NMR}^{[a]}$		$^{13}\text{C-NMR}$	
	CBGV	CBGB	CBGV	CBGB
1	-	-	154.80	154.81
2	6.25 (s)	6.25 (s)	108.42	108.37
3	-	-	142.50	142.71
4	6.25 (s)	6.25 (s)	108.42	108.37
5	-	-	154.80	154.81
6	-	-	110.61	110.58
1'	3.39 (d)	3.39 (d)	22.26	22.32
2'	5.29-5.25 (m)	5.29-5.25 (m)	121.68	121.68
3'	-	-	139.00	138.99
4'	2.12-2.06 (m)	2.10-2.06 (m)	39.69	39.69
5'	2.12-2.06 (m)	2.10-2.06 (m)	26.39	26.39
6'	5.07-5.04 (m)	5.06-5.04 (m)	123.75	123.75
7'	-	-	132.05	132.08
8'	1.68 (s)	1.67 (s)	17.69	17.59
9'	1.81 (s)	1.81 (s)	16.19	16.19
10'	1.62-1.57 (m)	1.59 (s)	25.66	25.66
1''	2.44 (t)	2.46 (t)	37.63	35.21
2''	1.62-1.57 (m)	1.57-1.53 (m)	24.17	33.24
3''	0.97 (t)	1.34 (sxt)	13.84	22.25
4''	-	0.91 (t)	-	13.93
OH	4.97 (bs)	4.96 (bs)	-	-

3.3. Method validation

Once the unambiguous identification of the two CBG impurities was accomplished, the HPLC-UV method developed was validated following the ICH guidelines to ensure linearity, low carry-over, high selectivity, sensitivity, accuracy, precision, and stability [15]. Validation was performed for both detection platforms demonstrating the robustness and reliability of the method.

Peak purity was assessed for the two analytes by comparing the UV trace at 210 nm for the start, the apex, and the end of each peak; no difference was found.

Linearity was assessed for both CBGV and CBGB in the range 0.01–1.00 g/mL with $R^2 > 0.997$ (Table S1).

CBGV and CBGB showed a LOD of 0.005 g/mL and a LLOQ of 0.01 g/mL (Fig. S5). The ULOQ was set at 1 g/mL.

The autosampler carry-over evaluated in blanks injected after the HQC, ULOQ, and a highly concentrated sample, was totally absent as no peaks at the retention time of the analytes were detected, thus ensuring good reliability of the quantification of the analytes.

Intra-day accuracy for CBGV was in the range of 101.7–106.7 %, and the intra-day precision ranged from 0.11 to 4.46%. CBGB showed an intra-day accuracy between 99.56 and 114.3 %, and an intra-day precision between 0.07 and 5.41 %. Inter-day accuracy resulted in the range 90.49–104.3 % and 87.76–106.0% for CBGV and CBGB respectively, while inter-day precision was found in the range 0.84–13.7 % and 0.64–13.4 % for CBGV and CBGB respectively. All data were within the limits established by the acceptance criteria of ICH guidelines (85–115 % for accuracy and below 15 % for precision) as reported in Table S2.

Short-term stability of the standard analytes was assessed at the three quality control levels (LQC, MQC, and HQC) and at the LLOQ, which generally shows major stability issues. Standard solutions were stored both on the bench-top and in the fridge and analyzed after 24 h. Both CBGV and CBGB were found stable at all levels as their concentration resulted within 15 % of the actual concentration based on a freshly prepared calibration curve (Table S3).

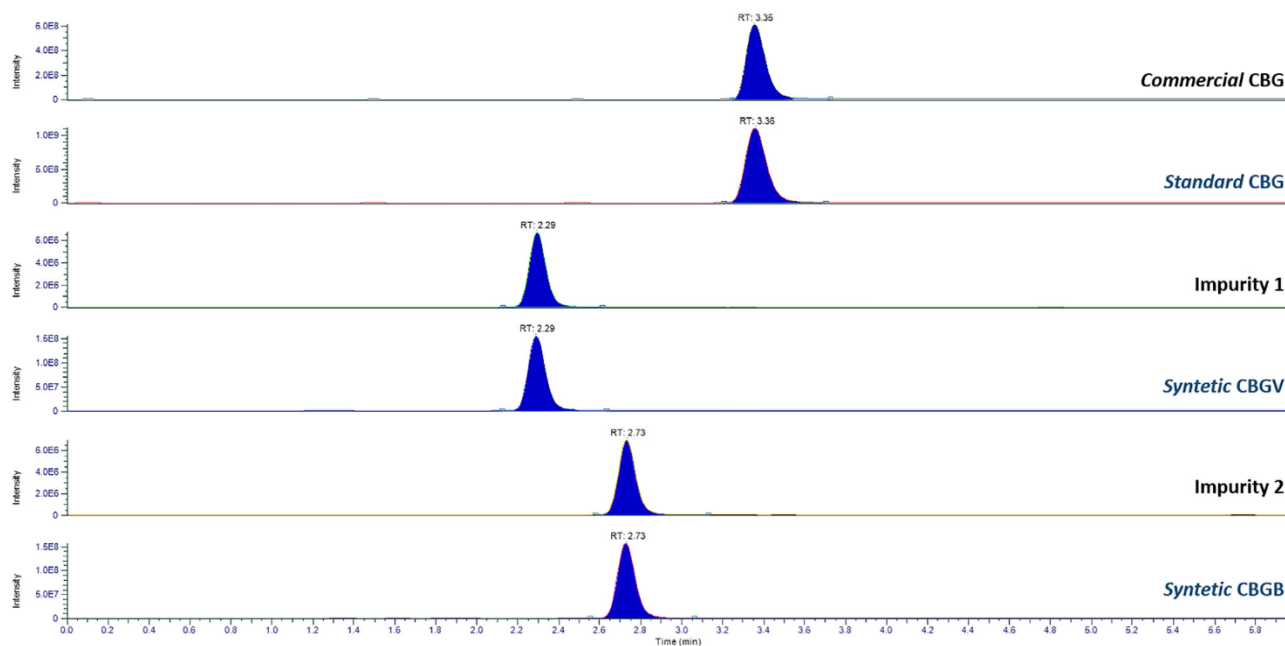


Fig. 4. Comparison of HPLC-HRMS traces of CBG, impurity 1 and impurity 2 with the corresponding standards in HESI + mode. Extracted ion chromatogram in stacked mode obtained in HESI + mode of the precursor ions of the analytes and the corresponding synthetic or commercial standards: m/z 317.2475 for CBG, m/z 303.2313 for CBGB, and m/z 289.2159 for CBGV.

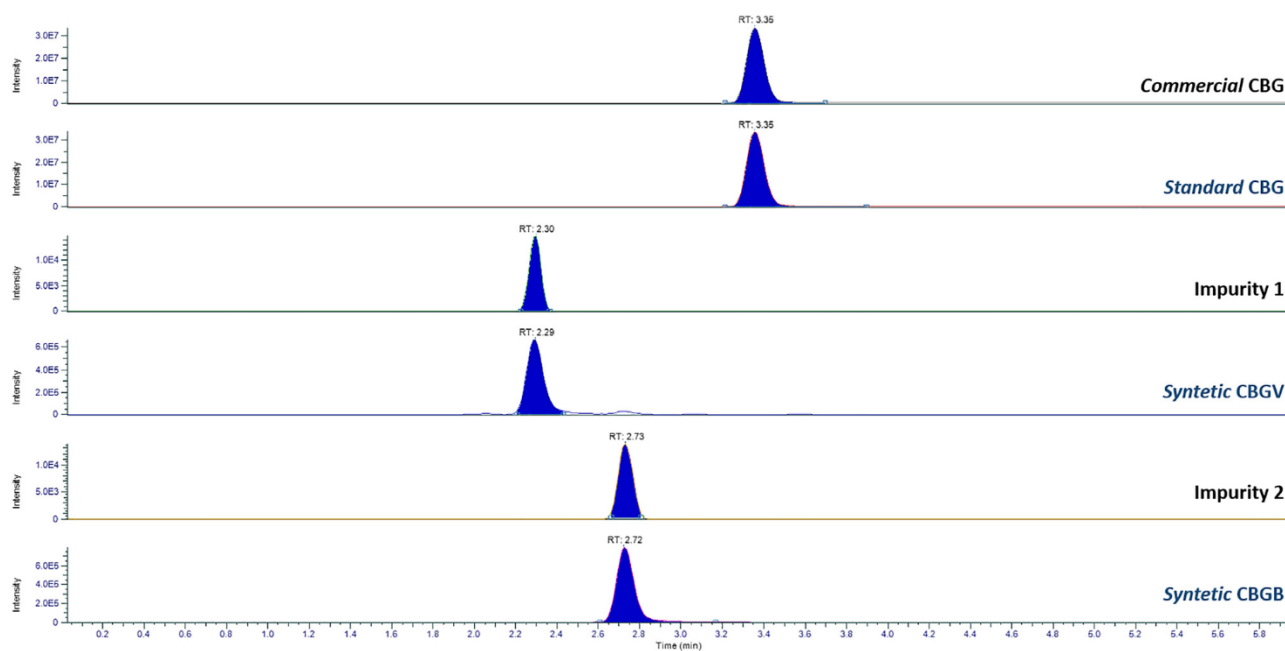


Fig. 5. Comparison of HPLC-HRMS traces of CBG, impurity 1 and impurity 2 with the corresponding standards in HESI- mode. Extracted ion chromatogram in stacked mode obtained in HESI- mode of the precursor ions of the analytes and the corresponding synthetic or commercial standards: m/z 315.2332 for CBG, m/z 301.2175 for CBGB, and m/z 287.2020 for CBGV.

3.4. Analysis of authentic CBG samples

The developed and validated method was applied to four commercial CBG samples in which the concentrations of the two impurities CBGV and CBGB were calculated. The results are reported in Table 2. The amount of CBGV in the CBG powder was found around 0.031 % for three samples and 2.215 % for one sample, while that of CBGB ranged from 0.115 to 0.295 %. Compared to previously reported results on the impurities of CBD samples [1], it appears that there is less variability in the ratio between the concentrations of the propyl and the butyl homologs, although the number of the samples limit any possible statistic speculation. On the other hand, while the ratio CBDV to CBDB mainly favored the propyl form [1], in the case of CBG homologs, this form was consistently about 4 times lower than the butyl one for three out of four samples. The fourth sample showed a completely different impurity profile as it presented an inverted ratio between CBGV and CBGB in favor of the former. Although both CBGV and CBGB have already been detected in some hemp/cannabis varieties [11,12,20], it is not cautious at this stage to assume that the concentration of such impurities in pure CBG samples are either simply reproduced from those of the belonging hemp variety or are to be addressed to the extraction process. In this regard, it would be essential to screen the concentrations of these two compounds and their ratios in different hemp varieties.

Table 2. Analysis of commercial CBG samples. The values are expressed as mean percentage±dev.st (w/w) of three analyses (n=3).

Sample	CBGV (%)	CBGB (%)
CBG-1	0.029±0.002	0.112±0.002
CBG-2	0.033±0.002	0.116±0.005
CBG-3	0.029±0.001	0.111±0.001

4. Conclusions

Cannabigerol (CBG) is a non-psychotropic phytocannabinoid from hemp with interesting pharmacological properties, which have attracted the attention of the hemp industry, pushing towards a new worldwide market. Commercially available “pure” CBG was analyzed in the present work by HPLC coupled to UV and HRMS, highlighting the presence of two main impurities, which were identified as cannabigerovarin (CBGV) and cannabigerobutol (CBGB), the propyl and butyl homologs of CBG, respectively. A fast and straightforward HPLC-UV method was developed and validated according to ICH guidelines to provide reliable quantification of such impurities in commercial CBG samples. Although the concentrations found were below 0.5 %, it should not be excluded that higher amounts might be present in the starting hemp material. Therefore, it could be crucial to determine such compounds in different hemp varieties and investigate their ratio to find out whether a correlation among the different CBG homologs exists. Lastly, the characterization of a new phytocannabinoid reported herein for the first time will be of foremost importance for a comprehensive phytocannabinome profiling of hemp varieties.

Author contribution

Giuseppe Cannazza and Cinzia Citti contributed to the study conception and design. Method development, data collection and analysis were performed by Francesco Tolomeo, Luigi Carbone, Anna Laura Capriotti and Aldo Laganà. Fabiana Russo, Maria Angela Vandelli and Giuseppe Biagini designed and performed synthesis and spectroscopic characterization. Giuseppe Cannazza and Giuseppe Gigli were involved in funding acquisition. Cinzia Citti and Giuseppe Cannazza supervised and coordinated all experimental activities. Cinzia Citti wrote the original draft of the manuscript and all authors commented and reviewed their part. All authors read and approved the final manuscript.

Acknowledgements

This work was supported by UNIHEMP research project “Use of Industrial Hemp biomass for Energy and new biochemicals Production” (ARS01 00668) funded by Fondo Europeo di

Sviluppo Regionale (FESR) and by Ministero dell'Istruzione, dell'Università e della Ricerca (MIUR) (within the PON R&I 2017-2020 – Axis2 – Action II – OS 1.b). Grant decree UNIHEMP prot. n. 2016 of 27/07/2018; CUP B76C18000520005.

References

- [1] C. Citti, P. Linciano, F. Forni, M.A. Vandelli, G. Gigli, A. Laganà, G. Cannazza, Analysis of impurities of cannabidiol from hemp. Isolation, characterization and synthesis of cannabidibutol, the novel cannabidiol butyl analog, *J. Pharm. Biomed. Anal.* 175 (2019), 112752.
- [2] C. Citti, P. Linciano, F. Forni, M.A. Vandelli, G. Gigli, A. Laganà, G. Cannazza, Chemical and spectroscopic characterization data of 'cannabidibutol', a novel cannabidiol butyl analog, *Data Brief* 26 (2019), 104463.
- [3] PubMed, Search Results for "cannabigerol", 2021 <https://pubmed.ncbi.nlm.nih.gov/?term=cannabigerol&sort=date>.
- [4] E.P.M. de Meijer, K.M. Hammond, The inheritance of chemical phenotype in *Cannabis sativa* L. (II): cannabigerol predominant plants, *Euphytica* 145 (1) (2005) 189–198.
- [5] M. Zagorcen, A. Čerenak, S. Kreft, Cannabigerol and cannabichromene in *Cannabis sativa* L., *Acta Pharm.* 71 (3) (2021) 355–364.
- [6] P. Linciano, C. Citti, L. Luongo, C. Belardo, M.A. Vandelli, F. Forni, G. Gigli, A. Laganà, C.M. Montone, G. Cannazza, Isolation of a high affinity cannabinoid for human CB1 receptor from a medicinal cannabis variety: D9-tetrahydrocannabutol, the butyl homologue of D9-tetrahydrocannabinol, *J. Nat. Prod.* 83 (2020) 88–98.
- [7] Y. Shoyama, H. Hirano, M. Oda, T. Somehara, I. Nishioka, Cannabichromevarin and cannabigerovar, two new propyl homologues of cannabichromene and cannabigerol, *Chem. Pharm. Bull. (Tokyo)* 23 (8) (1975) 1894–1895.
- [8] A. Oláh, A. Markovics, J. Szabó-Papp, P.T. Szabó, C. Stott, C.C. Zouboulis, T. Bíró, Differential effectiveness of selected non-psychoactive phytocannabinoids on human sebocyte functions implicates their introduction in dry/seborrhoeic skin and acne treatment, *Exp. Dermatol.* 25 (9) (2016) 701–707.
- [9] L. De Petrocellis, A. Ligresti, A. Schiano Moriello, M. Iappelli, R. Verde, C.G. Stott, L. Cristino, P. Orlando, V. Di Marzo, Non-THC cannabinoids inhibit prostate carcinoma growth in vitro and in vivo: pro-apoptotic effects and underlying mechanisms, *Br. J. Pharmacol.* 168 (1) (2013) 79–102.
- [10] L. De Petrocellis, P. Orlando, A.S. Moriello, G. Aviello, C. Stott, A.A. Izzo, V. Di Marzo, Cannabinoid actions at TRPV channels: effects on TRPV3 and TRPV4 and their potential relevance to gastrointestinal inflammation, *Acta Physiol.* 204 (2) (2012) 255–266.
- [11] P. Berman, L. Sulimani, A. Gelfand, K. Amsalem, G.M. Lewitus, D. Meiri, Cannabinoidomics – an analytical approach to understand the effect of medical Cannabis treatment on the endocannabinoid metabolome, *Talanta* 219 (2020), 121336.
- [12] P. Berman, K. Futoran, G.M. Lewitus, D. Mukha, M. Benami, T. Shlomi, D. Meiri, A new ESI-LC/MS approach for comprehensive metabolic profiling of phytocannabinoids in Cannabis, *Sci. Rep.* 8 (1) (2018) 14280.
- [13] P. Linciano, C. Citti, F. Russo, F. Tolomeo, A. Laganà, A.L. Capriotti, L. Luongo, M. Iannotta, C. Belardo, S. Maione, F. Forni, M.A. Vandelli, G. Gigli, G. Cannazza, Identification of a new cannabidiol n-hexyl homolog in a medicinal cannabis variety with an antinociceptive activity in mice: cannabidihexol, *Sci. Rep.* 10 (1) (2020) 22019.
- [14] C. Citti, P. Linciano, F. Russo, L. Luongo, M. Iannotta, S. Maione, A. Laganà, A.L. Capriotti, F. Forni, M.A. Vandelli, G. Gigli, G. Cannazza, A novel phytocannabinoid isolated from Cannabis sativa L. with an in vivo cannabimimetic activity higher than 9-tetrahydrocannabinol: 9-tetrahydrocannabiphorol, *Sci. Rep.* 9 (1) (2019) 20335.
- [15] International Conference on Harmonization, Draft revised guidance on impurities in new drug substances, *Federal Register Q3A(R)* 65 (140) (2000) 45085, 2000.
- [16] S. Takashina, Y. Igarashi, M. Takahashi, Y. Kondo, K. Inoue, Screening method for the quality evaluation

of cannabidiols in water-based products using liquid chromatography tandem mass spectrometry, *Anal. Sci.* 36 (11) (2020) 1427–1430.

[17] A. Nemeskalová, K. Hájková, L. Mikulová, D. Sykora, M. Kuchar, Combination of UV and MS/MS detection for the LC analysis of cannabidiol-rich products, *Talanta* 219 (2020), 121250.

[18] C. Citti, F. Russo, S. Sgrò, A. Gallo, A. Zanutto, F. Forni, M.A. Vandelli, A. Laganà, C.M. Montone, G. Gigli, G. Cannazza, Pitfalls in the analysis of phytocannabinoids in cannabis inflorescence, *Anal. Bioanal. Chem.* 412 (17) (2020) 4009–4022.

[19] Y.H. Choi, A. Hazekamp, A.M.G. Peltenburg-Looman, M. Frédérix, C. Erkelens, A.W.M. Lefeber, R. Verpoorte, NMR assignments of the major cannabinoids and cannabiflavonoids isolated from flowers of *Cannabis sativa*, *Phytochem. Anal.* 15 (6) (2004) 345–354.

[20] C.M. Montone, A. Cerrato, B. Botta, G. Cannazza, A.L. Capriotti, C. Cavaliere, C.

Citti, F. Ghirga, S. Piovesana, A. Laganà, Improved identification of phytocannabinoids using a dedicated structure-based workflow, *Talanta* 219 (2020), 121310.

Supplementary data

HPLC-UV-HRMS Analysis of Cannabigerovarin and Cannabigerobutol, the two impurities of Cannabigerol extracted from hemp

Francesco Tolomeo^{a,1}, Fabiana Russo^{b,c,†}, Maria Angela Vandelli^b, Giuseppe Biagini^d, Aldo Laganà^{a,e}, Giuseppe Gigli^a, Giuseppe Cannazza^{a,b,*}, Cinzia Citti^{a,b}

Institute of Nanotechnology – CNR NANOTEC, Campus Ecotekne, Via Monteroni, 73100 – Lecce, Italy

^b Department of Life Sciences, University of Modena and Reggio Emilia, Via Campi 103, 41125 – Modena, Italy

^c Clinical and Experimental Medicine PhD Program, University of Modena and Reggio Emilia, 41125 – Modena, Italy

^d Department of Biomedical, Metabolic and Neural Sciences, University of Modena and Reggio Emilia, 41125 – Modena, Italy

^e Department of Chemistry, Sapienza University of Rome, Piazzale Aldo Moro 5, 00185 – Rome, Italy

Table of content

¹H-NMR, ¹³C-NMR, COSY, HSQC, HMBC for synthetic CBGB	---SI-2
¹H-NMR, ¹³C-NMR, COSY, HSQC, HMBC for synthetic CBGV	---SI-9
FT-IR spectra of standard CBG, synthetic CBGV and synthetic CBGB	---SI-17
Comparison of the UV spectra of CBG impurities and standards	---SI-20
HPLC-UV method validation	---SI-21

¹ These authors contributed equally to the work.

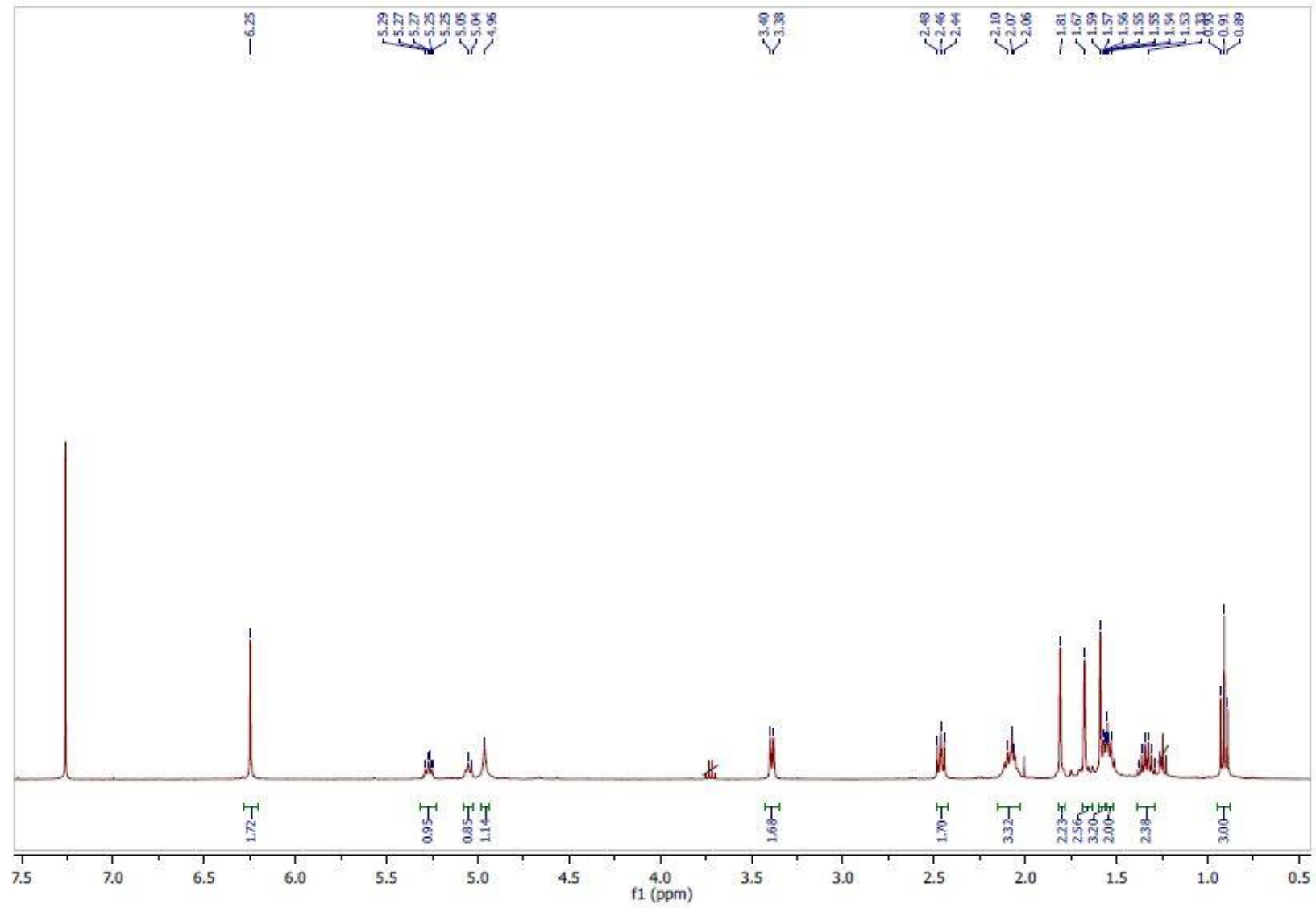
* Corresponding author: Giuseppe Cannazza, Ph.D., Email: giuseppe.cannazza@unimore.it; Tel.: +39 059 2055013.; Fax: +39 059 2055750.

¹H-NMR, ¹³C-NMR, COSY, HSQC, HMBC and IR for synthetic (*E*)-5-butyl-2-(3,7-dimethylocta-2,6-dien-1-yl)benzene-1,3-diol (CBGB)

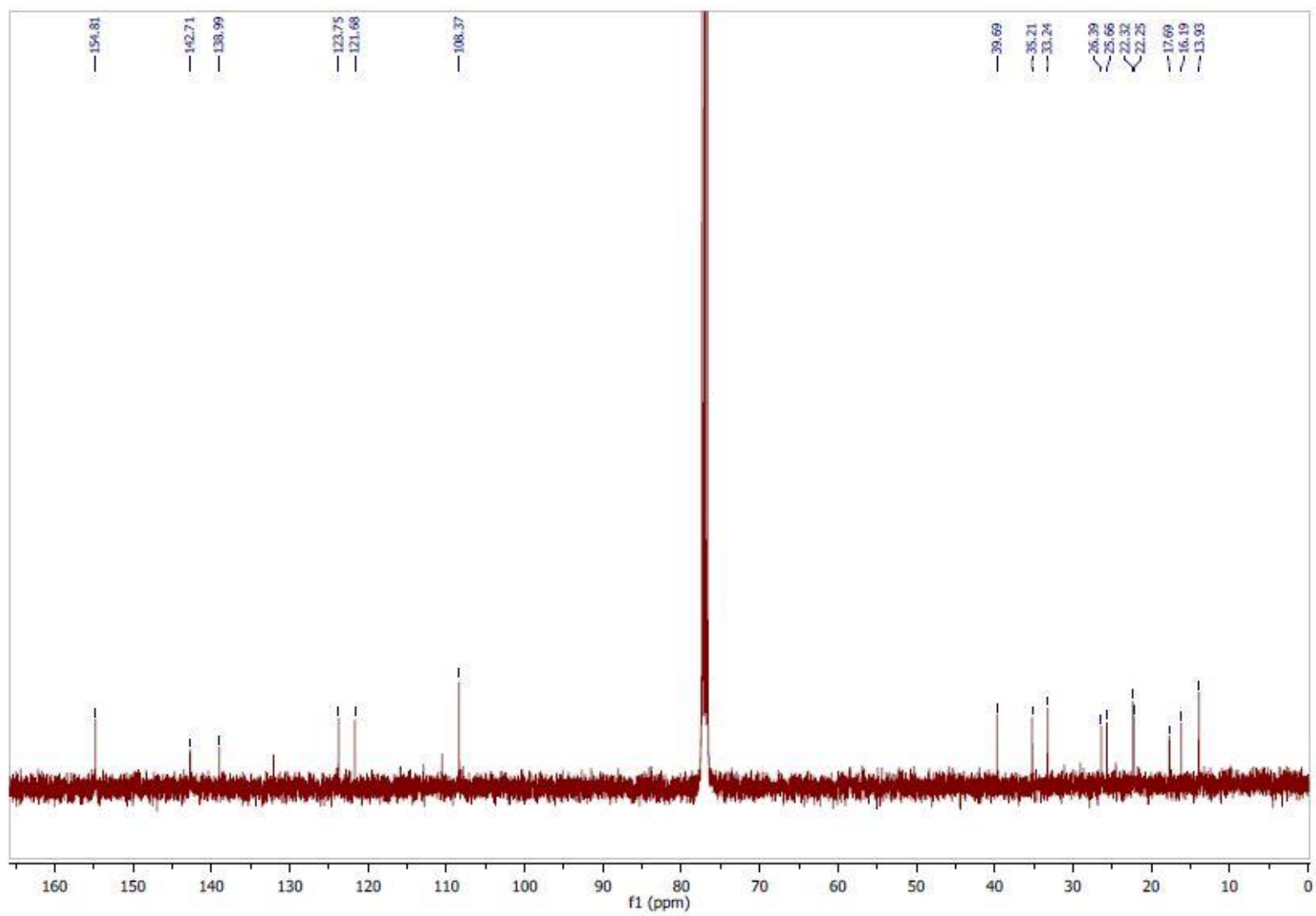
The reaction was performed as reported in general procedure. Reagents: 5-butylbenzene-1,3-diol (100 mg, 0.6 mmol); geraniol (105 μ L, 0.6 mmol); *p*TSA (9 mg); Anhydrous toluene (600 μ L). Chromatography: crude/silica gel ratio 1:100, eluent: CE/DCM 6:4 (v/v). Yellow oil (25% yield).

¹H NMR (400 MHz, CDCl₃) δ 6.25 (s, 2H), 5.29-5.25 (m, 1H), 5.06-5.04 (m, 1H), 4.96 (bs, 2H), 3.39 (d, *J* = 8 Hz, 2H), 2.46 (t, *J* = 8 Hz, 2H), 2.10-2.06 (m, 4H), 1.81 (s, 3H), 1.67 (s, 3H), 1.59 (s, 3H), 1.57-1.53 (m, 2H), 1.34 (sxt, *J* = 8 Hz, 2H), 0.91 (t, *J* = 8 Hz, 3H).

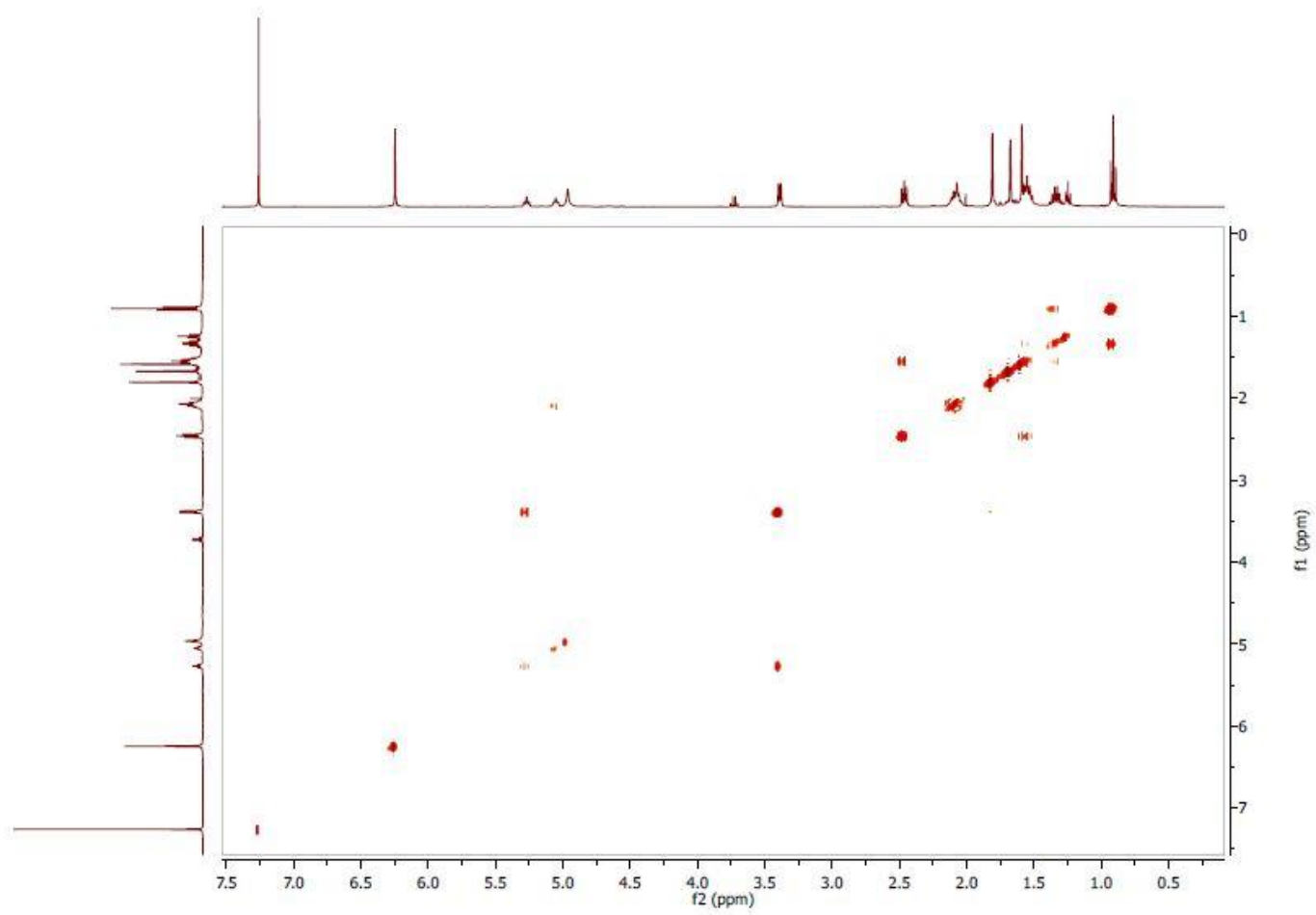
¹³C NMR (100MHz, CDCl₃) δ 154.81, 142.71, 138.99, 132.08, 123.75, 121.68, 110.58, 108.37, 39.69, 35.21, 33.24, 26.39, 25.66, 22.32, 22.25, 17.69, 16.19, 13.93.



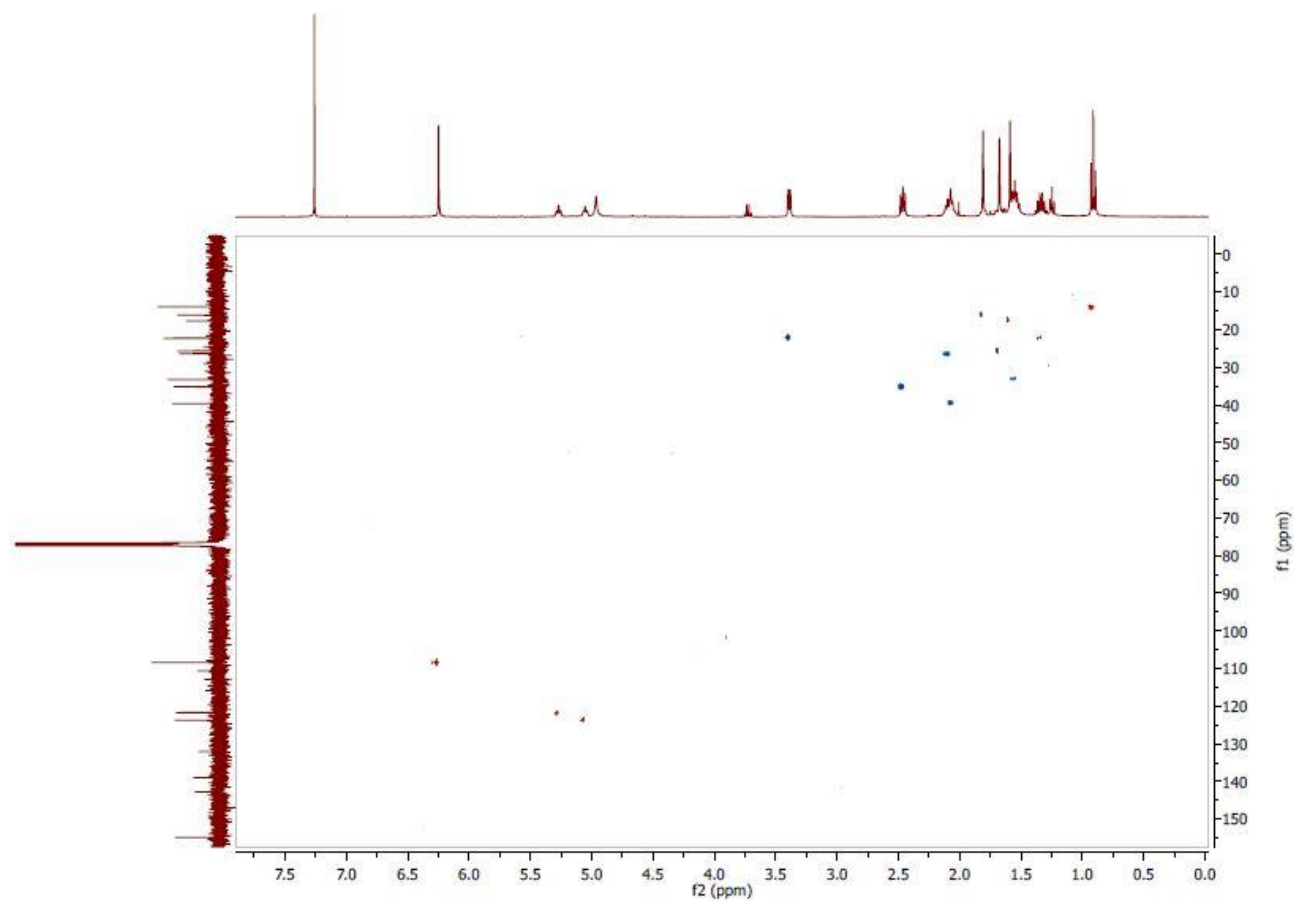
S4



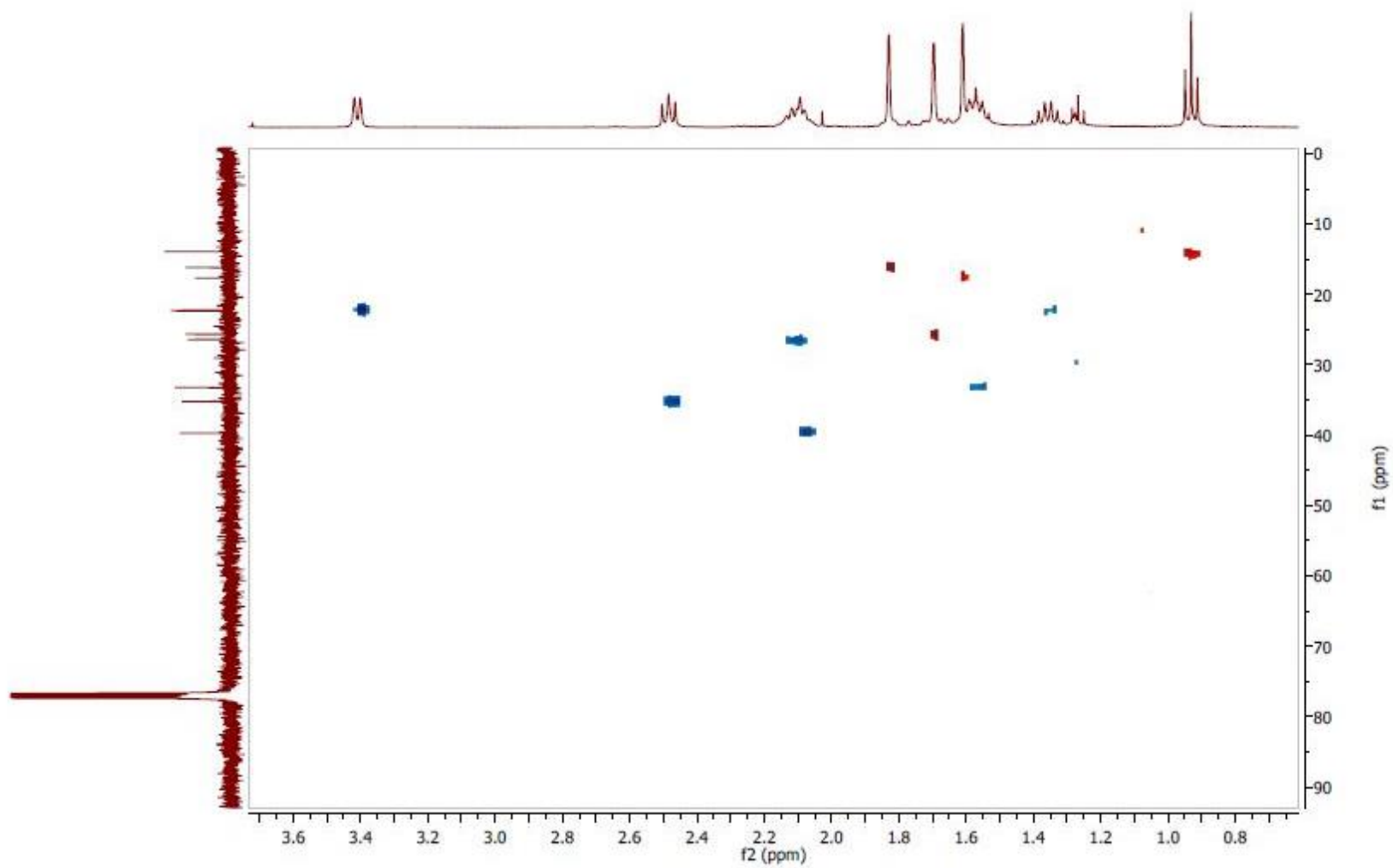
S5

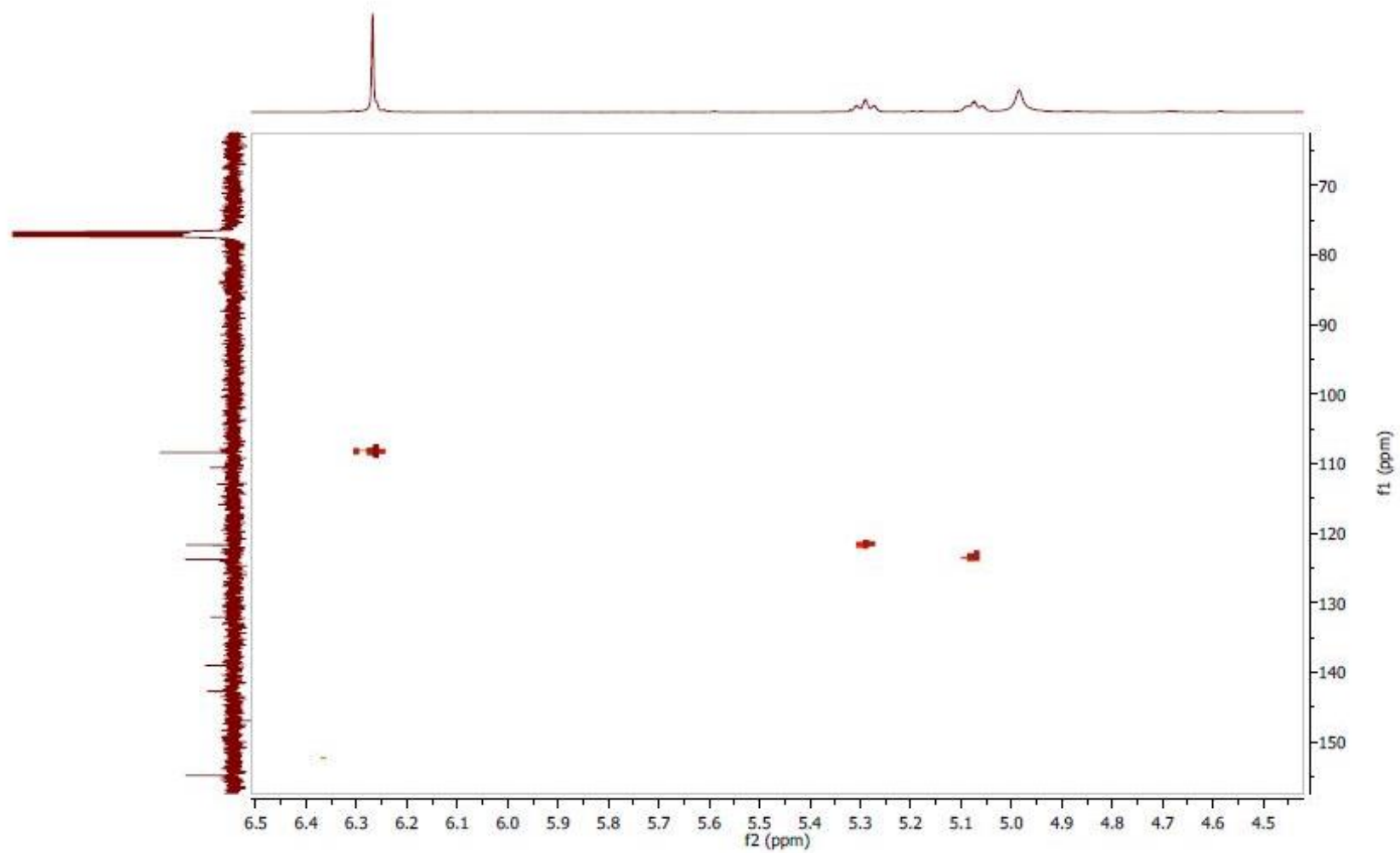


S6



S7



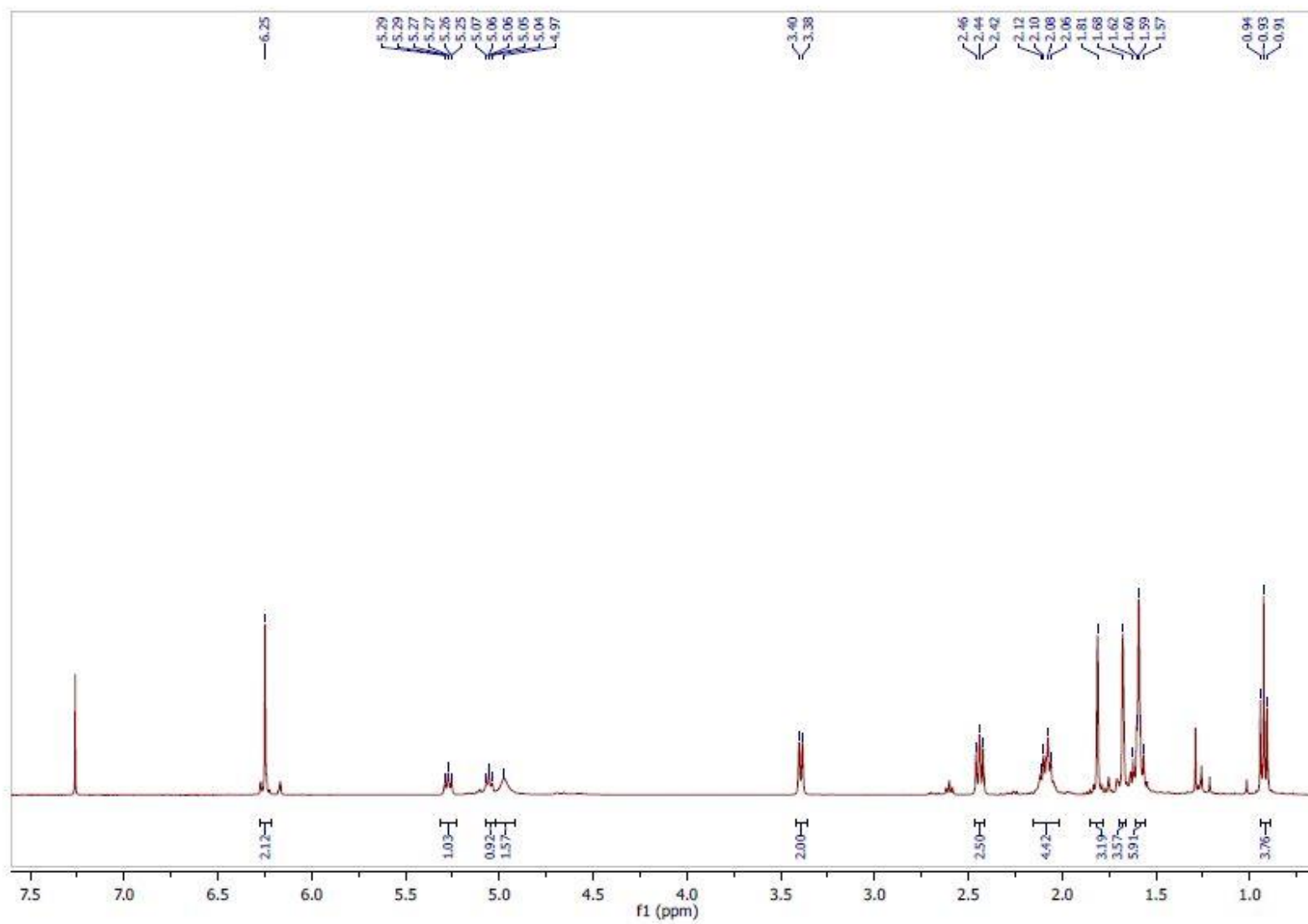


¹H NMR, ¹³C NMR, COSY, HSQC and HMBC for synthetic (*E*)-2-(3,7-dimethylocta-2,6-dien-1-yl)-5-propylbenzene-1,3-diol (CBGV)

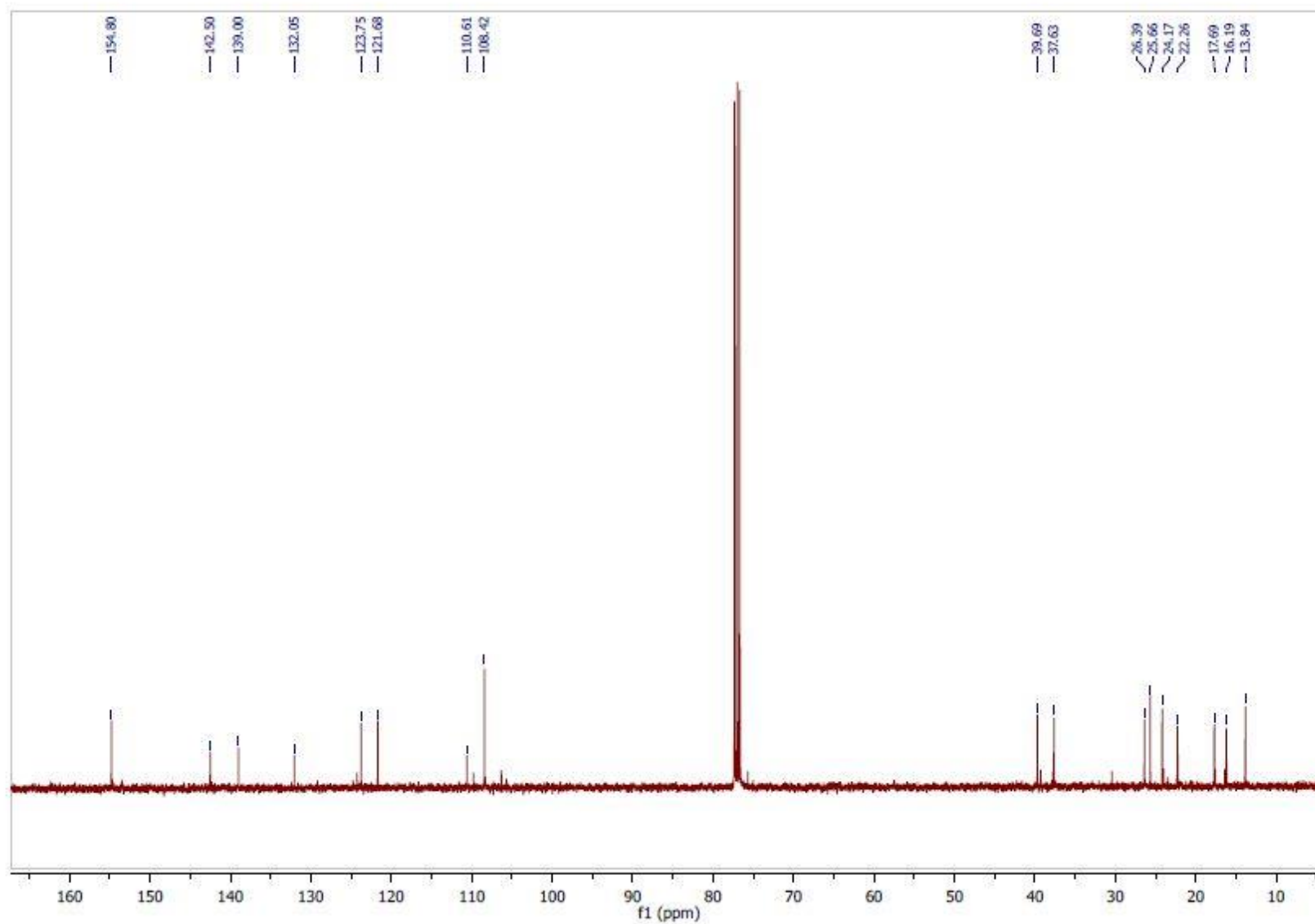
The reaction was performed as reported in general procedure. Reagents: 5-propylbenzene-1,3-diol (250mg, 1.6 mmol); geraniol (281 μ L, 1.6 mmol); *p*TSA (24 mg); Anhydrous toluene (1.6 mL). Chromatography: crude/silica gel ratio 1:100, eluent: CE/DCM 6:4 (v/v). Yellow oil (22% yield).

¹H NMR (400 MHz, CDCl₃) δ 6.25 (s, 2H), 5.29-5.25 (m, 1H), 5.07-5.04 (m, 1H), 4.97 (bs, 2H), 3.39 (d, *J* = 8 Hz, 2H), 2.44 (t, *J* = 8 Hz, 2H), 2.12-2.06 (m, 4H), 1.81 (s, 3H), 1.68 (s, 3H), 1.62-1.57 (m, 5H), 0.93 (t, *J* = 8 Hz, 3H).

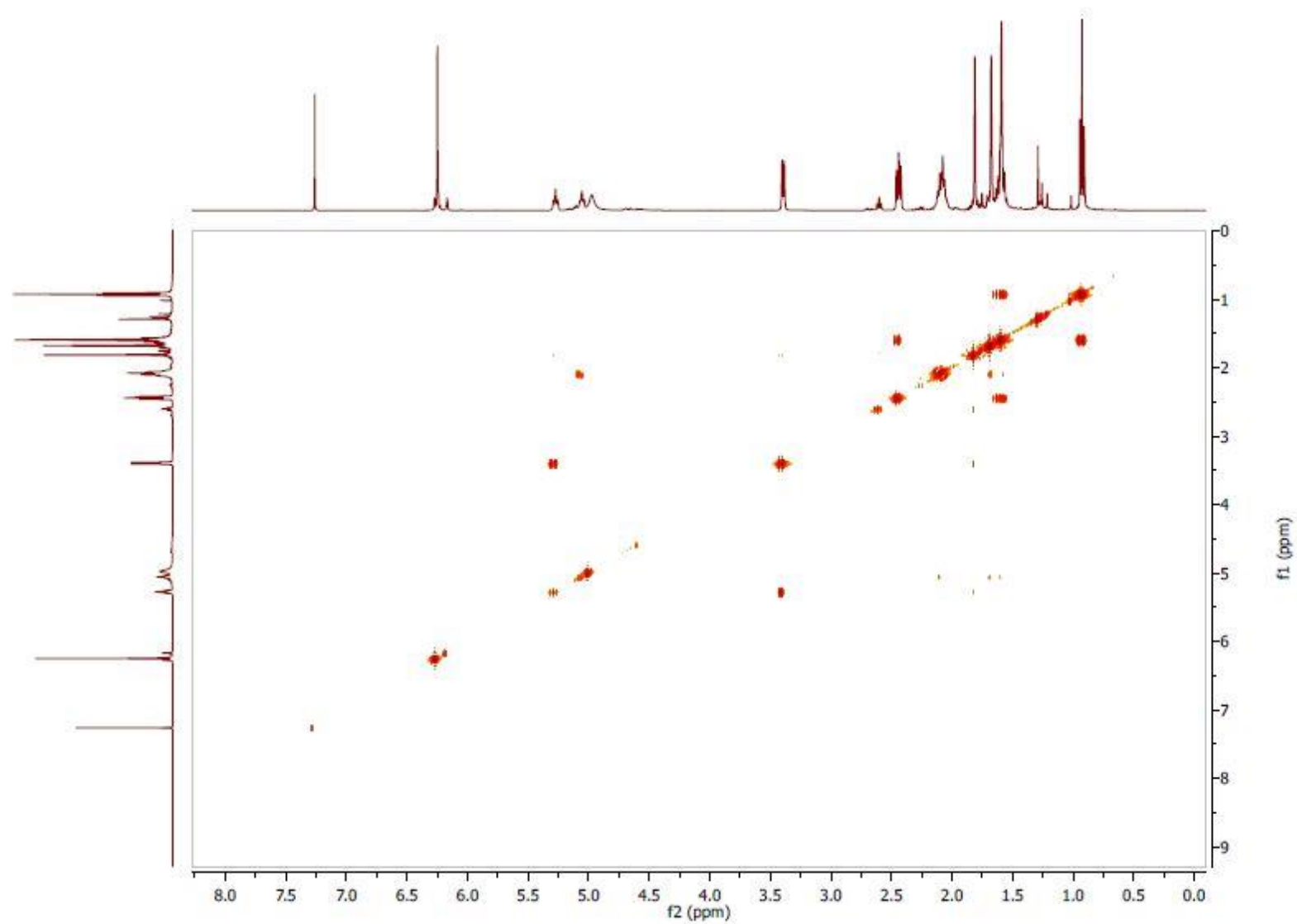
¹³C NMR (100 MHz, CDCl₃) δ 154.80, 142.50, 139.00, 132.05, 123.75, 121.68, 110.61, 108.42, 39.69, 37.63, 26.39, 25.66, 24.17, 22.26, 17.69, 16.19, 13.84.



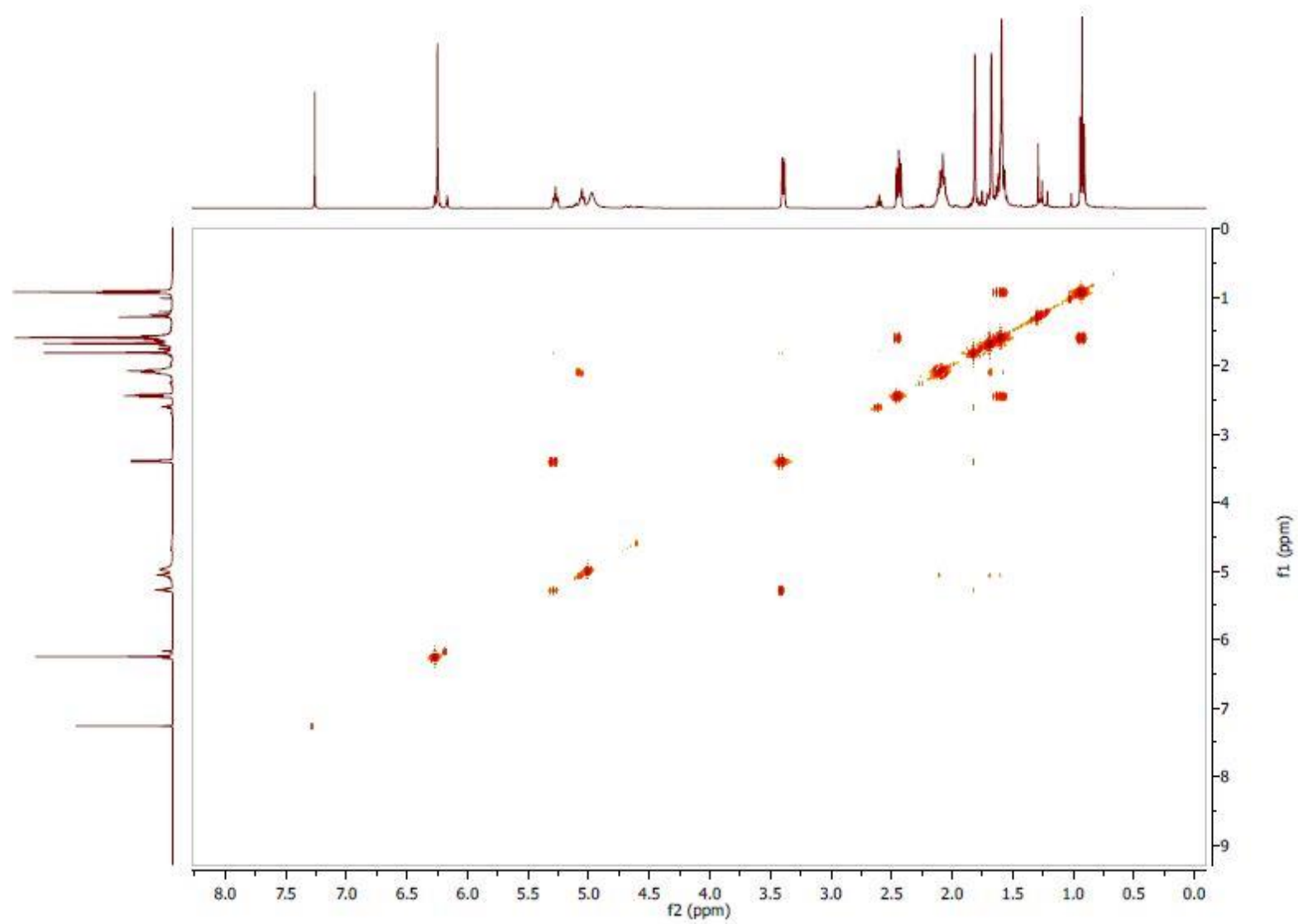
S11



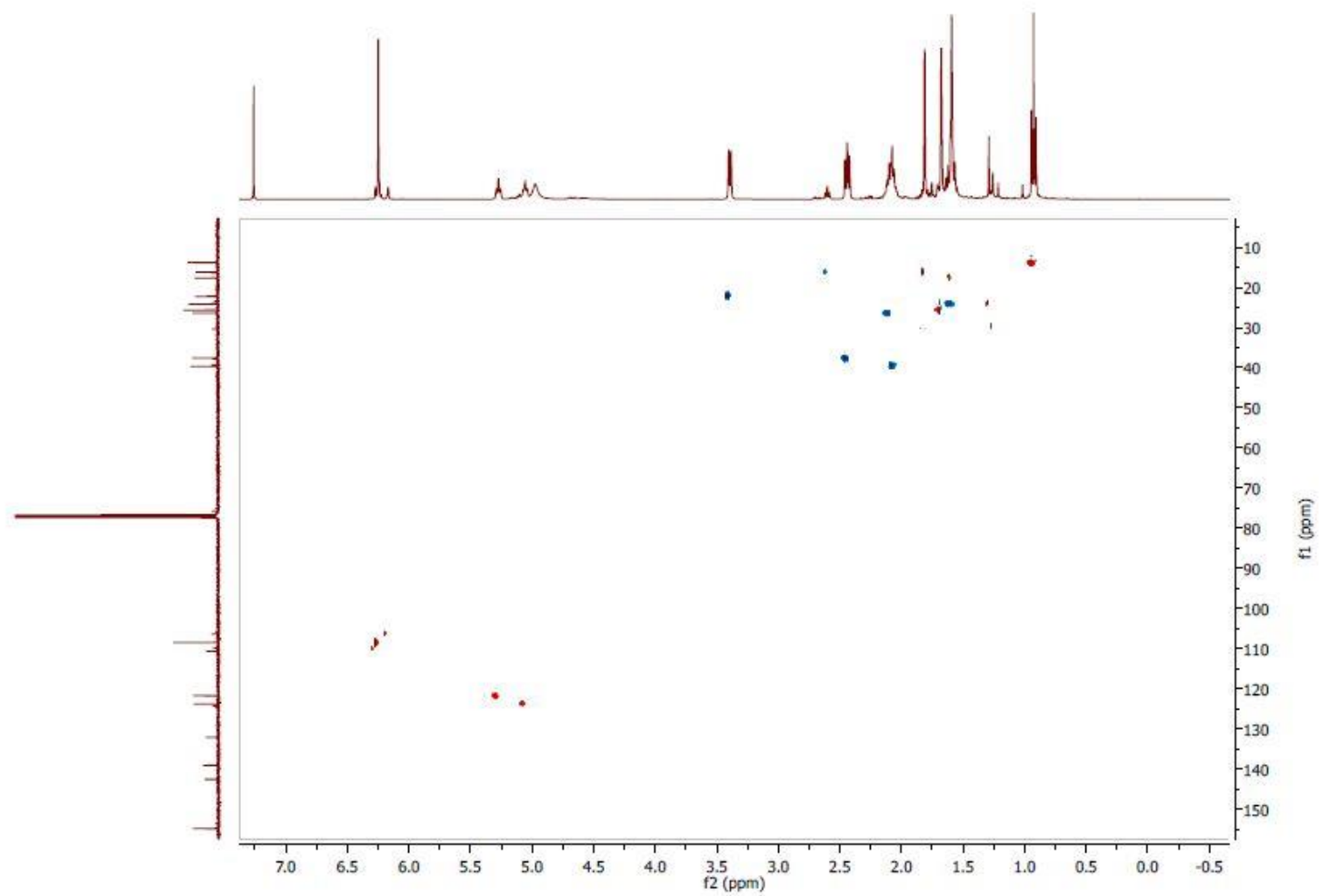
S12



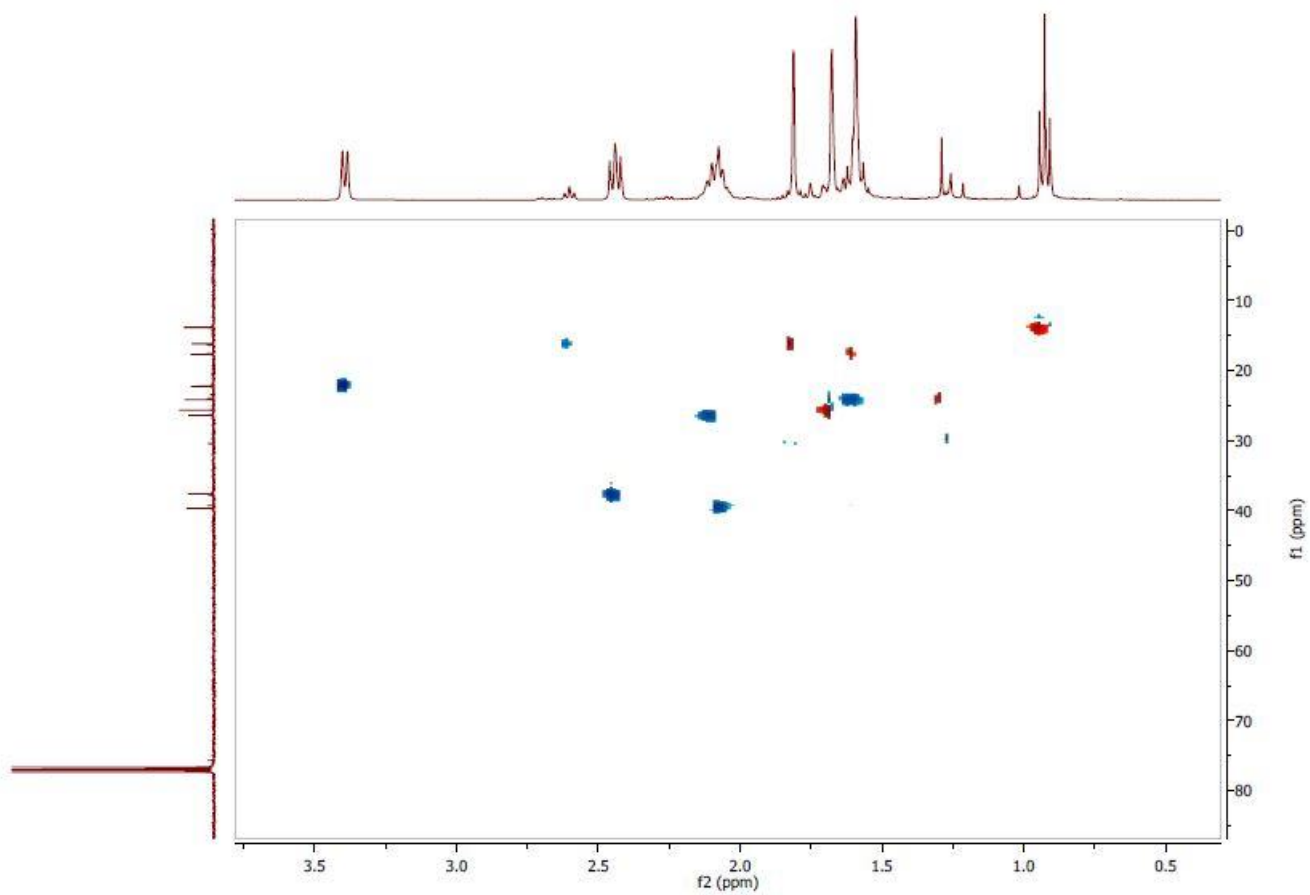
S13



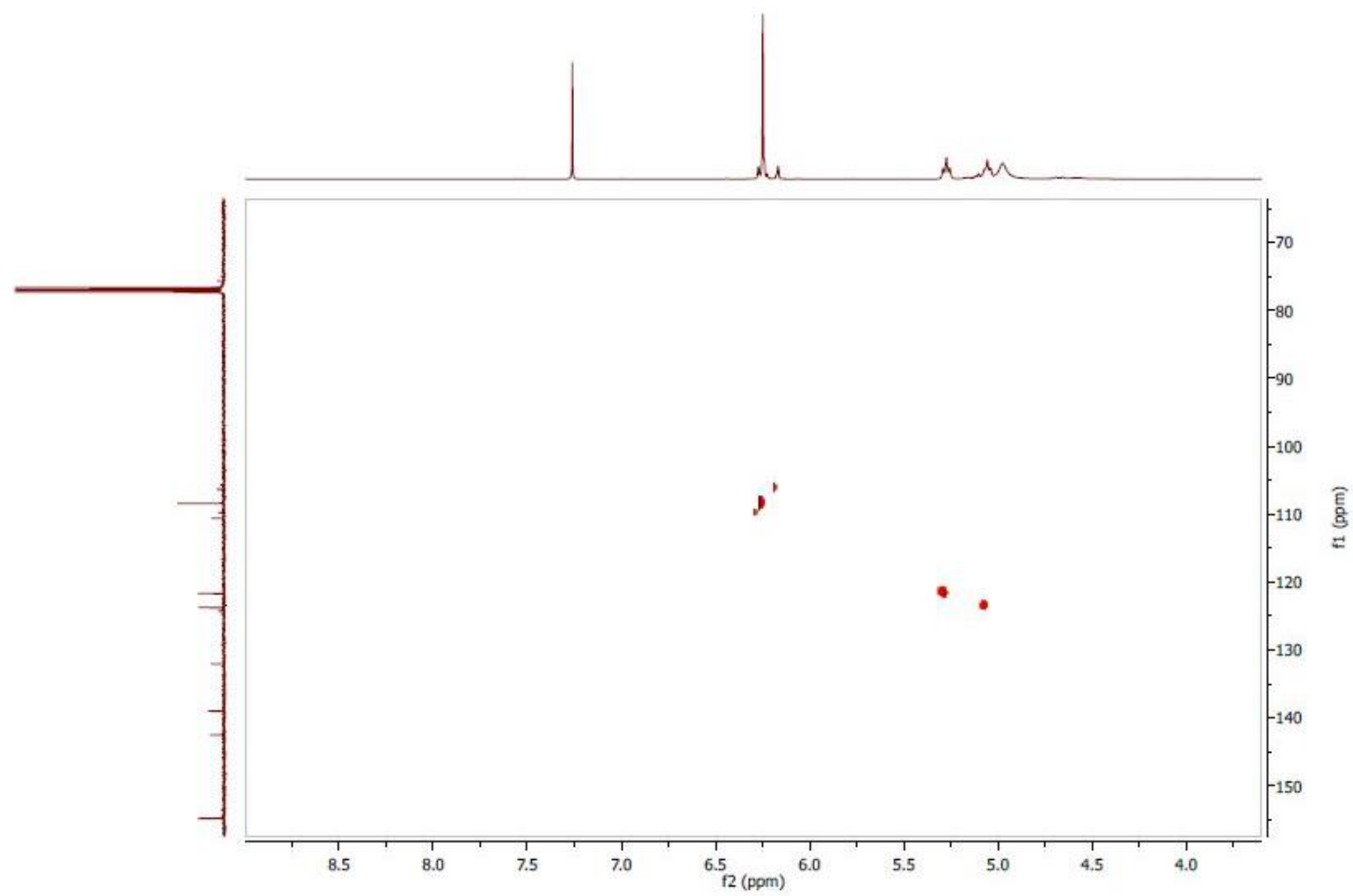
S14



S15



S16



FT-IR spectra of standard CBG, synthetic CBGV and synthetic CBGB

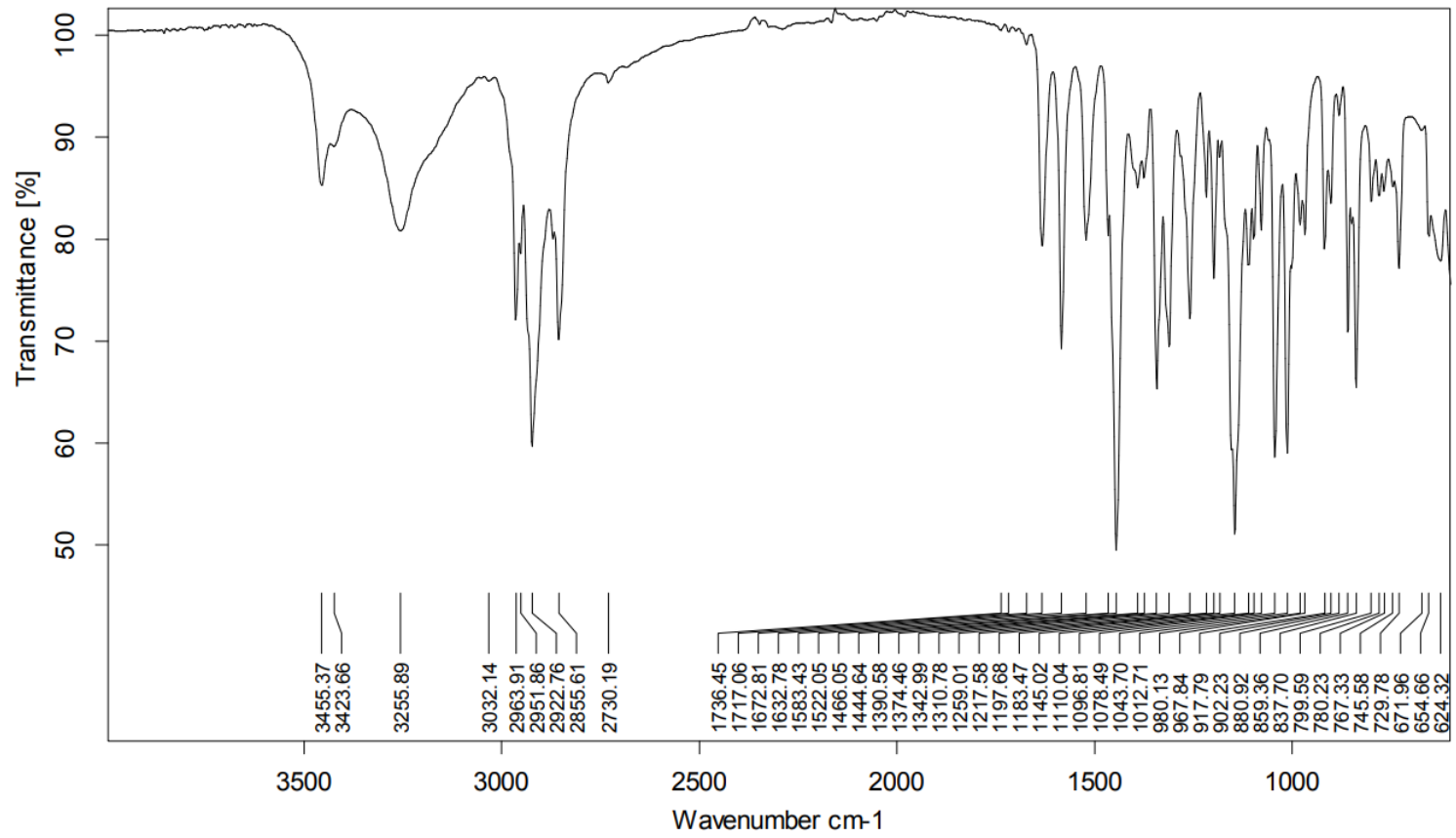


Figure S 1. FT-IR spectrum of standard CBG.

S18

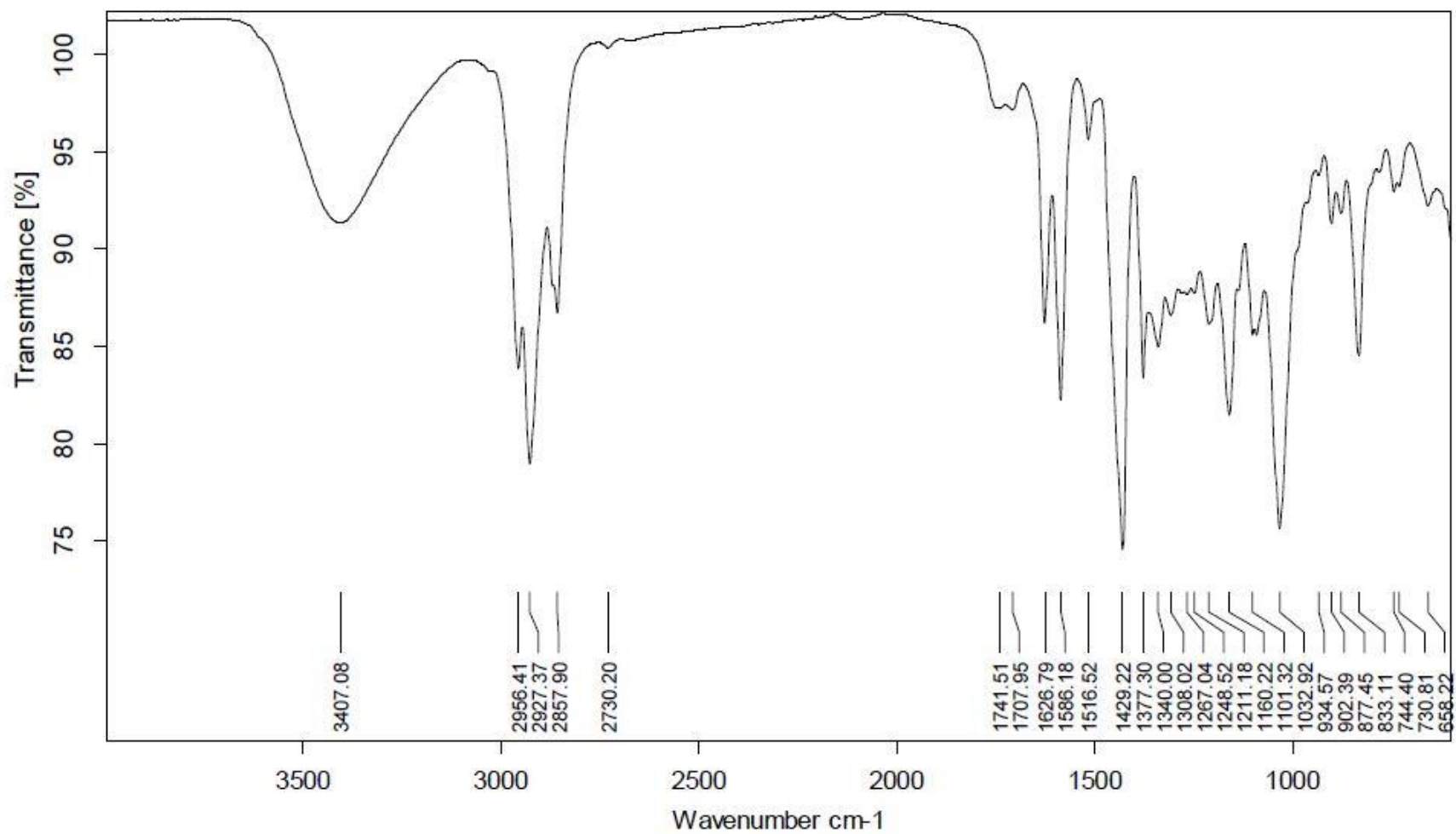


Figure S 2. FT-IR spectrum of CBGV.

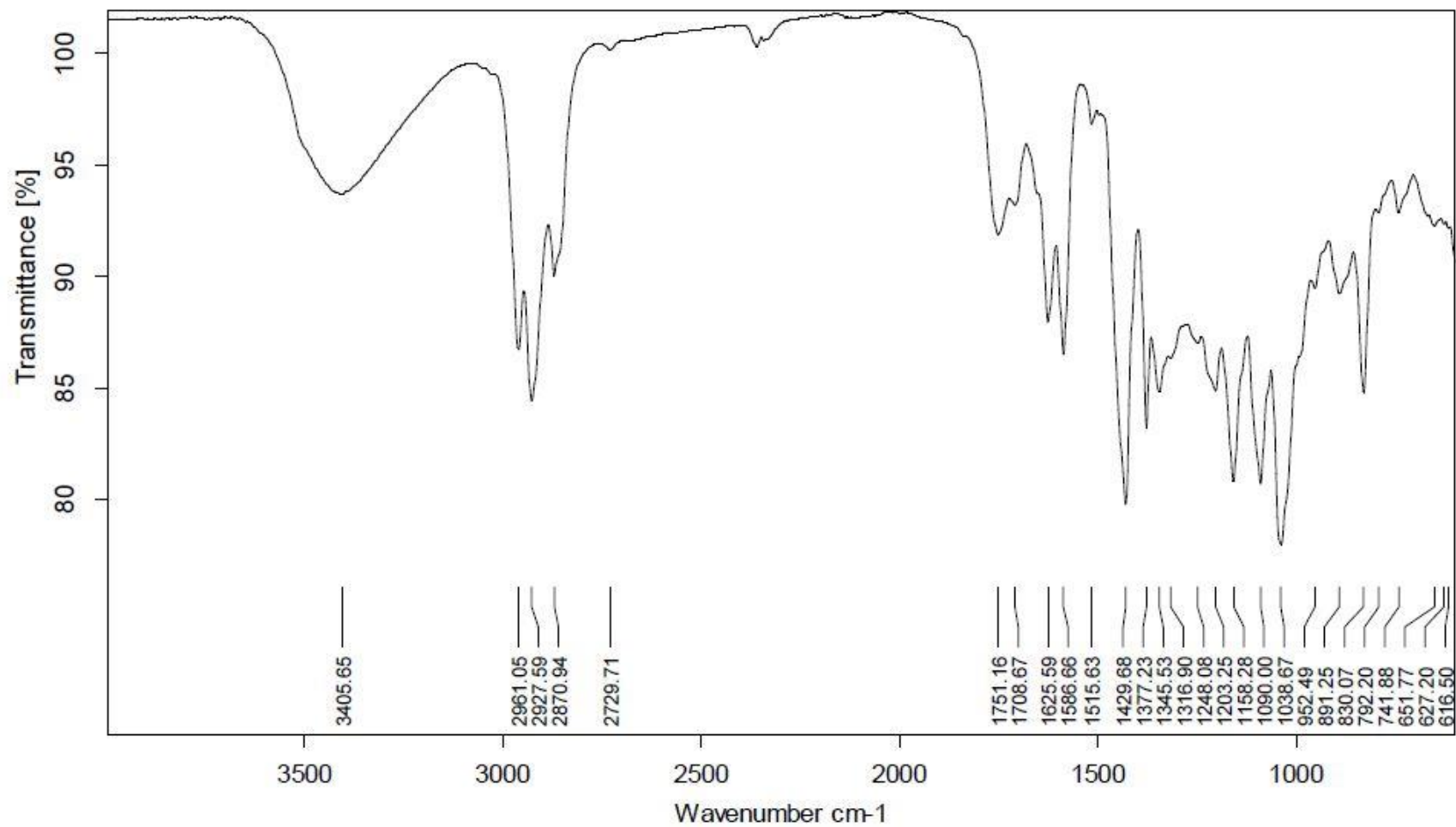


Figure S 3. FT-IR spectrum of CBGB.

UV spectra of synthetic standards and impurities

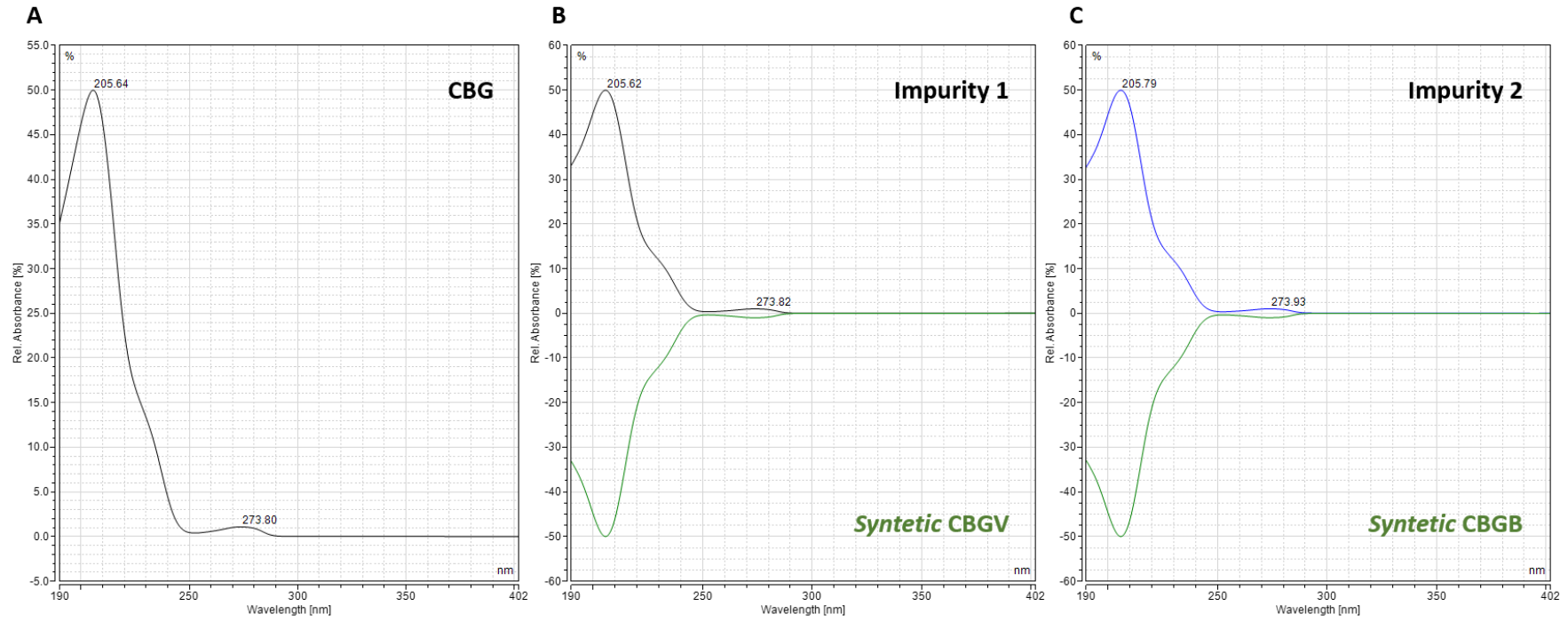


Figure S 4. A) UV spectra of CBG; B) Stacked UV trace of impurity 1 (black) and synthetic CBGV (green); C) Stacked UV trace of impurity 2 (blue) and synthetic CBGB (green).

HPLC-UV method validation

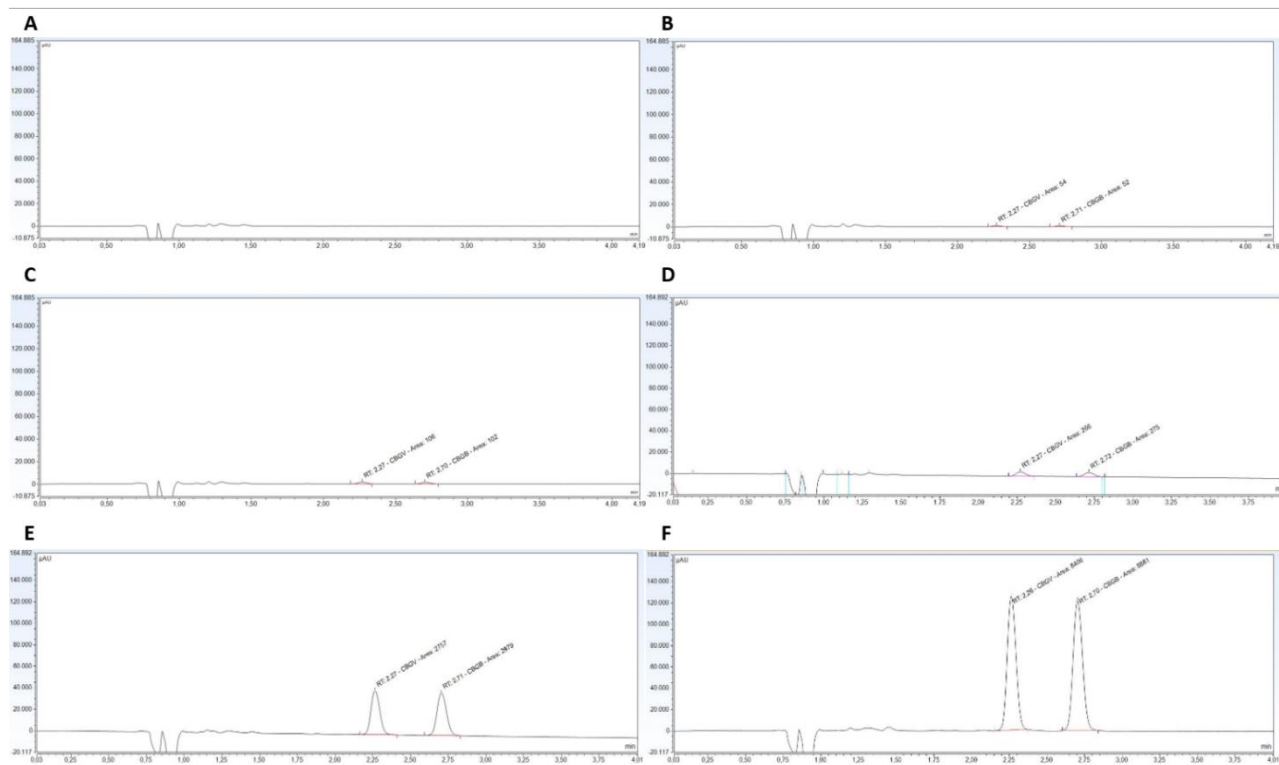


Table S 1. Linearity parameters for CBGV and CBGB (slope, intercept and R²weighted). Values are expressed as mean±standard error (n=3).

Compound	Slope	Intercept	R ² (weighted)
CBGV	1.38828±0.02410	0.00304±0.00253	0.9997
CBGB	1.23956±0.00436	0.00440±0.00353	0.9998

Table S 2. Intra-day and inter-day accuracy and precision of CBGV and CBGB at four concentration levels (LLOQ, LCQ, MQC and HQC). Values are expressed as mean of three analyses for intra-day accuracy and precision and 15 analyses for inter-day accuracy and precision (n=3 for 5 consecutive days).

		CBGV		CBGB	
		Accuracy	Precision (CV)	Accuracy	Precision (CV)
Intra-day (n = 3)	LLOQ	101.7	4.46	114.3	5.41
	LQC	106.7	1.78	110.9	2.14
	MQC	103.0	0.13	99.56	0.07
	HQC	103.5	0.11	100.8	0.07
Inter-day (n = 15)	LLOQ	90.49	13.7	87.76	13.4
	LQC	91.82	8.74	92.21	13.1
	MQC	104.3	2.79	106.0	6.66
	HQC	102.2	0.84	100.0	0.64

Table S 3. Stability data (bench-top and under refrigeration) for CBGV and CBGB calculated as mean of three analyses compared to nominal concentration of freshly prepared calibration curves.

Stability	QC level	CBGV	CBGB
Bench-top (25 °C, 24 h)	LLOQ	100.7	99.58
	LQC	98.11	101.5
	MQC	98.00	102.4
	HQC	100.1	109.4
Refrigeration (2-8 °C, 24 h)	LLOQ	100.6	110.1
	LQC	98.74	100.1
	MQC	108.4	111.4
	HQC	100.1	100.3

IDENTIFICATION OF A NEW CANNABIDIOL N-HEXYL HOMOLOG IN A MEDICINAL CANNABIS VARIETY WITH ANTINOCICEPTIVE ACTIVITY IN MICE: CANNABIDIHEXOL

**Pasquale Linciano^{1,6}, Cinzia Citti^{1,2,3,6}, Fabiana Russo¹, Francesco Tolomeo²,
Aldo Laganà^{3,4}, Anna Laura Capriotti⁴, Livio Luongo⁵, Monica Iannotta⁵, Carmela
Belardo⁵, Sabatino Maione⁵, Flavio Forni¹, Maria Angela Vandelli¹, Giuseppe Gigli³ &
Giuseppe Cannazza***

1 Department of Life Sciences, University of Modena and Reggio Emilia, Via Campi 103, 41125 Modena, Italy.

2 Meditekology (CNR Spin-Off Company), Via Arnesano, 73100 Lecce, Italy.

3 CNR NANOTEC, Istituto di Nanotecnologia, Via Monteroni, 73100 Lecce, Italy.

4 Department of Chemistry, Sapienza University of Rome, Piazzale Aldo Moro 5, 00185 Rome, Italy.

5 Division of Pharmacology, Università degli studi della Campania "L. Vanvitelli", Via Costantinopoli, 16, 80138 Naples, Italy.

6 These authors contributed equally: Pasquale Linciano and Cinzia Citti.

Published in: *Scientific Report* 10, 22019 (2020).
doi.org/10.1038/s41598-020-79042-2

*email: giuseppe.cannazza@unimore.it

ABSTRACT

The two most important and studied phytocannabinoids present in *Cannabis sativa* L. are undoubtedly cannabidiol (CBD), a non-psychotropic compound, but with other pharmacological properties, and Δ^9 -tetrahydrocannabinol (Δ^9 -THC), which instead possesses psychotropic activity and is responsible for the recreative use of hemp. Recently, the homolog series of both CBDs and THCs has been expanded by the isolation in a medicinal cannabis variety of four new phytocannabinoids possessing on the resorcinyl moiety a butyl- (in CBDB and Δ^9 -THCB) and a heptyl- (in CBDP and Δ^9 -THCP) aliphatic chain. In this work we report a new series of phytocannabinoids that fills the gap between the pentyl and heptyl homologs of CBD and Δ^9 -THC, bearing a n-hexyl side chain on the resorcinyl moiety that we named cannabidihexol (CBDH) and Δ^9 -tetrahydrocannabihexol (Δ^9 -THCH), respectively. However, some cannabinoids with the same molecular formula and molecular weight of CBDH and Δ^9 -THCH have been already identified and reported as monomethyl ether derivatives of the canonical phytocannabinoids, namely cannabigerol monomethyl ether (CBGM), cannabidiol monomethyl ether (CBDM) and Δ^9 -tetrahydrocannabinol monomethyl ether (Δ^9 -THCM). The unambiguously identification in cannabis extract of the n-hexyl homologues of CBD and Δ^9 -THC different from the corresponding methylated isomers (CBDM, CBGM and Δ^9 -THCM) was achieved by comparison of the retention time, molecular ion, and fragmentation spectra with those of the authentic standards obtained via stereoselective synthesis, and a semi-quantification of these cannabinoids in the FM2 medical cannabis variety was provided. Conversely, no trace of Δ^9 -THCM was detected. Moreover, CBDH was isolated by semipreparative HPLC and its identity was confirmed by comparison with the spectroscopic data of the corresponding synthetic standard. Thus, the proper recognition of CBDH, CBDM and Δ^9 -THCH closes the loop and might serve in the future for researchers to distinguish between these phytocannabinoids isomers that show a very similar analytical behaviour. Lastly, CBDH was assessed for biological tests *in vivo* showing interesting analgesic activity at low doses in mice.

Introduction

Cannabis research has made great progresses in the latest years in both clinical and academic field. For example, new cannabis-based drugs, like Epidiolex, have been placed on the market for the treatment of severe forms of infant epilepsy not responding to conventional therapies¹. In the academic research, new insights on cannabis chemistry have been disclosed thanks to the high-

performing technological platforms for the identification of new compounds²⁻⁶. Although there is still much to do in the cannabis chemistry research, almost 150 phytocannabinoids can be count on the most updated inventory⁷. Our most recent works have disclosed the existence of new phytocannabinoids series besides those of the orcinoids, varinoids and olivetoids, belonging to the cannabidiol (CBD) and Δ^9 -tetrahydrocannabinol (Δ^9 -THC) type cannabinoids^{4,8}. The new series of phytocannabinoids share the terpenophenolic core of CBD and Δ^9 -THC and differ for the length of the linear alkyl side chain; specifically, cannabidibutol (CBDB), and Δ^9 -tetrahydrocannabutol (Δ^9 -THCB) have a n-butyl side chain⁸, whereas cannabidiphorol (CBDP) and Δ^9 -tetrahydrocannabiphorol (Δ^9 -THCP) have a n-heptyl side chain⁴. The discovery of new phytocannabinoids, which were both directly isolated from the plant and synthetically prepared in the lab, has opened new gaps on their still unexplored biological activity, making us wondering about their pharmacological effects on humans.

To further complicate the already intricate scenario, we report a new series of phytocannabinoids that fills the gap between the pentyl and heptyl homologs of CBD and Δ^9 -THC, bearing a n-hexyl side chain on the resorcinylic moiety. At the best of our knowledge and according to the literature, no case of hexyl derivatives of cannabinoid has been reported so far. Conversely, cannabinoids with the same molecular formula and molecular weight have been classified as monomethyl ether derivatives of canonical phytocannabinoids, namely cannabigerol monomethyl ether (CBGM), cannabidiol monomethyl ether (CBDM) and Δ^9 -tetrahydrocannabinol monomethyl ether (Δ^9 -THCM)⁹. Whilst CBGM and CBDM have been already isolated and characterized^{10,11}, Δ^9 -THCM has been detected in cannabis smoke¹² and some authors reported that it is present in the plant, but they were not able to isolate it due to chromatographic issues¹³. Our findings on the presence of the hexyl homologs of CBD and Δ^9 -THC, which we named cannabidihexol (CBDH) and Δ^9 -tetrahydrocannabihexol (Δ^9 -THCH) respectively, were supported by the stereoselective synthesis of the corresponding pure standards that are found in the plant prior to decarboxylation.

Results

Identification of CBD and Δ^9 -THC hexyl homologs by UHPLC-HESI-Orbitrap. In the attempt to provide a complete characterization of the FM2 cannabis variety, we noticed the presence of two major peaks at 18.13 and 20.21, and a minor one at 21.46 min, corresponding to the molecular formula $C_{23}H_{32}O_4$, suggesting the presence of the carboxylic group. The analysis of the fragmentation spectra in negative ionization mode confirmed this hypothesis but showed three different fragmentation patterns (Fig. 1A). The two major peaks A and B presented very similar spectra differing only for the

relative intensity of the fragments, whereas the minor peak C showed very poor fragmentation. Peak A at 18.13 min could be associated to a CBDA-like molecule (Fig. 1B), while peak B at 20.21 min had lower intensity for the fragment corresponding to $[M-H_2O]^-$ at m/z 353 and presented a new fragment at m/z 178, not found in the other spectra (Fig. 1C). Peak C at 21.46 min showed a THCA-like fragmentation characterized by the very low intensity of the fragment $[M-H_2O]^-$ and the absence of other major fragments besides the one corresponding to $[M-CO_2]^-$ at m/z 327 (Fig. 1D).

In order to identify these compounds, but being unable to isolate acidic species, we moved to work on the decarboxylated forms of such cannabinoids. Therefore, the ethanolic extract of FM2 was heated and the new mixture was analysed employing the same conditions by UHPLC-HESI-Orbitrap. As expected, in place of the previously detected peaks, three new peaks appeared at different retention times, 18.62, 20.62, and 20.77 min, with the molecular formula $C_{22}H_{32}O_2$ corresponding exactly to the loss of a CO_2 molecule. Figure 1E shows a second chromatogram with the decarboxylated compounds Ad, Bd, and Cd. Surprisingly, peaks Bd and Cd had inverted elution order and peaks Ad and Cd presented superimposable fragmentation spectra in positive ionization mode with the same pattern as CBD and THC. Moreover, peaks Ad and Bd were very similar and differed for the relative intensity of the molecular ion $[M+H]^+$ at m/z 329 and the base peak at m/z 207. We concluded that peak A and B could be acidic CBD-type cannabinoids, whereas peak C could be an acidic THC-type cannabinoid (Fig. 1F–H).

According to the literature, cannabinoids with such molecular formula and molecular ions are reported as monomethyl ethers of CBDA and THCA, named cannabidiolic acid monomethyl ether (CBDMA) and tetrahydrocannabinolic acid monomethyl ether (THCMA). Similarly, cannabinoids with molecular formula $C_{22}H_{32}O_2$ could be the corresponding decarboxylated derivatives, the already known cannabidiol monomethyl ether (CBDM) and the putative tetrahydrocannabinol monomethyl ether (THCM). However, we found three peaks corresponding to the same formula but different MS2 spectra. By a comparison with other CBD and THC homologs present in our spectral library, such as cannabidivarin (CBDV), cannabidibutol (CBDB), cannabidiphorol (CBDP), Δ^9 -tetrahydrocannabivarin (Δ^9 -THCV), Δ^9 -tetrahydrocannabutol (Δ^9 -THCB), and Δ^9 -tetrahydrocannabiphorol (Δ^9 -THCP), we were able to putatively identify two new homologs of CBD and THC with a hexyl side chain. As shown in Fig. 2, the new compounds differ exactly by a $-CH_2$ unit (14 amu) from the corresponding pentyl (CBD and Δ^9 -THC) and the recently identified heptyl homologs (CBDP and THCP), not only for the molecular ion $[M+H]^+$ but also for all fragments. For both CBD (Fig. 2A) and THC (Fig. 2B) homologs, it was evident that the molecular ion $[M+H]^+$ and

the base peak inverted their relative intensity as the length of the side chain increased from the propyl to the heptyl homologs, most likely due to the increasing stability of the molecular ion.

In order to confirm the identity of these two new cannabinoids and unambiguously identify peak B_d, a stereoselective synthesis of the putatively identified cannabinoids, which for sake of simplicity and consistency were called cannabidihexol (CBDH) and Δ^9 -tetrahydrocannabihexol (Δ^9 -THCH), and the monomethyl ether derivatives of CBD and Δ^9 -THC (CBDM and Δ^9 -THCM) was performed.

Identification of CBGM by UHPLC-HESI-Orbitrap. Given the results obtained for CBD and Δ^9 -THC, we hypothesized the presence in the FM2 variety of the hexyl homolog of CBG, which has a molecular formula C₂₂H₃₄O₂ and [M+H]⁺ ion at m/z 331.2632. Only one peak resulted from the specific ion search, thus instilling the doubt about its identity as hexyl or methyl ether derivative. The fragmentation spectrum of its acidic precursor in the FM2 native extract showed a pattern different from that of cannabigerolic acid (CBGA), for which the analytical standard was available, and from those reported in the literature for the other series of CBG like cannabigerovarin (CBGV)¹⁴ and cannabigerobutol (CBGB)⁹. The match of retention time (20.98 min) and fragmentation spectrum with those of synthetic CBGM and the comparison with spectral data reported in the literature for the same cannabinoid confirmed that the additional methyl group was attached to the oxygen of the resorcinyloxy moiety and was not part of the alkyl side chain.

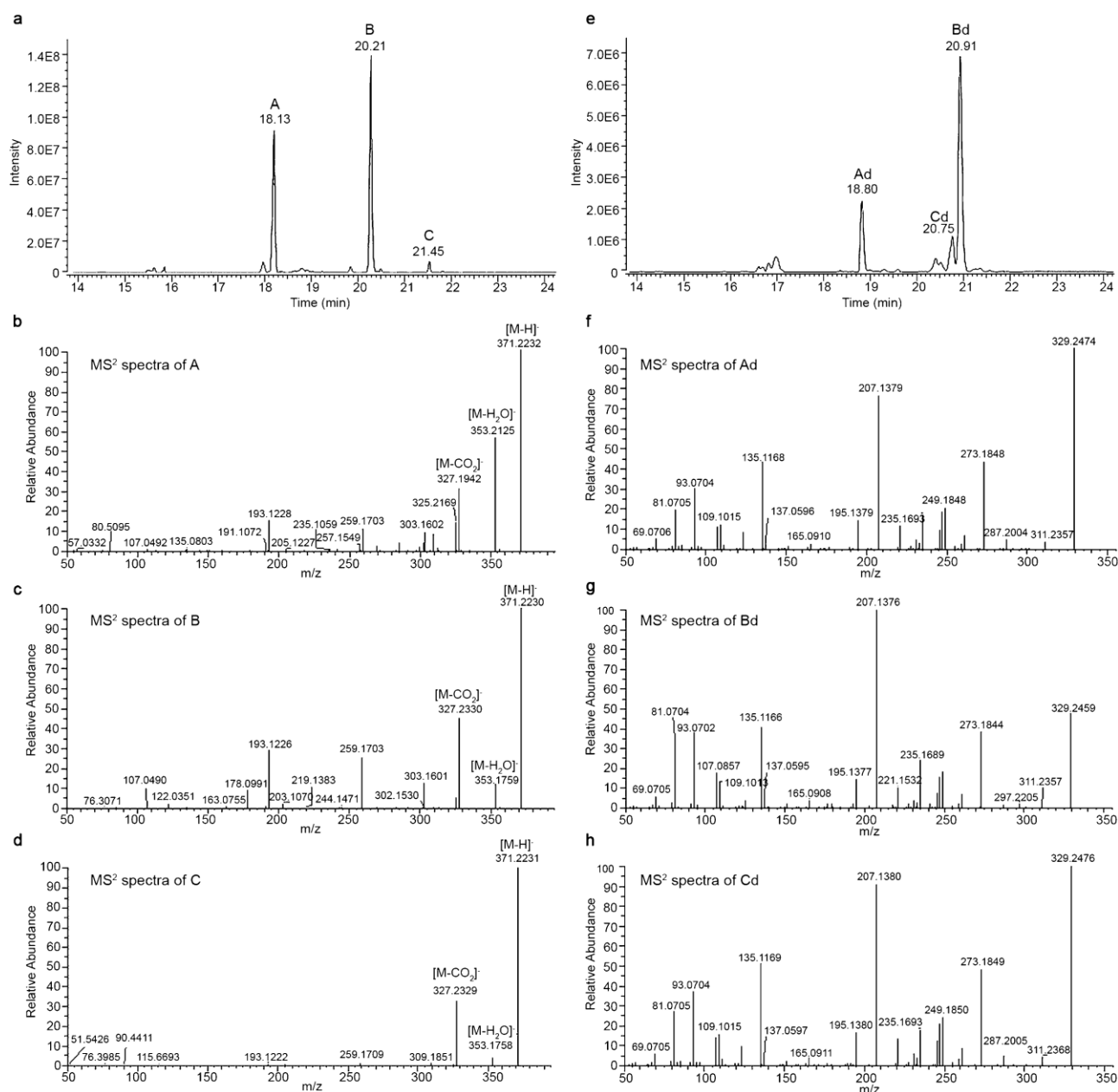


Figure 1. Identification of compounds corresponding to the molecular formula $C_{23}H_{32}O_4$ in *C. sativa* FM2. (A) UHPLC-HRMS extracted ion chromatogram (EIC) for molecular formula $C_{23}H_{32}O_4$ in native FM2 and the relative fragmentation spectra, in negative ionization mode, for the identified peaks A (panel B), B (panel C) and C (panel D). (E) UHPLC-HRMS extracted ion chromatogram (EIC) for molecular formula $C_{22}H_{31}O_2$ in decarboxylated FM2 and the relative fragmentation spectra, in negative ionization mode, for the identified peaks Ad (panel F), Bd (panel G) and Cd (panel H).

Stereoselective synthesis of CBDH, Δ^9 -THCH and monomethyl derivatives CBDM, Δ^9 -THCM and CBGM.

The stereoselective synthesis of (–)-trans-cannabidiol ((–)-trans-CBDH) and (–)-trans- Δ^9 -tetrahydrocannabidiol ((–)-trans- Δ^9 -THCH) was performed as previously reported for the synthesis of the corresponding homologs (–)-trans-CBDB, (–)-trans-CBDP, (–)-trans- Δ^9 -THCB and (–)-trans- Δ^9 -THCP^{2-4,8}. The appropriate 5-hexylbenzene-1,3-diol (**4**) was prepared first as reported in Fig. 3A, Scheme 1. (3,5-dimethoxybenzyl)triphenylphosphonium bromide (**1**) was easily prepared in

quantitative yield by reaction of 1-(bromomethyl)-3,5-dimethoxybenzene with triphenylphosphine in refluxing toluene for 6 h. Wittig's reaction between 1 and valeraldehyde in 0.1 M K_2CO_3 aqueous solution at reflux for 24 h gave 1-(hex-1-en-1-yl)-3,5-dimethoxybenzene (2) as a 55:45 E/Z mixture which was hydrogenated using the ThalesNano H-Cube flow reactor, to give the corresponding 1-hexyl-3,5-dimethoxybenzene (3) in 91% yield. The demethylation performed using BBr_3 in anhydrous DCM, overnight at room temperature and under nitrogen atmosphere, gave 5-hexyl-resorcinol (4) in quantitative yield. In our previous works CBDB and CBDP were synthesized first by condensation of the appropriate resorcinol with (1*S*,4*R*)-1-methyl-4-(prop-1-en-2-yl)cycloex-2-enol, using pTSA as catalyst and stopping the reaction before CBDs evolve to THCs in the same conditions. Conversely, for the selective synthesis of (-)-trans- Δ^9 -THCB and (-)-trans- Δ^9 -THCP a longer procedure was adopted. The appropriate resorcinol was condensed with (1*S*,4*R*)-1-methyl-4-(prop-1-en-2-yl)cycloex-2-enol in the same condition described above for a longer reaction time (usually 48 h). In this way, the CBDs were quantitatively converted into the corresponding Δ^8 -THCs. Hydrochlorination of the Δ^8 double bond of (-)-trans- Δ^8 -THCs, allowed to obtain (-)-trans-HCl-THCs, which were successively converted to (-)-trans- Δ^9 -THCs by selective elimination on position 2 of the terpene moiety using potassium t-amylate as base. Although this procedure allowed to selectively prepare (-)-trans- Δ^9 -THCs, it has the inconvenience to be time consuming, and with low atom economy. Because the conversion of CBDs to Δ^8 -THCs passes through the formation of Δ^9 -THCs first, for the synthesis of (-)-trans-CBDH and (-)-trans- Δ^9 -THCH we evaluated the possibility to stop the reaction before Δ^9 -THCH starts to convert into Δ^8 -THCH. Therefore, 5-hexyl-resorcinol (4) was condensed with (1*S*,4*R*)-1-methyl-4-(prop-1-en-2-yl)cycloex-2-enol using pTSA as catalyst and the progression of the reaction was monitored every 15 min by HPLC–UV/Vis. After approximately 2 h, almost the 50% of (-)-trans-CBDH converted in (-)-trans- Δ^9 -THCH, but no traces of Δ^8 -THCH were detected. The reaction was therefore stopped and (-)-trans-CBDH and (-)-trans- Δ^9 -THCH were purified as reported in Material and Methods section. (-)-trans-CBDH and (-)-trans- Δ^9 -THCH were obtained in 17% and 20% yield, respectively. The total yield of the two phytocannabinoids was 37%, which is in line with the yield obtained for the sole synthesis of CBDB or CBDP using the same procedure but quenching the reaction after the consumption of the starting materials and before that CBDs started to isomerize into THCs (usually 30 min–1 h). Therefore, strictly monitoring the codensation of the appropriate resorcinol with (1*S*,4*R*)-1-methyl-4-(prop-1-en-2-yl)cycloex-2-enol it is possible to prepare in one-pot reaction both (-)-trans-CBDs and (-)-trans- Δ^9 -THCs, avoiding cumbersome and longer procedure to selectively prepare the (-)-trans- Δ^9 -THCs, without the awkward formation of their Δ^8 isomers. The synthesis of the monomethyl ether derivatives of CBD, THC and CBG is reported in Fig. 3A, Scheme 2. (-)-trans- CBDM and CBGM

were easily prepared by methylation of the commercially available CBD and CBG by reaction with 0.5 equivalents of dimethylsulfate, in DMF at room temperature, using K_2CO_3 as base (Fig. 3A, Scheme 3). In contrast (-)-trans- Δ^9 -THCM was prepared from (-)-trans-CBDM, through cyclization catalyzed by pTSA (Fig. 3A, Scheme 2). The chemical identification of synthetic (-)-trans-CBDH, (-)-trans- Δ^9 -THCH, (-)-trans-CBDM, (-)-trans- Δ^9 -THCM and CBGM, and their unambiguous 1H and ^{13}C assignments were achieved by NMR spectroscopy (Figure SI-1–5, Supporting Information). In particular for (-)-trans-CBDH and (-)-trans- Δ^9 -THCH, as already stated during the synthesis of (-)-trans-CBDB, (-)-trans-CBDP, (-)-trans- Δ^9 -THCB and (-)-trans- Δ^9 -THCP, and by comparison with the well-known homologs (CBD, CBDV, Δ^9 -THC, and Δ^9 -THCV) no significant differences in the proton and carbon chemical shifts of the terpene and aromatic moieties were observed among CBD and Δ^9 -THC homologs. The sole exception observed regards the integration of the multiplet in the range 1.4–1.2 ppm in the 1H spectra and the number of carbon signals in the range 20–30 ppm of the ^{13}C spectra, corresponding to the central methylene units of the alkyl chain on the resorcinyly moiety. The perfect match in the chemical shift of the terpene and aromatic moieties between the synthesized (-)-trans-CBDH and (-)-trans- Δ^9 -THCH and the respective homologues^{2-4,8}, combined with the mass spectra and fragmentation pattern, allowed us to unambiguously confirm the chemical structures of the two new synthetic cannabinoids. The trans (1*R*,6*R*) configuration at the terpene moiety was confirmed by optical rotatory power. The new cannabinoids (-)-trans-CBDH, (-)-trans- Δ^9 -THCH, (-)-trans-CBDM and (-)-trans- Δ^9 -THCM showed an $[\alpha]_D^{20}$ of -146° , -166° , -113° and -161° , respectively, in chloroform. The $[\alpha]_D^{20}$ values were in line with those of the homologs^{2,8,15}, suggesting a (1*R*,6*R*) configuration for the four phytocannabinoids. Lastly, the perfect superimposition between the 1H and ^{13}C NMR spectra of both synthetic and extracted (-)-trans-CBDH was observed, confirming the identity of the new cannabinoids identified in the FM2 cannabis variety (Figure SI-6, Supporting Information). A comparison of the retention time, molecular ion and fragmentation spectra of each pure synthesized standard with those found in FM2 led us to conclude that the first peak Ad could be assigned to CBDH and the second one B_d to CBDM (Fig. 3B). The third peak Cd could most likely be associated to Δ^9 -THCH although it's very low abundance and the presence of other interferents in the fragmentation spectrum from the FM2 extract did not allow an unambiguous assignment of its chemical structure (Fig. 3B). Moreover, no trace of Δ^9 -THCM was found. Fragmentation in negative ionization mode helped us to distinguish between CBDH and Δ^9 -THCH, which were identical in positive ionization mode, whereas no ionization was obtained in negative mode for Δ^9 -THCM due to the lack of free hydroxyl groups to be deprotonated (Fig. 3B). Confirmation of the identification of CBDH was achieved by isolation of pure fractions from the FM2 extract containing the acidic precursor CBDHA by semipreparative liquid chromatography. The pure

compound was decarboxylated by heat and analysed by UHPLC-HESI-Orbitrap. Unfortunately, it was not possible to isolate fractions of FM2 containing THCHA due to its very low abundance. However, the stereoselective synthesis of Δ^9 -THCH allowed to assign a certain chemical structure to the corresponding peak in the FM2 sample.

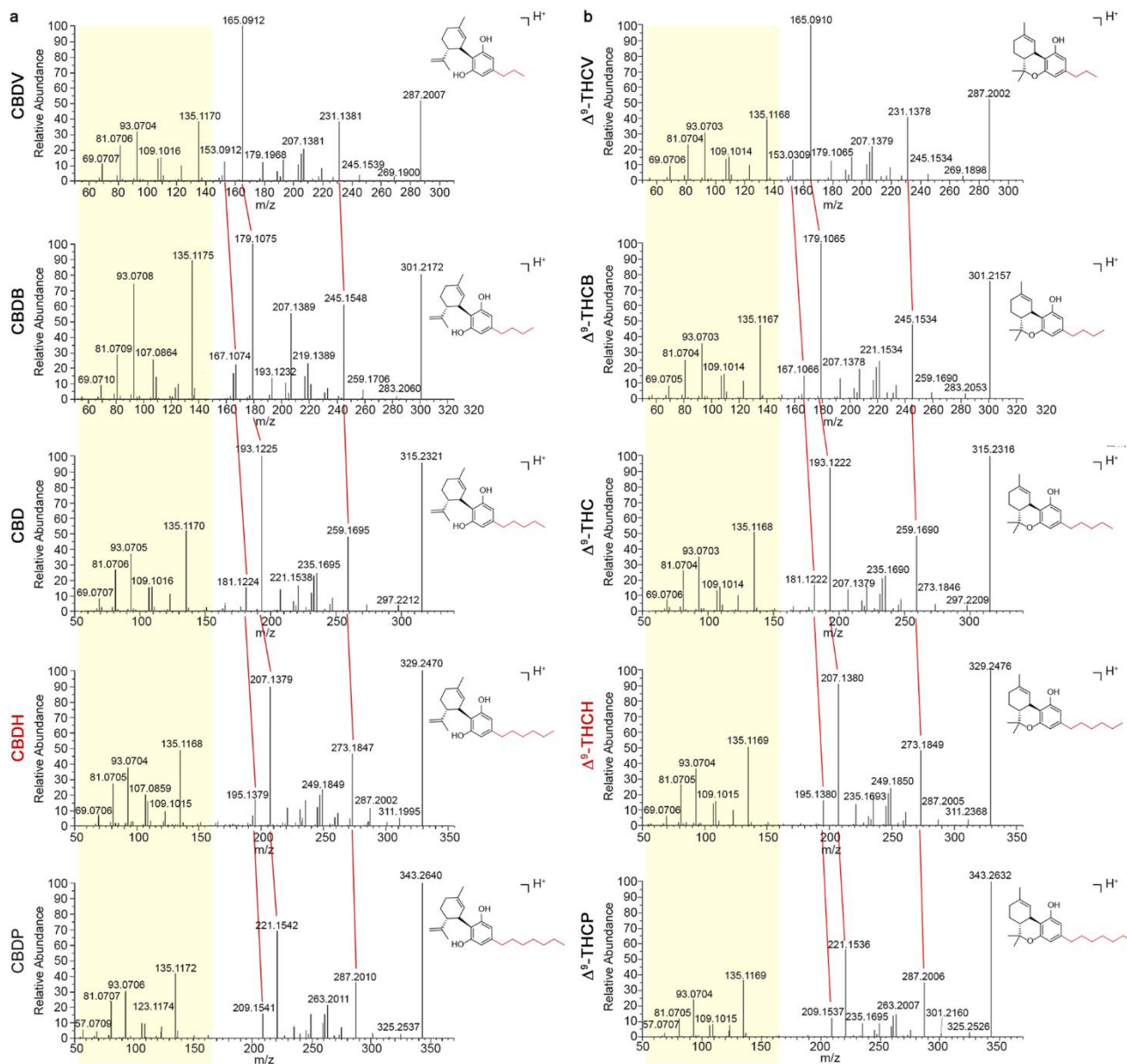


Figure 2. MS/MS spectra library of CBD and Δ^9 -THC homologs by UHPLC-HESI-Orbitrap. Comparison of the high-resolution fragmentation spectra in positive (ESI⁺) mode for CBD (panel A) and Δ^9 -THC (panel B) homologs. The pale-yellow box point out the constant terpenic portion. The red lines highlight the shift of some fragments corresponding to the loss of a methylene portion (CH₂, m/z = 14) moving from CBDP (or Δ^9 -THCP) to CBDV (or Δ^9 -THCV).

Semi-quantification of CBDH and Δ^9 -THCH in the FM2 extract. Thanks to the synthetically prepared analytical standards of CBDH, Δ^9 -THCH, CBDM and CBGM, we were able to provide a semi-quantification of these cannabinoids in the FM2 cannabis variety by building the corresponding

calibration curves. The results of concentration were in the order of the $\mu\text{g/g}$, while the main cannabinoids CBD and $\Delta^9\text{-THC}$ were in the order of the mg/g (56 and 39 mg/g respectively). In particular, the hexyl homologs of CBD and $\Delta^9\text{-THC}$ resulted 27 $\mu\text{g/g}$ and 7 $\mu\text{g/g}$, while the methyl ether derivatives CBDM and CBGM were 50 $\mu\text{g/g}$ and 102 $\mu\text{g/g}$. No $\Delta^9\text{-THCM}$ was detected in the FM2.

Effects of CBDH on the formalin test in mice.

Formalin paw injection is a solid and widely used model of nociception with high face validity when tested with analgesic drugs. A nociceptive response to subcutaneous formalin induced an early, short-lasting first phase (0–7 min) followed by a quiescent period, and then a second, prolonged phase (15–60 min) of tonic hyperalgesia (Fig. 3C). In the tonic phase, two-way ANOVA revealed that CBDH (1, 2 mg/kg , i.p.) significantly reduced the late phase of the formalin-induced nocifensive behavior when compared to the vehicle-treated group (treatment $F(4,288) = 17.32$, $P < 0.0001$, time $F(12,288) = 67.80$, $P < 0.0001$ and interaction $F(48,288) = 3.02$, $P < 0.0001$); also, the dose of 2 mg/kg had a significant antinociceptive effect as compared to the vehicle group. The doses of 3 and 5 mg/kg had no effect on the formalin test (Fig. 3C).

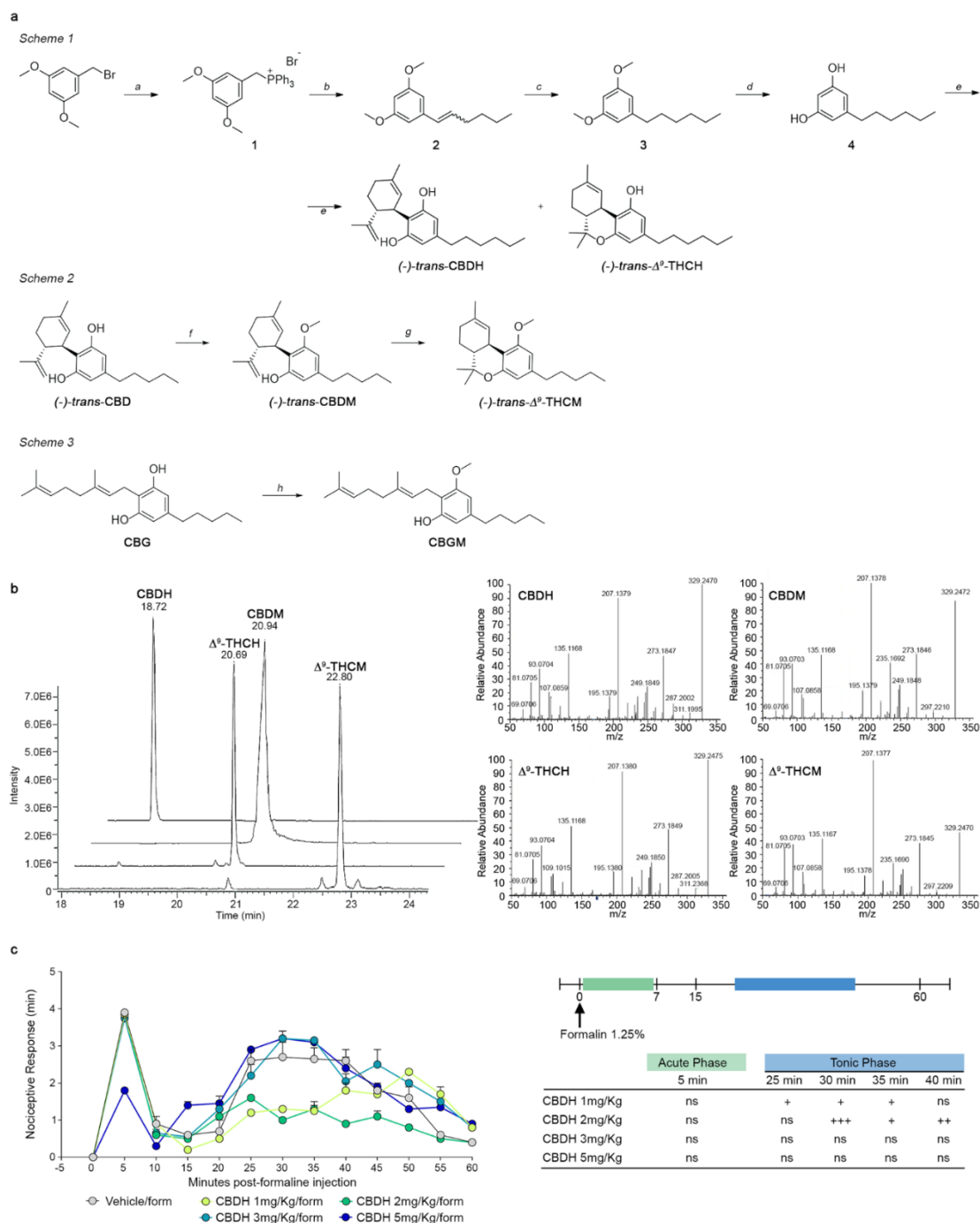


Figure 3. Synthesis and UHPLC-HRMS identification of CBDH, CBDM, Δ^9 -THCH and Δ^9 -THCM, and in vivo activity of CBDH. (A) Scheme 1. Reagents and conditions: (a) triphenylphosphine (1.1 equiv.), toluene, reflux, 6 h, quant. yield; (b) valeraldehyde (1.5 equiv.), 0.1 M K_2CO_3 aq. (10 mL per mmol of 1), reflux, 5 h, 81% yield; (c) H-Cube ThalesNano H_2 -Pd/C, EtOH, 30 °C, 20 bar, 1 mL/min, 91% yield; (d) BBr_3 1 M in DCM (2.2 eq.), anhydrous DCM, N_2 atmosphere, $-15\text{ }^\circ\text{C} \rightarrow \text{r.t.}$, 24 h, quant. yield; (e) (1S,4R)-1-methyl-4-(prop-1-en-2-yl)cyclohex-2-enol (0.9 equiv.), pTSA (0.1 equiv.), DCM, r.t., argon, 2 h, 17% yield for (-)-trans-CBDH and 20% yield for (-)-trans- Δ^9 -THCH. Scheme 2. Reagents and conditions: dimethylsulphate (0.5 equiv.), K_2CO_3 (1 equiv.), DMF, r.t. 62% yield for (-)-trans-CBDM and 57% yield for CBGM. Scheme 3. Reagents and conditions: p-TSA (0.1 equiv.), dry DCM, r.t., 1 h, 43% yield. (B) Superimposition of extracted UHPLC-HRMS ion chromatograms (EICs) of synthetic cannabinoid n-hexyl and monomethyl ether homologs. and relative fragmentation spectra, in positive ionization mode. EICs were chosen based on the exact mass calculated for $C_{23}H_{32}O_4$. (C) Effects of CBDH (1, 2, 3, and 5 mg/kg, i.p.) or vehicle in the formalin test in mice. The total time of the nociceptive response was measured every 5 min and expressed in min (see “Experimental” section). Data are represented as means \pm SEM (n = 5–6). +,+++ indicate statistically significant differences versus veh/form, $p < 0.05$ and $p < 0.001$, respectively. 2-way ANOVA followed by Bonferroni’s post hoc tests was used for statistical analysis.

Discussion

The comprehensive characterization of the chemical profile of a cannabis variety is a rather arduous task as the analytical tools in the chemist's hand are not able to cover such a broad range of compounds. However, the high sensitivity and selectivity of the high-resolution mass spectrometry, for example those achieved with the Orbitrap technology, can enable the identification of a reasonable number of molecules, even when present in very small traces. This approach allowed for the identification of new series of cannabinoids, CBD and THC homologs, with different lengths of the alkyl side chain, which were recently reported by our group^{2-4,8}. The present work expanded the scope of cannabinoids identification completing the series of homologs with different alkyl side chain from three to seven methylene units. Up to now, only cannabinoids with an odd number of carbon atoms on the side chain have been reported and those with an even number of carbon atoms have been supposed to be artifacts derived from fungal ω -oxidation of their corresponding homologs⁷. The investigation of the origin of these species, such as those with a butyl and hexyl side chain, is beyond the scope of this work, but, although surprising, it is certain that such cannabinoids are actually present in a medicinal cannabis variety. The literature reports the existence of monomethyl ether derivatives of the canonical pentyl cannabinoids to justify the presence of compounds bearing an additional methyl group. Although on one side the structural identity of such derivatives was confirmed, our findings pointed out a new series of cannabinoids with the same molecular formula of the monomethyl ethers but with a different arrangement. Their origin, whether it is from the plant or from microorganisms, should be investigated as this might disclose new insights in the cannabis biochemistry. It is certainly important to underline that it is very easy to confuse CBDH and CBDM, as well as Δ^9 -THCH and Δ^9 -THCM. However, the match of the high-resolution fragmentation patterns with their pure synthetic standards was determinant to assign the respective chemical structure. This work might serve in the future for any researcher to distinguish between two species that show a very similar analytical behaviour. In a similar way, the methyl ether derivative of CBG was also identified (CBGM). It is worth noting that no Δ^9 -THCM was detected in the FM2 variety. On the other hand, both CBDM and CBGM showed a high peak as well as their native precursors CBDMA and CBGMA. Achieved results are in accordance with what reported by Lumir Ondrej Hanus et al., which showed that the cannabigerol monomethyl ether is always presents in greater quantities than its products, THCMA and CBDMA^{7,16}. de Meijer et al. demonstrated that the cannabinoid acid synthases (THCAS, CBDAS) show a different affinity for CBGA alkyl homologues. This concept would explain the achieved results. CBDAS could be competitively stronger than THCAS when the substrate is CBGMA^{17,18}. The comparison of the results obtained for the concentrations of unorthodox cannabinoids in the FM2 variety suggested that there is no relationship

between the different series as the same CBD to THC ratio is not respected. Considering our recent work on the heptyl derivatives of CBD and Δ^9 -THC, CBDP and Δ^9 -THCP were found in the FM2 at the concentration of 243 $\mu\text{g/g}$ and 29 $\mu\text{g/g}$ ⁴; whereas, in the same cannabis variety, the butyl series of CBD and THC was found at the concentration of 500 $\mu\text{g/g}$ and 400 $\mu\text{g/g}$ for CBDB and Δ^9 -THCB respectively⁸. In this work, we found 27 $\mu\text{g/g}$ and 7 $\mu\text{g/g}$ for CBDH and Δ^9 -THCH respectively. However, this data should be verified considering a larger number of different varieties in order to provide a reliable statistical significance. The CBDH could have pleiotropic mechanisms of action through which it can exert its pharmacological effect. We found that the doses of the 1 and 2 mg/Kg significantly reduced the late phase of the formalin-induced nocifensive behavior, whereas the higher doses 3 and 5 mg/Kg were ineffective. This could be due, at least in part, assuming that at these doses CBDH can activate receptor facilitating nociception such as TRPV1 or other channels. On the other hand, we can speculate that CBDH at the higher doses could block receptors involved in antinociception such as CB1 or CB2. However, further pharmacological studies are needed to better investigate the pharmacodynamics profile of this interesting compound. Another piece of knowledge towards understanding Cannabis Sativa L. cannabinoma has been added with this work. In particular, clarity has been made about the possible confusion between phytocannabinoids with a 6-term alkyl chain (CBDH, THCH) and those with a methylated resorcinolic hydroxyl group (CBDM, THCM). Furthermore, two new phytocannabinoids CBDH and THCH have been identified in the FM2 variety by comparison with their respective authentic synthesized compounds. In particular, CBDH has been isolated, and its pharmacological activity has been evaluated in vivo in mice. At extremely low doses (1 mg/kg) it showed an interesting nocifensive activity. However, the CBDH concentration of 27 $\mu\text{g/g}$ found in the FM2 variety is too low to exert the pharmacological effect, but it is not excluded that other cannabis varieties may contain higher concentrations. More in-depth pharmacological studies are currently underway to clarify the mechanism of action of this new phytocannabinoid.

Methods

Plant material

FM2 cannabis variety is produced from the strain CIN-RO bred by the Council for Agricultural Research and Economics (CREA) in Rovigo (Italy) and supplied to the Military Chemical Pharmaceutical Institute (MCPI, Firenze, Italy). Experiments on FM2 inflorescence (batch n. 6A32/1) were performed with the authorization of the Italian Ministry of Health (prot. n. SP/062). Two 5 g packs were finely grinded (< 2 mm particle size) and divided into two batches: 500 mg were extracted with 50 mL of ethanol 96% according to the procedure reported in the monograph of Cannabis Flos of the German Pharmacopoeia¹⁹ and analyzed by UHPLC-HESI-Orbitrap without further dilution.

The remaining 9.5 g were treated according to the protocol of Pellati et al. with minor changes²⁰. Briefly, freeze-dried plant material was sonicated with 400 mL of n-hexane for 15 min in an ice bath. After centrifugation for 10 min at $2000 \times g$ the pellets were discarded. The same procedure was repeated twice more. The supernatants were then dried under reduced pressure and resuspended in 10 mL of acetonitrile, filtered and passed through a semi-preparative liquid chromatography for the isolation of the acidic species of the cannabinoids of interest.

Isolation of natural CBDH.

A semi-preparative LC system (Octave 10 Semba Bioscience, Madison, USA) was used to separate the FM2 mixture into 80 fractions in a total run time of 80 min. The chromatographic conditions used are reported in the paper by Citti et al.⁴. A Luna C18 with a fully porous silica stationary phase (Luna 5 μm C18(2) 100 Å, 250 \times 10 mm) (Phenomenex, Bologna, Italy) was the column employed and a mixture of acetonitrile:0.1% aqueous formic acid 70:30 (v/v) was used as mobile phase at a constant flow rate of 5 mL/min. The fractions containing CBDHA (retention time 13.0 min) was isolated as reported in our previous work². The fractions containing CBDHA (13.0 min) were analyzed by UHPLC-HESI-Orbitrap and dried on the rotavapor at 70 °C. The residue was placed in an oven at 120 °C for 2 h to achieve decarboxylation. An amount of about 0.3 mg of CBDH was obtained.

UHPLC-HESI-Orbitrap metabolomic analysis.

Analyses on FM2 extracts were performed on a Thermo Fisher Scientific Ultimate 3000 provided with a vacuum degasser, a binary pump, a thermostated autosampler, a thermostated column compartment and interfaced to a heated electrospray ionization source and a Q-Exactive Orbitrap mass spectrometer (UHPLC-HESI-Orbitrap). The HESI and Orbitrap parameters were set following our previous work⁴. Briefly, the capillary temperature was set at 320 °C, the vaporizer temperature at 280 °C, the electrospray voltage at 4.2 kV (for the positive ionization mode) and 3.8 kV (for the negative mode), the sheath gas and the auxiliary gas at 55 and 30 arbitrary units respectively, the RF level of the S lens at 45. Analyses were acquired in full scan data-dependent acquisition (FS-dd-MS2) in positive and negative mode with a resolving power of 70,000 FWHM and m/z of 200 using the Xcalibur 3.0 software (Thermo Fisher Scientific, San Jose, CA, USA). For the Orbitrap mass analyzer, a scan range of m/z 250–400, an AGC of 3e6, an injection time of 100 ms and an isolation window of m/z 0.7 were chosen as the optimal parameters. The collision energy for the fragmentation of the molecular ions was set at 20 eV. The exact masses of the $[\text{M}+\text{H}]^+$ and $[\text{M}-\text{H}]^-$ molecular ions were extracted from the total ion chromatogram (TIC) of the FM2 extracts and matched with pure analytical standards for accuracy of the exact mass (5 ppm), retention time and MS/MS spectrum. The chromatographic separation was carried out on a core shell C18 stationary

phase (Poroshell 120 SB-C18, 3.0×100 mm, $2.7 \mu\text{m}$, Agilent, Milan, Italy) following the conditions employed for our previous work⁴. A semi-quantitative analysis of Δ^9 -THC and CBD, their hexyl homologs CBDH and Δ^9 -THCH, and the methyl ether derivatives of CBD and CBG, CBDM and CBGM, was carried out using a calibration curve with the external standard method. A stock solution of CBD and Δ^9 -THC (1 mg/mL) was properly diluted to obtain five non-zero calibration points at the final concentrations of 50, 100, 250, 500 and 1000 ng/mL; a stock solution of CBDH, CBDM, Δ^9 -THCH, CBDM and CBGM was diluted to obtain the final concentrations of 5, 25, 50, 100 and 250 ng/mL. The linearity was assessed by the coefficient of determination (R^2), which was greater than 0.992 for each analyte.

Synthetic procedure.

The reagents and the solvents used for the synthesis of the analytical standards were purchased from Sigma-Aldrich and VWR, respectively. In the synthetic procedures, the solvents were abbreviated as following: acetonitrile (ACN); chloroform (CHCl_3); cyclohexane (CE); dichloromethane (DCM); diethyl ether (Et_2O); dimethyl sulfoxide (DMSO); ethyl acetate (AcOEt). The reactions were monitored by thin-layer chromatography (TLC) using 60F-254 silica gel plates (from Merck) and inspected with UV lamp, or alkaline KMnO_4 stain. Purification of the synthesized products was performed by flash chromatography on silica gel ($40\text{--}63 \mu\text{m}$). The mobile phase is specified in the respective following monographies. NMR spectra were recorded on a Bruker 400 (at 400.134 MHz for ^1H and 100.62 MHz for ^{13}C) or on a Bruker 600 (at 600.130 MHz for ^1H and 150.902 MHz for ^{13}C) spectrometer. Chemical shifts (δ) are reported in parts per million (ppm) and referenced to the solvent residual peaks. Coupling constants are reported in hertz (Hz) and the splitting pattern is reported as: singlet (s), doublet (d), triplet (t), quartet (q), double doublet (dd), quintet (quin), multiplet (m), broad signal (b). Monodimensional and bidimensional spectra were acquired using the same parameters previously reported^{3-5,8}. Optical rotation (α) was acquired with a Polarimeter 240C from Perkin-Elmer (Milan, Italy), using a cell with a length of 100 mm, and a volume 1 mL.

Synthesis of (3,5-dimethoxybenzyl)triphenylphosphonium bromide (1).

Triphenylphosphine (6.3 g, 23.8 mmol, 1.1 equiv.) was added to a stirred solution of 1-(bromomethyl)-3,5-dimethoxybenzene (5.0 g, 21.6 mmol, 1 equiv.), in 30 mL of toluene and refluxed for 6 h. After standing at room temperature overnight, the precipitate formed was collected by filtration, washed with diethyl ether and dried to give 10.4 g of a white solid (quant. yield).

$^1\text{H-NMR}$ (400 MHz, CDCl_3) δ 7.78–7.76 (m, 9H), 7.66–7.63 (m, 6H), 6.35 (t, 2H, $J = 2.3$ Hz), 6.30 (q, 1H, $J = 2.3$ Hz), 5.32 (d, 2H, $J = 14.3$ Hz), 3.54 (s, 6H).

Synthesis of (E/Z)-1-(hexyl-1-en-1-yl)-3,5-dimethoxybenzene (2).

Valeraldehyde (0.48 mL, 4.56 mmol, 1.5 equiv.) was added to a stirred suspension of 1 (1.5 g, 3.04 mmol, 1 equiv.) in 20 mL of aqueous 0.1 M K₂CO₃. The mixture was refluxed overnight and chilled down at 0 °C. Cyclohexane (20 mL) was added, and the biphasic mixture was vigorously stirred in the same condition for two hours in order to precipitate triphenylphosphine oxide. The solid was removed by filtration and the organic phase separated. The aqueous layer was extracted two more times with cyclohexane. The combined organic phase was washed with brine, dried over anhydrous Na₂SO₄ and concentrated to give 540 mg (81% yield) of a yellow oil. The product was obtained as a 55:45 E/Z mixture of alkene, pure enough to be used in the next step without further purification.

¹H NMR (400 MHz, CDCl₃, Z-isomer) δ 6.43 (d, 2H, J = 2.2 Hz), 6.35 (t, 1H, J = 2.2 Hz), 6.31 (d, 1H, J = 11.5 Hz), 5.66 (dt, 1H, J = 11.5, 7.0 Hz), 3.79 (s, 6H), 2.37–2.30 (m, 2H), 1.47–1.31 (m, 4H), 0.90 (t, 3H, J = 7.1 Hz); ¹H NMR (400 MHz, CDCl₃, E-isomer) δ 6.51 (d, 2H, J = 2.2 Hz), 6.29 (bm, 1H), 6.21 (dt, 1H, J = 15.9, 6.85 Hz), 3.79 (s, 6H), 2.24–2.18 (m, 2H), 1.47–1.31 (m, 4H, overlap with the same signals of Z-isomer), 0.92 (t, 3H, J = 7.1 Hz).

Synthesis of 1-hexyl-3,5-dimethoxybenzene (3).

The mixture of (E/Z)-1-(hept-1-en-1-yl)-3,5-dimethoxybenzene (2), solubilized in EtOH, was selectively reduced at the double bond by hydrogenation with the flux reactor H-Cube Mini Plus ThalesNano using the following conditions: temperature 30 °C, H₂ 20 psi, cartridge Pd/C, solvent EtOH, flow 1 mL/min. The solvent was evaporated obtaining 495 mg (91% yield) of a colourless liquid pure enough to be used in the next step without further purification.

¹H NMR (400 MHz, CDCl₃) δ 6.37 (d, J = 2.3 Hz, 2H), 6.32 (t, J = 2.3 Hz, 1H), 3.80 (s, 6H), 2.57 (t, J = 7.48 Hz, 2H), 1.61 (qnt, 2H, J = 6.9 Hz), 1.39–1.28 (m, 6H), 0.91 (t, J = 6.4 Hz, 3H). ¹³C NMR (101 MHz, CDCl₃) δ 160.67, 145.43, 106.48, 97.55, 55.23, 36.32, 31.73, 31.25, 29.02, 22.61, 14.10.

Synthesis of 5-hexylbenzene-1,3-diol (4).

3 (495 mg, 2.23 mmol, 1 equiv.) was solubilized in anhydrous DCM at – 15 °C and under argon atmosphere, and a 1 M solution of BBr₃ in anhydrous DCM (5 mL, 4.9 mmol, 2.2 equiv.) was added dropwise over a period of 30 min. The mixture was stirred at room temperature overnight and quenched with an aqueous saturated solution of NaHCO₃. The organic phase was washed with water, brine, dried over anhydrous Na₂SO₄ and concentrated to give 430 mg (99% yield) of an orange liquid which crystalized upon standing.

¹H NMR (400 MHz, CDCl₃) δ 6.24 (d, 2H, J = 2.3 Hz), 6.17 (t, 1H, J = 2.3 Hz), 4.71 (bs, 2H), 2.49 (t, 2H, J = 8.0 Hz), 1.57 (qnt, 2H, J = 8.0 Hz), 1.35–1.23 (bm, 6H), 0.88 (t, 3H, J = 6.8 Hz). ¹³C NMR (101 MHz, CDCl₃) δ 156.57, 146.16, 108.04, 100.12, 35.82, 31.74, 31.01, 28.94, 22.59, 14.09.

Synthesis of 1'R,2'R)-4-hexyl-5'-methyl-2'-(prop-1-en-2-yl)-1',2',3',4'-tetrahydro-[1,1'-biphenyl]-

2,6-diol, (-)-*trans*-CBDH and (6*aR*,10*aR*)-3-hexyl-6,6,9-trimethyl-6*a*,7,8,10*a*-tetrahydro-6*H*-benzo[*c*]chromen-1-ol, (-)-*trans*- Δ^9 -THCH.

(1*S*,4*R*)-1-methyl-4-(prop-1-en-2-yl)cycloex-2-enol (304 mg, 2.0 mmol, 0.9 eq.), solubilized in 20 mL of anhydrous DCM, was added dropwise over a period of 20 min to a stirred solution of 5-hexylbenzene-1,3-diol (1) (433 mg, 2.23 mmol, 1 eq.) and *p*-toluenesulfonic acid (40 mg, 0.2 mmol, 0.1 eq.) in anhydrous DCM (20 mL) at room temperature and under argon atmosphere. The reaction was stirred in the same conditions and monitored every 15 min by HPLC, following the same chromatographic method using for the analytic characterization. After for 2 h, the putative ratio between CBDH and THCH was almost 1:1 and no traces of Δ^8 -THCH were detected. The reaction was therefore quenched with 20 mL of a saturated aqueous solution of NaHCO₃. The organic layer was washed with brine, dried over anhydrous Na₂SO₄ and evaporated. The crude was chromatographed over silica gel (ratio crude:silica 1/150, eluent: CE:DCM 8/2). All the chromatographic fractions were analyzed by HPLC–UV and UHPLC-HESI-Orbitrap and only the fractions containing exclusively CBDH and THCH were separately collected to give 65 mg of CBDH as colorless oil (10% yield, purity > 99%) and 71 mg of THCH as a light purple oil (11% yield, purity > 99%). These two fractions were used as pure analytic standards for spectroscopic and analytic characterization. The chromatographic fraction containing both CBDH and THCH (c.a. 150 mg) was purified by semipreparative HPLC on a C18 reverse phase using ACN:water 70:30 as mobile phase. Two other aliquots of CBDH (45 mg) and THCH (60 mg) were obtained.

(-)-*trans*-CBDH: colorless oil. 110 mg (17% yield). ¹H NMR (400 MHz, CDCl₃) δ 6.10–6.32 (bm, 2H), 5.97 (bs, 1H), 5.57 (s, 1H), 4.73–4.59 (bm, 2H), 4.56 (s, 1H), 3.88–3.81 (m, 1H), 2.46–2.36 (m, 3H), 2.27–2.20 (m, 1H), 2.09 (ddt, *J* = 2.4, 5.0, 18.0 Hz, 1H), 1.85–1.76 (m, 5H), 1.65 (s, 3H), 1.58–1.51 (m, 2H), 1.31–1.25 (m, 6H), 0.87 (t, *J* = 6.7 Hz, 3H). ¹³C NMR (101 MHz, CDCl₃) δ 156.14, 153.98, 149.54, 143.20, 140.19, 124.26, 113.89, 110.97, 109.78, 108.12, 46.29, 37.42, 35.65, 31.86, 31.05, 30.54, 29.09, 28.54, 23.82, 22.73, 20.67, 14.22. HRMS *m/z* [M+H]⁺ calcd. for C₂₂H₃₃O₂⁺: 329.2475. Found: 343.2629; [M–H][–] calcd. for C₂₂H₃₁O₂[–]: 327.2330. Found: 341.2482. [α]_D²⁰ = –146° (c = 1.0, ACN).

(-)-*trans*- Δ^9 -THCH: light purple oil. 131 mg (20% yield). ¹H NMR (400 MHz, CDCl₃) δ 6.30 (bt, 1H), 6.27 (bd, 1H), 6.14 (bd, 1H), 4.78 (s, 1H), 3.20 (dt, *J* = 2.5, 10.8 Hz, 1H), 2.43 (t, *J* = 7.5 Hz, 2H), 2.16–2.18 (m, 2H), 1.95–1.88 (m, 1H), 1.71–1.65 (m, 4H), 1.58–1.51 (m, 2H), 1.43–1.36 (m, 4H), 1.34–1.24 (m, 6H), 1.09 (s, 3H), 0.88 (t, *J* = 6.8 Hz, 3H). ¹³C NMR (101 MHz, CDCl₃) δ 154.91, 154.29, 142.97, 134.54, 123.87, 110.24, 109.17, 107.69, 77.35, 45.95, 35.66, 33.72, 31.88, 31.31, 31.08, 29.16, 27.71, 25.16, 23.51, 22.73, 19.41, 14.25. HRMS *m/z* [M+H]⁺ calcd. for C₂₂H₃₃O₂⁺: 329.2475. Found: 343.2629; [M–H][–] calcd. for C₂₂H₃₁O₂[–]: 327.2330. Found: 341.2482. [α]_D²⁰ = –166° (c 1.0, ACN).

Synthesis of (1*R*,2*R*)-6-methoxy-5'-methyl-4-pentyl-2'-(prop-1-en-2-yl)-1',2',3',4'-tetrahydro-[1,1'-biphenyl]-2-ol, (-)-*trans*-CBDM.

To a solution of (-)-trans-CBD (500 mg, 1.6 mmol, 1 equiv.) in dry DMF (5 mL), K₂CO₃ (414 mg, 3.2 mmol, 2 equiv.) and dimethylsulphate (76 μ L, 0.8 mmol, 0.5 equiv.) were added and stirred at room temperature overnight. The mixture was quenched with water and extracted with Et₂O. The organic phase was washed with brine, dried over anhydrous Na₂SO₄ and concentrated. The titled compound was purified by column chromatography (eluent CE:AcOEt 95:5) to give 162 mg (31% yield) of an amber liquid.

¹H NMR (400 MHz, CDCl₃) δ 6.30 (s, 1H), 6.22 (s, 1H), 5.99 (bs, 1H), 5.57 (bs, 1H), 4.49 (s, 1H), 4.32 (s, 1H), 3.99 (bd, 1H), 3.70 (s, 3H), 2.49 (t, J = 7.6 Hz, 2H), 2.43–2.37 (m, 1H), 2.25–2.19 (m, 1H), 2.07 (bdt, 1H), 1.80–1.74 (m, 6H), 1.65 (s, 3H), 1.62–1.55 (m, 3H), 1.35–1.26 (m, 4H), 0.87 (t, J = 6.8 Hz, 3H). ¹³C NMR (101 MHz, CDCl₃) δ 158.31, 155.88, 147.41, 142.82, 139.70, 124.68, 115.20, 111.02, 109.67, 103.27, 55.70, 46.81, 36.16, 35.65, 31.71, 30.97, 30.51, 28.26, 23.84, 22.70, 18.87, 14.19. HRMS m/z [M+H]⁺ calcd. for C₂₂H₃₃O₂⁺: 329.2475. Found: 343.2629; [M-H]⁻ calcd. for C₂₂H₃₁O₂⁻: 327.2330. Found: 341.2482. [α]_D²⁰ = -113° (c 1.0, ACN).

Synthesis of (E)-2-(3,7-dimethylocta-2,6-dien-1-yl)-3-methoxy-5-pentylphenol (CBGM).

The title compound was synthesized and purified according to the procedure described for (-)-trans-CBDM. Yellow liquid (57% yield). ¹H NMR (400 MHz, CDCl₃) δ 6.33 (s, 1H), 6.31 (s, 1H), 5.24 (dt, J = 7.6, 1.6 Hz, 1H), 5.20 (s, 1H), 5.05 (dt, J = 7.6, 1.6 Hz, 1H), 3.80 (s, 3H), 3.38 (d, J = 7.2 Hz, 2H), 2.51 (t, J = 7.2 Hz, 2H), 2.10–2.03 (m, 4H), 1.79 (s, 3H), 1.67 (s, 3H), 1.64–1.57 (m, 5H), 1.34–1.29 (m, 4H), 0.89 (t, J = 6.8 Hz, 3H). ¹³C NMR (101 MHz, CDCl₃) δ 157.84, 155.54, 142.67, 138.09, 131.98, 124.08, 122.34, 112.42, 109.04, 103.71, 55.62, 39.87, 36.21, 31.73, 31.14, 26.63, 25.80, 22.71, 22.21, 17.83, 16.28, 14.18. HRMS m/z [M+H]⁺ calcd. for C₂₂H₃₅O₂: 331.2632. Found: 343.2629; [M-H]⁻ calcd. for C₂₂H₃₃O₂⁻: 329.2486. Found: 341.2482.

Synthesis of (6aR,10aR)-1-methoxy-6,6,9-trimethyl-3-pentyl-6a,7,8,10a-tetrahydro-6H-benzo[c]chromene, (-)-trans-THCM.

To a solution of (-)-trans-CBDM (100 mg, 0.32 mmol, 1 equiv.) in dry DCM (10 mL), at room temperature and under nitrogen atmosphere, pTSA (5 mg, 0.03 mmol, 0.1 equiv.) was added. The solution was stirred in the same condition, monitoring the progress of the reaction by HPLC–UV/Vis in order to avoid the further conversion of the forming (-)-trans- Δ^9 -THCM into the Δ^8 isomer. After 1 h, the conversion is completed, and the reaction was quenched with NaHCO₃ aqueous. The organic phase was washed with brine, dried over anhydrous Na₂SO₄ and concentrated. The crude was purified by column chromatography (eluent CE:DCM 9:1) to give 45 mg (43% yield) of colorless liquid.

¹H NMR (400 MHz, CDCl₃) δ 6.30 (s, 1H), 6.26 (s, 1H), 6.23 (s, 1H), 3.84 (s, 3H), 3.17 (dt, J = 11.8, 2.0 Hz, 1H), 2.50 (t, J = 7.6 Hz, 2H), 2.16–2.14 (m, 2H), 1.93–1.88 (m, 1H), 1.70–1.57 (m, 7H), 1.43–1.30 (m, 11H), 1.08 (s, 3H), 0.89 (t, J = 6.4 Hz, 3H). ¹³C NMR (101 MHz, CDCl₃) δ 158.52, 154.50, 142.70, 133.59, 124.98, 110.52, 110.37, 103.07, 55.31, 46.05, 36.19, 34.06, 31.76, 31.44, 30.98, 27.72, 27.07, 25.30, 23.55, 22.71, 19.29, 14.18. HRMS m/z [M+H]⁺ calcd. for C₂₂H₃₃O₂⁺: 329.2475. Found: 343.2629; [M-H]⁻ calcd. for C₂₂H₃₁O₂⁻: 327.2330. Found: 341.2482. [α]_D²⁰ = -161° (c 1.0, ACN).

Formalin test in mice.

The formalin test assay was performed as previously reported in Linciano et al.⁸. In detail, male C57BL/6J mice, 6–8 weeks (Envigo, Italy), were housed under controlled conditions (12 h light/12 h dark cycle; temperature 20–22 °C; humidity 55–60%) with chow and tap water available ad libitum. All surgeries and experimental procedures were approved by the Animal Ethics Committee of the University of Campania “L. Vanvitelli”, Naples (prot. no. 1066/2016 PR). Animal care was in compliance with Italian (D.L. 116/92) and European Commission (O.J. of E.C. L358/1 18/12/86) regulations on the protection of laboratory animals. Efforts were made to minimize animal suffering and to reduce the number of animals used. All experiments were performed in a randomized manner by the same operator blind to pharmacological treatments. Mice were used after a 1-week acclimation period and received formalin (1.25% in saline, 30 µL) in the dorsal surface of one side of the hind paw. Each mouse, randomly assigned to one of the experimental groups (n = 5–6), was placed in a plexiglass cage and allowed to move freely for 15–20 min. A mirror was placed at a 45° angle under the cage to allow full view of the hind paws. Lifting, favoring, licking, shaking, and flinching of the injected paw were recorded as nocifensive behavior. The total time of the nociceptive response was measured every 5 min for 1 h and expressed in minutes (mean ± SEM). Mice received vehicle (0.5% DMSO in saline) or different doses of CBDH (1, 2, 3, and 5 mg/kg, i.p.) 20 min before formalin injection⁸.

References

1. Zhu, L. et al. Effect and mechanism of quorum sensing on horizontal transfer of multidrug plasmid RP4 in BAC biofilm. *Sci. Total Environ.* 698, 134236 (2020).
2. Citti, C. et al. Analysis of impurities of cannabidiol from hemp. Isolation, characterization and synthesis of cannabidibutol, the novel cannabidiol butyl analog. *J. Pharm. Biomed. Anal.* 175, 666 (2019).
3. Citti, C. et al. Chemical and spectroscopic characterization data of ‘cannabidibutol’, a novel cannabidiol butyl analog. *Data Br.* <https://doi.org/10.1016/j.dib.2019.104463> (2019).
4. Citti, C. et al. A novel phytocannabinoid isolated from *Cannabis sativa* L. with an in vivo cannabimimetic activity higher than Δ^9 -tetrahydrocannabinol: Δ^9 -Tetrahydrocannabiphorol. *Sci. Rep.* 9, 1–13 (2019).
5. Cerrato, A. et al. A new software-assisted analytical workflow based on high-resolution mass spectrometry for the systematic study of phenolic compounds in complex matrices. *Talanta* 209, 120573 (2020).
6. Antonelli, M. et al. New insights in hemp chemical composition: a comprehensive polar lipidome characterization by combining solid phase enrichment, high-resolution mass spectrometry, and cheminformatics. *Anal. Bioanal. Chem.* 412, 413–423 (2020).
7. Hanuš, L. O., Meyer, S. M., Muñoz, E., Tagliatalata-Scafati, O. & Appendino, G. Phytocannabinoids: A unified critical inventory. *Nat. Prod. Rep.* 33, 1357–1392 (2016).
8. Linciano, P. et al. Isolation of a high-affinity cannabinoid for the human CB1 receptor from a medicinal *cannabis sativa* variety: Δ^9 -tetrahydrocannabutol, the butyl homologue of Δ^9 -tetrahydrocannabinol. *J. Nat. Prod.* 83, 88–98 (2020).

9. Berman, P. et al. A new ESI-LC/MS approach for comprehensive metabolic profiling of phytocannabinoids in Cannabis. *Sci. Rep.* 8, 14280 (2018).
10. Shoyama, Y., Yamauchi, T., Nishioka, I. & Cannabis, V. Cannabigerolic acid monomethyl ether and cannabinolic acid. *Chem. Pharm. Bull.* 18, 1327–1332 (1970).
11. Shoyama, Y., Kuboe, K., Nishioka, I. & Yamauchi, T. Cannabidiol monomethyl ether. A new neutral cannabinoid. *Chem. Pharm. Bull.* 20, 2072 (1972).
12. Kettenes-Van Den Bosch, J. J. & Salemink, C. A. Cannabis: XVI. Constituents of marihuana smoke condensate. *J. Chromatogr. A* 131, 422–424 (1977).
13. Bercht, C. A. L. et al. Cannabis: VII. Identification of cannabinol methyl ether from hashish. *J. Chromatogr. A* 81, 163–166 (1973).
14. Shoyama, Y., Hirano, H., Oda, M., Somehara, T. & Nishioka, I. Cannabichromevarin and cannabigerovarin, two new propyl homologues of cannabichromene and cannabigerol. *Chem. Pharm. Bull. Tokyo* 23, 1894–1895 (1975).
15. Mechoulam, R., Braun, P. & Gaoni, Y. 1972 Syntheses of Δ^9 -tetrahydrocannabinol and related cannabinoids. *J. Am. Chem. Soc.* 94, 6159–6165 (1972).
16. Yamauchi, T., Shoyama, Y., Matsuo, Y. & Nishioka, I. Cannabigerol monomethyl ether, a new component of hemp. *Chem. Pharm. Bull. Pharm. Bull.* 16, 1164–1165 (1968).
17. de Meijer, E. P. M. et al. The inheritance of chemical phenotype in Cannabis sativa L. *Genetics* 163, 335–346 (2003).
18. de Meijer, E. P. M., Hammond, K. M. & Sutton, A. The inheritance of chemical phenotype in Cannabis sativa L. (IV): cannabinoid-free plants. *Euphytica* 168, 95–112 (2009).
19. Cannabis Flos; New Text of the German Pharmacopoeia. (2018).
20. Compounds, B. et al. New methods for the comprehensive analysis. *Molecules* 23, 2639 (2018).

Acknowledgements

This work was supported by UNIHEMP research project “Use of industrial Hemp biomass for Energy and new biochemicals Production” (ARS01_00668) funded by Fondo Europeo di Sviluppo Regionale (FESR) (within the PON R&I 2017-2020—Axis 2—Action II—OS 1.b). Grant decree UNIHEMP prot. n. 2016 of 27/07/2018; CUP B76C18000520005. We are also thankful to the Military Chemical Pharmaceutical Institute of Florence for providing the FM2 cannabis inflorescence.

Author contributions

G.C. developed and supervised the project, P.L. and C.C. conceived the experiments plan and drafted the manuscript, C.C., F.R. and F.T. carried out the UHPLC-HRMS analyses, P.L. performed the stereoselective syntheses and characterization, L.L., M.I., C.B. and S.M. performed the formalin test in mice, A.L. processed the UHPLC-HRMS data. G.G., F.F. and M.A.V. revised and implemented the manuscript. All authors reviewed the manuscript.

Supporting information.

Identification of a new cannabidiol n-hexyl homolog in a medicinal cannabis variety with an antinociceptive activity in mice: cannabidihexol.

Pasquale Linciano^{1,†}, Cinzia Citti^{1,2,3,†}, Fabiana Russo¹, Francesco Tolomeo², Aldo Laganà^{3,4}, Anna Laura Capriotti⁴, Livio Luongo⁵, Monica Iannotta⁵, Carmela Belardo⁵, Sabatino Maione⁵, Flavio Forni¹, Maria Angela Vandelli¹, Giuseppe Gigli³, Giuseppe Cannazza^{1,3,*}

¹ Department of Life Sciences, University of Modena and Reggio Emilia, Via Campi 103, 41125 Modena, Italy

² Mediteknology (CNR spin-off company), Via Arnesano, 73100 Lecce

³ CNR NANOTEC, Istituto di Nanotecnologia, Via Monteroni, 73100 Lecce, Italy

⁴ Department of Chemistry, Sapienza University of Rome, Piazzale Aldo Moro 5, 00185 Rome, Italy

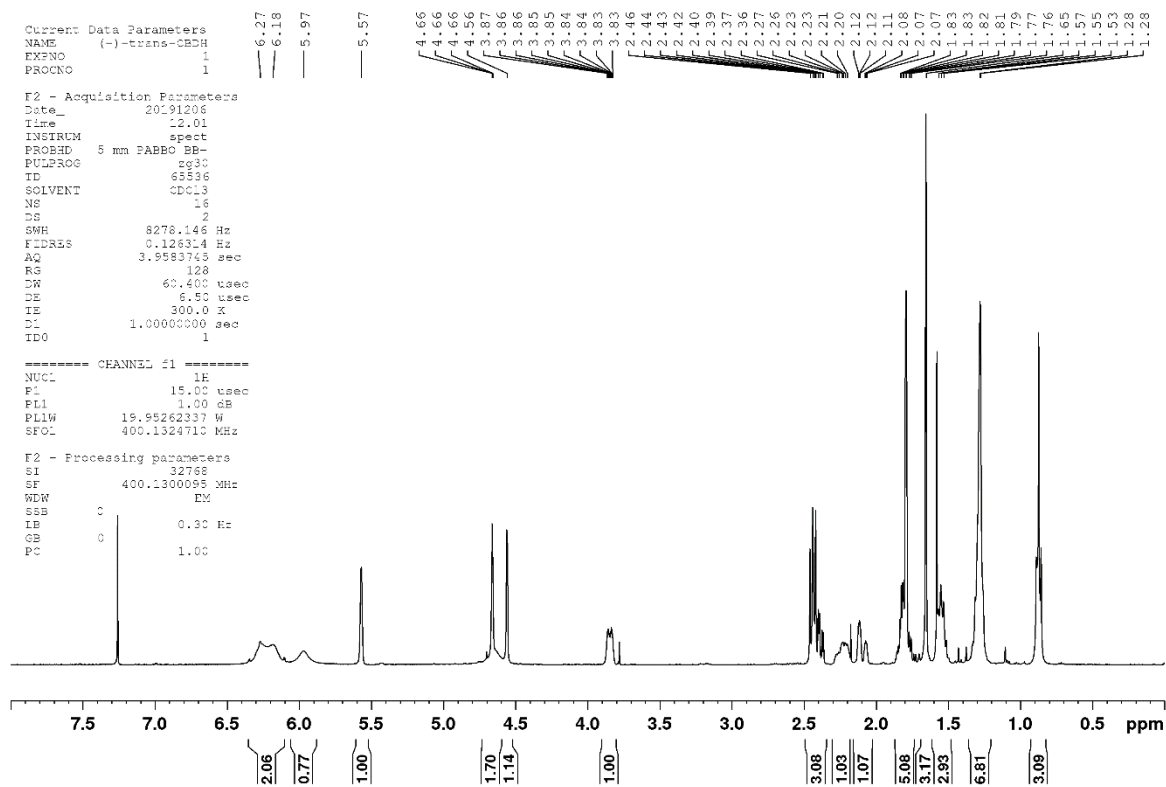
⁵ Division of Pharmacology, Università degli studi della Campania "L. Vanvitelli", Via Costantinopoli, 16, 80138, Naples, Italy

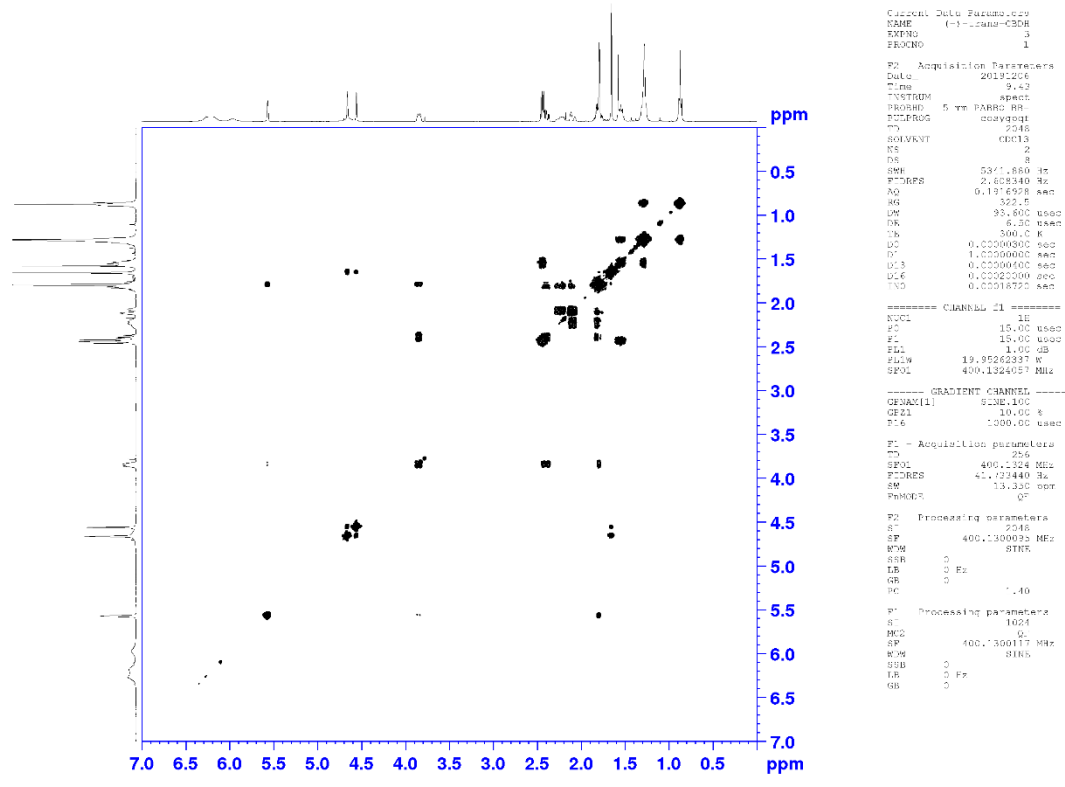
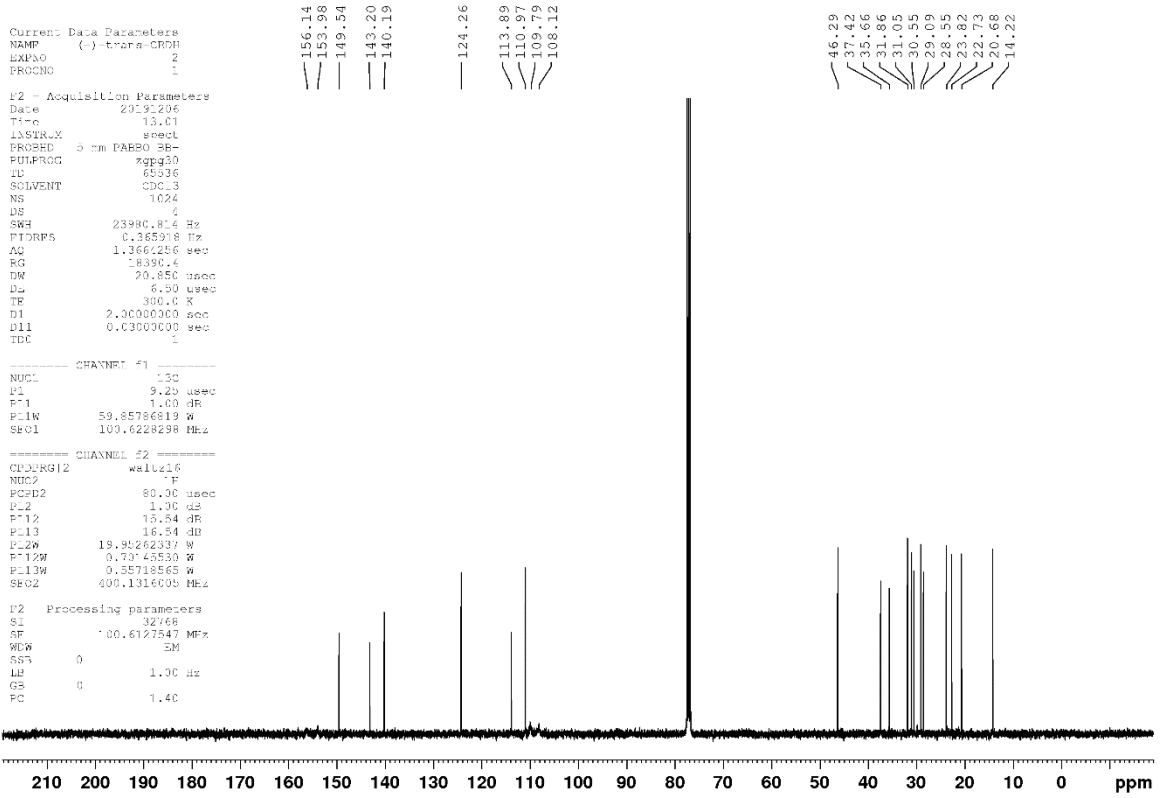
† These authors contributed equally to the work

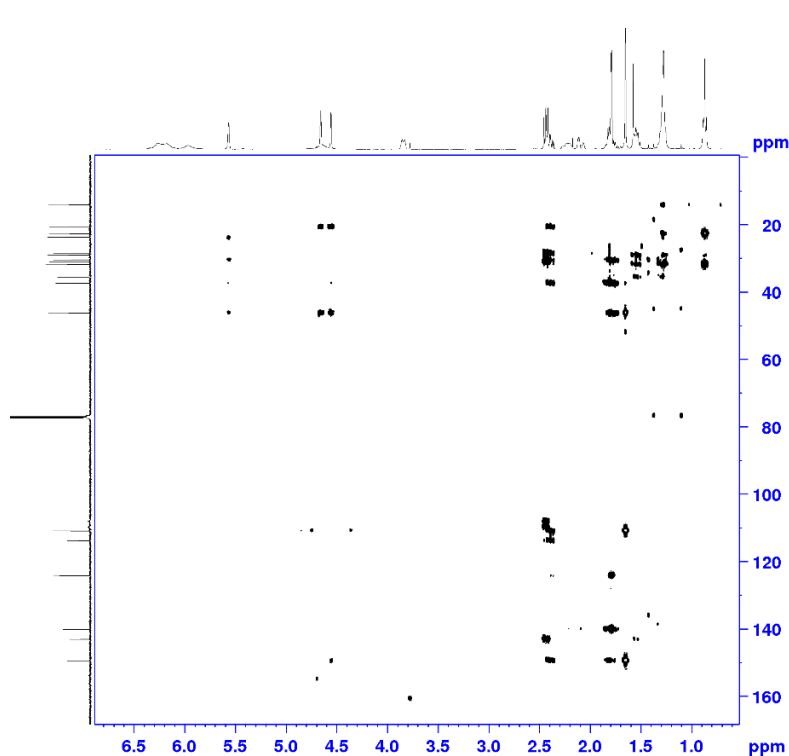
* Corresponding author: giuseppe.cannazza@unimore.it, tel: +39 059 2055013, fax: +39 059 2055750, ORCID ID: 0000-0002-7347-7315

Table of Content

Figure SI-1. NMR spectroscopic characterization of synthetic (-)- <i>trans</i> -CBDH	... SI-2
Figure SI-2. NMR spectroscopic characterization of synthetic (-)- <i>trans</i> - Δ^9 -THCH	... SI-5
Figure SI-3. NMR spectroscopic characterization of synthetic (-)- <i>trans</i> -CBDM	... SI-8
Figure SI-4. NMR spectroscopic characterization of synthetic (-)- <i>trans</i> - Δ^9 -THCM	... SI-9
Figure SI-5. NMR spectroscopic characterization of synthetic CBGM	...SI-10
Figure SI-6. Superimposition of ¹ H-NMR and ¹³ C-NMR spectra of synthetic and extracted (-)- <i>trans</i> -CBDH	...SI-11

Figure SI-1. NMR spectroscopic characterization of synthetic (-)-*trans*-CBDH





```

Current Data Parameters
NAME      (-)-trans-CBDL
EXINFO   3
PROCNO    1

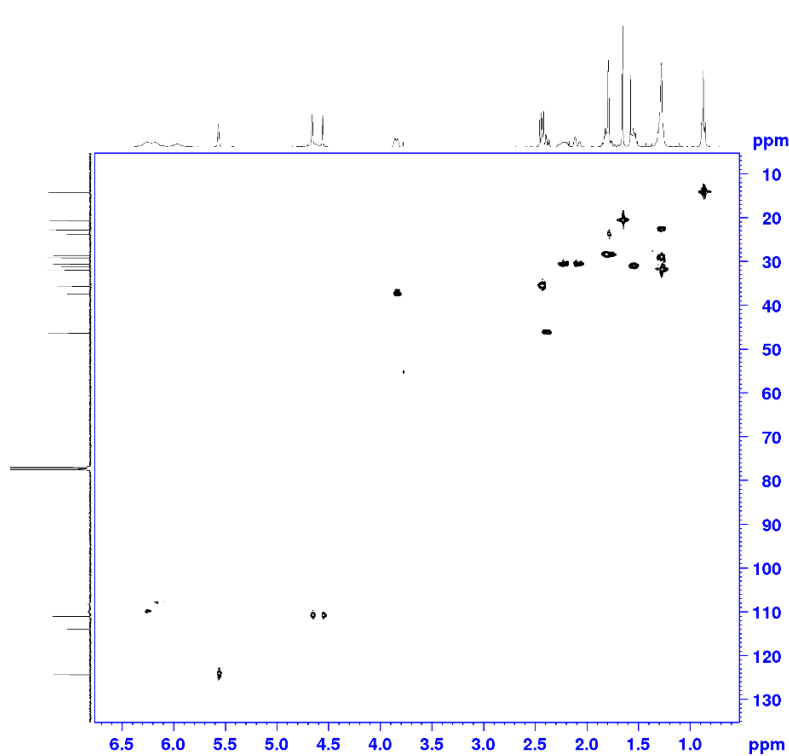
F2 - Acquisition Parameters
Date_     20191206
Time      10.18
INSTRUM   spect
PROBHD    5 mm PABBO-DE
PULPROG   hmgcp1pdzf
TD         4096
SOLVENT   CDCl3
NS         16
DS         16
SWH        5208.333 Hz
F2REFS    2.77166 Hz
AQ         0.393769 sec
RG         4096
DM         96.000 usec
DE         6.50 usec
TE         300.0 K
CNSF2     145.000000
CNSF13    8.000000
D0         0.0000000 sec
D1         1.0000000 sec
D2         0.00341828 sec
D6         0.0635000 sec
D16        0.0020000 sec
LNO        0.0002235 sec

----- CHANNEL f1 -----
NUC1       1H
P1         15.00 usec
P2         30.00 usec
PL1        1.00 dB
PL12       19.55262337 W
PL12#      100.6278138 MHz
SFO1       400.1325208 MHz

----- CHANNEL f2 -----
NUC2       13C
P3         9.20 usec
P4         18.00 usec
PL2        1.00 dB
PL2#       59.8578683 W
PL2#       100.6278138 MHz

----- GRADIENT CHANNEL -----
CPNAM[1]   SINE.100
CPNAM[2]   SINE.100
CPNAM[4]   SINE.100
GPZ1       30.00 s
SPZ2       30.00 s
CPZ3       40.00 s
PL6        1000.00 usec

F1 Acquisition parameters
TD         656
    
```



```

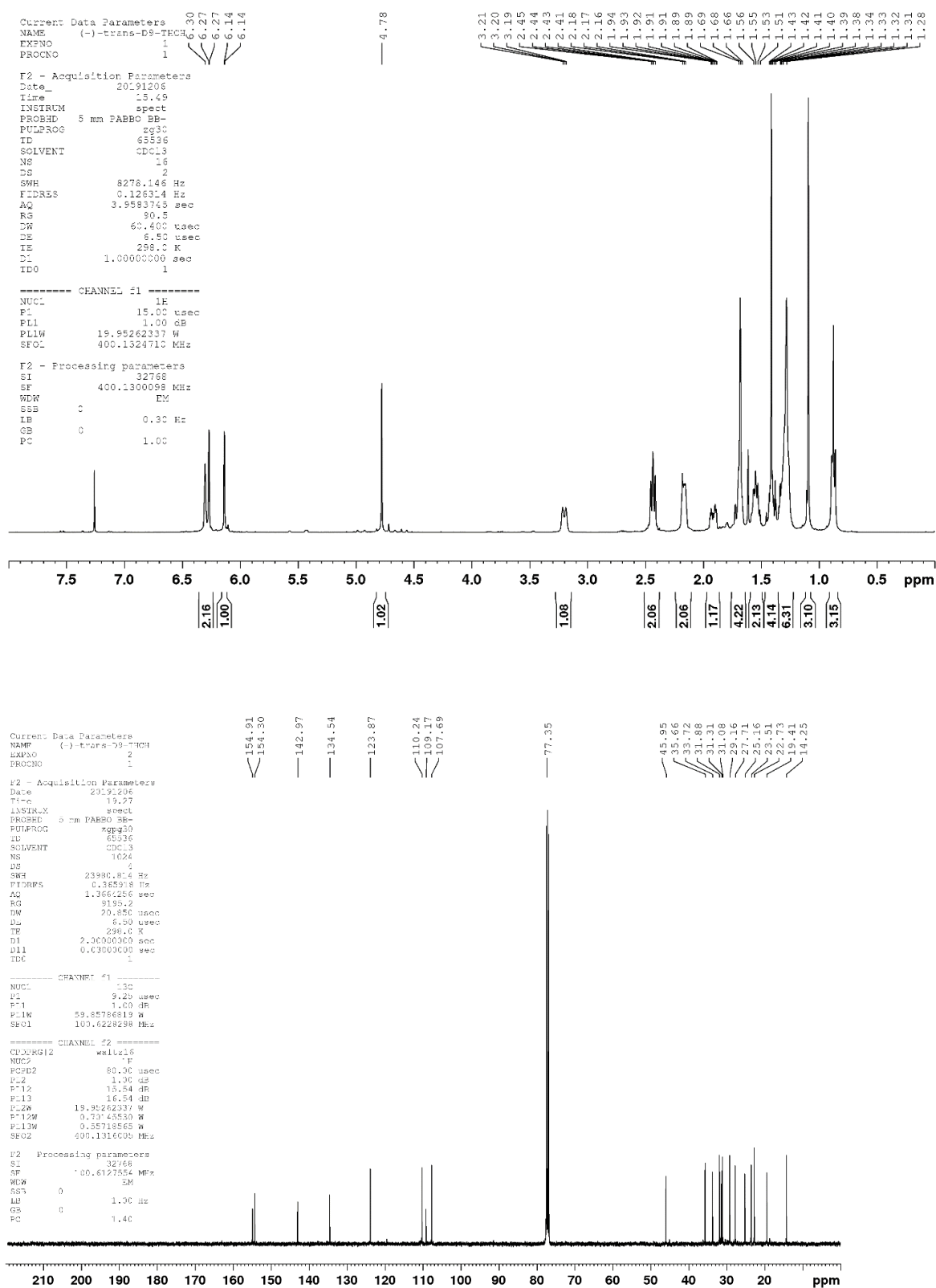
Current Data Parameters
NAME      (-)-trans-CBDL
EXINFO   4
PROCNO    1

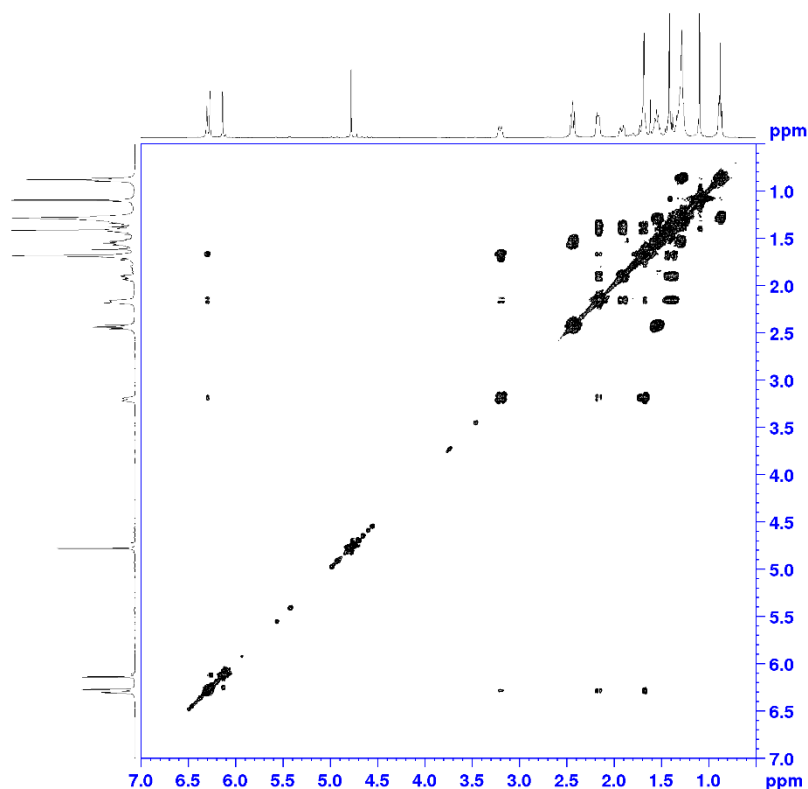
F2 - Acquisition Parameters
Date_     20191206
Time      9.56
INSTRUM   spect
PROBHD    5 mm PABBO-DE
PULPROG   hsqzdepp
TD         2048
SOLVENT   CDCl3
NS         4
DS         16
SWH        5341.680 Hz
F2REFS    2.806340 Hz
AQ         0.1916928 sec
RG         4096
DM         93.600 usec
DE         6.50 usec
TE         300.0 K
CNSF2     145.000000
D0         0.0000000 sec
D1         1.0000000 sec
D4         0.00172614 sec
D11        0.0000000 sec
D13        0.0000400 sec
D16        0.0020000 sec
D21        0.0034500 sec
LNO        0.0003000 sec
ZSOFHAS

----- CHANNEL f1 -----
NUC1       1H
P1         15.00 usec
P2         30.00 usec
P2#        18.00 usec
PL2        1.00 dB
PL2#       59.8578683 W
PL2#       100.6278138 MHz
SFO1       400.1324657 MHz

----- CHANNEL f2 -----
CPNAM[1]   SINE.100
CPNAM[2]   SINE.100
CPNAM[4]   SINE.100
GPZ1       30.00 s
SPZ2       30.00 s
CPZ3       40.00 s
PL6        1000.00 usec

F1 Acquisition parameters
TD         656
    
```


Figure SI-2. NMR spectroscopic characterization of synthetic (-)-*trans*- Δ^9 -THCH



Current Data Parameters
 NAME (-)-trans-29-THCE
 EXNO 2
 PROCNO 1

F1 - Acquisition Parameters
 Date_ 20191206
 Time 18.16
 INSTRUM spect
 PROBP2 5 mm PARBO 90
 PULPROG cosyzgq
 TD 2048
 SOLVENT CDCl3
 NS 2
 DS 8
 SFR 5341.880 Hz
 FIDRES 0.498340 Hz
 AQ 0.1916928 sec
 RG 61
 DW 93.600 usec
 DP 6.50 usec
 TP 298.0 K
 D0 0.0000000 sec
 D1 0.0000000 sec
 D15 0.0000000 sec
 D16 0.0000000 sec
 TMO 0.0001870 sec

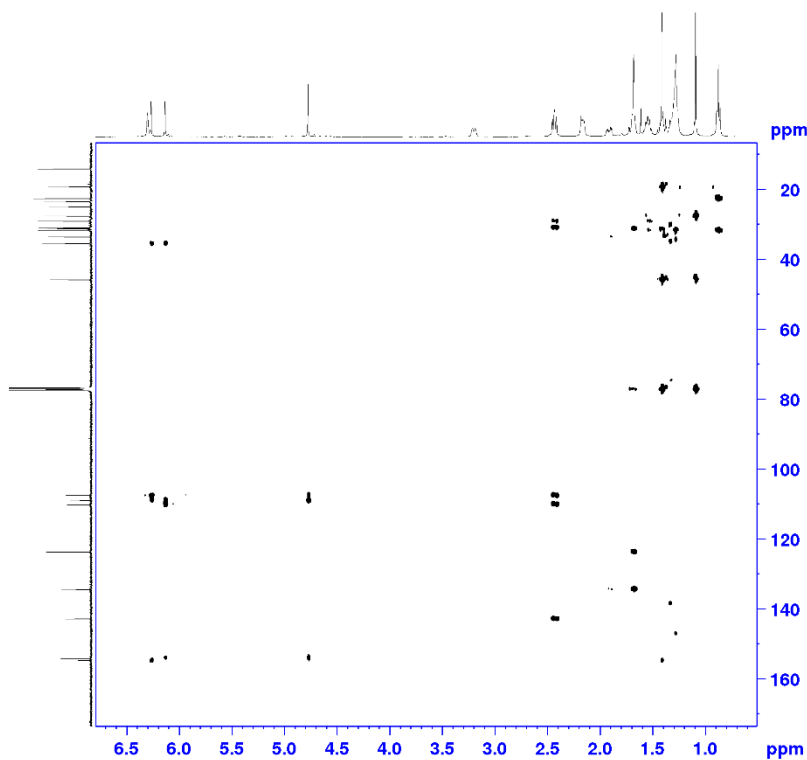
----- CHANNEL f1 -----
 NUC1 1H
 P1 15.00 usec
 P2 15.00 usec
 PL1 1.00 dB
 PLW 19.95262337 W
 SFO1 400.1324051 MHz

----- GRADIENT CHANNEL -----
 CPNMR[1] SINE,100
 CPZ1 10.00 %
 PL6 1000.00 usec

F1 - Acquisition parameters
 TD 256
 SFO1 400.1324 MHz
 FIDRES 41.733440 Hz
 SW 13.130 ppm
 FHM00 0F

F1 - Processing parameters
 ST 2048
 SF 400.1300129 MHz
 MR 8196
 GB 0 Hz
 GR 0
 PC 1.40

F1 Processing parameters
 ST 1024
 SF 400.1300146 MHz
 MR 0
 GB 0 Hz
 GR 0



Current Data Parameters
 NAME (-)-trans-19-THCE
 EXNO 4
 PROCNO 1

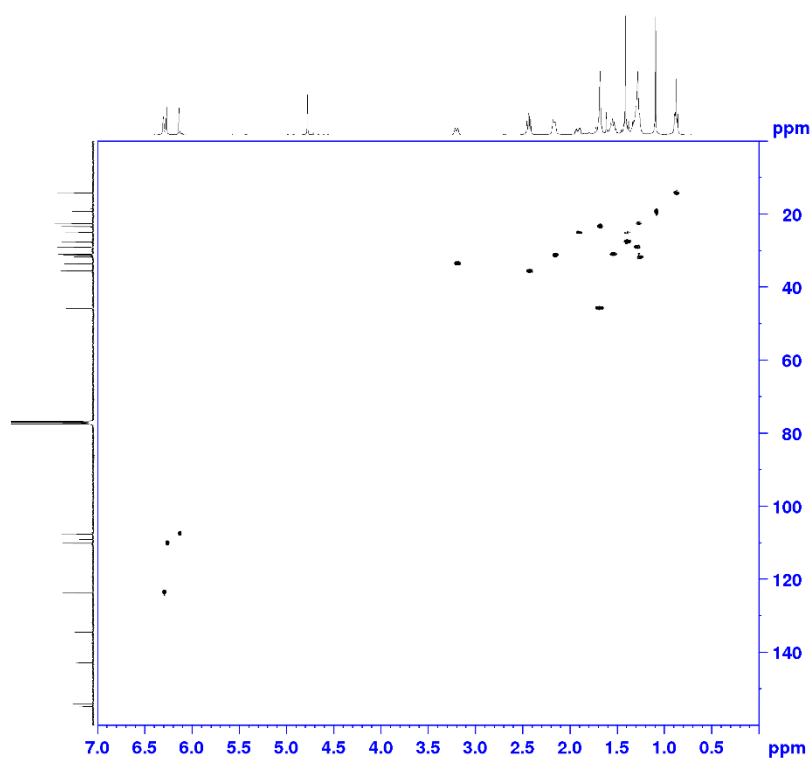
F2 - Acquisition Parameters
 Date_ 20191206
 Time 18.35
 INSTRUM spect
 PROBP2 5 mm PARBO 90
 PULPROG hbhsp1pndqf
 TD 4096
 SOLVENT CDCl3
 NS 16
 DS 16
 SFR 5208.333 Hz
 FIDRES 1.27566 Hz
 AQ 0.993760 sec
 RG 4096
 DW 96.000 usec
 DE 6.50 usec
 TR 299.2 K
 CNST1 145.0000000
 CNST13 8.0000000
 D0 0.0000000 sec
 D1 1.0000000 sec
 D2 0.03341828 sec
 D4 0.06250000 sec
 D16 0.00020000 sec
 LNO 0.00032135 sec

----- CHANNEL f1 -----
 NUC1 1H
 P1 15.00 usec
 P2 30.00 usec
 PL1 1.00 dB
 PLW 19.95262337 W
 SFO1 400.1325208 MHz

----- CHANNEL f2 -----
 NUC2 13C
 P3 9.00 usec
 P12 1.00 dB
 PLW 59.85786619 W
 SFO2 100.6208138 MHz

----- GRADIENT CHANNEL -----
 CPNMR[1] SINE,100
 CPNMR[2] SINE,100
 CPNMR[3] SINE,100
 CPZ1 50.00 %
 CPZ2 30.00 %
 CPZ3 40.00 %
 PL6 1000.00 usec

F1 Acquisition parameters
 TD 256



```

Current Data Parameters
NAME      (-)-trans-59-1bCl
EXPNO    3
PROCNO   1

F2 - Acquisition Parameters
Date_    20121206
Time     16.12
INSTRUM spect
PROBHD   5 mm ZABSO 2B-
PULPROG hsqcdeap
TD       2648
SOLVENT  CDCl3
NS       4
DS       16
SWH      5341.880 Hz
FIDRES   2.638340 Hz
AQ       0.1918928 sec
RG       4096
DM       93.609 usec
DE       6.59 usec
TE       298.2 K
CONST   145.000000
D0       0.0000000 sec
D1       1.0000000 sec
D4       0.00172414 sec
D11      0.03000000 sec
D13      0.00000000 sec
D16      0.00200000 sec
D21      0.00345000 sec
IN0      0.00000000 sec
ZSOLVBS

===== CHANNEL f1 =====
NUC1     13C
P1       15.00 usec
P2       30.00 usec
P2R      1.00 usec
PL1      1.00 dB
PL1W     19.95262337 W
SFO1     100.6261272 MHz

===== CHANNEL f2 =====
CPDPRG2  gpgp
NUC2     1H
P2       9.23 usec
P4       18.46 usec
PCPD2    70.00 usec
PL2      1.00 dB
PL12     18.00 dB
PL12W    59.85786819 W
PL12W    1.19432151 W
SFO2     400.1324657 MHz

===== GRADIENT CHANNEL =====
GPNAM1[1] SIML100
GPNAM1[2] S W 1.00
  
```

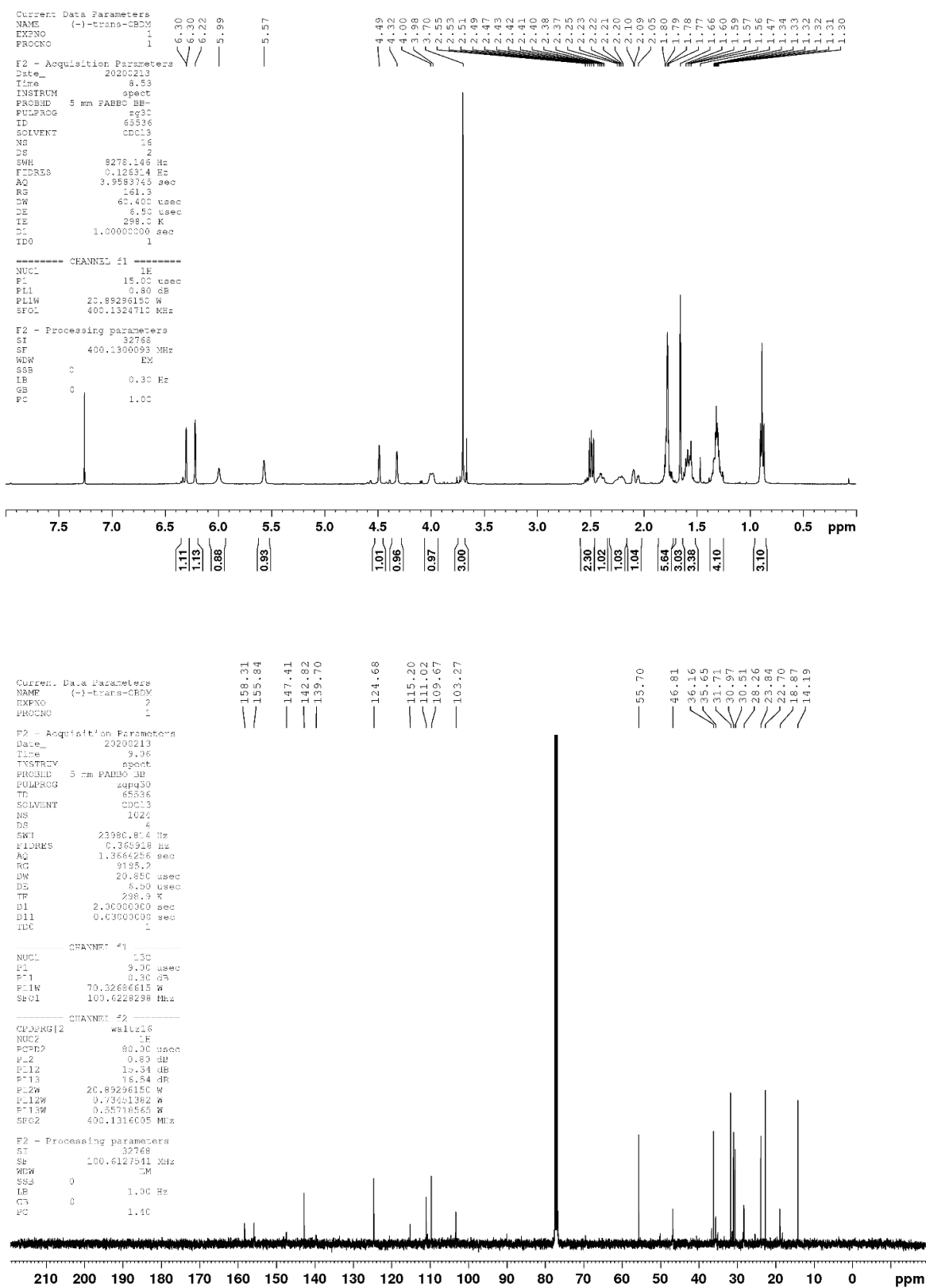
Figure SI-3. NMR spectroscopic characterization of synthetic (-)-*trans*-CBDM

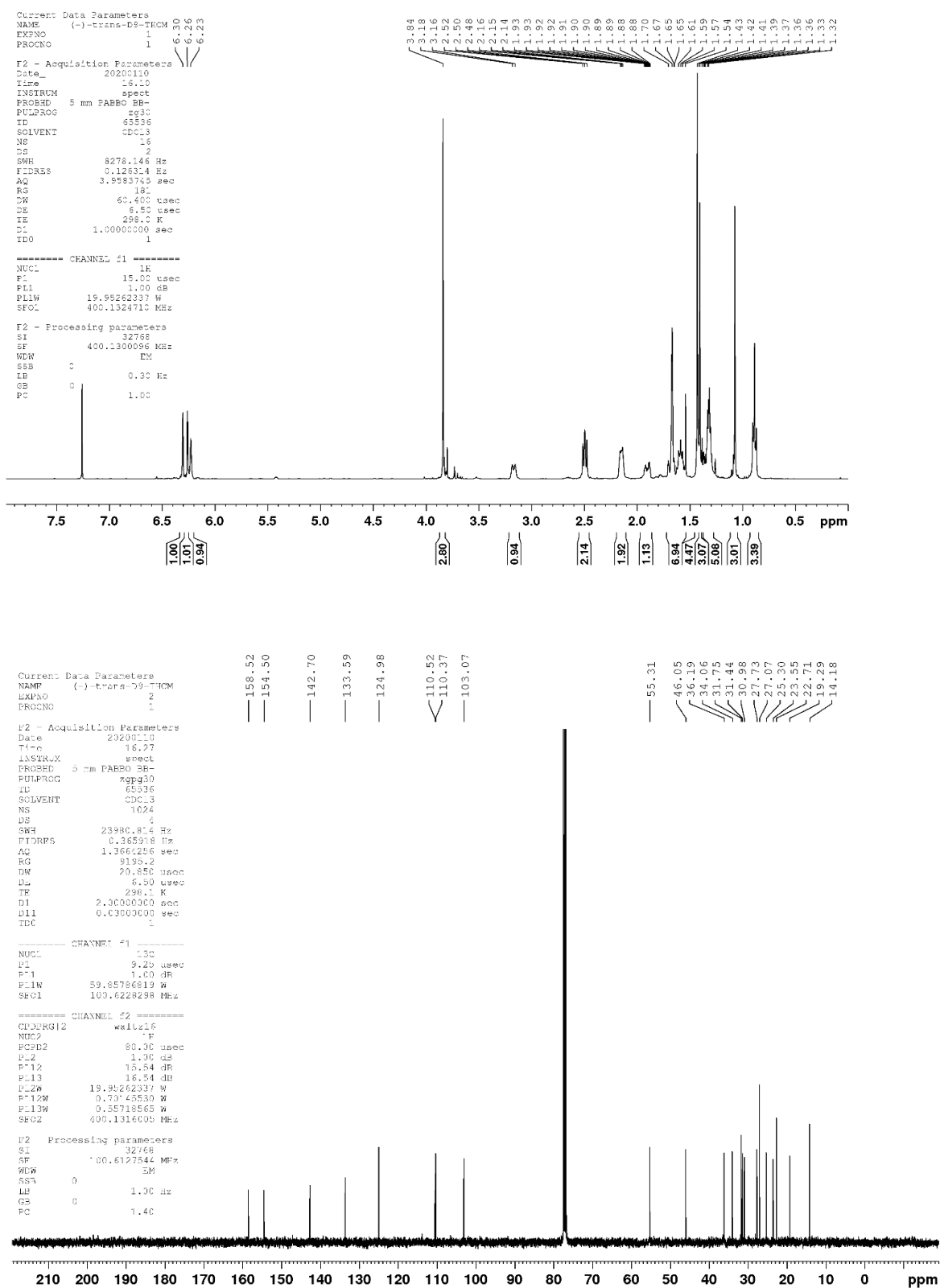
Figure SI-4. NMR spectroscopic characterization of synthetic (-)-*trans*- Δ^9 -THCM

Figure SI-5. NMR spectroscopic characterization of synthetic CBGM

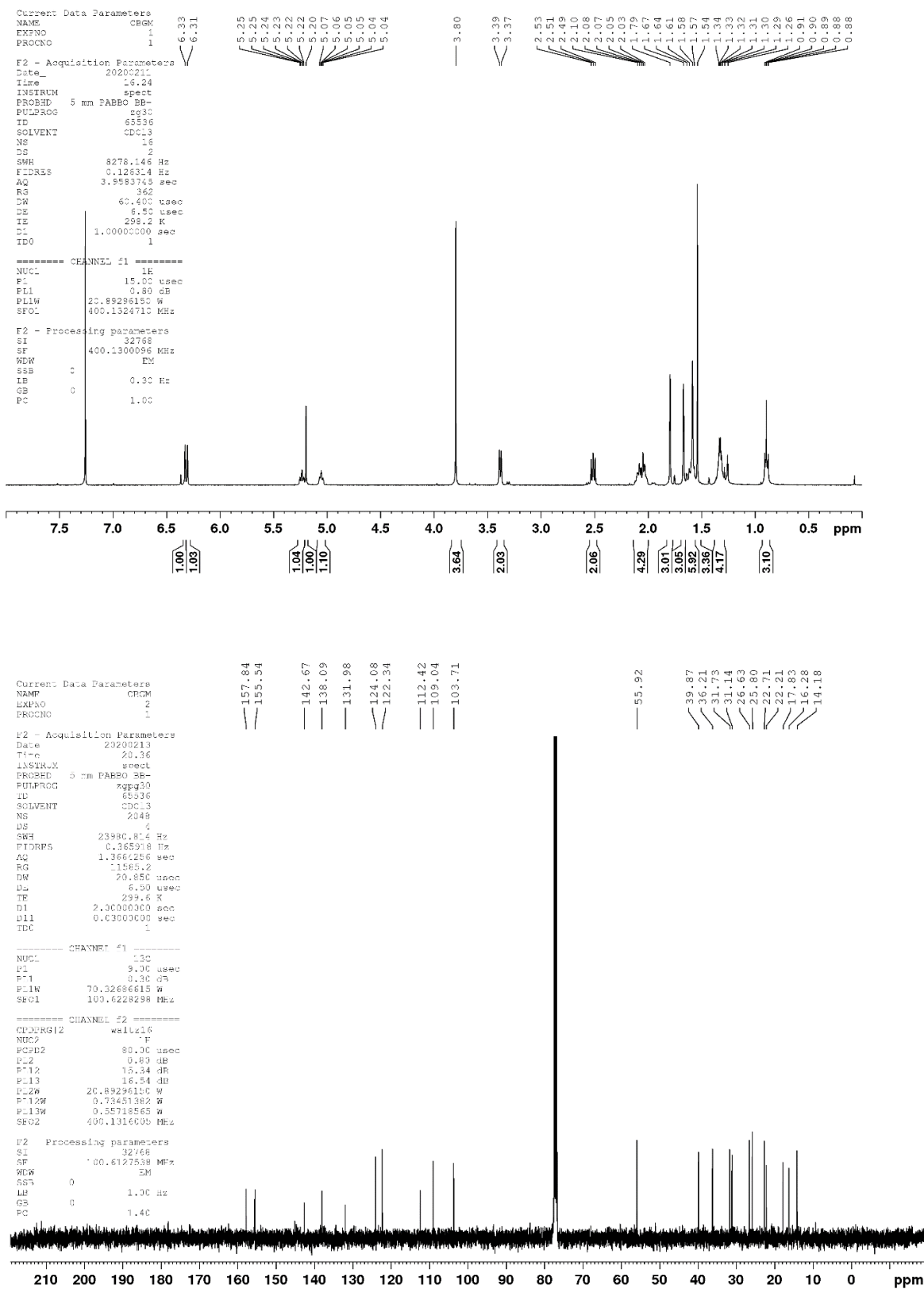
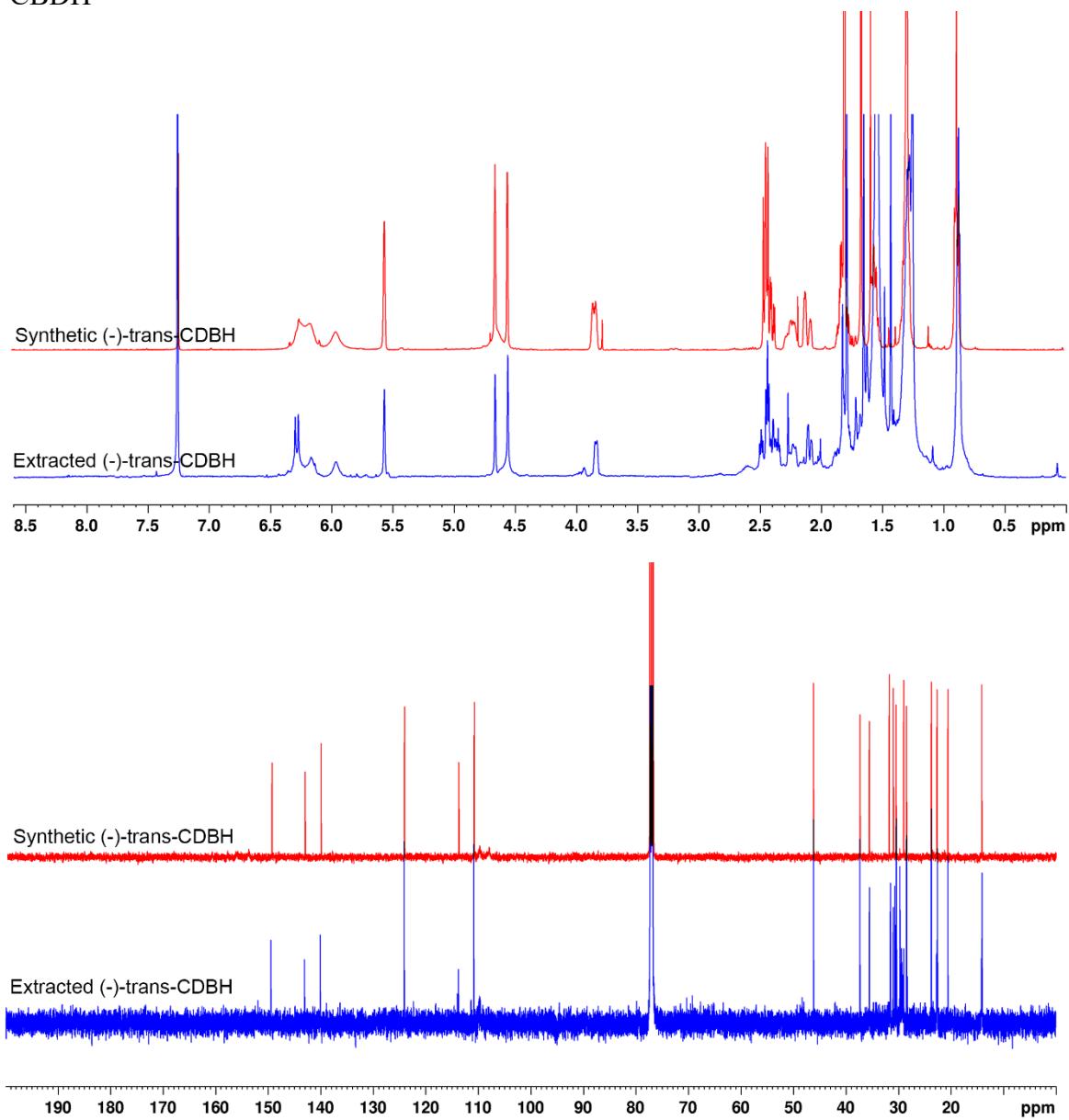


Figure SI-6. Superimposition of ^1H -NMR and ^{13}C -NMR spectra of synthetic and extracted (-)-trans-CBDH



THE NOVEL HEPTYL PHOROLIC ACID CANNABINOIDS CONTENT IN DIFFERENT CANNABIS SATIVA L. ACCESSIONS

Pasquale Linciano^{a,b}, Fabiana Russo^a, Cinzia Citti^{a,c,*}, Francesco Tolomeo^c, Roberta Paris^d, Flavia Fulvio^d, Nicola Pecchioni^e, Maria Angela Vandelli^a, Aldo Lagana^{e,f}, Anna Laura Capriotti^f, Giuseppe Biagini^g, Luigi Carbone^c, Giuseppe Gigli^c, Giuseppe Cannazza^{a,c}

a Department of Life Sciences, University of Modena and Reggio Emilia, Via G. Campi 103, 41125, Modena, Italy

b School of Pharmacy, University of Pavia, Viale Taramelli 12, 27100, Pavia, Italy

c Institute of Nanotechnology, CNR NANOTEC, Via Monteroni, 73100, Lecce, Italy

d CREA-Research Center for Cereal and Industrial Crops, Via di Corticella 133, 40128, Bologna, Italy

e CREA-Research Center for Cereal and Industrial Crops, S.S. 673 Km 25,200, 71122, Foggia, Italy

f Department of Chemistry, Sapienza University of Rome, Piazzale Aldo Moro 5, 00185, Rome, Italy

g Department of Biomedical, Metabolic and Neural Sciences, University of Modena and Reggio Emilia, Via G. Campi 287, 41125, Modena, Italy

Published in: *Talanta*. 2021.

doi: 10.1016/j.talanta.2021.122704

* Corresponding author. Institute of Nanotechnology, CNR NANOTEC, Via Monteroni, 73100, Lecce, Italy.

E-mail addresses: cinzia.citti@unimore.it, cinzia.citti@nanotec.cnr.it (C. Citti).

ABSTRACT

The recent discovery of the novel heptyl phytocannabinoids cannabidiphorol (CBDP) and Δ^9 -tetrahydrocannabiphorol (Δ^9 -THCP) raised a series of questions relating to the presence and abundance of these new unorthodox compounds in cannabis inflorescence or derived products. As fresh inflorescence contains mainly their acid precursors, which are not commercially available, an ad hoc stereoselective synthesis was performed in order to obtain cannabidiphorolic acid (CBDPA) and Δ^9 -tetrahydrocannabiphorolic acid (THCPA) to be used as analytical standards for quantitative purposes. The present work reports an unprecedented targeted analysis of both pentyl (C5) and heptyl (C7) CBD- and THC-type compounds in forty-nine cannabis samples representing four different chemotypes. Moreover, the ultrahigh performance liquid chromatography coupled to high-resolution mass spectrometry-based method was applied for the putative identification of other heptyl homologs of the most common phytocannabinoid acids, including cannabigerophorolic acid (CBGPA), cannabichromophorolic acid (CBCPA), cannabinophorolic acid (CBNPA), cannabielsophorolic acid (CBEPA), cannabicycophorolic acid (CBLPA), cannabitriophorolic acid (CBTPA), and cannabiripsophorolic acid (CBRPA). Cannabis research has made great progresses in the last few years thanks to a renewed interest in this plant from both public institutions and private companies. The attention towards cannabis is particularly due to the well-known class of phytocannabinoids, which includes the non-psychoactive cannabidiol (CBD) and the psychoactive Δ^9 -tetrahydrocannabinol (Δ^9 -THC) (Fig. 1). Since their discovery in the early 60s by Mechoulam and co-workers [1,2], the inventory of phytocannabinoids has grown to a very large extent reaching a number slightly below 150 [3]. In this regard, in the last two years six new phytocannabinoids, homologs of CBD and Δ^9 -THC, have been discovered, tearing down previous beliefs on the chemistry of cannabis [4–8]. The new homologs differ from canonical compounds in the length of the alkyl side chain on the resorcinyl group. In particular, cannabidibutol (CBDDB) [4–6] and Δ^9 -tetrahydrocannabutol (Δ^9 -THCB) [6] present a four-term linear ($-\text{CH}_2(\text{CH}_2)_2\text{CH}_3$) side chain, while cannabidihexol (CBDH) [8] and Δ^9 -tetrahydrocannabihexol (Δ^9 -THCH) [8] share a n-hexyl ($-\text{CH}_2(\text{CH}_2)_4\text{CH}_3$) side chain, and cannabidiphorol (CBDP) [7] and Δ^9 -tetrahydrocannabiphorol (Δ^9 -THCP) [7] are characterized by a seven-term linear ($-\text{CH}_2(\text{CH}_2)_5\text{CH}_3$) side chain (Fig. 1). All these new phytocannabinoids derive from their acid precursors cannabidibutolic acid (CBDDBA), tetrahydrocannabutolic acid (THCBA), cannabidihexolic acid (CBDHA), tetrahydrocannabihexolic acid (THCHA), cannabidiphorolic acid (CBDPA), and tetrahydrocannabiphorolic acid (THCPA), as they were putatively identified in samples of cannabis inflorescence [6–8]. Whilst the biological activity of CBD homologs has still to be evaluated, with the exception of the analgesic activity of CBDH [8], Δ^9 -THCB [6] and Δ^9 -THCP [7] were tested in both in vitro and in vivo assays. In details, preliminary investigations indicated that

Δ^9 -THCB has an affinity for CB1 receptors similar to that of Δ^9 -THC and a partial agonistic activity in behavioural tests [6]. On the other hand, Δ^9 -THCP showed a surprisingly 30 fold affinity for CB1 receptors compared to Δ^9 -THC and an in vivo cannabimimetic activity similar to Δ^9 -THC but at half the dose [7]. Besides the bewildering biological activity of Δ^9 -THCP, a natural cannabinoid with a side chain longer than five carbon atoms has never been reported nor even hypothesized until now, and these findings have baffled the scientific community on this topic [7]. As a result, these studies have paved the way to the identification of a new series of phytocannabinoids, the butyl [6], hexyl [8] and heptyl homologs [7] of CBD and THC, but have also disclosed the existence of a phytocannabinoid in a cannabis variety with a psychotropic activity potentially higher than THC, hitherto considered the main psychotropic constituent of cannabis. In our recent work, the identification of both CBDP and Δ^9 -THCP was accomplished after thermal decarboxylation of their putative acidic precursors, namely cannabidiphorolic acid (CBDPA) and Δ^9 -tetrahydrocannabiphorolic acid (Δ^9 -THCPA), which bear a carboxylic group on the resorcinylic moiety similarly to all phytocannabinoid precursors [7]. The experiments were performed on the medicinal cannabis variety FM2 bred as CINRO by CREA-CI (Research Centre for Cereal and Industrial Crops) site in Rovigo (Italy) and supplied by the Military Chemical Pharmaceutical Institute (Florence, Italy) [7]. It is known that the decarboxylation process can lead to a degradation of the phytocannabinoid molecules, thus not reflecting the actual concentrations of the original compounds in the plant [9–11]. The unambiguous identification of a new phytocannabinoid requires the confirmation of the retention time, mass to charge ratio (m/z), and MS/MS spectrum match with a pure analytical standard. As these novel phytocannabinoids are not commercially available, an in house stereoselective synthesis reported in the present work allowed to confirm our putative identification of CBDPA and Δ^9 -THCPA in the FM2 cannabis variety. On the other hand, the finding of new phytocannabinoids opened important questions: are they present in other cannabis accessions? If so, what are their actual concentrations? The present work aims to answer these open questions through the analysis of samples collected from forty-nine cannabis accessions provided by CREA-CI (Rovigo, Italy) and belonging to I-IV chemotypes [12] by an ultrahigh performance liquid chromatography coupled to high-resolution mass spectrometry (UHPLC-HRMS) method. Our research was not only limited to the determination of CBDPA and THCPA, but also to the putative identification of other species of this series of phytocannabinoids, such as cannabigerophorolic acid (CBGPA), cannabichromophorolic acid (CBCPA), and cannabielsoforolic acid (CBEPA), cannabiripsophorolic acid (CBRPA), cannabitriophorolic acid (CBTA), cannabicyclophorolic acid (CBLPA), and cannabinophorolic acid (CBNPA) (Fig. 1).

2. Materials and methods

2.1. Materials

Analytical grade ethanol 96% (Carlo Erba) was used for the extraction of the various cannabis inflorescence samples. LC-MS grade acetonitrile, water and formic acid were purchased from Carlo Erba (Milan, Italy) and employed in the UHPLC-HRMS analyses. Δ^9 -Tetrahydrocannabinol (Δ^9 -THC), Δ^9 -tetrahydrocannabinolic acid (THCA), cannabidiol (CBD), cannabidiolic acid (CBDA), cannabichromenic acid (CBCA), and cannabigerolic acid (CBGA) were purchased as Cerilliant certified analytical standards (Sigma-Aldrich, Milan, Italy). Cannabidiphorol (CBDP) and Δ^9 -tetrahydrocannabiphorol (Δ^9 -THCP) were prepared following our in house synthesis, as previously reported [7]. Reagents and solvents for synthesis were purchased from Sigma-Aldrich and used as arrived, unless otherwise specified. Organic solvents were abbreviated as follows: chloroform (CHCl_3); deuterium-chloroform (CDCl_3); cyclohexane (CE); dichloromethane (DCM); diethyl ether (Et_2O); dimethyl formamide (DMF).

2.2. Synthesis and characterization of CBDPA and THCPA

Reaction monitoring was performed by thin-layer chromatography on silica gel (60F-254, E. Merck) and checked by UV light or alkaline KMnO_4 aqueous solution. Reaction products were purified by flash chromatography on silica gel (40–63 μm) with the solvent system indicated. NMR spectra were recorded on a Bruker 400 spectrometer working at 400.134 MHz for ^1H and at 100.62 MHz for ^{13}C . Chemical shifts (δ) are reported in parts per million (ppm) and they were referenced to the solvent residual peaks (CDCl_3 $\delta = 7.26$ ppm for proton and $\delta = 77.20$ ppm for carbon); coupling constants are reported in hertz (Hz); splitting patterns are expressed with the following abbreviations: singlet (s), doublet (d), triplet (t), quartet (q), double doublet (dd), quintet (qnt), multiplet (m), broad signal (b). COSY spectra were recorded as a 2048×256 matrix with 2 transients per t1 increment and processed as a 2048×1024 matrix; the HSQC spectra were collected as a 2048×256 matrix with 4 transients per t1 increment and processed as a 2048×1024 matrix, and the one-bond heteronuclear coupling value was set to 145 Hz; the HMBC spectra were collected as a 4096×256 matrix with 16 transients per t1 increment and processed as a 4096×1024 matrix, and the long-range coupling value was set to 8 Hz. Optical rotation (α) was measured with a Polarimeter 240C (cell- length 100 mm, volume 1 mL) from PerkinElmer (Milan, Italy).

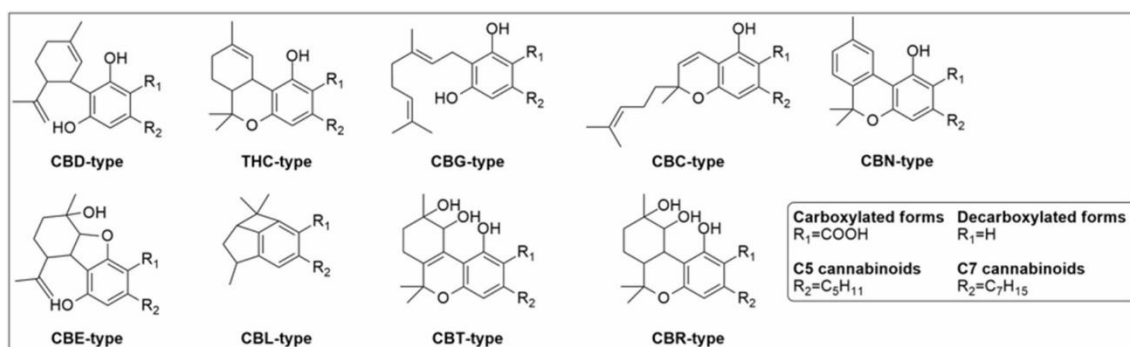


Fig. 1. General chemical structure of C5 and C7 phytocannabinoids. General chemical structure of C5 and C7 acid (carboxylated) and neutral (decarboxylated) phytocannabinoids, including CBD-, THC-, CBG-, CBC-, CBN-, CBE-, CBL-, CBT-, and CBR-type compounds.

2.3. Plant material and sample preparation

The female or monoecious inflorescences collected at maturity from forty-nine cannabis varieties/accessions were obtained from Cannabis germplasm collection available at the Research Centre for Cereal and Industrial Crops (CREA-CI) in Rovigo (Italy). In particular, seventeen samples were female inflorescences collected from chemotype I plants, with high THC levels (and poor in other cannabinoids); six samples were from chemotype II genotypes, with a balanced level of THC and CBD; twenty samples were from chemotype III varieties/accessions with a high CBD content (and low content of other cannabinoids); and six samples taken from chemotype IV genotypes, characterized by a prevalence of CBG. Chemotype V varieties were not taken into consideration as they have amounts of cannabinoids close to zero. More details on the genotypes (geographical origin, designation and use, harvest date, plant material, sex, drying process, cultivation) are given in Table S1 (Appendix A, Supplementary Material). Varieties are indicated with their names while other accessions are indicated with a code starting with S or a V depending whether they are propagated by seed or vegetatively. Cultivation of *Cannabis sativa* L. plants for scientific purposes on field areas and greenhouses with THC limit 5% and 10% respectively was authorized according to art. 26 of the D.P.R. 309/90 (authorization n. SP/052, March 31, 2017); indoor cultivations of cannabis plants with THC limit of 25% were granted with authorization n. SP/041 on March 13, 2017 according to art. 26 of the D.P.R. 309/90. Cultivation started in March 2018 and the harvesting was concluded in November 2018. Samples (2 g each) were finely ground and extracted in ethanol 96% according to the monograph of Cannabis flos of the German Pharmacopoeia and as previously reported in other works (500 mg in 50 mL of solvent) [7,13–15]. For the determination of the pentyl phytocannabinoids the samples were 1000-fold diluted with mobile phase, while the heptyl homologs were determined by diluting the sample 10-fold.

2.4. UHPLC-HRMS analysis

The analysis of the samples was carried out on a Thermo Fisher Scientific Ultimate 3000 UHPLC system provided with a vacuum degasser, a binary pump, a thermostated autosampler set at 4 °C, and a thermostated column compartment set at 25 °C. The chromatographic apparatus was interfaced to a heated electrospray ionization source and a Q-Exactive Orbitrap mass spectrometer (UHPLC-HESI-Orbitrap). For an optimal detection of the species under investigation, the parameters of the HESI source employed in our previous work were applied: capillary temperature, 320 °C; vaporizer temperature, 280 °C; electrospray voltage, 4.2 kV (positive mode) and 3.8 kV (negative mode); sheath gas, 55 arbitrary units; auxiliary gas, 30 arbitrary units; S lens RF level, 45 [4]. The analyses were acquired with Xcalibur 3.0 software (Thermo Fisher Scientific, San Jose, CA, USA) in full scan data-dependent acquisition (FS-dd-MS2) in positive (HESI⁺) and negative (HESI⁻) mode at a resolving power of 70,000 FWHM at m/z 200; the scan range was set in the window of m/z 150–750 to achieve a higher sensitivity for the molecular weight of cannabinoids, the AGC target was set at 3e6, the injection time at 100 ms and the isolation window for the filtration of the precursor ions at m/z 0.7 to improve selectivity [4]. A collision energy of 20 eV was used to fragment the precursor ions. $[M+H]^+$ and $[M-H]^-$ molecular ions were extracted from the total ion chromatogram (TIC) of each extracts and matched with pure analytical standards for accuracy of the exact mass ($\Delta = 5$ ppm), retention time ($\Delta = 0.1$ min) and MS/MS spectrum. The chromatographic separation was carried out on a column with a core-shell based stationary phase (Poroshell 120 SB-C18, 3 × 100 mm, 2.7 μ m, Agilent, Milan, Italy) and a mobile phase composed of 0.1% (v/v) aqueous formic acid (A) and acetonitrile (B) following the conditions employed in our previous work with a linear gradient from 70 to 98% B (0–25 min), an isocratic elution with 98% B (25.1–28.0) min, and a final re-equilibration with 70% B (28.1–30.0 min) [4,16]. A semi-quantitative analysis of CBD, Δ^9 -THC, CBDP, Δ^9 -THCP, CBDA, THCA, CBDPA, and THCPA was achieved by building the corresponding calibration curves using external standards. A stock solution of all analytes (1 mg/mL) was properly diluted to obtain five non-zero calibration points at the final concentrations of 10, 50, 100, 500 and 1000 ng/mL. The linearity was assessed by the coefficient of determination (R^2), which was greater than 0.997 for each analyte.

2.5. Statistical analysis

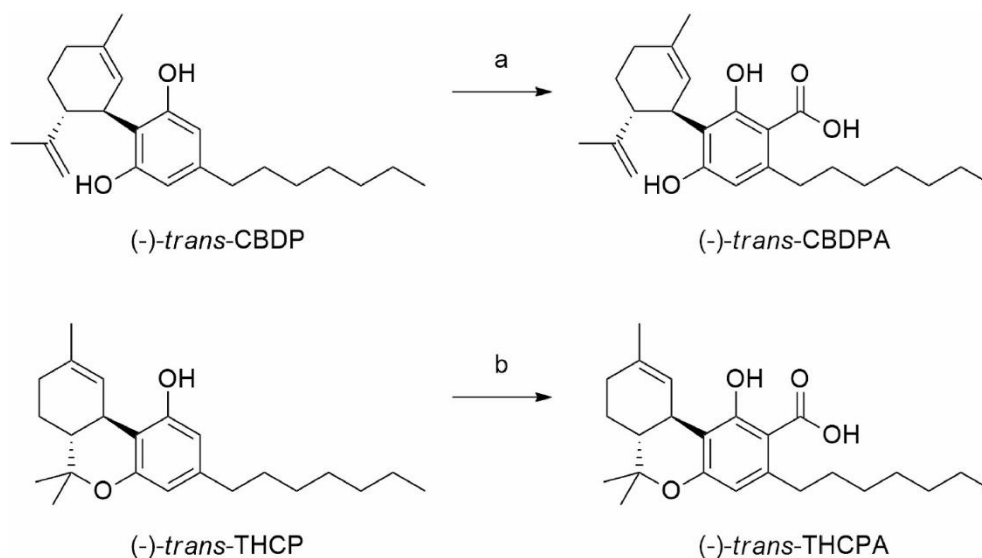
Data have been compared by one-way analysis of variance (ANOVA) followed by Bonferroni's correction for multiple comparisons. All the analyses were performed with GraphPad Prism 8 (GraphPad Software Inc., San Diego, CA, USA). Results are illustrated by mean values and standard errors of the mean and considered significant at $p < 0.05$.

3. Results and discussion

3.1. Synthesis and characterization of CBDPA and THCPA

Mechoulam already reported the chemical conversion of (-)-trans- CBD and (-)-trans- Δ^9 -THC into their corresponding acid (carboxylated) forms [17]. Accordingly, in the present study, the synthesis of the analytical standards of (-)-trans-CBDPA and (-)-trans- Δ^9 -THCPA was performed starting from the corresponding neutral (decarboxylated) cannabinoids (-)-trans-CBDP and (-)-trans- Δ^9 -THCP, which were prepared as previously reported by our research group [7]. As reported in Scheme 1, (-)-trans-CBDP and (-)-trans- Δ^9 -THCP were reacted in a Kolbe-like reaction, using 2 M methyl magnesium carbonate (MMC) in DMF as carboxylating agent, at 120–130 °C for 3 h for (-)-trans-CBDPA) or overnight for (-)-trans- Δ^9 -THCPA). Of note, the reaction was performed in close vessels in order to avoid the loss of carbon dioxide thus promoting the shift of the reaction equilibrium towards the product. The two standards were obtained in 39% and 7% yield for (-)-trans-CBDPA and (-)-trans- Δ^9 -THCPA, respectively, and the yields are in line with those reported by Mechoulam [17]. One of the main issues related to the acid forms of CBDs and THCs is their poor chemical stability, since they easily and spontaneously undergo decarboxylation, especially by heating. It was therefore necessary to set up a protocol to purify the CBDPA and THCPA from the unreacted starting materials and by-products, in particular using low-boiling solvents that could be evaporated at low temperature and under modest reduced pressure. CBDPA and THCPA were purified by solid phase extraction on silica gel. The reaction crude was eluted first using a mixture of CE/DCM 1:1 to remove the unreacted starting materials and by-products. In these conditions, CBDPA and THCPA were completely retained by silica gel. Thereafter, by elution with 100% Et₂O it was possible to recover the sole desired product. Moreover, since Et₂O is a very low-boiling solvent (boiling temperature 34.6 °C) it was removed at room temperature without affecting the stability of the final compounds that were thus achieved in high purity (>98%) as stated by UHPLC-UV/MS analysis. The chemical identification of synthetic (-)-trans-CBDPA and (-)-trans- Δ^9 -THCPA was confirmed by NMR spectroscopy and HRMS. The monodimensional (¹H and ¹³C) and bidimensional (COSY, HSQC and HMBC) NMR spectra are reported in the Material and Methods section and in Appendix B (Supplementary Material). Since (-)-trans-CBDPA and (-)-trans- Δ^9 -THCPA differ from the respective homologs (-)-trans-CBDA and (-)-trans- Δ^9 -THCA solely for the length of the alkyl chain on the resorcinylic moiety, no significant differences in the proton and carbon chemical shifts of the terpene and aromatic moieties were expected. The perfect match in the chemical shift of the terpene and aromatic moieties between the synthesized (-)-trans-CBDPA and (-)-trans- Δ^9 -THCPA and the respective homologs (-)-trans-CBDA and (-)-trans- Δ^9 -THCA [18], combined with the HRMS spectra and fragmentation pattern, allowed us to unambiguously confirm the chemical structures of the two new synthetic cannabinoids. Lastly, the stereochemistry of the starting materials (-)-trans-CBDP and (-)-trans- Δ^9 -THCP was fully

investigated and confirmed in our previous study [8]. We were confident that the synthetic conditions adopted for the synthesis of the corresponding acids did not affect the absolute configuration of the two stereocenters, and the position of the double bond. For these reasons, we could confirm the Δ^9 position of the double bond and the 1' R, 2' R and 6aR, 10aR absolute configuration for (-)-trans-CBDPA and (-)-trans- Δ^9 -THCPA, respectively. Description of the synthetic procedure and characterization of the two new compounds are reported in Appendix B (Supplementary Material).



Scheme 1. Reagents and conditions: a) 2 M MMC in DCM, 120 °C, 3 h. b) 2 M MMC in DCM, 130 °C, 18 h.

3.2. Identification of CBDPA and THCPA

The acidic precursors of CBDP and Δ^9 -THCP, namely cannabidiphorolic acid (CBDPA) and tetrahydrocannabiphorolic acid (THCPA), were putatively identified and reported in a previous paper [7]. In the present work, these phytocannabinoid acids were identified in the forty-nine varieties by means of high-resolution Orbitrap mass spectrometry and confirmed by match with pure synthesized standards. In details, CBDPA and THCPA presented the same molecular ions in both positive and negative ionization mode with $[M+H]^+$ at m/z 387.2530 and $[M-H]^-$ at m/z 385.2384, respectively, and molecular formula $C_{24}H_{34}O_4$. CBDPA and THCPA eluted at 18.78 min and 22.18 min respectively (Fig. 2). As expected, the fragmentation spectra of the two compounds were identical in positive ionization mode (HESI⁺), while they could be distinguished in negative ionization mode (HESI⁻). In HESI⁺ mode, the molecular ion was barely visible, as well as the fragment corresponding to the loss of the carboxylic moiety at m/z 341; the loss of water, instead, generated the base peak at m/z 369. The fragment at m/z 289 was produced by the loss of water and part of the terpene moiety, followed by the complete loss of the latter to generate the fragment at m/z 247. On the other hand, the relative abundance of the fragments in HESI⁻ mode was diagnostic of the cannabinoid type since CBD-type cannabinoids generally present a fragment rich spectrum, whereas THC-type spectra are usually

characterized by a reduced number of fragment peaks. The only common features were the base peak, which corresponded to the precursor ion, and the fragment generated by the loss of CO₂ at m/z 341. The loss of water generated the fragment at m/z 367, which was visible only in the spectrum of CBDPA. The fragment at m/z 273, higher in the spectrum of CBDPA, was produced by the loss of water and part of the terpene moiety, while the fragment at m/z 207, lacking the whole terpene moiety, was observed only in the CBDPA spectrum. Fig. 2 shows the match of retention times in both HESI⁺ and HESI⁻ mode of CBDPA and THCPA in a synthetic standard mixture (100 ng/mL) and in a real sample (from the medical variety CINRO cultivated indoor); comparison of the high-resolution mass fragmentation spectra of the two compounds in both ionization modes are also reported. Fragmentation patterns of both C7 phytocannabinoid acids confirmed the data previously reported for putatively identified CBDPA and THCPA [16].

3.3. Putative identification of heptyl phytocannabinoid acids

The discovery of CBDPA and THCPA in the pharmaceutical cultivar CINRO [7] prompted the research of other phytocannabinoids of the heptyl series. Therefore, the possible existence of cannabigerophoric acid (CBGPA), cannabichromophoric acid (CBCPA), cannabielsohporolic acid (CBEPA), cannabicyclophoric acid (CBLPA), cannabitriflorolic acid (CBTPA), and cannabiripsophoric acid (CBRPA), heptyl homologs of the most common phytocannabinoid acids, was further investigated (Fig. 1). The corresponding precursor ions were searched in both HESI⁺ and HESI⁻ mode, but only two of the aforementioned compounds were detected and only in HESI⁻ mode, which is generally more sensitive for carboxylated cannabinoids. Due to the likely scarce abundance of such homologs, it was not possible to detect the HESI⁺ peak and HRMS spectra. The [M-H]⁻ ion at m/z 387.2546 corresponding to the chemical formula C₂₄H₃₆O₄ was putatively identified as CBGPA given the perfect correspondence of the fragments and relative abundance in the HRMS spectrum with its pentyl homolog cannabigerolic acid (CBGA) with the addition of two methylene units (28.0313 amu), as shown in Figure S1 (Appendix B, Supplementary Material). CBGPA precursor ion [M-H]⁻ at m/z 387 is considerably higher than that of CBGA at m/z 359. Such phenomenon occurs also for the other C7 species like THCPA and CBDPA, for which the precursor ion exceeds by approximately twice that of their C5 homologs THCA and CBDA, most likely because C7 precursor ion needs higher collision energies for a stronger fragmentation. The loss of water produces the base peak for both CBGA and CBGPA at m/z 341 and 369 respectively. Besides the fragment generated by the loss of CO₂ at m/z 315 and 343 for CBGA and CBGPA respectively, the other fragments showed very low abundance. In the same way, CBCPA was putatively identified from its [M-H]⁻ molecular ion and chemical formula, which are identical to those of CBDPA and THCPA. Moreover,

the HRMS spectrum of the putative CBCPA was comparable to that of its pentyl homolog cannabichromenic acid (CBCA) with two additional methylene units (Figure S2, Appendix B, Supplementary Material). The highest signal for the peak area of CBGPA and CBCPA was registered in the sample from the female inflorescence of the experimental accession “V_02”. The other heptyl phytocannabinoid acids were not found, although all the pentyl homologs, cannabiripsolic acid (CBRA), cannabitrilic acid (CBTA) and cannabielsoic acid (CBEA), with the exception of cannabicyclolic acid (CBLA), were detected based on the putative identification reported in the literature [14,19].

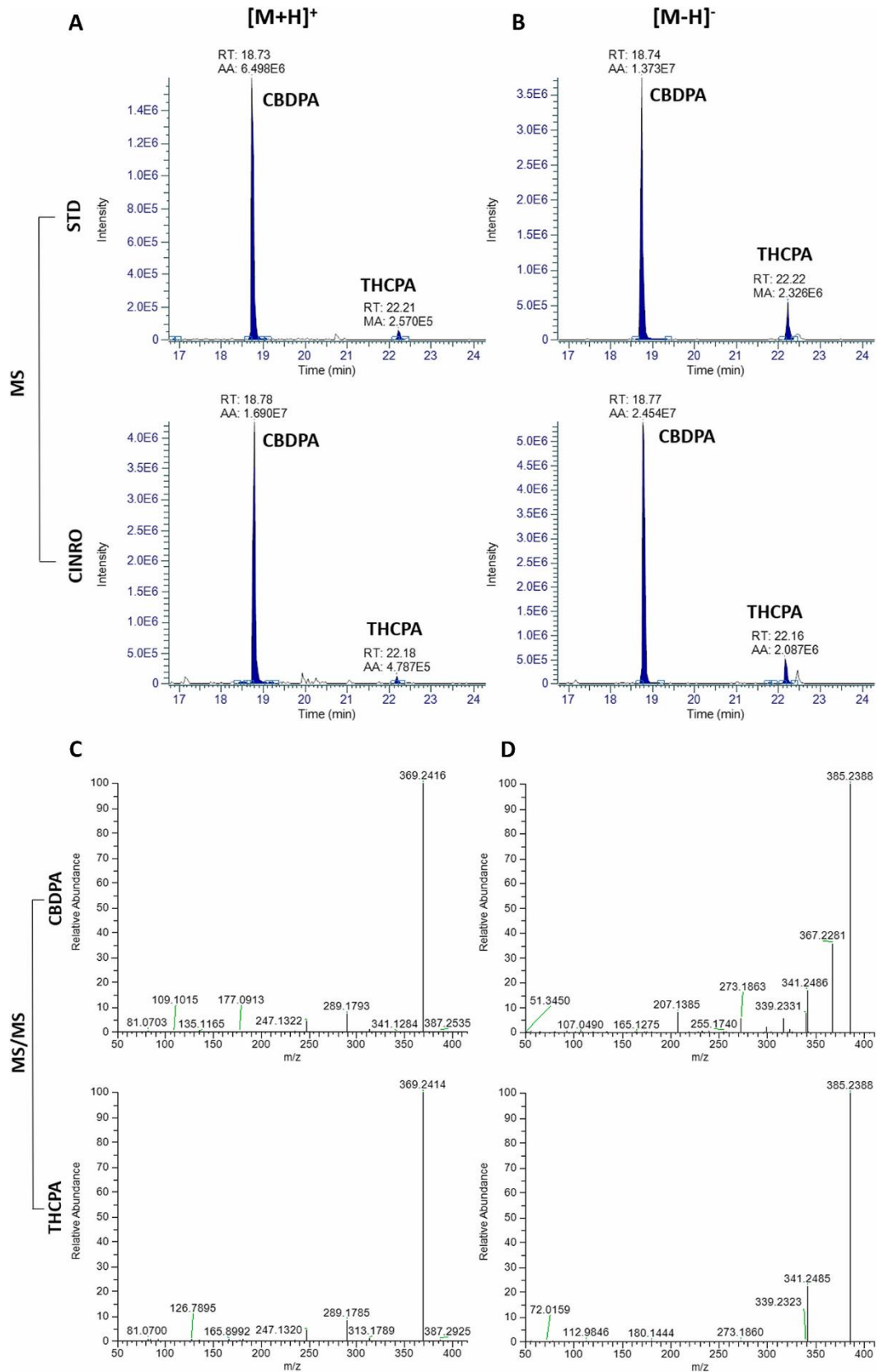


Fig. 2. Match of standard and natural CBDPA and THCPA. HPLC-HRMS chromatograms of standard CBDPA and THCPA obtained by stereoselective synthesis and the same compounds found in a cannabis variety (CINRO) in both positive (A) and negative (B) ionization mode. Tandem HRMS fragmentation spectra of CBDPA and THCPA in both positive (C) and negative (D) ionization mode.

3.4. Semi-quantification of pentyl and heptyl phytocannabinoids

The synthesized pure standards, obtained with a purity greater than 98%, were used to build the calibration curves for the semi-quantification of CBDPA and THCPA. Moreover, the authentic standards of CBDP and Δ^9 -THCP were available from previous in-house synthesis [7]. These calibrations allowed to provide a reasonably accurate measure of the concentration of the new heptyl phytocannabinoids, along with their pentyl counterparts CBDA, THCA, CBD, and Δ^9 -THC for which the pure analytical standards are commercially available. Δ^8 -THC was not detected. According to their optimal ionization parameters, the phytocannabinoid acids were determined in the cannabis samples in HESI⁻ mode, whereas the decarboxylated phytocannabinoids were quantified in HESI⁺ mode. Good coefficients of linear correlation were obtained in the range 10–1000 ng/mL for all analytes. The results were obtained from the analysis of three replicates for each sample and summarized per chemotype in Fig. 3. Data are graphed as micrograms of phytocannabinoid per gram of plant material. Detailed data of phytocannabinoids concentrations in each cannabis accession is given in Appendix B (Supplementary Material, Figures S3 and S4). THCPA was present in half of the samples in concentrations above 100 $\mu\text{g/g}$ reaching the highest amount of 446 $\mu\text{g/g}$ in the CREA experimental accession “V_08–2018” (chemotype I) and 433 $\mu\text{g/g}$ in the variety “CINRO” (chemotype II) ($p < 0.001$, Figure S4). CBDPA reached the highest concentration value of about 1030 $\mu\text{g/g}$ in the floral sample taken from accession “V_02” ($p < 0.001$, Figure S3), which has a chemotype III. Both accessions were selected at CREA-CI for pharmaceutical purposes, with V_08 bearing a prevalence of THCA and V_02 a prevalence of CBDA. These samples showed a proportion of heptyl cannabinoids in the total of main C5 and C7 cannabinoid fraction equal to 0.95% and 0.89% respectively (calculated as $C7/(C5+C7)$). The highest amount of C7 THC and CBD homologs was found in the female inflorescence of CINRO medical variety (cultivated indoor) with about 1221 $\mu\text{g/g}$, equal to 1.20% out of the total amount of C5 and C7 cannabinoids and with 67.8% of purity in total CBDP ($\text{CBDP}/C7$) ($p < 0.001$). This variety is a chemotype II with $\text{THCA} + \text{CBDA} = 15\%$ in a 2:3 ratio. Instead, the highest proportion of C7 homologs was found in samples from chemotype I Chinese landraces (S1770, S1605, S1639, and V_11), with a mean value of 1.18% of $C7/(C5+C7)$ cannabinoids ($p < 0.001$). Among the European hemp varieties with chemotype III, the proportion of heptyl homologs ranged from 0.23% to 0.55%. In the same group, the average of total CBD and total THC concentrations showed a similar pattern to total CBDP and THCP concentrations ($p > 0.05$) respectively. A straightforward picture of total CBD vs total CBDP and total THC vs total THCP in percentage is illustrated in Fig. 4 (both CBD and THC percentages were calculated out of total C5 cannabinoids, as well as CBDP and THCP results were calculated out of total C7 cannabinoids). As expected, in THC-predominant plants THC and THCP covered the almost total percentage of total

C5 and C7 cannabinoid fractions respectively, while CBD and CBDP represented only a small percentage ($p < 0.001$, Fig. 4). The opposite trend (low THC and THCP and high CBD and CBDP content) was observed in CBD-rich plants belonging to chemotype III ($p < 0.001$). No significant difference was observed in the percentages of total THCP/C7 compared to total THC/C5, as well as between total CBDP/C7 and total CBD/C5 in chemotype III plants ($p > 0.05$), suggesting that the distribution of the C7 phytocannabinoids follows that of their C5 homologs, thus being representative of the belonging chemotype. Only chemotype IV presented significant differences between the investigated couples of phytocannabinoids ($p < 0.001$), most likely due to the very low if not null concentrations of C7 species in this chemotype ($p < 0.05$). Compared to their C5 counterpart, C7 homologs are consistently less abundant in all accessions, thus suggesting that the final concentrations of these new phytocannabinoids are generated from less abundant substrates. Considering that CBGA is the substrates used by CBDA- and THCA synthase to produce CBD-type and THC-type compounds respectively, the concentrations of C7 phytocannabinoids should be strictly connected to those of CBGPA and its precursors [20] and to a different affinity and catalytic activity of THCAS and CBDAS towards alkyl homologs [21]. As a result, C7 cannabinoids represented only a small percentage out of the sum of C5 and C7 cannabinoids ($p < 0.001$) ranging from 0.11% to 1.27%, which might reflect the low abundance of the substrate CBGPA (and its phorolic precursors). The experimental data indicated that almost all the samples tested presented a variable amount of the novel C7 phytocannabinoids, whose pharmacology is still unexplored. From preliminary results, Δ^9 -THCP showed an extraordinary activity profile with 33-fold in vitro affinity for CB1 receptors compared to its C5 homolog and a cannabimimetic behavior similar to Δ^9 -THC but at lower doses [7]. Although Δ^9 -THCP concentrations here reported were in the order of $\mu\text{g/g}$, a potential therapeutic effect should not be completely ruled out. In this regard, fiber-type and drug-type cannabis can be distinguished by a THC cut-off of 0.2%, above which the plant is classified as drug-type. The highest level of THCP was registered for CINRO at about 0.5 mg/g (0.05% on inflorescence dry weight). Considering the higher biological activity compared to THC and the complexity of its pharmacokinetics in the human body, such potency could hypothetically be equivalent to a plant with a THC content higher than 1%. Moreover, it should be taken into account that thanks to the new frontiers in cannabis chemotype breeding it is possible to produce high potency plants with increased levels of these novel phytocannabinoids. On the other hand, although CBDP pharmacological role has not been cleared to date, plants rich in this phytocannabinoid could be potentially bred for the treatment of important inflammatory pathologies.

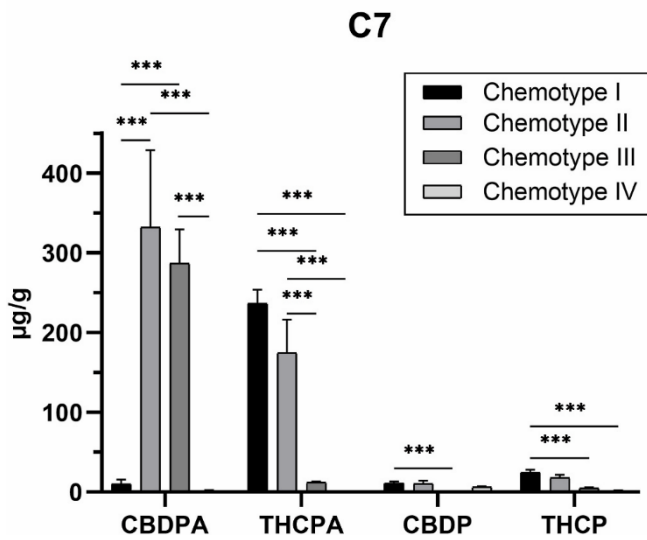
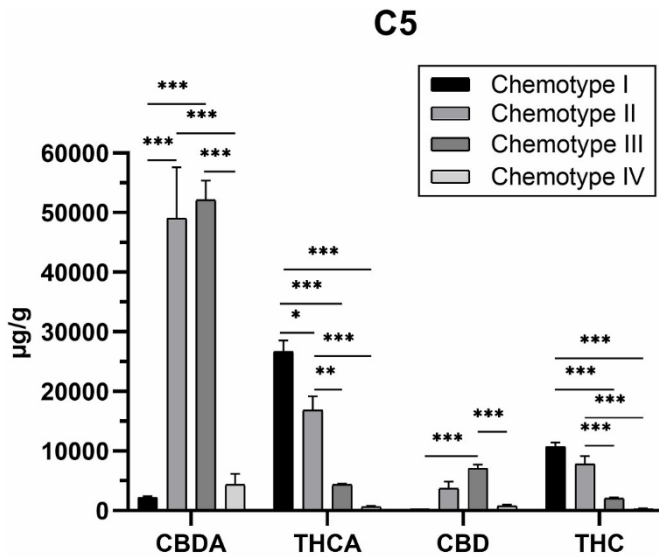


Fig. 3. Distribution of C5 and C7 CBD-type phytocannabinoids among chemotypes I-IV. Average amount of CBDA, CBD, THCA, and THC (C5) in the four chemotypes (I, II, III, and IV) calculated as $\mu\text{g/g}$ and reported as mean \pm SEM ($n = 3$) (top). Average amount of CBDPA, CBDP, THCPA, and THCP (C7) in the four chemotypes (I, II, III, and IV) calculated as $\mu\text{g/g}$ and reported as mean \pm SEM ($n = 3$) (bottom). Significant difference is expressed through asterisks: * $p < 0.05$, ** $p < 0.01$, *** $p < 0.001$.

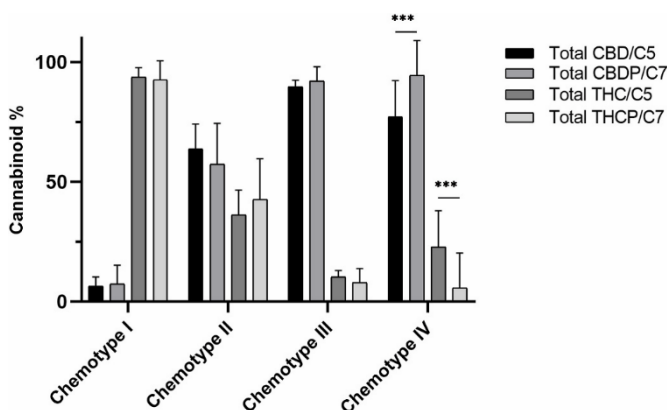


Fig. 4. Distribution of total CBD-type and total THC-type phytocannabinoids among chemotypes I-IV. Percentages of total CBDP (calculated as the sum of $(\text{CBDPA} \cdot 0.877) + \text{CBDP}$ out of C7 phytocannabinoids), total CBD (calculated as the sum of $(\text{CBDA} \cdot 0.877) + \text{CBD}$ out of C5 phytocannabinoids), total THCP ($(\text{THCPA} \cdot 0.877) + \text{THCP}$)/C7), and total THC ($(\text{THCA} \cdot 0.877) + \Delta^9\text{-THC}$ /C5) in the four chemotypes (I, II, III, and IV). Significant difference is expressed through asterisks: * $p < 0.05$, ** $p < 0.01$, *** $p < 0.001$.

4. Conclusions

The identification of the novel C7 phytocannabinoids, THCP and CBDP, has given the opportunity to study their distribution in cannabis germplasm. In order to provide a reliable estimate of their amount in fresh cannabis plants it is necessary to quantify the native acidic species of phlorolic cannabinoids. A stereoselective synthesis of these compounds has allowed for the first time to obtain the analytical standards for a semi-quantitative determination. By employing the UHPLC-HRMS method based on a targeted approach towards both C5 and C7 acidic and neutral phytocannabinoids, it was possible to highlight a heterogeneous distribution of such compounds among forty-nine samples with different chemotypes. Although they represented only a small percentage out of total C5 and C7 species, it should be taken into account that the C7 THC homolog resulted more active than THC itself. Therefore, the concentration of the C7 species observed in the present study for some accessions could be considered relevant for therapeutic purposes. In particular, C7 phytocannabinoids showed a trend of concentrations strictly depending on the chemotype, with high THCP concentrations in chemotype I accessions (almost pure in THC) and high CBDP concentrations in chemotype III plants (almost pure in CBD). As a result, a future direction of cannabis research may focus on the screening and selection of favourable genetics with high content of C7 phytocannabinoids to be employed in the treatment of specific pathologies.

Declaration of competing interest

The authors declare that they have no known competing financial interests or personal relationships that could have appeared to influence the work reported in this paper.

Acknowledgments

This work was funded by UNIHEMP research project “Use of iNdustrIal Hemp biomass for Energy and new biocheMicals Production” (ARS01_00668) funded by Fondo Europeo di Sviluppo Regionale (FESR) (within the PON R&I 2017–2020 – Axis 2 – Action II – OS 1. b). Grant decree UNIHEMP prot. n. 2016 of July 27, 2018; CUP B76C18000520005.

Credit author statement

C. Citti, P. Linciano: Supervision, Investigation, Writing-original draft; C. Citti, F. Tolomeo, L. Carbone: (UHPLC-HRMS) Investigation, Formal analysis; P. Linciano, F. Russo, G. Biagini: (Synthesis) Investi- gation; G. Biagini: (Statistical analysis) Formal analysis; R. Paris, F. Fulvio, N. Pecchioni: Resources; Writing – original draft; A. Lagana`, A. L. Capriotti, M. A. Vandelli: Data

curation; G. Gigli: Resources; G. Cannazza: Conceptualization, Funding acquisition, Project administration; all authors: Writing-review & editing.

References

- [1] Y. Gaoni, R. Mechoulam, Isolation, structure, and partial synthesis of an active constituent of hashish, *J. Am. Chem. Soc.* 86 (8) (1964) 1646–1647.
- [2] R. Mechoulam, Y. Shvo, Hashish—I: the structure of cannabidiol, *Tetrahedron* 19 (12) (1963) 2073–2078.
- [3] L.O. Hanuš, S.M. Meyer, E. Muñoz, O. Tagliatalata-Scafati, G. Appendino, Phytocannabinoids: a unified critical inventory, *Nat. Prod. Rep.* 33 (12) (2016) 1357–1392.
- [4] C. Citti, P. Linciano, F. Forni, M.A. Vandelli, G. Gigli, A. Lagana, G. Cannazza, Analysis of impurities of cannabidiol from hemp. Isolation, characterization and synthesis of cannabidibutol, the novel cannabidiol butyl analog, *J. Pharmaceut. Biomed. Anal.* 175 (2019) 112752.
- [5] C. Citti, P. Linciano, F. Forni, M.A. Vandelli, G. Gigli, A. Lagana, G. Cannazza, Chemical and spectroscopic characterization data of ‘cannabidibutol’, a novel cannabidiol butyl analog, *Data in Brief* 26 (2019) 104463.
- [6] P. Linciano, C. Citti, L. Luongo, C. Belardo, S. Maione, M.A. Vandelli, F. Forni, G. Gigli, A. Lagana, C.M. Montone, G. Cannazza, Isolation of a high-affinity cannabinoid for the human CB1 receptor from a medicinal *Cannabis sativa* variety: Δ^9 -Tetrahydrocannabutol, the butyl homologue of Δ^9 -Tetrahydrocannabinol, *J. Nat. Prod.* 83 (1) (2020) 88–98.
- [7] C. Citti, P. Linciano, F. Russo, L. Luongo, M. Iannotta, S. Maione, A. Lagana, A.L. Capriotti, F. Forni, M.A. Vandelli, G. Gigli, G. Cannazza, A novel phytocannabinoid isolated from *Cannabis sativa* L. with an in vivo cannabimimetic activity higher than Δ^9 -tetrahydrocannabinol: Δ^9 -Tetrahydrocannabiphorol, *Sci. Rep.* 9 (1) (2019) 20335.
- [8] P. Linciano, C. Citti, F. Russo, F. Tolomeo, A. Lagana, A.L. Capriotti, L. Luongo, M. Iannotta, C. Belardo, S. Maione, F. Forni, M.A. Vandelli, G. Gigli, G. Cannazza, Identification of a new cannabidiol n-hexyl homolog in a medicinal cannabis variety with an antinociceptive activity in mice: cannabidihexol, *Sci. Rep.* 10 (1) (2020) 22019.
- [9] C. Citti, B. Pacchetti, M.A. Vandelli, F. Forni, G. Cannazza, Analysis of cannabinoids in commercial hemp seed oil and decarboxylation kinetics studies of cannabidiolic acid (CBDA), *J. Pharmaceut. Biomed. Anal.* 149 (2018) 532–540.
- [10] Mei Wang, Yan-Hong Wang, Bharathi Avula, Mohamed M. Radwan, Amir S. Wanas, John van Antwerp, Jon F. Parcher, Mahmoud A. ElSohly, Ikhlas A. Khan, Decarboxylation study of acidic cannabinoids: a novel

approach using ultra-high- performance supercritical fluid chromatography/photodiode array-mass spectrometry, *Cannabis and cannabinoid research* 1 (1) (2016) 262–271.

[11] F.E. Dussy, C. Hamberg, M. Luginbuhl, T. Schwerzmann, T.A. Briellmann, Isolation of Delta9-THCA-A from hemp and analytical aspects concerning the determination of Delta9-THC in cannabis products, *Forensic Sci. Int.* 149 (1) (2005) 3–10.

[12] G. Mandolino, A. Carboni, Potential of marker-assisted selection in hemp genetic improvement, *Euphytica* 140 (1–2) (2004) 107–120.

[13] P. Linciano, C. Citti, L. Luongo, C. Belardo, M.A. Vandelli, F. Forni, G. Gigli,

A. Lagana`, C.M. Montone, G. Cannazza, Isolation of a high affinity cannabinoid for human CB1 receptor from a medicinal cannabis variety: D9-Tetrahydrocannabinol, the butyl homologue of D9-tetrahydrocannabinol, *J. Nat. Prod.* (2019) in press.

[14] C.M. Montone, A. Cerrato, B. Botta, G. Cannazza, A.L. Capriotti, C. Cavaliere, C. Citti, F. Ghirga, S. Piovesana, A. Lagana, Improved identification of phytocannabinoids using a dedicated structure-based workflow, *Talanta* 219 (2020) 121310.

[15] *Cannabis Flos*, New Text of the German Pharmacopoeia, 2018. Bonn, Germany.

[16] A. Cerrato, C. Citti, G. Cannazza, A.L. Capriotti, C. Cavaliere, G. Grassi, F. Marini, C.M. Montone, R. Paris, S. Piovesana, A. Lagana`, Phytocannabinomics: untargeted metabolomics as a tool for cannabis chemovar differentiation, *Talanta* 230 (2021) 122313.

[17] R. Mechoulam, Z. Ben-Zvi, Carboxylation of resorcinols with methylmagnesium carbonate. Synthesis of cannabinoid acids, *J. Chem. Soc. D Chem. Commun.* (7) (1969) 343–344.

[18] Y.H. Choi, A. Hazekamp, A.M.G. Peltenburg-Looman, M. Fr'ederich, C. Erkelens, A. W.M. Lefeber, R. Verpoorte, NMR assignments of the major cannabinoids and cannabiflavonoids isolated from flowers of *Cannabis sativa*, *Phytochem. Anal.* 15 (6) (2004) 345–354.

[19] P. Berman, K. Futoran, G.M. Lewitus, D. Mukha, M. Benami, T. Shlomi, D. Meiri, A new ESI-LC/MS approach for comprehensive metabolic profiling of phytocannabinoids in *Cannabis*, *Sci. Rep.* 8 (1) (2018) 14280.

[20] X. Luo, M.A. Reiter, L. d'Espaux, J. Wong, C.M. Denby, A. Lechner, Y. Zhang, A. T. Grzybowski, S. Harth, W. Lin, H. Lee, C. Yu, J. Shin, K. Deng, V.T. Benites, G. Wang, E.E.K. Baidoo, Y. Chen, I. Dev, C.J. Petzold, J.D. Keasling, Complete biosynthesis of cannabinoids and their unnatural analogues in yeast, *Nature* 567 (7746) (2019) 123–126.

[21] M.T. Welling, L. Liu, C.A. Raymond, T. Kretzschmar, O. Ansari, G.J. King, Complex patterns of cannabinoid alkyl side-chain inheritance in *Cannabis*, *Sci. Rep.* 9 (1) (2019) 11421.

SUPPLEMENTARY MATERIAL

The novel heptyl phorolic acid cannabinoids content in different *Cannabis sativa*

L. accessions

Pasquale Linciano^{2,3}, Fabiana Russo¹, Cinzia Citti^{1,4,*}, Francesco Tolomeo³, Roberta Paris⁵, Flavia Fulvio⁴, Nicola Pecchioni⁶, Maria Angela Vandelli¹, Aldo Laganà^{3,7}, Anna Laura Capriotti⁶, Giuseppe Biagini⁸, Luigi Carbone³, Giuseppe Gigli³, Giuseppe Cannazza^{1,3}

Table of content

Putative identification of CBGPA and CBCPA	---SI-2
Synthesis and characterization of CBDPA and THCPA	---SI-4
¹H-NMR, ¹³C-NMR, COSY, HSQC, HMBC for synthetic CBDPA	---SI-5
¹H-NMR, ¹³C-NMR, COSY, HSQC, HMBC for synthetic THCPA	---SI-10
Distribution of C5 and C7 phytocannabinoids in different <i>Cannabis sativa</i> L. accessions	---SI-15

² Department of Life Sciences, University of Modena and Reggio Emilia, Via G. Campi 103, 41125 – Modena, Italy

³ Present address: School of Pharmacy, University of Pavia, Viale Taramelli 12, 27100 – Pavia, Italy

⁴ Institute of Nanotechnology – CNR NANOTEC, Via Monteroni, 73100 – Lecce, Italy

⁵ CREA-Research Center for Cereal and Industrial Crops, Via di Corticella 133, 40128 – Bologna, Italy

⁶ CREA-Research Center for Cereal and Industrial Crops, S.S. 673 Km 25,200 - 71122 - Foggia, Italy

⁷ Department of Chemistry, Sapienza University of Rome, Piazzale Aldo Moro 5, 00185 – Rome, Italy

⁸ Department of Biomedical, Metabolic and Neural Sciences, University of Modena and Reggio Emilia, Via G. Campi 287, 41125 – Modena, Italy

* Address correspondence to: Cinzia Citti, PhD. Phone: +39 0832 319206; e-mail: cinzia.citti@unimore.it.

Putative identification of CBGPA and CBCPA

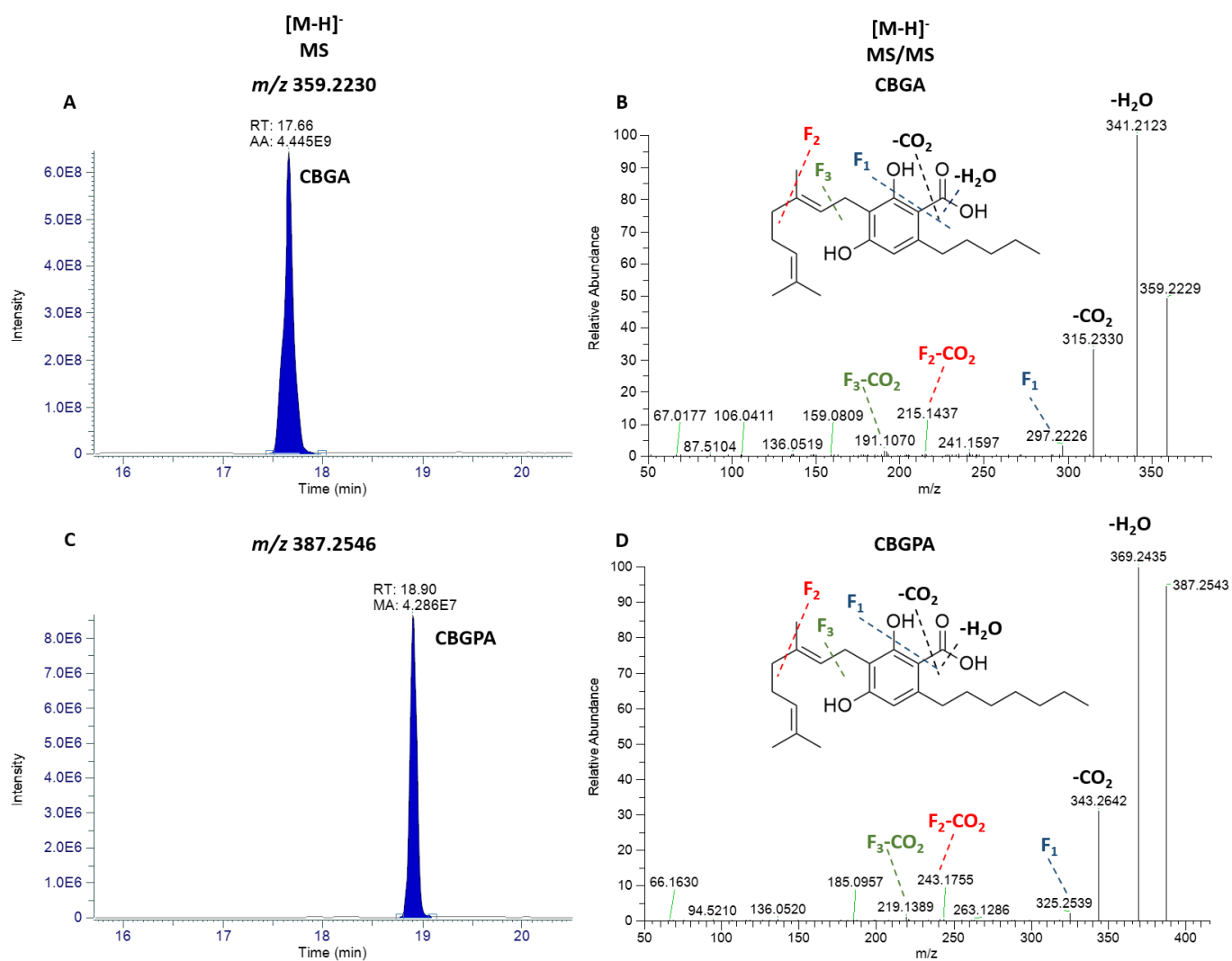


Figure S 5. Extracted HPLC-HRMS chromatograms in negative ionization mode of CBGA and CBGPA and their corresponding HRMS/MS spectra with a proposed fragmentation pattern.

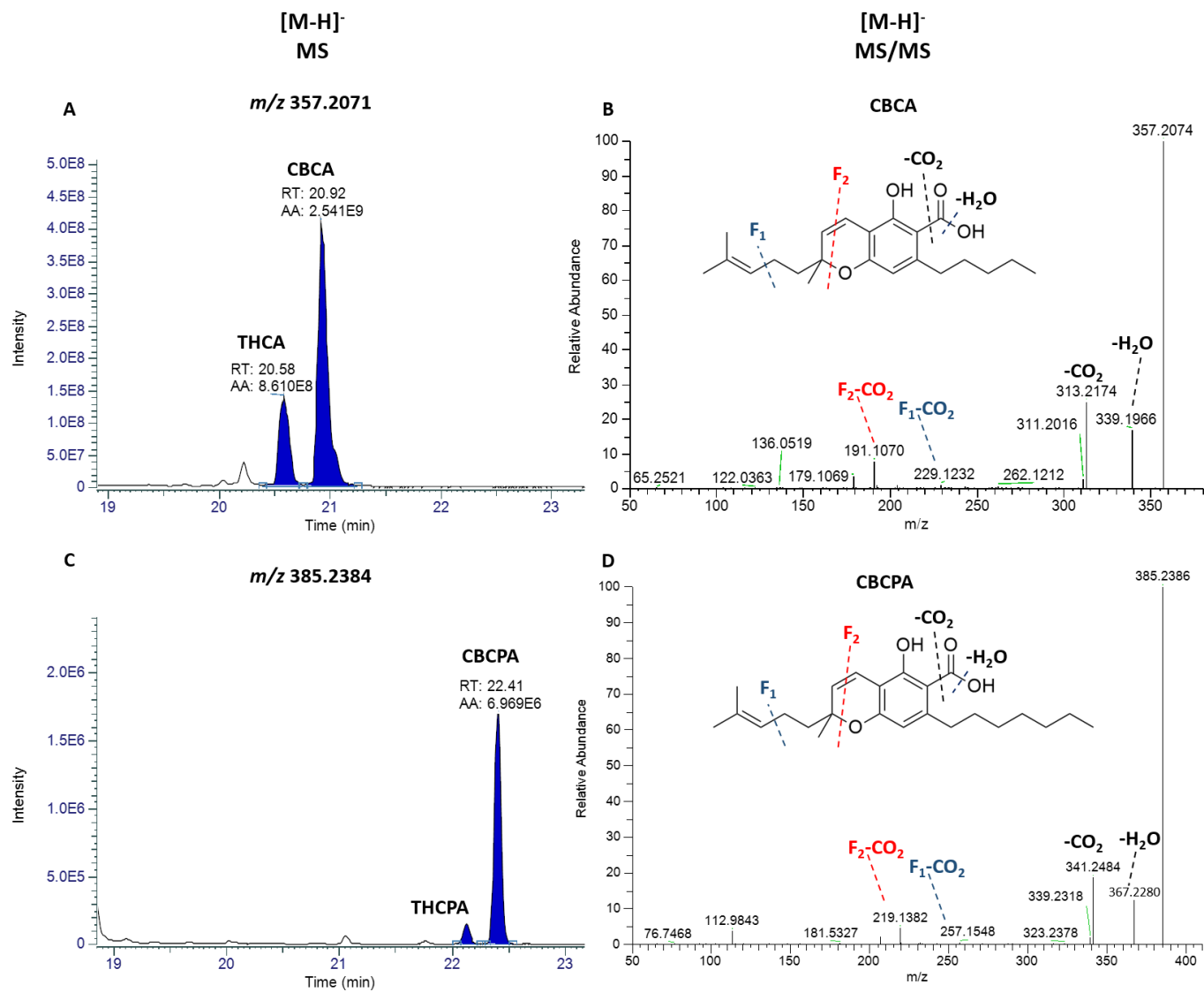


Figure S 6. Extracted HPLC-HRMS chromatograms in negative ionization mode of CBCA and CBCPA and their corresponding HRMS/MS spectra with a proposed fragmentation pattern.

Synthesis and characterization of (-)-*trans*-CBDPA and (-)-*trans*- Δ^9 -THCPA

Synthesis of (1'R,2'R)-4-heptyl-2,6-dihydroxy-5'-methyl-2'-(prop-1-en-2-yl)-1',2',3',4'-tetrahydro-[1,1'-biphenyl]-3-carboxylic acid, (-)-trans-CBDPA

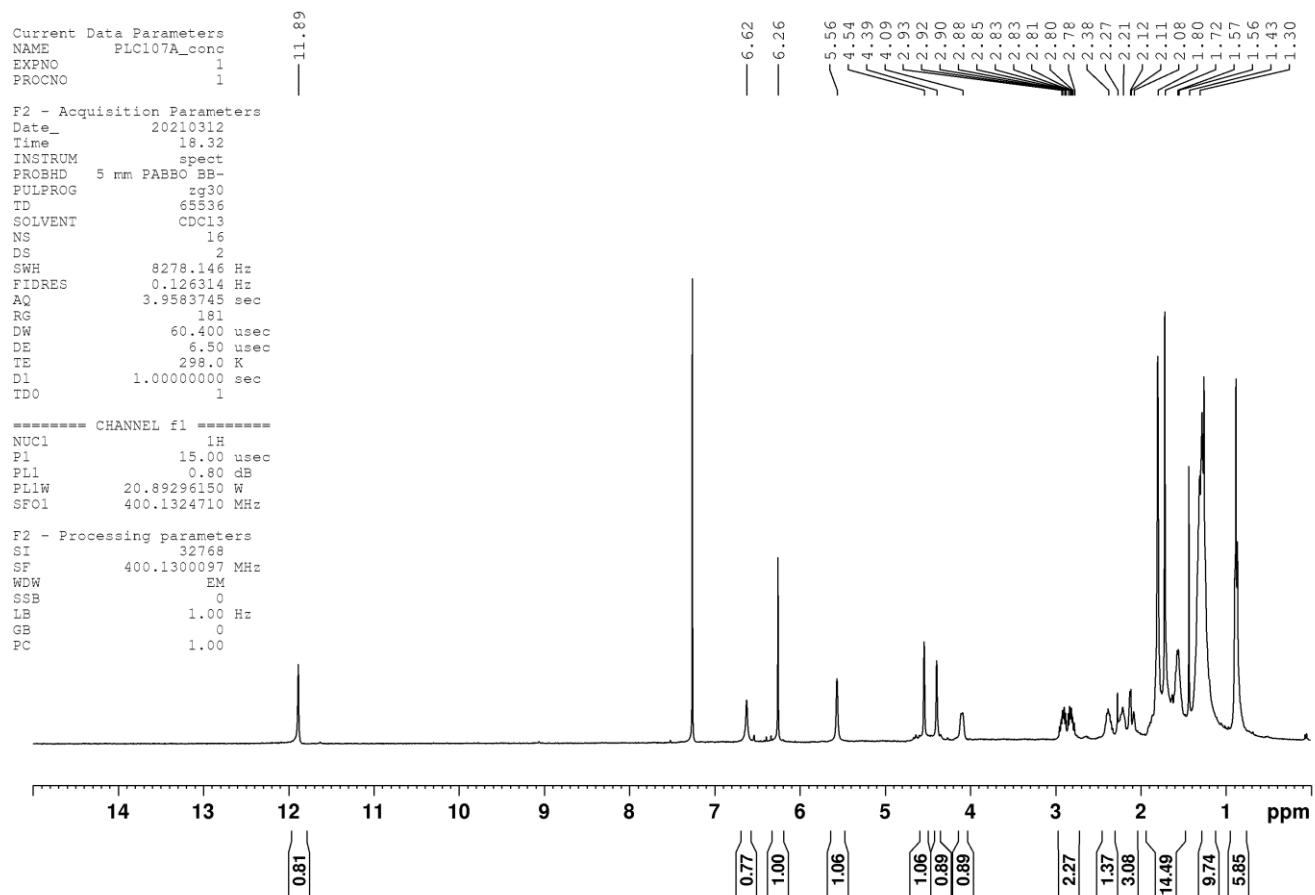
To a 2 M solution of MMC in DMF (600 μ L), CBDP (60 mg, 0.15 mmol) was added. The reaction was stirred at 120°C for 3 hours. Thereafter, the reaction was cooled down to room temperature, diluted with Et₂O and acidified with 1 N HCl. The organic layer was washed with a saturated solution of NaCl, dried over anhydrous Na₂SO₄, filtered and concentrated. The crude was purified over silica gel (eluent CE/DCM 1:1 (v/v) and then Et₂O 100%) to give 20 mg of brown liquid (39% yield). $[\alpha]_D^{20} = +61.9^\circ$ (c. 2.9, CHCl₃).

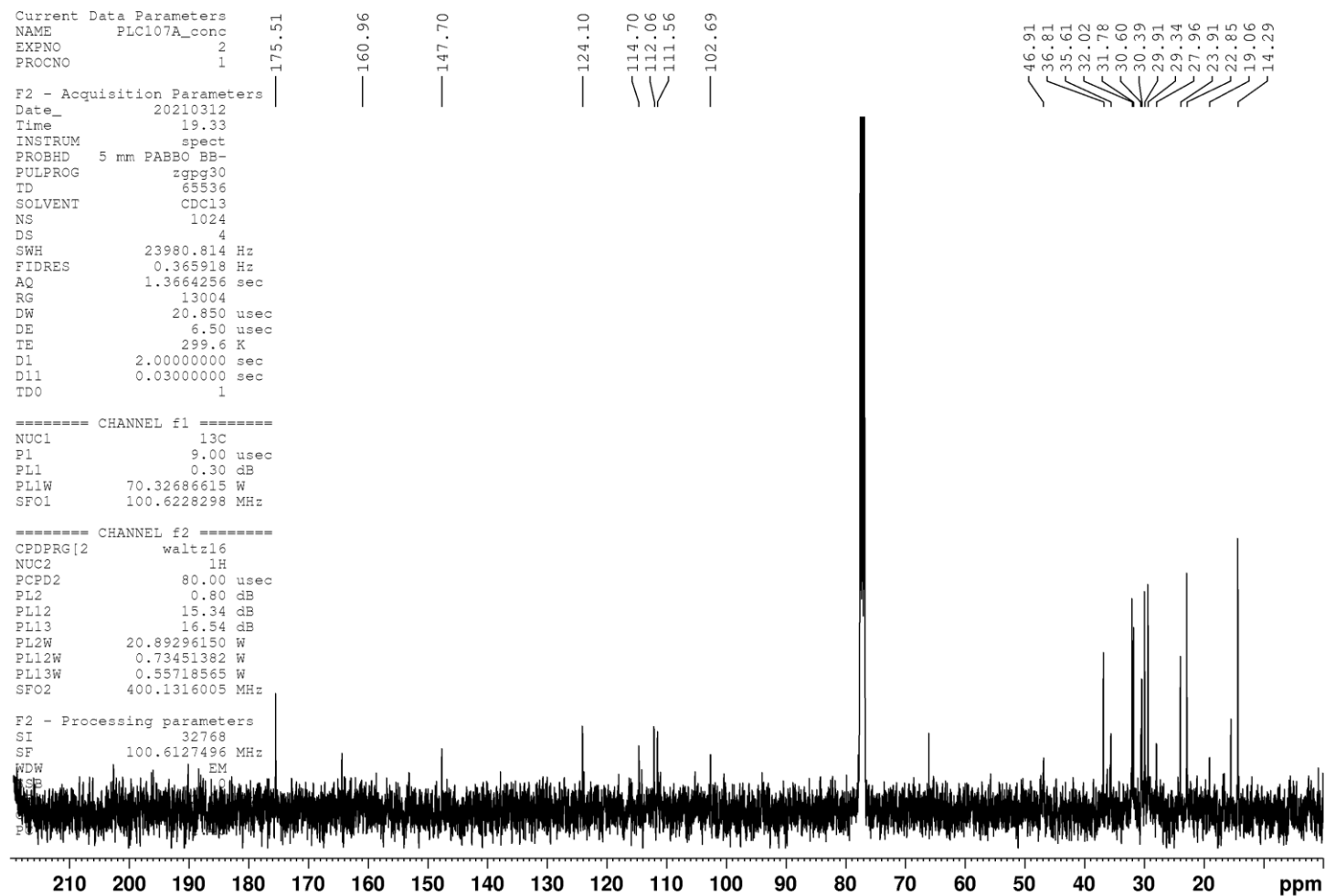
¹H NMR (400 MHz, CDCl₃) δ 11.88 (bs, OH), 6.62 (s, 1H), 6.26 (s, 1H), 5.56 (s, 1H), 4.54 (s, 1H), 4.39 (s, 1H), 4.11-4.09 (m, 1H), 2.93-2.88 (m, 1H), 2.85-2.78 (m, 1H), 2.40-2.33 (m, 1H), 2.27-2.21 (m, 1H), 2.12-2.08 (m, 1H), 1.80 (s, 3H), 1.72 (s, 3H), 1.57-1.55 (m, 3H), 1.30-1.19 (m, 10H), 0.86 (t, 3H, $J = 7.6$ Hz). ¹³C NMR (100 Hz, CDCl₃) δ 14.29, 19.06, 22.85, 23.91, 27.96, 29.34, 29.91, 30.39, 30.60, 31.78, 32.02, 35.61, 36.80, 46.91, 102.69, 111.56, 112.06, 114.70, 124.10, 135.91 (from HMBC), 140.76 (from HMBC), 147.70, 160.96, 175.51. HRMS m/z [M+H]⁺ calcd. for C₂₄H₃₅O₄⁺: 387.2530. Found: 387.2535; [M-H]⁻ calcd. for C₂₄H₃₃O₄⁻: 385.2384. Found: 385.2388.

Synthesis of (6aR,10aR)-3-heptyl-1-hydroxy-6,6,9-trimethyl-6a,7,8,10a-tetrahydro-6H-benzo[c]chromene-2-carboxylic acid, (-)-trans- Δ^9 -THCPA

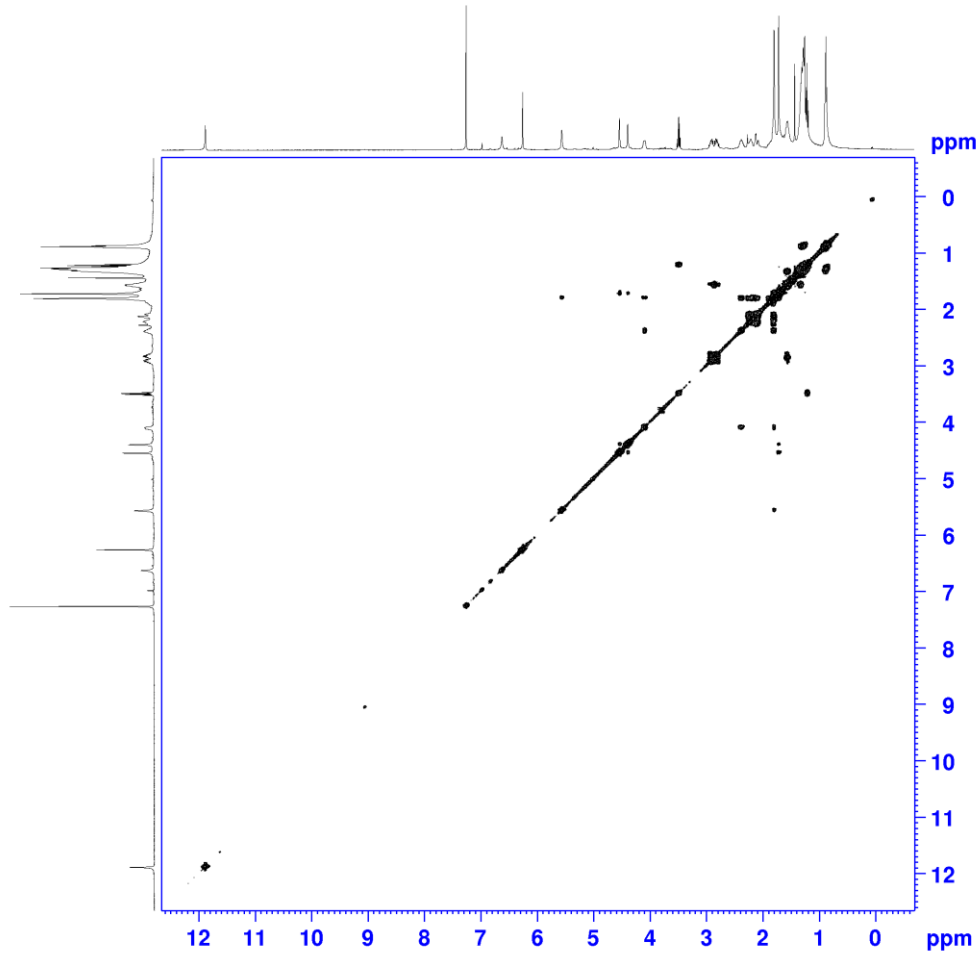
To a 2 M solution of MMC in DMF (700 μ L), THCP (120 mg, 0.35 mmol) was added. The reaction was stirred at 130 °C for 18 h hours. Thereafter, the reaction was cooled at room temperature, diluted with Et₂O and acidified with 1 N HCl. The organic layer was washed with a saturated solution of NaCl, dried over anhydrous Na₂SO₄, filtered and concentrated. The crude was purified over silica gel (eluent CE/DCM 1:1 (v/v) and then Et₂O 100%) to give 10 mg (7% yield) of brown liquid.

¹H NMR (400 MHz, CDCl₃) δ 12.28 (bs, OH), 6.39 (s, 1H) 6.25 (s, 1H), 3.23 (d, $J = 10.5$ Hz, 1H), 2.98-2.90 (m, 1H), 2.81-2.74 (m, 1H), 2.21-2.12 (bm, 2H), 1.93-1.90 (m, 1H), 1.72-1.68 (m, 4H), 1.60-1.52 (m, 2H), 1.44 (s, 3H), 1.40-1.25 (m, 10H), 1.11 (s, 3H), 0.88 (t, $J = 6.0$ Hz, 3H) ¹³C NMR (400Hz, CDCl₃) δ 14.16, 19.56, 22.73, 23.37, 25.05, 27.44, 29.21, 29.84, 31.27, 31.66, 31.87, 33.53, 36.59, 45.67, 78.85, 102.29, 109.88, 112.58, 123.71, 133.83, 146.84, 159.70, 164.71, 175.57. HRMS m/z [M+H]⁺ calcd. for C₂₄H₃₅O₄⁺: 387.2530. Found: 387.2925; [M-H]⁻ calcd. for C₂₄H₃₃O₄⁻: 385.2384. Found: 385.2388.

NMR spectra of (-)-*trans*-CBDPA



S7



```
Current Data Parameters
NAME      PLC107A_conc
EXPNO     3
PROCNO    1

F2 - Acquisition Parameters
Date_     20210312
Time      19.34
INSTRUM   spect
PROBHD    5 mm PABBO BB-
PULPROG   cosygpcqf
TD         2048
SOLVENT   CDC13
NS         2
DS         3
SWH        5341.880 Hz
FIDRES     2.608340 Hz
AQ         0.1916928 sec
RG         362
DW         93.600 usec
DE         6.50 usec
TE         298.6 K
DO         0.00000300 sec
D1         1.00000000 sec
D13        0.00000400 sec
D16        0.00020000 sec
INO        0.00018720 sec

===== CHANNEL f1 =====
NUC1       1H
PO         15.00 usec
P1         15.00 usec
PL1        0.80 dB
PL1W       20.89296150 W
SFO1       400.1324057 MHz

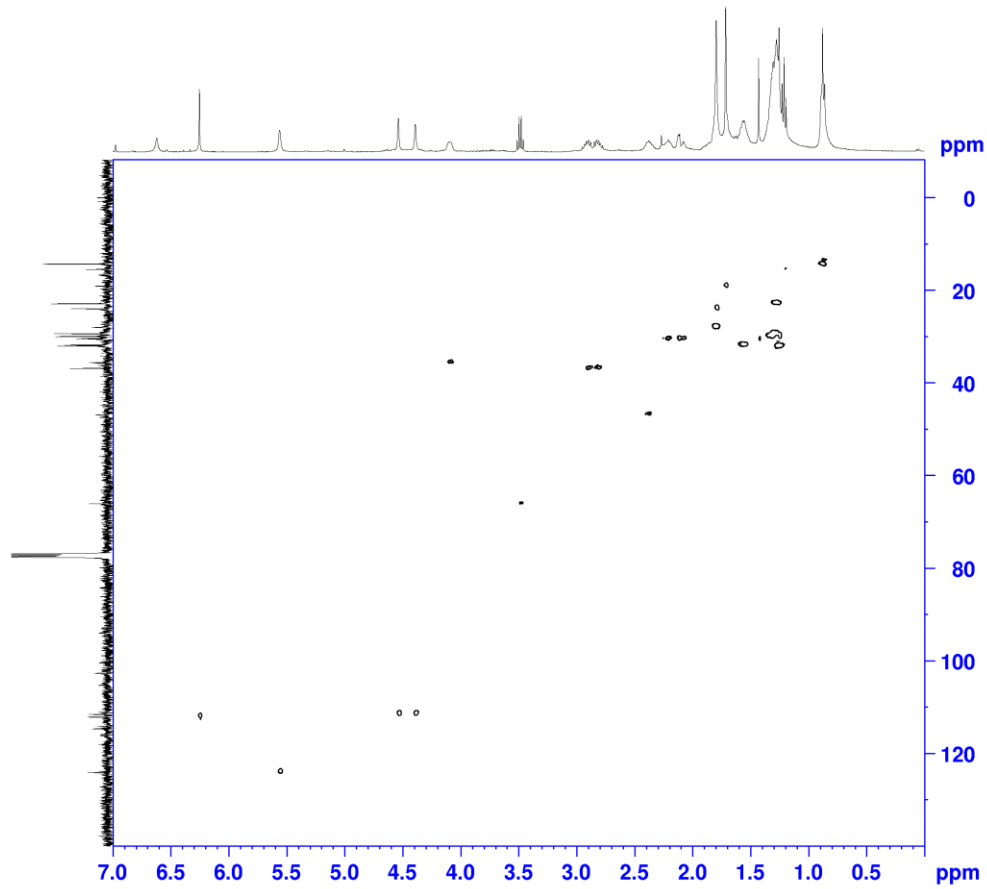
===== GRADIENT CHANNEL =====
GPNAM[1]   SINE.100
GPZ1       10.00 %
P16        1000.00 usec

F1 - Acquisition parameters
TD         256
SFO1       400.1324 MHz
FIDRES     41.733440 Hz
SW         13.350 ppm
FnMODE     QF

F2 - Processing parameters
SI         2048
SF         400.1300101 MHz
WDW        SINE
SSB        0
LB         0 Hz
GB         0
PC         1.40

F1 - Processing parameters
SI         1024
MC2        QF
SF         400.1300117 MHz
WDW        SINE
SSB        0
LB         0 Hz
GB         0
```

S8



```
Current Data Parameters
NAME      PLC107A_conc
EXPNO     4
PROCNO    1

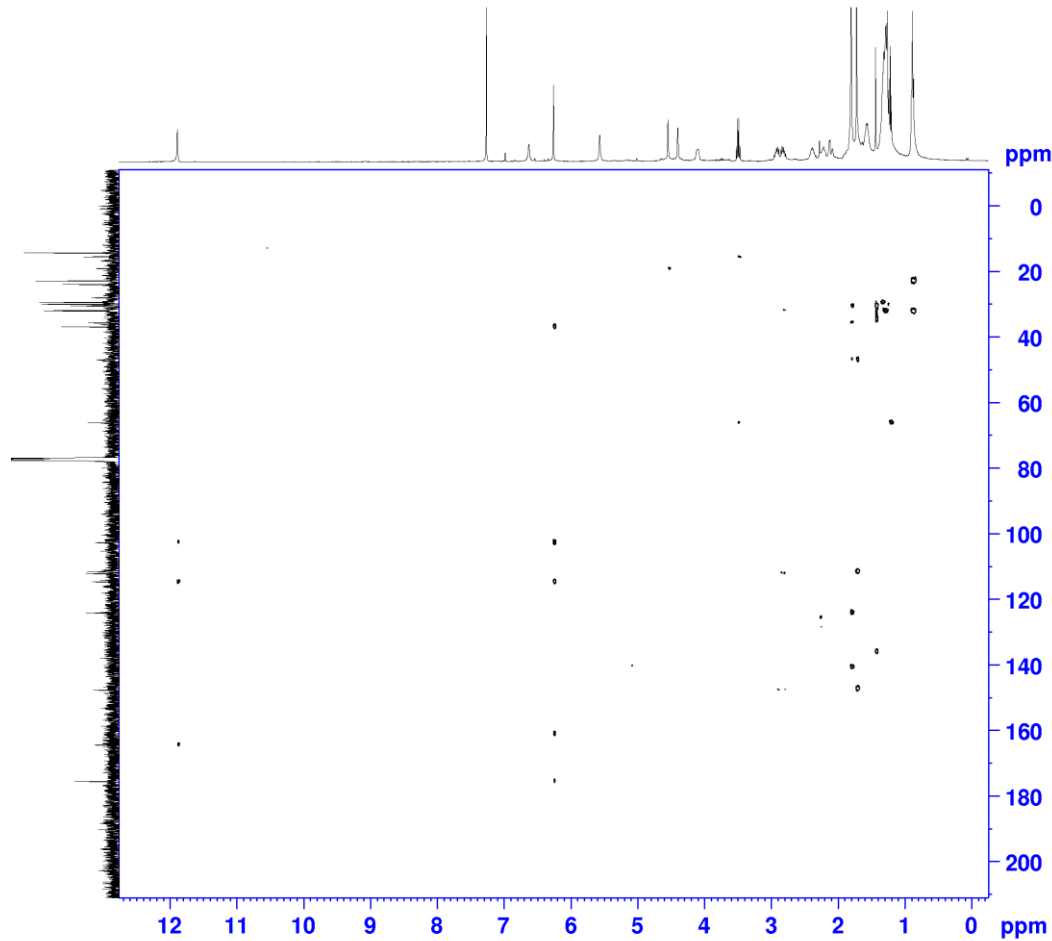
F2 - Acquisition Parameters
Date_     20210312
Time      19.46
INSTRUM   spect
PROBHD    5 mm PABBO BB-
PULPROG   hsqcetgcp
TD         2048
SOLVENT   CDCl3
NS         4
DS         16
SWH       5341.880 Hz
FIDRES    2.608340 Hz
AQ         0.1916928 sec
RG         4096
DW         93.600 usec
DE         6.50 usec
TE         298.4 K
CNST2     145.0000000
D0         0.00000300 sec
D1         1.00000000 sec
D4         0.00172414 sec
D11        0.03000000 sec
D13        0.00000400 sec
D16        0.00020000 sec
D21        0.00345000 sec
IN0        0.00003000 sec
ZGOPTNS

===== CHANNEL f1 =====
NUC1       1H
P1         15.00 usec
P2         30.00 usec
P28        1.00 usec
PL1        0.80 dB
PL1W       20.89296150 W
SFO1       400.1324057 MHz

===== CHANNEL f2 =====
CPDPRG[2]  garp
NUC2       13C
P3         9.00 usec
P4         18.00 usec
PCPD2     70.00 usec
PL2        0.30 dB
PL12       18.12 dB
PL2W       70.32686615 W
PL12W     1.16177273 W
SFO2       100.6202727 MHz

===== GRADIENT CHANNEL =====
GPNAM[1]   SINE.100
GPNAM[2]   SINE.100
```


S9



```
Current Data Parameters
NAME      PLC107A_conc
EXPNO    5
PROCNO   1

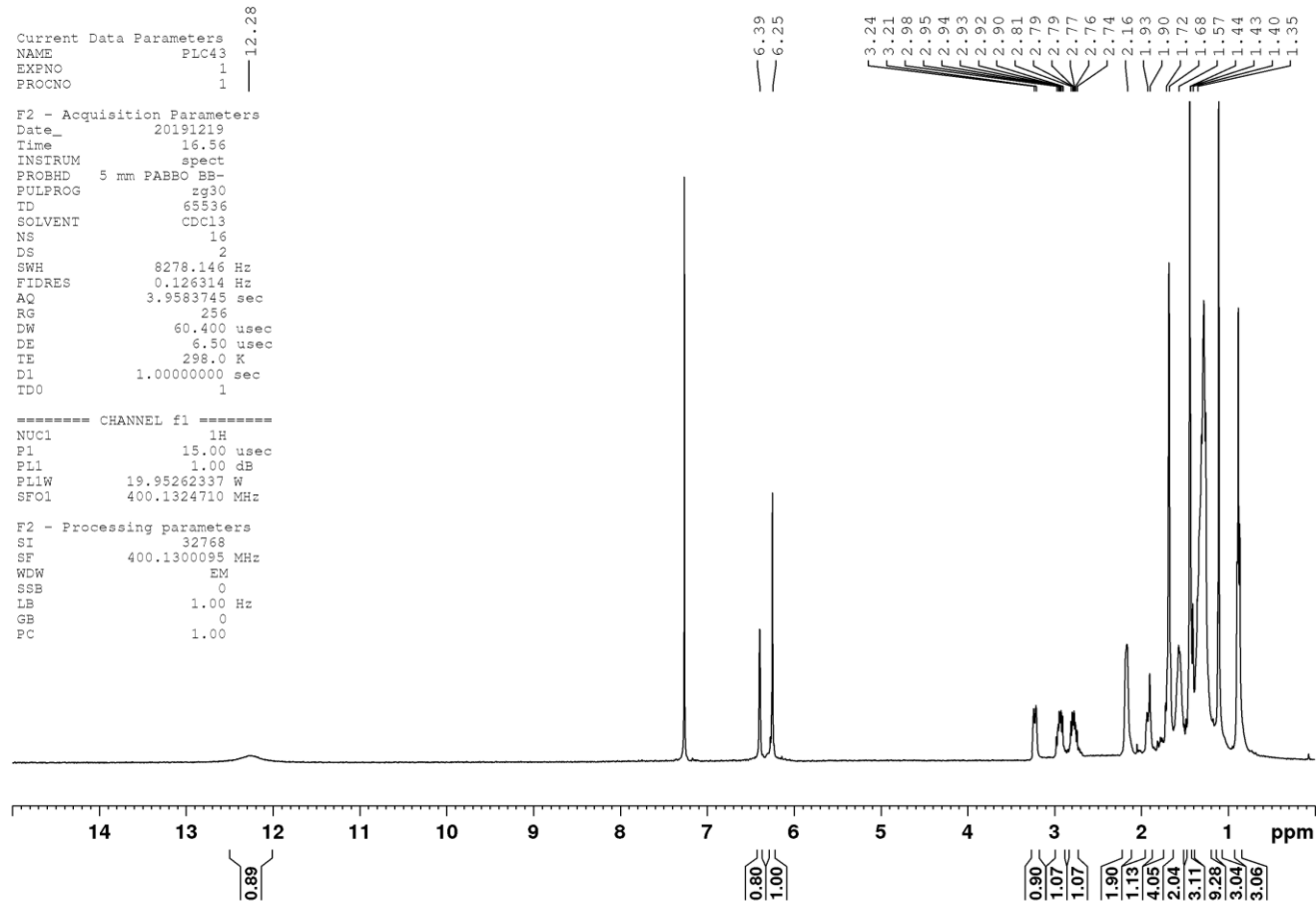
F2 - Acquisition Parameters
Date_    20210312
Time     20.09
INSTRUM  spect
PROBHD   5 mm PABBO BB-
PULPROG  hmbcgp1pdqf
TD       4096
SOLVENT  CDCl3
NS       16
DS       16
SWH      5208.333 Hz
FIDRES   1.271566 Hz
AQ       0.3932160 sec
RG       4096
DW       96.000 usec
DE       6.50 usec
TE       298.2 K
CNST2    145.0000000
CNST13   8.0000000
D0       0.00000300 sec
D1       1.00000000 sec
D2       0.00344828 sec
D6       0.06250000 sec
D16      0.00020000 sec
IN0      0.00002235 sec

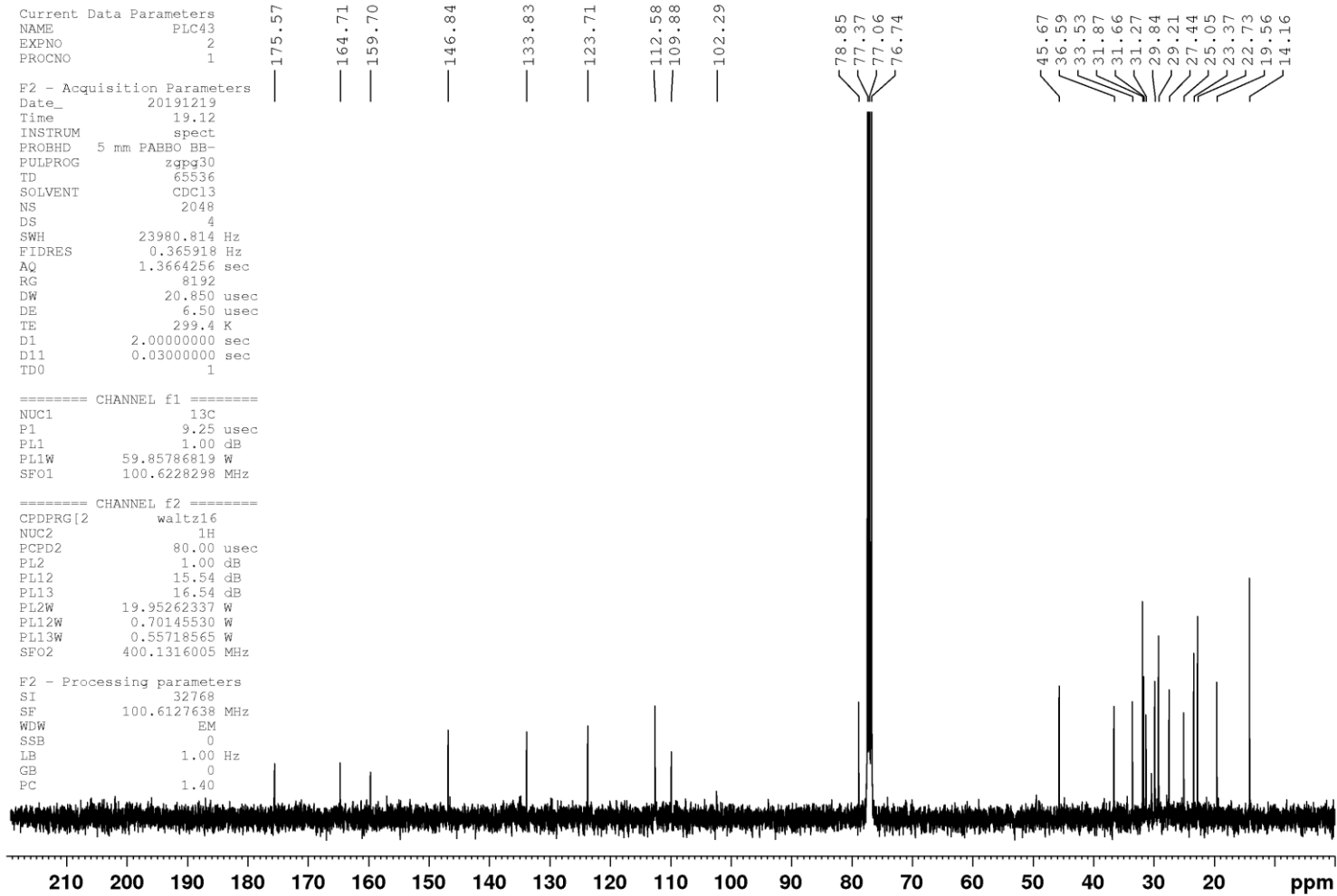
===== CHANNEL f1 =====
NUC1     1H
P1       15.00 usec
P2       30.00 usec
PL1      0.80 dB
PL1W     20.89296150 W
SFO1     400.1325208 MHz

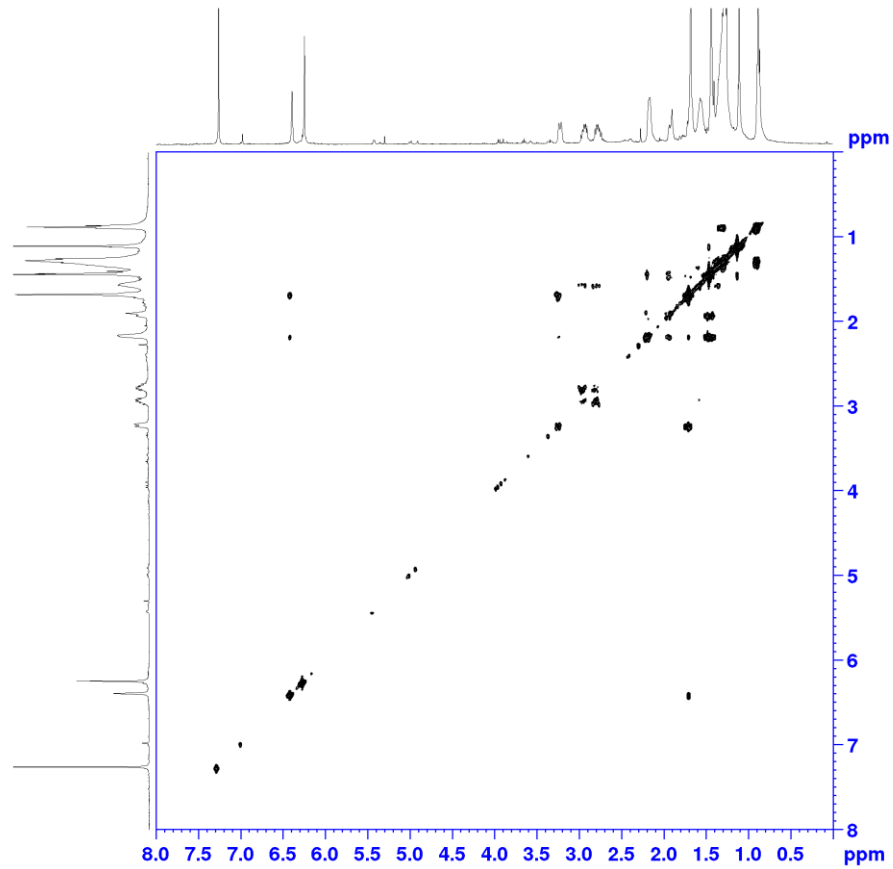
===== CHANNEL f2 =====
NUC2     13C
P3       9.00 usec
P2       0.30 dB
PL2W     70.32686615 W
SFO2     100.6228138 MHz

===== GRADIENT CHANNEL =====
GPNAM[1] SINE.100
GPNAM[2] SINE.100
GPNAM[3] SINE.100
GFZ1     50.00 %
GFZ2     30.00 %
GFZ3     40.10 %
P16      1000.00 usec

F1 - Acquisition parameters
TD       256
```

NMR spectra of (-)-*trans*-THCPA





```

Current Data Parameters
NAME          PLC43
EXPNO         3
PROCNO        1

F2 - Acquisition Parameters
Date_         20191219
Time          19.13
INSTRUM       spect
PROBHD        5 mm PABBO BB-
PULPROG       cosygpcqf
TD            2048
SOLVENT       CDCl3
NS            2
DS            8
SWH           5341.880 Hz
FIDRES        2.608340 Hz
AQ            0.1916928 sec
RG            512
DW            93.600 usec
DE            6.50 usec
TE            298.3 K
D0            0.00000300 sec
D1            1.00000000 sec
D13           0.00000400 sec
D16           0.00020000 sec
IN0           0.00018720 sec

===== CHANNEL f1 =====
NUC1           1H
P0             15.00 usec
P1             15.00 usec
PL1            1.00 dB
PL1W           19.95262337 W
SF01           400.1324057 MHz

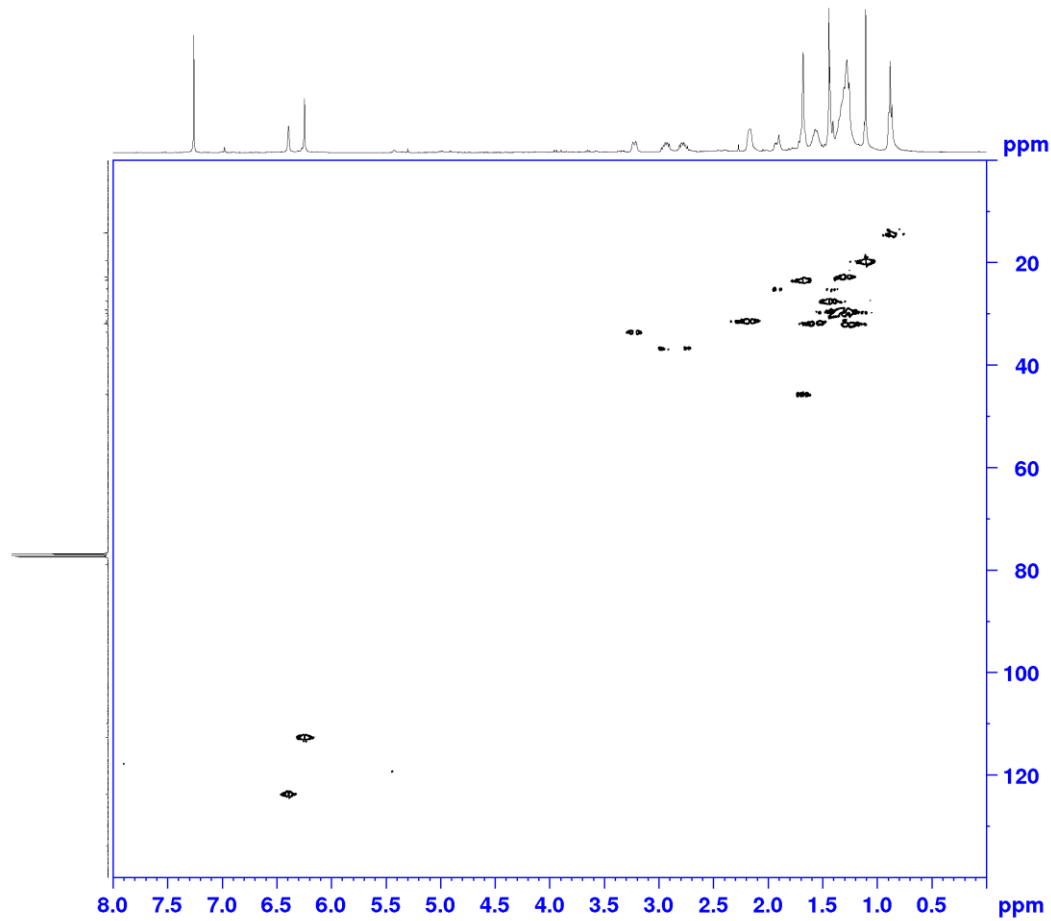
===== GRADIENT CHANNEL =====
GPNAM[1]       SINE.100
GPZ1           10.00 %
P16            1000.00 usec

F1 - Acquisition parameters
TD             256
SF01           400.1324 MHz
FIDRES         41.733440 Hz
SW             13.350 ppm
FnMODE         QF

F2 - Processing parameters
SI             2048
SF             400.1300000 MHz
WDW            SINE
SSB            0
LB             0 Hz
GB             0
PC             1.40

```

S13



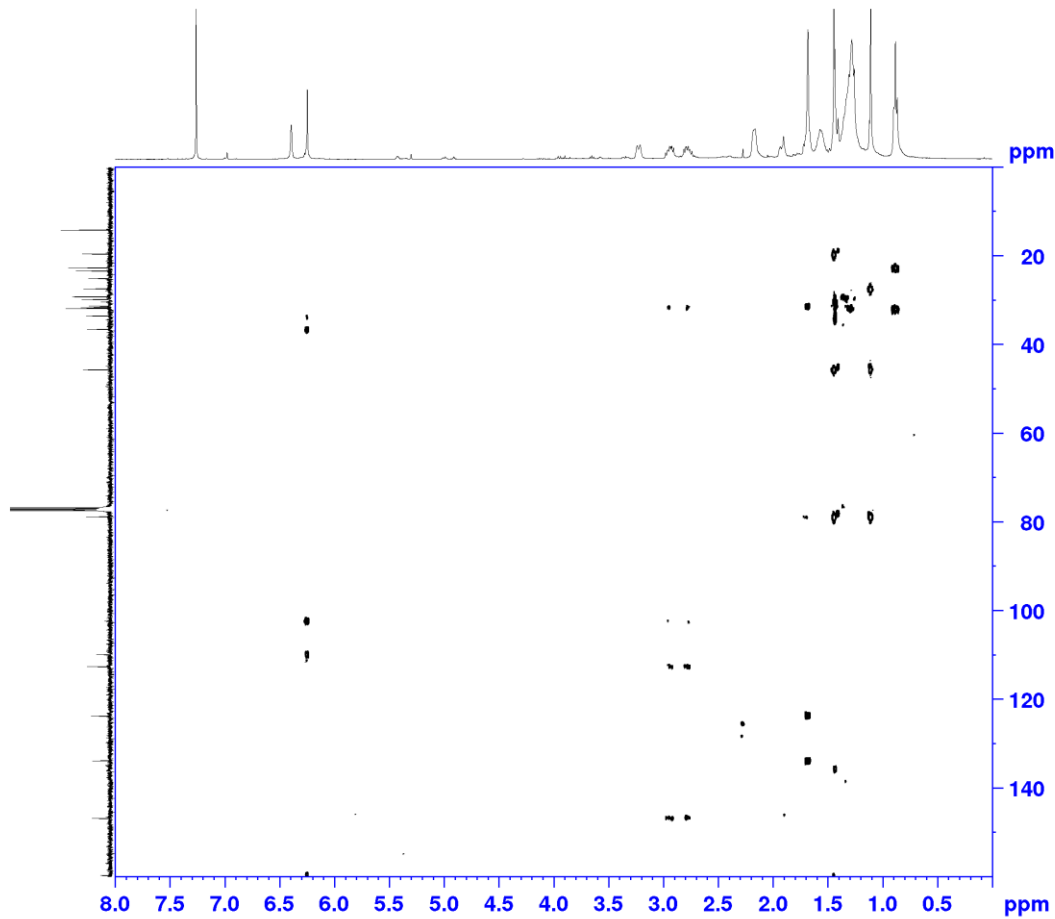
Current Data Parameters
NAME PLC43
EXPNO 4
PROCNO 1

F2 - Acquisition Parameters
Date_ 20191219
Time 19.26
INSTRUM spect
PROBHD 5 mm PABBO BB-
PULPROG hsqcedetgp
TD 2048
SOLVENT CDCl3
NS 4
DS 16
SWH 5341.880 Hz
FIDRES 2.608340 Hz
AQ 0.1916928 sec
RG 4096
DW 93.600 usec
DE 6.50 usec
TE 298.3 K
CNST2 145.0000000
D0 0.00000300 sec
D1 1.00000000 sec
D4 0.00172414 sec
D11 0.03000000 sec
D13 0.00000400 sec
D16 0.00020000 sec
D21 0.00345000 sec
IN0 0.00003000 sec
ZGOPTNS

===== CHANNEL f1 =====
NUC1 1H
P1 15.00 usec
P2 30.00 usec
P28 1.00 usec
PL1 1.00 dB
PL1W 19.95262337 W
SFO1 400.1324057 MHz

===== CHANNEL f2 =====
CPDPRG[2] garp
NUC2 13C
P3 9.25 usec
P4 18.50 usec
PCPD2 70.00 usec
PL2 1.00 dB
PL12 18.00 dB
PL2W 59.85786819 W
PL12W 1.19432151 W
SFO2 100.6202727 MHz

S14



Current Data Parameters
 NAME PLC43
 EXPNO 5
 PROCNO 1

F2 - Acquisition Parameters
 Date_ 20191219
 Time 19.49
 INSTRUM spect
 PROBHD 5 mm PABBO BB-
 PULPROG hmbcgp1pndgf
 TD 4096
 SOLVENT CDCl3
 NS 16
 DS 16
 SWH 5208.333 Hz
 FIDRES 1.271566 Hz
 AQ 0.3932160 sec
 RG 4096
 DW 96.000 usec
 DE 6.50 usec
 TE 297.9 K
 CNST2 145.0000000
 CNST13 8.0000000
 D0 0.00000300 sec
 D1 1.00000000 sec
 D2 0.00344828 sec
 D6 0.06250000 sec
 D16 0.00020000 sec
 IN0 0.00002235 sec

===== CHANNEL f1 =====
 NUC1 1H
 P1 15.00 usec
 P2 30.00 usec
 PL1 1.00 dB
 PL1W 19.95262337 W
 SFO1 400.1325208 MHz

===== CHANNEL f2 =====
 NUC2 13C
 P3 9.25 usec
 PL2 1.00 dB
 PL2W 59.85786819 W
 SFO2 100.6228138 MHz

===== GRADIENT CHANNEL =====
 GPNAM[1] SINE.100
 GPNAM[2] SINE.100
 GPNAM[3] SINE.100
 GPZ1 50.00 %
 GPZ2 30.00 %
 GPZ3 40.10 %
 P16 1000.00 usec

Distribution of C5 and C7 phytocannabinoids in different *Cannabis sativa* L. accessions

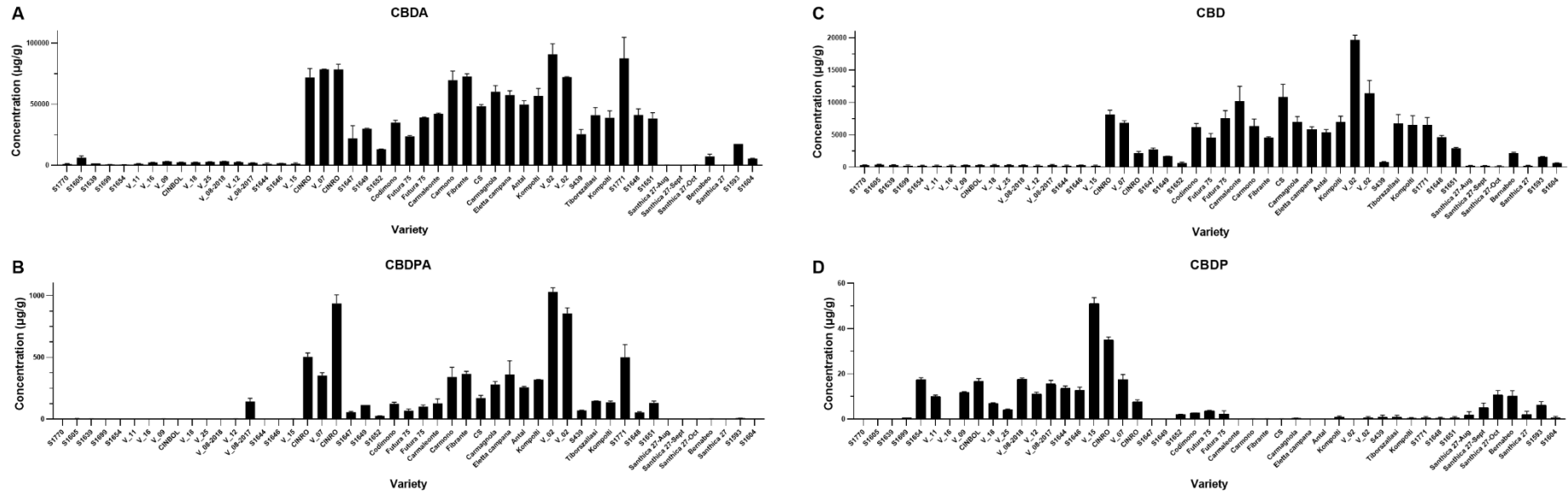


Figure S 7. Concentrations in µg/g of C5 and C7 CBD-type phytocannabinoids in each cannabis accession. Values are expressed as mean±st.dev (n=3).

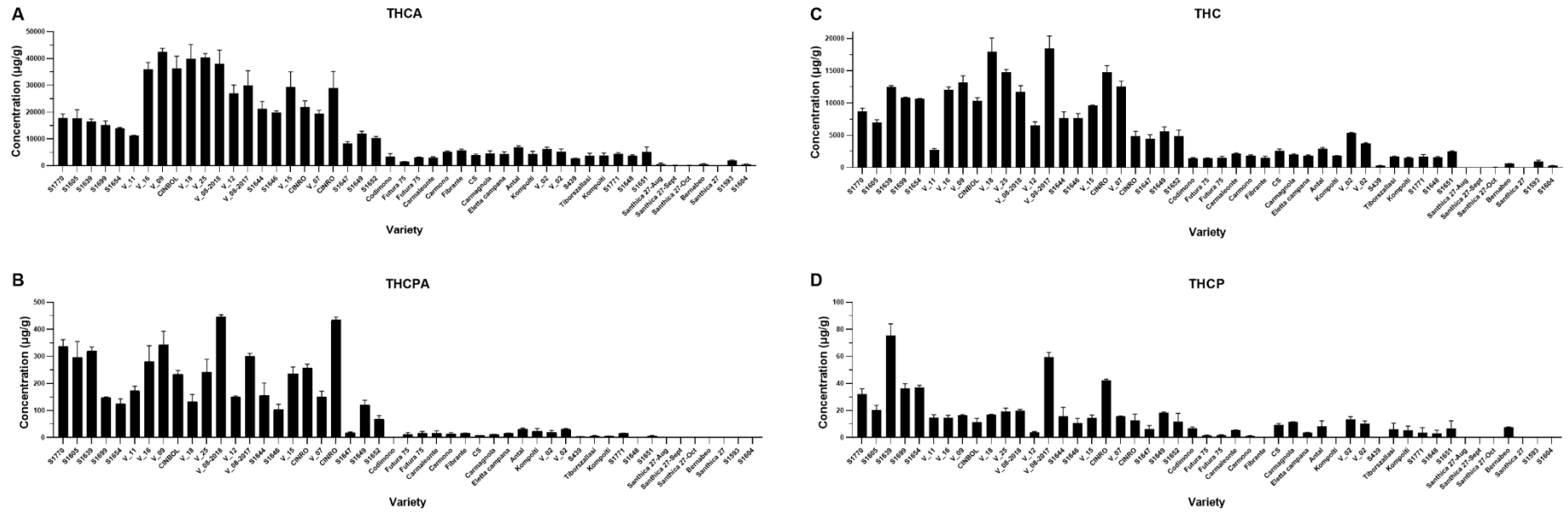


Figure S 8. Concentrations in µg/g of C5 and C7 THC-type phytocannabinoids in each cannabis accession. Values are expressed as mean±st.dev (n=3).

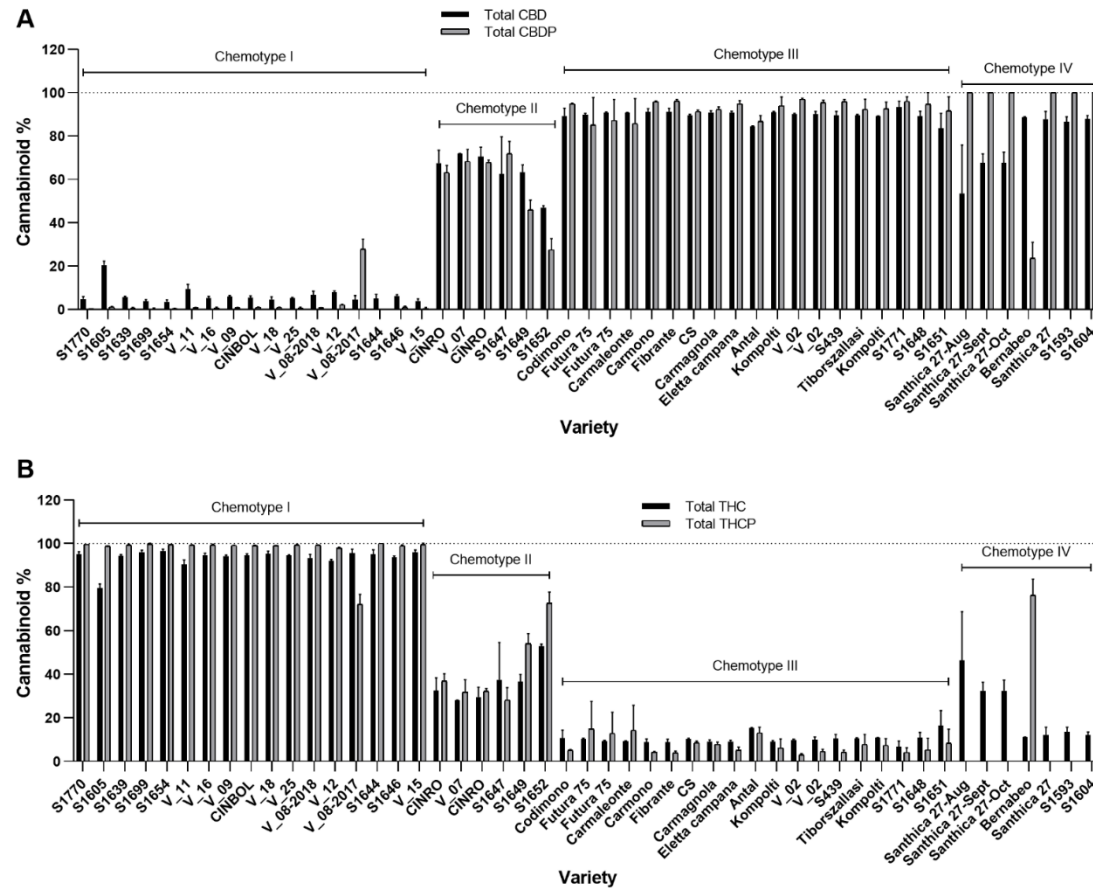


Figure S 9. A) Percentages of total CBD out of C5 cannabinoids and total CBDP out of C7 cannabinoids in each cannabis accession. B) Percentages of total THC out C5 cannabinoids and total THCP out of total C7 cannabinoids in each cannabis accession. Values are expressed as mean \pm st.dev (n=3).

CHAPTER 2

DEVELOPMENT OF ANALYTICAL METHODS TO ASSESS THE STEREOISOMERIC COMPOSITION OF THE MAIN PHYTOCANNABINOIDS IN CANNABIS SATIVA

CIS- Δ^9 -TETRAHYDROCANNABINOLIC ACID OCCURRENCE IN CANNABIS SATIVA L

Francesco Tolomeo ^{a,1}, Fabiana Russo ^{b,c,1}, Dominika Kaczorova ^{d,e}, Maria Angela Vandelli ^f, Giuseppe Biagini ^c, Aldo Lagana ^{a,g}, Anna Laura Capriotti ^g, Roberta Paris ^h, Flavia Fulvio ^h, Luigi Carbone ^a, Elisabetta Perrone ^a, Giuseppe Gigli ^a, Giuseppe Cannazza ^{a, f, *}, Cinzia Citti ^{a, f, *}

a Institute of Nanotechnology – CNR NANOTEC, Campus Ecotekne, Via Monteroni, 73100 Lecce, Italy

b Clinical and Experimental Medicine PhD Program, University of Modena and Reggio Emilia, 41125 Modena, Italy

c Department of Biomedical, Metabolic and Neural Sciences, University of Modena and Reggio Emilia, 41125 Modena, Italy

d Centre of the Region Han'á for Biotechnological and Agricultural Research, Department of Genetic Resources for Vegetables, Medicinal and Special Plants, Crop Research Institute, Šlechtitelů 29, 78371 Olomouc, Czech Republic

e Department of Biochemistry, Faculty of Science, Palacký University, Šlechtitelů 27, 78371 Olomouc, Czech Republic

f Department of Life Sciences, University of Modena and Reggio Emilia, Via Campi 103, 41125 Modena, Italy

g Department of Chemistry, Sapienza University of Rome, Piazzale Aldo Moro 5, 00185 Rome, Italy

h CREA – Research Center for Cereal and Industrial Crops, Via di Corticella 133, 40128 Bologna, Italy

Published in: *J Pharm Biomed Anal.* (2022).
doi: 10.1016/j.jpba.2022.114958

* Corresponding author at: Department of Life Sciences, University of Modena and Reggio Emilia, Via Campi 103, 41125 Modena, Italy.

** Corresponding author at: Institute of Nanotechnology – CNR NANOTEC, Campus Ecotekne, Via Monteroni, 73100 Lecce, Italy.

E-mail addresses: giuseppe.cannazza@unimore.it (G. Cannazza), cinzia.citti@unimore.it (C. Citti).

1 These authors contributed equally to the work.

Abstract

Cannabidiolic acid (CBDA) and *trans*- Δ^9 -tetrahydrocannabinolic acid (*trans*- Δ^9 -THCA) are known to be the major phytocannabinoids in *Cannabis sativa* L., along with their decarboxylated derivatives cannabidiol (CBD) and *trans*- Δ^9 -tetrahydrocannabinol (*trans*- Δ^9 -THC). The *cis* isomer of Δ^9 -THC has been recently identified, characterized and quantified in several *Cannabis sativa* varieties, which had been heated (decarboxylated) before the analysis. Since decarboxylation alters the original phytocannabinoids composition of the plant, this work reports the identification and characterization of the carboxylated precursor *cis*- Δ^9 -THCA. The compound was also synthesized and used as analytical standard for the development and validation of a liquid chromatography coupled to high resolution mass spectrometry-based method for its quantification in ten *Cannabis sativa* L. samples from different chemotypes. The highest concentrations of *cis*- Δ^9 -THCA were found in CBD-rich varieties, lower levels were observed in cannabigerol (CBG)-rich varieties (chemotype IV) and in those varieties with a balanced level of both CBD and THC (chemotype III), while its levels were not detectable in cannabichromene (CBC)-rich varieties (chemotype VI). The presence of the *cis* isomer of THC and THCA raises the question on whether to include or not this species in the calculation of the total amount of THC to classify a cannabis variety as a drug-type or a fiber-type (hemp).

1. Introduction

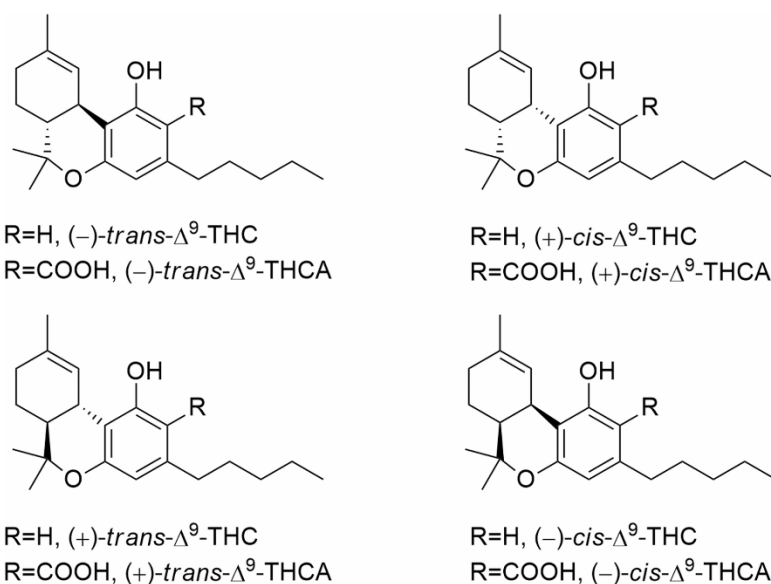
Cannabis sativa L. is known for its uncountable properties, which cover the pharmaceutical [1], cosmetic [2] and nutraceutical [3] sphere. Characteristic euphoriant effects are generally ascribed to cannabis extracts rich in Δ^9 -tetrahydrocannabinol (Δ^9 -THC), the psychoactive compound derived from the conversion of the naturally occurring tetrahydrocannabinolic acid (THCA) via heat-assisted decarboxylation [4]. Traces of Δ^9 -THC can be also found in unheated cannabis inflorescence following spontaneous chemical decarboxylation due to heat and/or light during drying or storage [5]. Whilst cannabidiolic acid (CBDA) and cannabidiol (CBD) represent the non-narcotic most abundant compounds found in cannabis [6], THCA and Δ^9 -THC are the most thoroughly studied phytocannabinoids in the cannabis plant, especially for the narcotic and therapeutic properties of the latter [1,7]. The molecule of Δ^9 -THC possesses two stereogenic centers, which potentially generate four stereoisomers: (-)-*trans*- Δ^9 -THC, (+)-*trans*- Δ^9 -THC, (-)-*cis*- Δ^9 -THC and (+)-*cis*- Δ^9 -THC (Fig. 1) [8]. As reported in the literature, the (-)-*trans* isomer is the most abundant form found in cannabis extracts, while the others are present only in trace [8]. Although Smith reported the isolation of *cis*- Δ^9 -THC by HPLC-UV in seized marijuana samples for the first time in 1977 [9], the real existence of *cis*- Δ^9 -THC has been dismissed until a work by Schafroth et al. appeared in 2021 [10]. The latter described the quantification of *cis*- Δ^9 -THC in low THC-containing industrial hemp, thus confirming

the natural occurrence of this stereoisomer of Δ^9 -THC. However, the authors declared they were unable to isolate the natural compound despite the apparently high amount, in most cases comparable to that of *trans*- Δ^9 -THC [10]. Their experiments led to the conclusion that *cis*- Δ^9 -THC might originate either from the same process that generates CBD and *trans*- Δ^9 -THC through a specific oxidocyclase or the one that leads to cannabichromene (CBC) from cannabigerolic acid (CBGA) through a pericyclic cyclase [10]. Nonetheless, the origin of this molecule is far from being elucidated as all analyses were carried out on heated cannabis extracts, which unavoidably are characterized by the predominant presence of the decarboxylated species of all phytocannabinoids [9,10]. Moreover, it is known that the decarboxylation reaction has different kinetics for each cannabinoid and is affected by several parameters [11,12], thus the concentration obtained for decarboxylated cannabinoids does not necessarily reflect the actual cannabinoid profile of the living plant. These hypotheses imply the existence of the carboxylated form of *cis*- Δ^9 -THC, *cis*- Δ^9 -tetrahydrocannabinolic acid (*cis*- Δ^9 -THCA) (Fig.1), which has never been reported in the literature so far. To the best of the authors' knowledge, this is the first time that the natural precursor of *cis*- Δ^9 -THC, namely Δ^9 -*cis*-THCA, is reported. This work aimed at identifying this compound by high performance liquid chromatography coupled to high-resolution mass spectrometry (HPLC-HRMS) and synthesizing the corresponding pure standard to be used for the development and validation of a quantitative analytical method according to ICH Q2(R1) harmonized guidelines [14]. *Cis*- Δ^9 -THCA, along with other nine cannabinoids, was successfully quantified in ten cannabis samples from different varieties and chemotypes, which were not subjected to heat before the analysis to preserve the original cannabinoid composition of the plant material.

2. Materials and methods

2.1. Materials

LC-MS grade water, acetonitrile and formic acid and analytical grade ethanol 96% (v/v) were purchased from Carlo Erba (Milan, Italy). Stock solutions of pure certified analytical standards of *trans*- Δ^9 -THCA, CBDA, cannabichromenic acid (CBCA), CBGA, *trans*- Δ^9 -THC, CBD, CBC, and CBG were bought from Cerilliant (Sigma-Aldrich Merck, Milan, Italy). *cis*- Δ^9 -THCA and *cis*- Δ^9 -THC were synthesized in house. Plant materials were taken from a germplasm collection maintained at CREA-CI (Research Centre of Cereals and Industrial Crops, Bologna, Italy), and comprise strains used for medical production (1), commercial hemp varieties (3-6), new breeding lines for medical (2) or industrial (7, 8,10) applications and a Chinese accession (9). Details on the origin and type of the samples are reported in the Supplementary Material.



2.2. Synthesis and characterization of *cis*- Δ^9 -THCA

The synthetic procedures to obtain *cis*- Δ^9 -THCA are reported in the Supplementary Material. Reactions were monitored through thin-layer chromatography on silica gel (60 F-254, E. Merck) and HPLC-UV ($\lambda = 230$ nm) following the same method employed for the identification of *cis*- Δ^9 -THCA described in the next paragraphs. Flash chromatography on silica gel (40–63 μm) was used to purify the desired reaction products, which were then characterized by mono- and bidimensional NMR. NMR spectra were acquired on a Bruker 400 spectrometer working at 400.134 MHz for ^1H and at 100.62 MHz for ^{13}C . Chemical shifts (δ) are reported in ppm with respect to the solvent residual peaks (CDCl_3 $\delta = 7.26$ ppm for proton and $\delta = 77.20$ ppm for carbon); coupling constants are reported in Hz; splitting patterns are expressed as follows: singlet (s), doublet (d), triplet (t), quartet (q), double doublet (dd), quintet (qnt), multiplet (m), broad signal (b). COSY spectra were recorded as a 2048×256 matrix with 2 transients per t1 increment and processed as a 2048×1024 matrix; the HSQC spectra were recorded as a 2048×256 matrix with 4 transients per t1 increment and processed as a 2048×1024 matrix, and the one-bond heteronuclear coupling value was set to 145 Hz; the HMBC spectra were recorded as a 4096×256 matrix with 16 transients per t1 increment and processed as a 4096×1024 matrix, and the long-range coupling value was set to 8 Hz.

2.3. Extraction of *Cannabis sativa* L. samples

Cannabis sativa L. samples were extracted according to the protocol of the German Pharmacopoeia and as reported in previous works [15–18]. Briefly, three extraction cycles of 15 min each with 20 mL, 12.5 mL and 12.5 mL of ethanol were performed on 500 mg of finely powdered biomass and the liquid phase was brought to 50 mL in a volumetric flask with fresh ethanol. A small aliquot (1 mL)

was filtered through a 0.45 μm syringe filter and diluted 1:10 with acetonitrile for the injection into the HPLC-HRMS apparatus. The extracts were analyzed straight after their preparation.

Table 1
 ^1H and ^{13}C NMR signals of *cis*- and *trans*- Δ^9 -THCA.

	^1H NMR (400 MHz, CDCl_3)		^{13}C NMR (100 Hz, CDCl_3)	
	(+/-)- <i>cis</i> -THCA	(-)- Δ^9 - <i>trans</i> -THCA	(+/-)- <i>cis</i> -THCA	(-)- Δ^9 - <i>trans</i> -THCA
COOH			175.39	176.82
-OH	12.20 (bc)	12.15 (s)	-	-
10a	3.57 (bt, 1 H, $J = 4$ Hz)	3.21 (d, 1 H, $J = 11.2$ Hz);	31.45	33.40
10	6.30 (bd)	6.38 (s);	122.30	123.61
9	-	-	134.28	133.62
11	1.68 (s)	1.67 (s)	23.78	23.25
8	1.91–2.03 (m)	2.14 (m)	29.81	31.14
7	1.91–2.03 (m, 1 H)	1.89 (m, 1 H) 1.42 (m, 1 H)	21.06	24.93
6a	1.43–1.48 (m, 1 H)	-	-	-
6	1.74–1.81 (m)	1.66 (m)	40.21	45.53
12	-	-	77.96	78.75
13	1.29 (s)	1.09 (s)	25.61	27.28
10b	1.42 (s)	1.42 (s)	25.89	19.43
1	-	-	110.65	109.80
2	-	-	165.47	164.65
3	-	-	102.85	102.32
4	-	-	146.61	146.96
5	6.22 (s)	6.24 (s);	112.64	112.63
1'	-	-	158.98	159.74
2'	2.75–2.84 (m, 1 H)	2.77 (dq, 1 H); 2.93 (dq, 1 H);	36.63	36.44
3'-4'	2.85–2.94 (m, 1 H)	-	-	-
5'	1.52–1.61 (m)	1.57 (m)	31.54	31.19
	1.31–1.35 (m)	1.34 (m)	32.27–22.70	31.97–22.45
	0.89 (t)	0.89 (t)	14.20	13.99

2.4. Identification of *cis*- Δ^9 -THCA in *Cannabis sativa* L

Cis- Δ^9 -THCA was identified by HPLC-HRMS using a Vanquish core system (Thermo Fisher Scientific, Waltham, Massachusetts, USA) equipped with a vacuum degasser, a binary pump, a thermostated autosampler set at 4 $^{\circ}\text{C}$, a thermostated column compartment set at 30 $^{\circ}\text{C}$, and a diode array detector (DAD) set at 230 nm and 306 nm. DAD was only employed as additional detector to monitor the analyses but not to quantify the analytes of interest. The chromatographic separation was achieved on a Poroshell EC-C18 column (3 \times 100 mm, 2.7 μm , Agilent, Milan, Italy) using a gradient elution program starting from 95% solvent A (0.1% aqueous formic acid (v/v)) and 5% B (acetonitrile with 0.1% formic acid (v/v)), which linearly increased to 95% B in 20 min and held for 3 min; after a washing step at 98% B for 7 min, the system was re-equilibrated at the initial condition for 6 min. The flow rate was maintained constant at 0.5 mL/min for a total run time of 36 min. The chromatographic apparatus was interfaced to an Exploris 120 Orbitrap mass spectrometer (Thermo Fisher Scientific) with a heated electrospray ionization source (HESI), which operated in both positive (HESI⁺) and negative (HESI⁻) mode. HESI⁻ mode was used for the detection of the carboxylated forms of cannabinoids due to a better signal obtained for these species compared to HESI⁺. Conversely, the decarboxylated species were extracted from the total ion current in HESI⁺ mode for the same reason. Simultaneous full scan (FS) and data- dependent acquisition (DDA) were

employed to run the untargeted metabolomics experiments and obtain the fragmentation spectra of the investigated analytes. The parameters of the HESI source were optimized to obtain the most intense instrument response: capillary temperature, 390°C; vaporizer temperature, 150°C; electrospray voltage, 4.2 kV (positive mode) and 3.8 kV (negative mode); sheath gas, 55 arbitrary units; auxiliary gas, 5 arbitrary units; S lens RF level, 45. Previously optimized parameters of the analyzer were used: resolution, 60,000 FWHM (full width at half maximum) at m/z 200 FS mode and 15,000 FWHM for DDA mode; scan range, m/z 75–750; maximum injection time, 54 ms for FS mode and 22 ms for DDA mode; isolation window, m/z 0.7 for FS mode and m/z 1.2 for DDA mode; stepped NCE (normalized collision energy), 20–40–100; [19]. An absolute collision energy of 20 eV was applied to obtain a different fragmentation spectrum for the *cis* and the *trans* isomer of THCA. The injection volume was 5 μ L. The analytes precursor ions $[M-H]^-$ and $[M+H]^+$ were extracted with a 5-ppm mass tolerance from the total ion current. The analyses were acquired with Xcalibur 3.0 (Thermo Fisher Scientific) and processed using TraceFinder 5.0 (Thermo Fisher Scientific).

2.5. Quantification of *cis*- Δ^9 -THCA and other phytocannabinoids in *Cannabis sativa* L

The same chromatographic parameters used for the identification of *cis*- Δ^9 -THCA in standard solutions and plant material were employed for its quantification. The mass analyzer operated in t-SIM (targeted selected ion monitoring) to improve selectivity and specificity. The t-SIM allowed to select the exact m/z of the $[M-H]^-$ precursor ion ($\Delta m/z = 0.4$) of *cis*- Δ^9 -THCA (357.2071) based on the chemical formula ($C_{22}H_{30}O_4$). A freshly prepared calibration curve was used to quantify *cis*- Δ^9 -THCA in ten cannabis samples. Calibration curves for the other phytocannabinoids (CBDA, CBGA, *trans*-THCA, CBCA, CBD, CBG, *cis*- Δ^9 -THC, *trans*- Δ^9 -THC, and CBC) were built using the same chromatographic and spectrometric conditions employed for *cis*- Δ^9 -THCA. All phytocannabinoids were quantified in *Cannabis sativa* L. samples, which were also run in the same analytical conditions.

2.5.1. Preparation of the standard solutions

Serial 1:10 dilutions of a *cis*- Δ^9 -THCA stock solution (1 mg/mL) were prepared and used to get stock solutions with the final concentrations of 100 and 10 μ g/mL. The latter were used to prepare five non-zero calibration points (10, 50, 100, 500, and 1000 ng/mL) and three (low, medium, and high) quality control (QC) samples (LQC 25 ng/mL, MQC 250 ng/mL, and HQC 750 ng/mL). All dilutions were prepared in amber glass vials by adding acetonitrile to the standard solutions.

2.5.2. Method validation

The method was validated according to ICH Q2(R1) guidelines [14] for linearity range, sensitivity, selectivity, repeatability, carry-over, accuracy, precision, recovery, matrix effect, short-term stability, freeze-thaw stability, and long-term stability.

2.5.2.1. Selectivity and purity.

Selectivity was evaluated by analyzing six hemp samples lacking *cis*- Δ^9 -THCA (Ermo variety) and verifying that no other interfering compounds with the same [M-H]⁻ precursor ion eluted at the same retention time. Reproducibility was evaluated by the standard deviation (SD) of the retention time of the analyte in all runs during the entire validation. This value should not exceed 2.5%. Peak purity was assessed by comparing the MS/MS spectrum of *cis*- Δ^9 -THCA at the start, apex, and end of the peak.

2.5.2.2. Sensitivity.

A properly diluted solution of *cis*- Δ^9 -THCA was prepared to obtain an instrument response lower than the one given by the sample known to contain the lowest amount of the analyte. The limit of detection (LOD) was then calculated as three times the SD obtained by analyzing ten times the prepared dilution. The lower limit of quantification (LLOQ) was calculated as ten times the SD of ten injections of the appropriately diluted standard. The upper limit of quantification (ULOQ) was set above the highest amount estimated in the hemp samples.

2.5.2.3. Linearity.

Linearity was assessed in the range 10–1000 ng/mL (accepting an R² of the calibration curve of *cis*- Δ^9 -THCA of at least 0.991). A calibration curve was built each day for five consecutive days and analyses were run in triplicate. The back-calculated concentration was considered acceptable if the mean precision (RSD or CV) was within $\pm 15\%$ of the nominal concentrations for all calibration points and $\pm 20\%$ of the LLOQ.

2.5.2.4. Repeatability and carry-over.

Repeatability was expressed as RSD of the retention time registered in all analytical runs included in the validation process and calculated as the percentage of the ratio between the standard deviation and the mean of the retention time values. RSD is considered acceptable if it is lower than 10%. Autosampler carry-over was assessed by injecting two blank samples after running a ULOQ and a hemp sample known to contain the highest amount of the analyte among all samples available. The carry-over was considered acceptable if the detector response for the analyte in the blanks was within $\pm 20\%$ of the LLOQ.

2.5.2.5. Accuracy and precision.

Precision and accuracy were evaluated at four concentration levels, LLOQ (10 ng/mL), LQC (25 ng/mL), MQC (250 ng/mL), and HQC (750 ng/mL). The intra-day precision and accuracy were calculated by analyzing each level three times ($n = 3$) within a single day and expressed respectively as relative standard deviation (RSD or coefficient of variation CV) and percentage of the mean calculated against nominal concentration. The inter-day precision and accuracy were calculated in the same way by analyzing three times freshly prepared standard solutions for five consecutive days ($n = 15$).

2.5.2.6. Recovery.

Recovery was evaluated on six blank matrix samples derived from cannabinoid-free hemp biomass (Ermo variety), where the analyte of interest is below the LOD. Three of these blanks were extracted with solvent spiked with a known amount of *cis*- Δ^9 -THCA standard solutions to obtain three extracts with the same concentrations as the QC levels (pre-spike). The other three blank matrix samples were first extracted and the analytical samples were spiked with *cis*- Δ^9 -THCA standard solutions to get the same concentrations as the QC levels (postspike). The recovery (%R) was calculated with Eq. 1 and the results were average recoveries ($n = 3$ each) of the investigated analyte:

$$\%R = \frac{\text{Pre - spike}}{\text{Average post - spike}} \times 100$$

The extraction method was considered efficient if %R was in the range 85–115%.

2.5.2.7. Matrix effect.

Matrix effect was evaluated using the same post spike samples used for the calculation of the recovery and QC samples freshly prepared with acetonitrile (neat QC). The matrix factor (MF) was calculated using the following equation (Eq. 2) and the results were average MF ($n = 3$ each) of the investigated analyte:

$$MF = \left[1 - \frac{\text{Post - spike}}{\text{Average neat QC}} \right] \times 100$$

MF was considered acceptable if values were below 15%.

2.5.2.8. Stability. Short-term stability was evaluated at the LLOQ and QC levels for two different storage conditions, bench-top (20°C) and fridge (4°C), in a 24-hour period. Moreover, three freeze-thaw cycles were performed to assess the stability after repeatedly freezing and thawing *cis*- Δ^9 -

THCA standard solutions. Long-term stability was assessed in a 45-days period at the QC levels in three storage conditions, bench-top (20°C), fridge (4°C), and freezer (-20°C).

2.5.3. Statistical analysis

Statistical analysis was performed with GraphPad Prism 8.0.1. Data of concentrations of *cis*- Δ^9 -THCA in each variety were compared with respect to the variable chemotype using one-way ANOVA analysis followed by Tukey's post hoc test. Trans to cis ratio variations among samples within the same chemotype were evaluated with two-way ANOVA and Tukey's post hoc test. Significant difference was considered from $P < 0.05$.

3. Results and discussion

3.1. Synthesis and characterization of *cis*- Δ^9 -THCA

Cis- Δ^9 -THCA was synthesized starting from the corresponding decarboxylated species *cis*- Δ^9 -THC as previously reported for other cannabinoid carboxylic acids following the procedure developed by Mechoulam et al. [13,17]. *Cis*- Δ^9 -THC was obtained by reacting citral with olivetol via pTSA catalysis as also reported by Schafroth et al. [10]. The complex mixture obtained mainly consisted of *trans*-CBD, *trans*- Δ^9 -THC, *cis*- Δ^9 -THC, and smaller amounts of other unknown by-products. A first separation on silica gel allowed to separate the CBD-containing fraction from the THC-containing fraction. The latter was then subject to a further separation on a C18 semi-preparative column to resolve *cis*- Δ^9 -THC and *trans*- Δ^9 -THC. Although the yield was relatively low (10%), a sufficient amount was recovered to undertake the next carboxylation step. *Cis*- Δ^9 -THCA was purified with diethyl ether in order to prevent decarboxylation and preserve its chemical stability. The pure compound was obtained in low yield (7%) in line with those previously reported by Mechoulam and our group [13,17]. Confirmation of the exact structure of *cis*- Δ^9 -THCA came from NMR spectroscopy and HRMS. Table 1 reports the comparison of the ^1H and ^{13}C NMR signals of the *cis* and *trans* isomer of THCA, the latter reported by Fellermeier et al. [20]. Significant differences were observed in ^1H NMR for H-10a and H-6a, the former shifted from 3.21 ppm to 3.57 ppm and the latter from 1.66 ppm to the range 1.77–1.81 ppm. Moreover, H-10a was found to give a broad triplet with a tighter coupling constant ($J=4$ Hz) compared to H-10a of *trans*- Δ^9 -THCA ($J=11.2$ Hz). The theoretical coupling constant for *cis* and *trans* isomers of THCA were reported to be 3.9 Hz and 11.9 Hz respectively [21,22]. The presence of the carboxylic acid group was confirmed by the two protons in 1' position, which appeared as a double multiplet, and the signal of OH-1, which shifted by about 8 ppm (at 12.2 ppm) with respect to the decarboxylated species *cis*- Δ^9 -THC (4.8 ppm). Such shift has been described by Choi et al. as probably due to an intra-molecular hydrogen bonding between the

OH and the ortho-COOH [21]. In ^{13}C NMR spectrum an upward shift of 5 ppm and 2 ppm were observed for C-6a and C-10a, respectively, in comparison with the same carbon atoms in *trans*- Δ^9 -THCA, respectively. Description of the synthetic procedure and characterization of the two new compounds with the mono-dimensional (^1H and ^{13}C) and bidimensional (COSY, HSQC and HMBC) NMR spectra of *cis*- Δ^9 -THCA and comparison with *cis*- Δ^9 -THC are reported in the Supplementary Material.

3.2. Identification of *cis*- Δ^9 -THCA in *Cannabis sativa* L

Untargeted metabolomics is a useful approach for the detection of a large number of polar and apolar compounds in a complex matrix such as plant extracts. *Cannabis sativa* extracts show completely different chemical compositions when heated before analysis [23]. The decarboxylation of the cannabinoid precursors allows only to give an estimation of the compounds present in the original plant material as the reaction does not take place with the same kinetics for all compounds [11,12,23–25]. Moreover, the formation of decarboxylated species could be addressed not only to decarboxylation processes but also to conversion from other cannabinoids. On the other hand, when the extraction is performed on unheated biomass it is possible to preserve the original chemical profile and determine the actual concentration of the carboxylated cannabinoid precursors. An extraction of the peaks corresponding to both carboxylated and decarboxylated phytocannabinoids from a chemotype III cannabis sample is reported in Fig. 2. Although it was not possible to distinguish the two isomers of THCA by mass spectrometry in negative ionization mode, which generally provides the highest signal, they showed a slightly different profile in positive mode (Fig. 3). In particular, a 20 eV collision energy was applied for the fragmentation of the two molecules and a lower relative abundance of the precursor ion $[\text{M}+\text{H}]^+$ was observed (50% for *cis* isomer vs 100% for *trans* isomer). From a chromatographic point of view, we can easily discriminate between the two isomers by the retention time, which is slightly different, 20.91 min and 21.29 min for *cis* and *trans* respectively.

3.3. Quantification of *cis*- Δ^9 -THCA

3.3.1. Method validation

The HPLC-HRMS method was developed in t-SIM mode in order to improve sensitivity and selectivity towards the analyte of interest. The HESI source was set in negative ionization mode to provide better signals for the carboxylated species. The method was validated according to the ICH guidelines to ensure reliable quantitative results for the species under investigation in *Cannabis sativa* biomass. Validation embraced selectivity, linearity, sensitivity, carry-over, accuracy, precision, and stability. The method proved to be selective and sensitive for *cis*- Δ^9 -THCA with LOD of 3 ng/mL and

LLOQ of 10 ng/mL. Linearity was assessed in the range 10–1000 ng/mL with R² greater than 0.995. No carry-over was observed by running blank samples after the analysis of ULOQ and highly concentrated samples. Repeatability was considered optimal as RSD was below 0.1%. Intra-day accuracy and precision were in the range 87.41–114.58% and 0.98–3.53% respectively, while inter-day accuracy and precision were in the range 95.42–110.99% and 4.92–7.71% respectively, thus within the accepted range for the validation of MS-based methods according to ICH Q2(R1) guidelines. Good recovery values were obtained comparing pre- and post-spike peak areas of *cis*- Δ^9 -THCA for all concentration levels, whereby pre- and post-spike related to blank matrices to which a known amount of analytical standard was added respectively either before or after the extraction. In the case of cannabinoids, it is very difficult to provide a blank matrix as it is almost genetically impossible to obtain a cannabis variety free of this class of compounds. A chemotype V variety (Ermo, with low content of cannabinoids) was thus employed as it showed undetectable amount of *cis*- Δ^9 -THCA (<LOD). Matrix effect is an important parameter to evaluate in MS-based methods as matrix can often affect the ionization efficiency of the molecules in a sample. The matrix factor obtained for all concentration levels was below 10%, thus meeting the ICH requirements, and the positive values indicated a slight but acceptable degree of ion suppression for *cis*- Δ^9 -THCA. Short-term stability was evaluated for both bench-top (20°C) and refrigerated conditions (4°C) in a 24-hours interval and provided acceptable results (within 15% of the nominal concentration of freshly prepared standards). Good results were also obtained for long-term stability assessed in a 45-days interval under three conditions: freezer (-20°C), fridge (4°C) and bench-top (20°C). Almost complete loss of the nominal concentration was obtained after three freeze-thaw cycles. The results of the validation are reported in the Supplementary material.

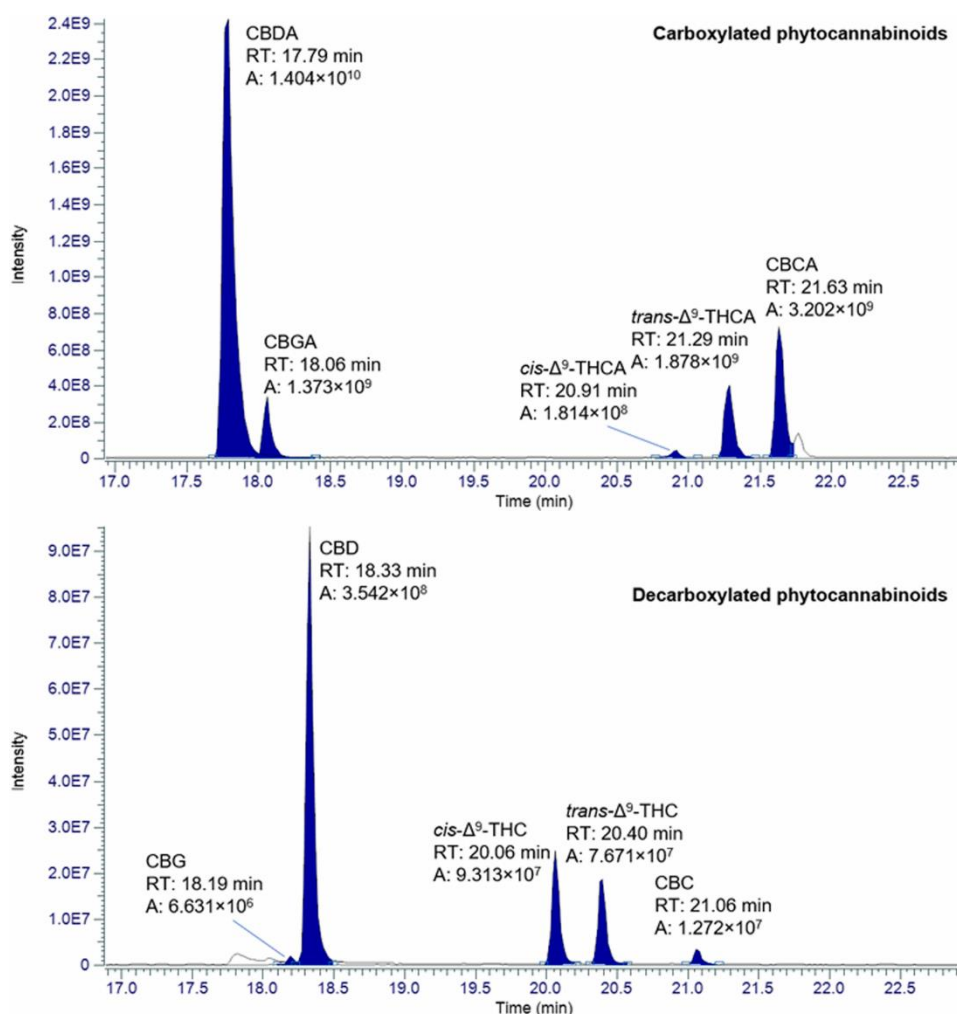


Fig.2. HPLC-HRMS traces of both carboxylated and decarboxylated phytocannabinoids in *Cannabis sativa* L. Extracted ion chromatograms of $[M-H]^-$ of carboxylated species (CBDA, CBGA, *cis*- Δ^9 -THCA, *trans*- Δ^9 -THCA, CBCA) and $[M+H]^+$ of the carboxylated species (CBD, CBG, *cis*- Δ^9 -THC, *trans*- Δ^9 -THC, CBC). Retention time and peak area are indicated.

3.3.2. Quantification of *cis*- Δ^9 -THCA in authentic *Cannabis sativa* L. samples

The pure standard obtained by chemical synthesis was employed to build a calibration curve and quantify *cis*- Δ^9 -THCA in ten cannabis samples with different chemical profiles (two samples for each chemotype), which included THC-rich varieties (chemotype I), varieties with balanced content of CBD and THC (chemotype II), CBD-rich varieties (chemotype III), CBG-rich varieties (chemotype IV), and CBC-rich samples (here indicated as chemotype VI). They are representative of five chemotypes (all except V) previously assessed by HPLC-UV-HRMS. Chemotype V was excluded from the experiments as it does not contain quantifiable levels of phytocannabinoids, while it finds a better use as blank matrix. Along with *cis*- Δ^9 -THCA, the other main cannabinoids (CBDA, CBGA, CBCA, and *trans*-THCA) and the corresponding decarboxylated derivatives (*cis*- Δ^9 -THC, *trans*- Δ^9 -THC, CBD, CBG, and CBC) were also detected and quantified (Tables 2 and 3, respectively). The

highest amount of *cis*- Δ^9 -THCA was found in chemotype III samples (up to about 0.6 mg/g of dry weight) ($P < 0.0001$), while chemotypes I, II and IV showed amounts five to fifteen times lower (0.041–0.110 mg/g) ($P < 0.0001$ for all comparisons). Samples characterized by a prevalence of CBC species presented no detectable levels of this phytocannabinoid. The number of samples available is too small to appreciate a correlation between the concentrations of *cis*-THCA and the belonging chemotype. Moreover, although there seems to exist a constant ratio between the *trans* and the *cis* isomer in each chemotype ($P > 0.05$, i.e. no variation of the *trans* to *cis* ratio between samples within the same chemotype), the investigation of the origin of this phytocannabinoid is beyond the scope of the present work. However, it is noteworthy that the ratio between the two isomeric forms was in favor of the *cis* isomer in chemotype III varieties when considering only the decarboxylated forms. Overall, the total amount of the carboxylated and decarboxylated species for each cannabinoid (calculated as the sum of the amount of the carboxylated species multiplied by 0.877 and that of the decarboxylated species) follows the same trend as that of the carboxylated species. This result is somehow in agreement with the data obtained by Schafroth et al. for *cis*- Δ^9 -THC, which showed higher levels in chemotype III varieties [10]. Considering that the authors decarboxylated the samples before the analysis, the concentration reported in their work should theoretically include both carboxylated and decarboxylated species [10]. The detection of *cis*-THCs in fiber-type cannabis varieties raises the question regarding the calculation of the total THC amount for legal purposes: should these species be included for the classification of a cannabis variety as drug-type or fiber-type? Considering that *cis*- Δ^9 -THC has a weak but efficacious cannabimimetic activity as reported by Schafroth et al. [10], it is reasonable to think that high amounts of *cis*- Δ^9 -THCA can contribute to the psychotropic THC-like effects of cannabis following decarboxylation (e.g. with smoking). As suggested by the same authors, no research has been carried out on the metabolism of *cis*- Δ^9 -THC, which could potentially interfere with forensic evaluation of THC metabolites [10]. Lastly, to the best of the authors' knowledge, no information is currently available on the potential isomerization of the *cis* into the *trans* form of either THCA or THC during decarboxylation. Hence, we cannot say whether all *cis*- Δ^9 -THCA is converted into the corresponding decarboxylated *cis* form or some undergoes isomerization giving the psychoactive *trans* species. Importantly, another compound has been added to the phytocannabinoid HRMS library [26–28] for its straightforward identification in complex biological matrices.

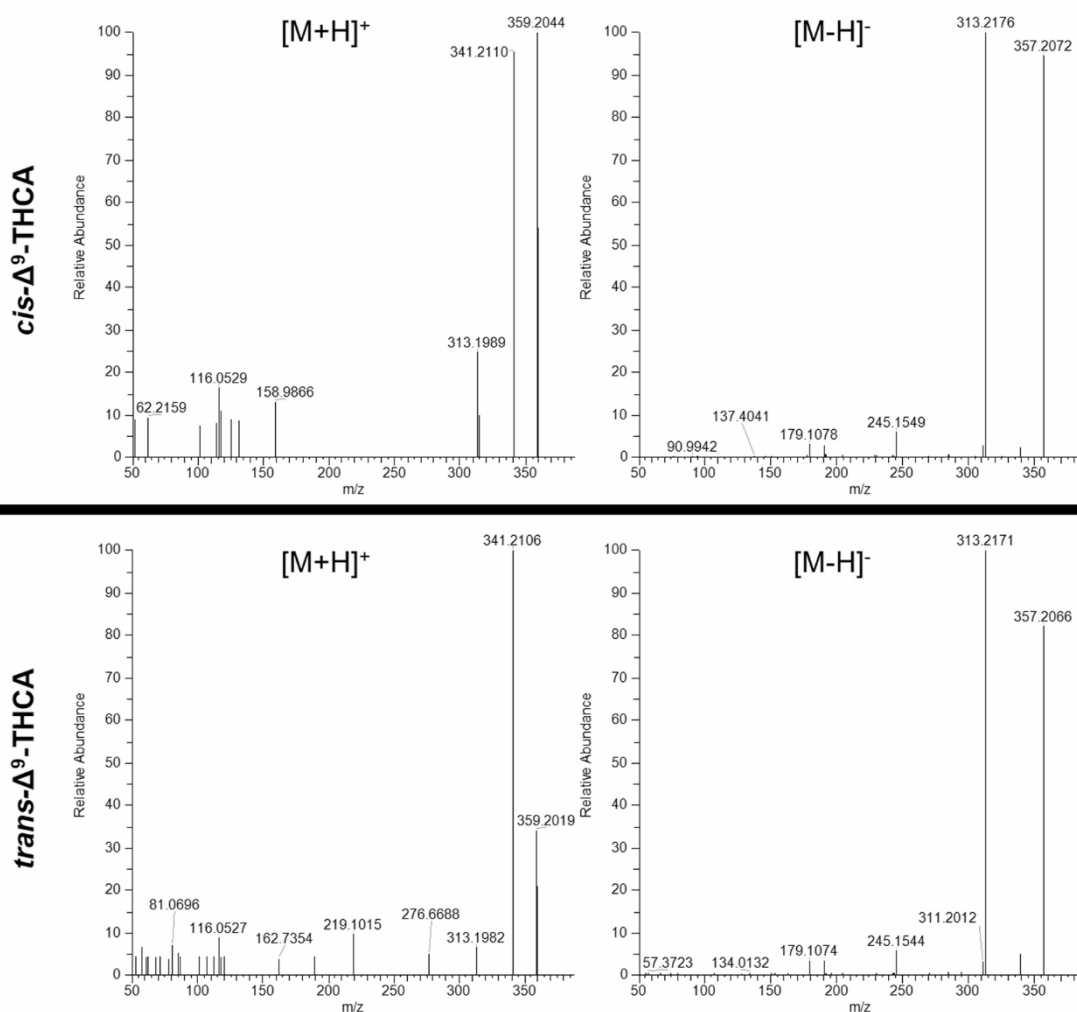


Fig.3. Mass spectrometric characterization of standard *cis*- Δ^9 -THCA and *trans*- Δ^9 -THCA. Mass fragmentation spectra (MS2) of the [M+H]⁺ and [M-H]⁻ of *cis*- Δ^9 - THCA and *trans*- Δ^9 -THCA at 20 eV of collision energy.

4. Conclusions

The *cis* isomer of THCA was identified and quantified in several *Cannabis sativa* samples from different chemotypes, along with all other main phytocannabinoids, resulting in concentrations comparable to or slightly lower than those of its well-known *trans* isomer, especially in CBD- and CBG-rich varieties (chemotypes II, III, and IV). Although the quantification of the decarboxylated species represents a more convenient way to analyze phytocannabinoids, as they are more stable than the corresponding carboxylated precursors, it does not reflect the actual abundance of the phytocannabinoids naturally occurring in the raw material. The availability of the analytical standard of *cis*- Δ^9 -THCA will enable its straightforward quantification in any matrix and open the way to the next step of the research that will disclose the origin of this phytocannabinoid.

Funding

This work was funded by UNIHEMP research project “Use of iNdustrIal Hemp biomass for Energy and new biocheMicals Production” (ARS01_00668) funded by Fondo Europeo di Sviluppo Regionale (FESR) (within the PON R&I 2017–2020 – Axis 2 – Action II – OS 1.b). Grant decree UNIHEMP prot. n. 2016 of 27/07/2018; CUP B76C18000520005. Part of the activity was supported by a project of the Czech Ministry of Education, Youth and Sports (CZ.02.2.69/0.0/0.0/18_053/0016953, Mobility of researchers to support new trends and methods of agricultural research).

CRedit authorship contribution statement

F. Russo, F. Tolomeo, D. Kaczorova: (Synthesis, characterization, method development) Investigation, Formal analysis. L. Carbone, E. Perrone: Validation. R. Paris, F. Fulvio: (Plant samples extraction) Investigation. G. Biagini: (Statistical analysis) Investigation. A. Lagan`a, A. L. Capriotti: (Method validation) Investigation. M.A. Vandelli: Data curation. G. Gigli, R. Paris: Resources. G. Cannazza, C. Citti: Conceptualization, Project administration, Methodology, Writing original draft. G. Cannazza: Funding acquisition. All authors: Writing –review & editing.

Declaration of Competing Interest

The authors declare that they have no known competing financial interests or personal relationships that could have appeared to influence the work reported in this paper.

Table 2

Concentrations of all carboxylated phytocannabinoids in ten cannabis samples. Values are expressed in mg/g (mg of substance per g of dry weight) as mean \pm dev.st (n = 3).

Sample	Chemotype	CBDA	CBGA	<i>trans</i> - Δ^9 -THCA	CBCA	<i>cis</i> - Δ^9 -THCA
1	I	1.503 \pm 0.055	9.146 \pm 0.252	49.173 \pm 0.730	6.076 \pm 0.466	0.058 \pm 0.004
2	I	0.992 \pm 0.015	6.624 \pm 0.061	47.221 \pm 3.575	17.700 \pm 1.459	0.110 \pm 0.009
3	II	11.741 \pm 0.199	1.133 \pm 0.026	14.937 \pm 0.378	1.190 \pm 0.017	0.097 \pm 0.002
4	II	10.167 \pm 0.303	1.087 \pm 0.007	14.262 \pm 0.667	1.044 \pm 0.059	0.089 \pm 0.005
5	III	38.662 \pm 0.636	3.076 \pm 0.093	1.596 \pm 0.060	20.678 \pm 1.140	0.586 \pm 0.017
6	III	42.216	4.628	1.784	20.920	0.636

		± 1.338	± 0.246	± 0.039	± 0.263	± 0.011
7	IV	10.414	35.256	0.104	0.766	0.041
		± 0.210	± 0.313	± 0.032	± 0.171	± 0.004
8	IV	12.500	38.213	0.154	0.996	0.057
		± 0.200	± 1.389	± 0.012	± 0.027	± 0.005
9	VI	0.002	0.330	0.238	28.355	<LOQ ^a
		± 0.000	± 0.008	± 0.003	± 0.546	
10	VI	0.464	0.629	0.386	22.028	<LOD ^b
		± 0.075	± 0.117	± 0.065	± 3.024	

Table 3

Concentrations of all decarboxylated phytocannabinoids in ten cannabis samples. Values are expressed in mg/g (mg of substance per g of dry weight) as mean ± dev.st (n = 3).

Sample	Chemotype	CBD	CBG	<i>trans</i> - Δ^9 -THC	CBC	<i>cis</i> - Δ^9 -THC
1	I	0.017	0.211	1.269	0.216	0.004
		± 0.001	± 0.002	± 0.054	± 0.003	± 0.000
2	I	0.013	0.157	2.748	0.813	0.006
		± 0.000	± 0.004	± 0.180	± 0.004	± 0.000
3	II	0.219	0.033	0.716	0.124	0.025
		± 0.05	± 0.000	± 0.025	± 0.005	± 0.001
4	II	0.152	0.020	0.478	0.093	0.019
		± 0.007	± 0.001	± 0.012	± 0.001	± 0.000
5	III	1.780	0.239	0.185	0.359	0.194
		± 0.050	± 0.007	± 0.002	± 0.014	± 0.002
6	III	1.433	0.454	0.178	0.281	0.229
		± 0.050	± 0.012	± 0.004	± 0.013	± 0.008
7	IV	0.161	1.044	0.017	0.053	0.011
		± 0.010	± 0.012	± 0.000	± 0.003	± 0.000
8	IV	0.145	0.817	0.019	0.049	0.014
		± 0.006	± 0.023	± 0.000	± 0.003	± 0.000
9	VI	<LOQ	0.093	<LOQ	0.081	<LOD
			± 0.010		± 0.003	
10	VI	<LOD	0.032	<LOQ	0.239	<LOD
			± 0.001		± 0.002	

Data availability

Data will be made available on request. Appendix A. Supporting information Supplementary data associated with this article can be found in the online version at doi:10.1016/j.jpba.2022.114958.

References

- [1] P. Kumar, D.K. Mahato, M. Kamle, R. Borah, B. Sharma, S. Pandhi, V. Tripathi, H. S. Yadav, S. Devi, U. Patil, J. Xiao, A.K. Mishra, Pharmacological properties, therapeutic potential, and legal status of *Cannabis sativa* L.: an overview, *Phytother. Res.* 35 (11) (2021) 6010–6029.
- [2] P.R. Cohen, Therapeutic and cosmetic uses of cannabis: cannabinoids for acne treatment and skin - rejuvenation, *Skinmed* (2021) 45–47.
- [3] P. Cerino, C. Buonerba, G. Cannazza, J. D'Auria, E. Ottoni, A. Fulgione, A.D. Stasio, B. Pierri, A. Gallo, A review of hemp as food and nutritional supplement, *Cannabis Cannabinoid Res.* 6 (1) (2021) 19–27.
- [4] M. Kimura, K. Okamoto, Distribution of tetrahydrocannabinolic acid in fresh wild cannabis, *Experientia* 26 (8) (1970) 819–820.
- [5] T. Yamauchi, Y. Shoyama, H. Aramaki, T. Azuma, I. Nishioka, Tetrahydrocannabinolic acid, a genuine substance of tetrahydrocannabinol, *Chem. Pharm. Bull.* 15 (7) (1967) 1075–1076.
- [6] J.A. Toth, G.M. Stack, A.R. Cala, C.H. Carlson, R.L. Wilk, J.L. Crawford, D. R. Viands, G. Philippe, C.D. Smart, J.K.C. Rose, L.B. Smart, Development and validation of genetic markers for sex and cannabinoid chemotype in *Cannabis sativa* L, *GCB Bioenergy* 12 (3) (2020) 213–222.
- [7] E. Carlini, The good and the bad effects of (-) *trans*-delta-9-tetrahydrocannabinol (Δ^9 -THC) on humans, *Toxicol* 44 (4) (2004) 461–467.
- [8] WHO, Fortieth report of the WHO Expert Committee on Drug Dependence, WHO Technical Report Series, N. 1013, World Health Organization, Geneva, 2018.
- [9] R.M. Smith, K.D. Kempfert, D1-3,4-*cis*-tetrahydrocannabinol in *Cannabis sativa*, *Phytochemistry* 16 (1977) 1088–1089.
- [10] M.A. Schafroth, G. Mazzocanti, I. Reynoso-Moreno, R. Erni, F. Pollastro, D. Caprioglio, B. Botta, G. Allegrone, G. Grassi, A. Chicca, F. Gasparrini, J. Gertsch, E.M. Carreira, G. Appendino, Δ^9 -*cis*-Tetrahydrocannabinol: natural occurrence, chirality, and pharmacology, *J. Nat. Prod.* 84 (9) (2021) 2502–2510.
- [11] C. Citti, B. Pacchetti, M.A. Vandelli, F. Forni, G. Cannazza, Analysis of cannabinoids in commercial hemp seed oil and decarboxylation kinetics studies of cannabidiolic acid (CBDA), *J. Pharm. Biomed. Anal.* 149 (2018) 532–540.

- [12] F.E. Dussy, C. Hamberg, M. Luginbuhl, T. Schwerzmann, T.A. Briellmann, Isolation of Delta9-THCA-A from hemp and analytical aspects concerning the determination of Delta9-THC in cannabis products, *Forensic Sci. Int.* 149 (1) (2005) 3–10.
- [13] R. Mechoulam, Z. Ben-Zvi, Carboxylation of resorcinols with methylmagnesium carbonate. Synthesis of cannabinoid acids, *J. Chem. Soc. Chem. Commun.* 7 (1969) 343–344.
- [14] EMA, ICH Harmonised Tripartite Guideline. Validation of Analytical Procedures: Text and Methodology Q2(R1), 2005.
- [15] Cannabis Flos; New Text of the German Pharmacopoeia, Bonn, Germany, 2018.
- [16] P. Linciano, C. Citti, F. Russo, F. Tolomeo, A. Lagan`a, A.L. Capriotti, L. Luongo, M. Iannotta, C. Belardo, S. Maione, F. Forni, M.A. Vandelli, G. Gigli, G. Cannazza, Identification of a new cannabidiol n-hexyl homolog in a medicinal cannabis variety with an antinociceptive activity in mice: cannabidihexol, *Sci. Rep.* 10 (1) (2020) 22019.
- [17] P. Linciano, F. Russo, C. Citti, F. Tolomeo, R. Paris, F. Fulvio, N. Pecchioni, M. A. Vandelli, A. Lagan`a, A.L. Capriotti, G. Biagini, L. Carbone, G. Gigli, G. Cannazza, The novel heptyl phorolic acid cannabinoids content in different Cannabis sativa L. accessions, *Talanta* 235 (2021), 122704.
- [18] F. Fulvio, R. Paris, M. Montanari, C. Citti, V. Cilento, L. Bassolino, A. Moschella, I. Alberti, N. Pecchioni, G. Cannazza, G. Mandolino, Analysis of sequence variability and transcriptional profile of cannabinoid synthase genes in Cannabis sativa L. chemotypes with a focus on cannabichromenic acid synthase, *Plants* 10 (9) (2021) 1857.
- [19] F. Tolomeo, F. Russo, M.A. Vandelli, G. Biagini, A.L. Capriotti, A. Laganà, L. Carbone, G. Gigli, G. Cannazza, C. Citti, HPLC-UV-HRMS analysis of cannabigerovarín and cannabigerobutol, the two impurities of cannabigerol extracted from hemp, *J. Pharm. Biomed. Anal.* 203 (2021), 114215.
- [20] M. Fellermeier, W. Eisenreich, A. Bacher, M.H. Zenk, Biosynthesis of cannabinoids. Incorporation experiments with (13)C-labeled glucoses, *Eur. J. Biochem.* 268 (6) (2001) 1596–1604.
- [21] Y.H. Choi, A. Hazekamp, A.M.G. Peltenburg-Looman, M. Fr´ed´erich, C. Erkelens, A. W.M. Lefeber, R. Verpoorte, NMR assignments of the major cannabinoids and cannabiflavonoids isolated from flowers of Cannabis sativa, *Phytochem. Anal.* 15 (6) (2004) 345–354.
- [22] M. Karplus, Contact electron-spin coupling of nuclear magnetic moments, *J. Chem. Phys.* 30 (1) (1959) 11–15.
- [23] C. Citti, F. Russo, S. Sgr`o, A. Gallo, A. Zanutto, F. Forni, M.A. Vandelli, A. Laganà, C.M. Montone, G. Gigli, G. Cannazza, Pitfalls in the analysis of phytocannabinoids in cannabis inflorescence, *Anal. Bioanal. Chem.* 412 (17) (2020) 4009–4022.

- [24] M. Wang, Y.-H. Wang, B. Avula, M.M. Radwan, A. Wanas, Jv Antwerp, J. F. Parcher, M.A. ElSohly, I.A. Khan, Decarboxylation study of acidic cannabinoids: a novel approach using ultra-high-performance supercritical fluid chromatography/photodiode array-mass spectrometry, *Cannabis Cannabinoid Res.* 1 (1) (2016) 262–271.
- [25] D. Wianowska, A.L. Dawidowicz, M. Kowalczyk, Transformations of Tetrahydrocannabinol, tetrahydrocannabinolic acid and cannabiniol during their extraction from *Cannabis sativa* L, *J. Anal. Chem.* 70 (8) (2015) 920–925.
- [26] C.M. Montone, A. Cerrato, B. Botta, G. Cannazza, A.L. Capriotti, C. Cavaliere, C. Citti, F. Ghirga, S. Piovesana, A. Laganà, Improved identification of phytocannabinoids using a dedicated structure-based workflow, *Talanta* 219 (2020), 121310.
- [27] A. Cerrato, C. Citti, G. Cannazza, A.L. Capriotti, C. Cavaliere, G. Grassi, F. Marini, C.M. Montone, R. Paris, S. Piovesana, A. Lagan`a, Phytocannabinomics: untargeted metabolomics as a tool for cannabis chemovar differentiation, *Talanta* 230 (2021), 122313.
- [28] A.L. Capriotti, G. Cannazza, M. Catani, C. Cavaliere, A. Cavazzini, A. Cerrato, C. Citti, S. Felletti, C.M. Montone, S. Piovesana, A. Laganà, Recent applications of mass spectrometry for the characterization of cannabis and hemp phytocannabinoids: from targeted to untargeted analysis, *J. Chromatogr. A* 2021 (1655), 462492.

Supplementary Material

*Cis- Δ^9 -tetrahydrocannabinolic acid occurrence in *Cannabis sativa* L.*

Francesco Tolomeo^{a,†††}, Fabiana Russo^{b,c,†}, Dominika Kaczorova^{d,e}, Maria Angela Vandelli^f, Giuseppe Biagini^c, Aldo Laganà^{a,g}, Anna Laura Capriotti^g, Roberta Paris^h, Flavia Fulvio^h, Luigi Carbone^a, Elisabetta Perrone^a, Giuseppe Gigli^a, Giuseppe Cannazza^{a,f,*}, Cinzia Citti^{a,f,*}

^a Institute of Nanotechnology – CNR NANOTEC, Campus Ecotekne, Via Monteroni, 73100 – Lecce, Italy

^b Clinical and Experimental Medicine PhD Program, University of Modena and Reggio Emilia, 41125 – Modena, Italy

^c Department of Biomedical, Metabolic and Neural Sciences, University of Modena and Reggio Emilia, 41125 – Modena, Italy

^d Centre of the Region Haná for Biotechnological and Agricultural Research, Department of Genetic Resources for Vegetables, Medicinal and Special Plants, Crop Research Institute, Šlechtitelů 29, 78371 Olomouc, Czech Republic

^e Department of Biochemistry, Faculty of Science, Palacký University, Šlechtitelů 27, 78371 Olomouc, Czech Republic

^f Department of Life Sciences, University of Modena and Reggio Emilia, Via Campi 103, 41125 – Modena, Italy

^g Department of Chemistry, Sapienza University of Rome, Piazzale Aldo Moro 5, 00185 – Rome, Italy

^h CREA – Research Center for Cereal and Industrial Crops, Via di Corticella 133, 40128, Bologna, Italy

Table of content

Synthesis of <i>cis-Δ^9-THCA</i>	---SI-2
¹H-NMR and ¹³C-NMR of <i>cis-Δ^9-THC</i>	---SI-4
¹H-NMR, ¹³C-NMR, COSY, HSQC and HMBC of <i>cis-Δ^9-THCA</i>	---SI-6
HPLC-HRMS method validation	---SI-13

††† These authors contributed equally to the work.

* Corresponding authors:

Giuseppe Cannazza, Ph.D., Email: giuseppe.cannazza@unimore.it; Tel.: +39 059 2055013.; Fax: +39 059 2055750.

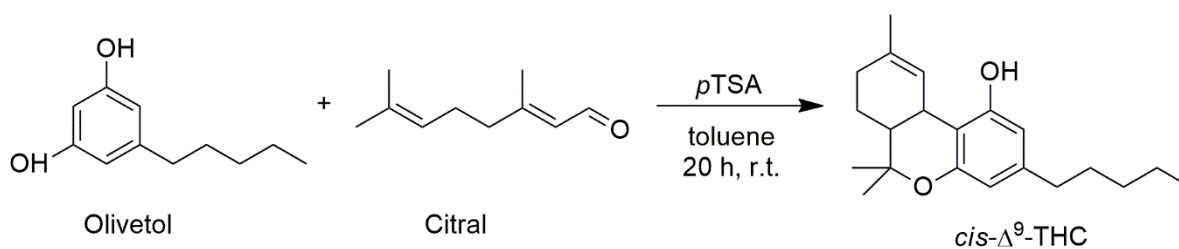
Cinzia Citti, Ph.D., Email: cinzia.citti@unimore.it; Tel.: +39 0832 319206.

Synthesis of *cis*- Δ^9 -THCA

Synthesis of 6,6,9-trimethyl-3-pentyl-6a,7,8,10a-tetrahydro-6H-benzo[*c*]chromen-1-ol (*cis*- Δ^9 -THC)

To a solution of olivetol (1eq; 3.4mmol) and citral (0.9eq., 3 mmol) in dry toluene (20 mL), under nitrogen atmosphere and at room temperature, *p*-toluenesulfonic acid (*p*TSA, 10% mol) was added according to the procedure reported by Schafroth et al. [1]. The reaction was stirred in the same conditions for 20 hours. The reaction was quenched with a saturated solution of NaHCO₃. The aqueous and organic phases were separated. The latter was washed with brine, dried over anhydrous Na₂SO₄ and concentrated in the rotavapor. The crude was purified over silica gel (ratio crude:silica 1:80, eluent CE:DCM 6/4) and subsequent semipreparative liquid chromatography (LC Column Luna® 5 μ m C18(2) 100Å 250×10 mm, Mobile phase 90% ACN 0.1% formic acid, 10 mL/min, loop 700 μ L) to give 106 mg of colourless oil (10%).

¹H NMR (400 MHz, CDCl₃) δ 6.25 (d, *J*=4Hz, 1H), 6.23-6.19 (m, 1H), 6.13(d, *J*=8Hz, 1H), 4.76 (s, 1H), 3.55 (bt, *J*=4Hz, 1H), 2.42 (t, *J*= 8Hz, 2H), 2.03-1.89 (m, 3H), 1.75-1.70 (m, 1H), 1.69s (s, 3H), 1.59-1.52 (m, 2H), 1.49-1.44 (m, 1H), 1.39 (s, 3H), 1.34-1.28 (m, 4H), 1.27 (s, 3H), 0.88 (t, *J*=4Hz, 3H). ¹³C NMR (101 MHz, CDCl₃) δ 154.95, 154.06, 142.64, 135.25, 122.14, 110.21, 108.16, 76.35, 40.24, 35.58, 31.76, 31.69, 30.76, 29.97, 26.11, 25.51, 23.86, 22.73, 20.85, 14.20.

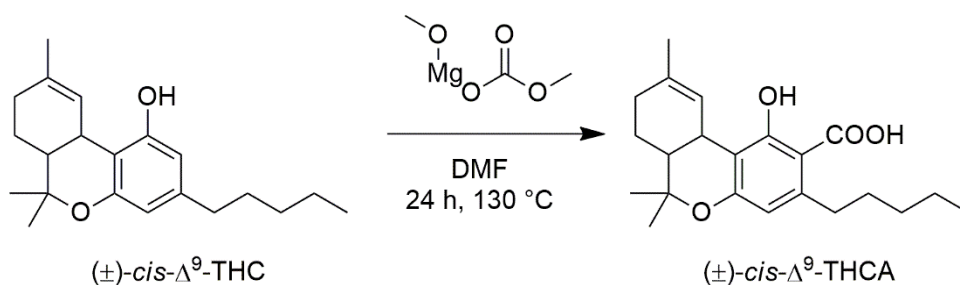


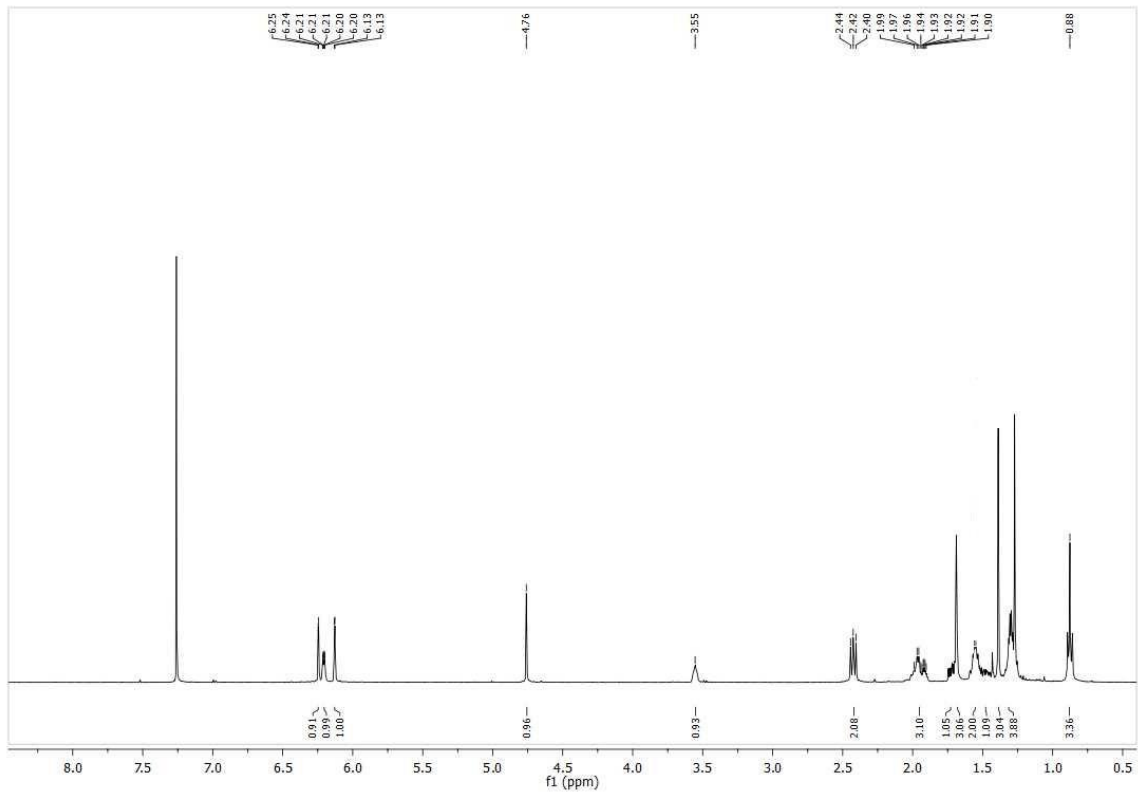
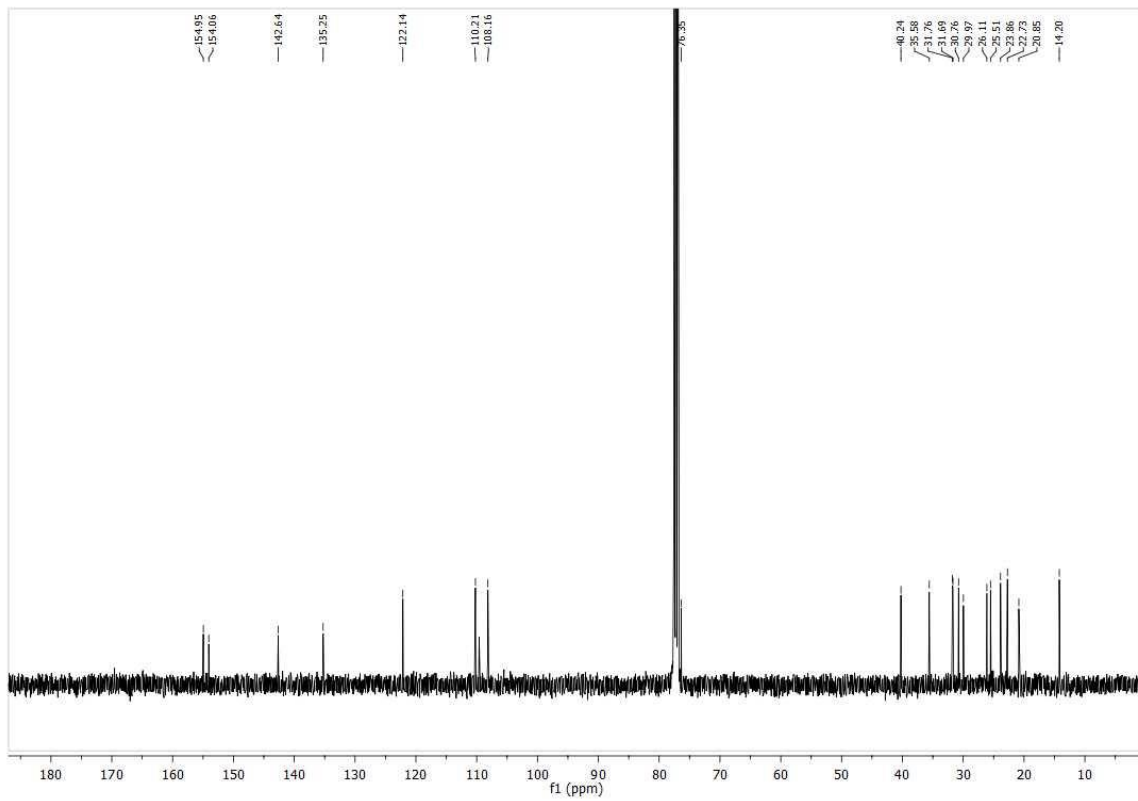
Scheme 1. Synthesis of cis- Δ^9 -THC.

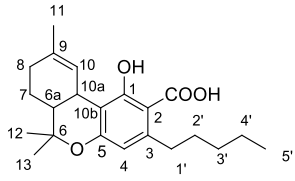
Synthesis of 1-hydroxy-6,6,9-trimethyl-3-pentyl-6a,7,8,10a-tetrahydro-6H-benzo[c]chromene-2-carboxylic acid (cis- Δ^9 -THCA)

cis- Δ^9 -THCA was synthesized as reported for *trans*-THCPA [2]. To a 2 M solution of MMC in DMF (0.34mmol/1eq), *cis*- Δ^9 -THC (0.34 mmol/1eq) was added. The reaction was stirred at 130 °C for 24 hours. Therefore, the reaction was cooled at room temperature, diluted with Et₂O and acidified with 1 N HCl. The organic layer was washed with brine, dried over anhydrous Na₂SO₄, filtered and concentrated. The crude was purified over silica gel (eluent CE/DCM 1:1 (v/v) and then Et₂O 100%) to give 8.5mg (7% yield) of colourless liquid.

¹H NMR (400 MHz, CDCl₃) δ 12.20 (s, 1H) 6.28 (bs, 1H), 6.20 (s, 1H), 3.55 (s, 1H), 2.93-2.71 (m, 2H), 2.02-1.85 (m, 3H), 1.79-1.71 (m, 1H), 1.66 (s, 3H), 1.59-1.50 (m, 2H), 1.45-1.40 (m, 1H), 1.39 (s, 3H), 1.33-1.28 (m, 4H), 1.26 (s, 3H), 0.87 (t, *J*=4Hz, 3H). ¹³C NMR (101 MHz, CDCl₃) δ 175.39, 165.47, 158.98, 146.61, 134.28, 122.30, 112.64, 110.65, 102.85, 77.96, 40.21, 36.63, 32.27, 31.54, 31.45, 30.57, 29.81, 25.89, 25.61, 23.78, 22.70, 21.06, 14.20.

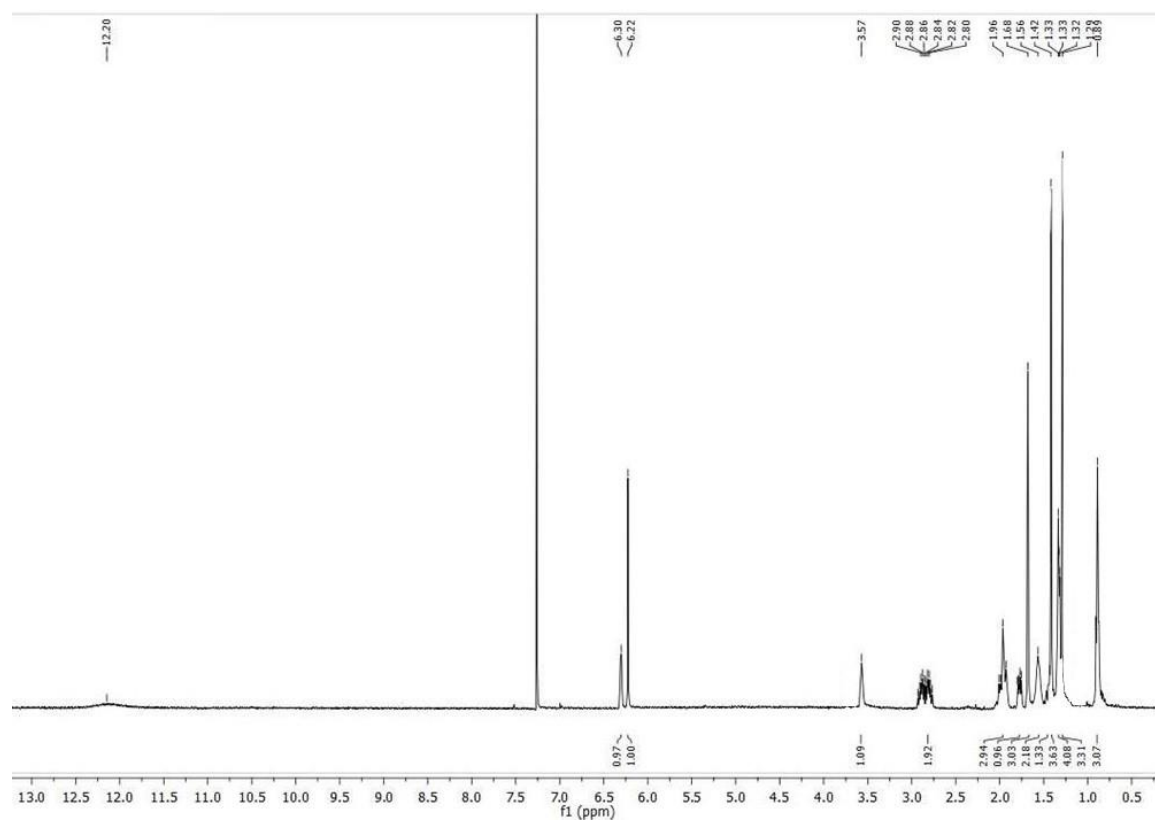
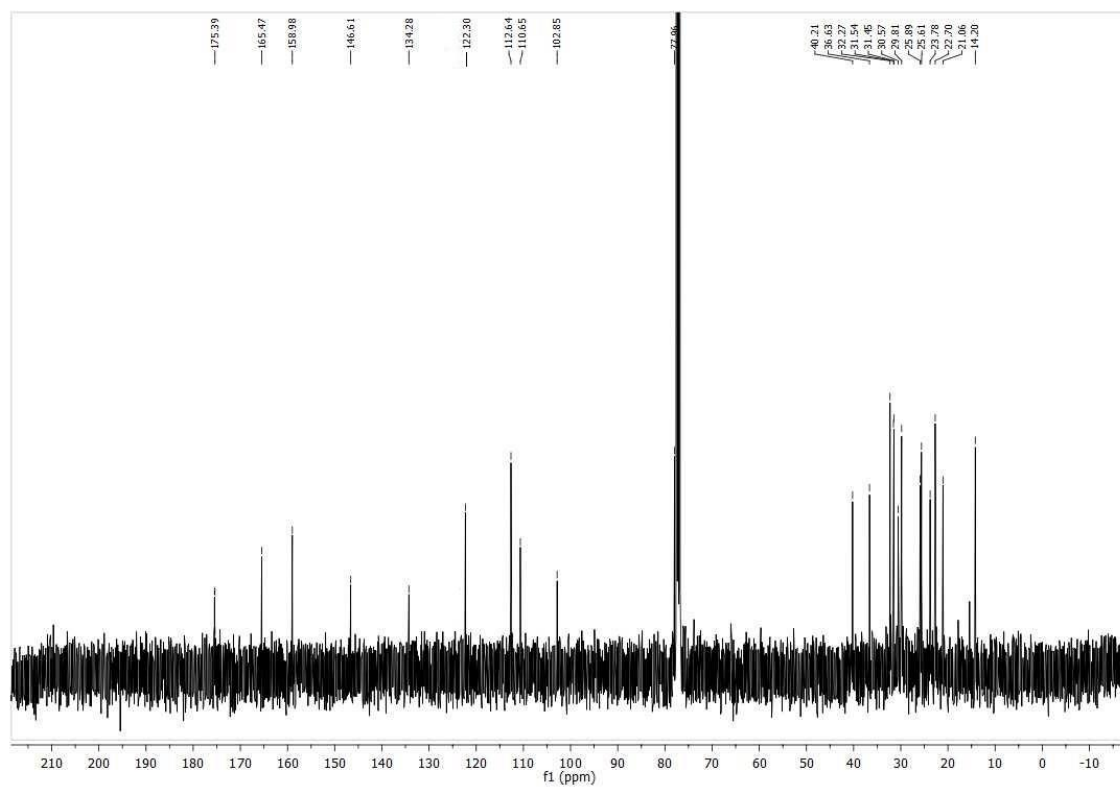


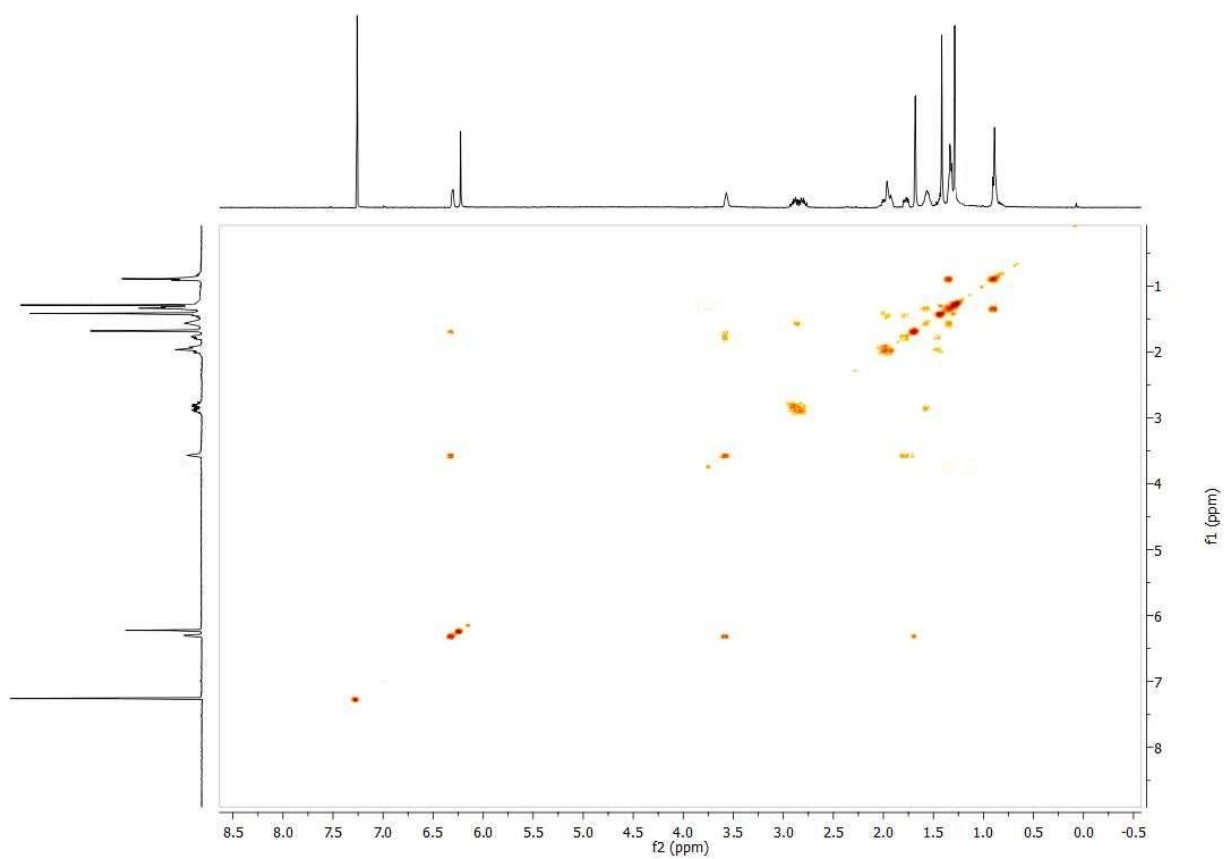
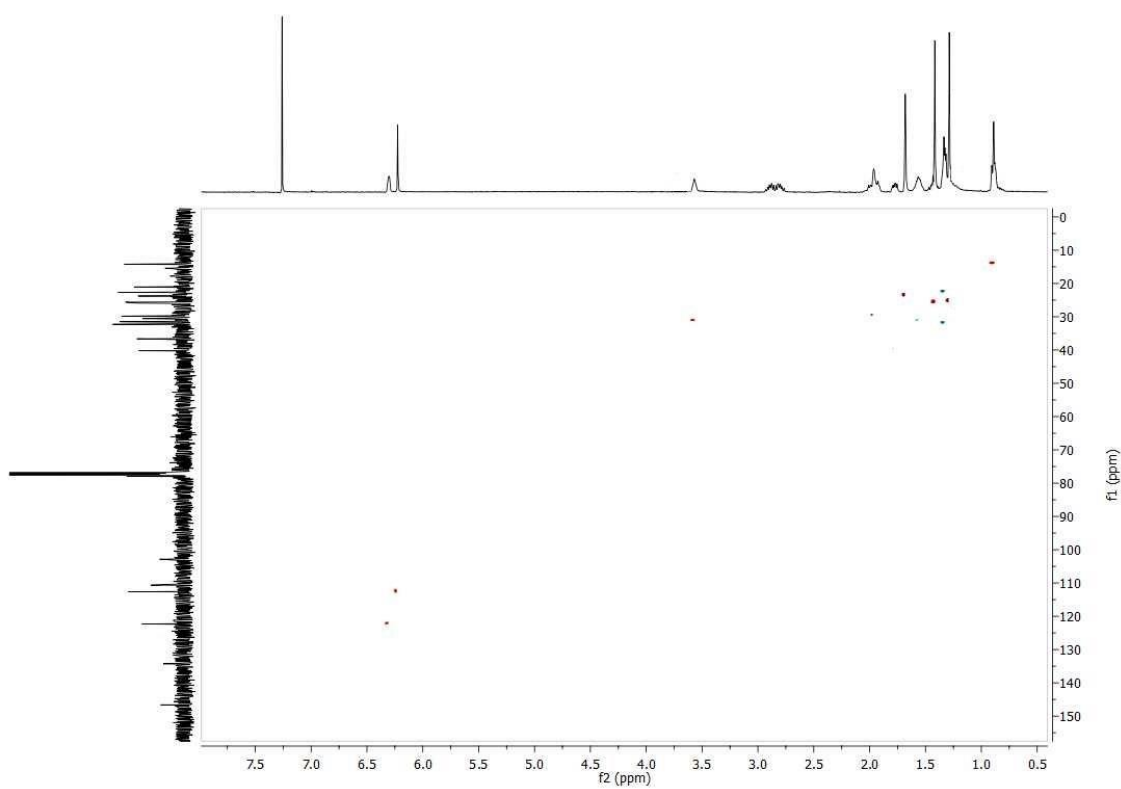
$^1\text{H-NMR}$ of *cis*- Δ^9 -THC **$^{13}\text{C-NMR}$ of *cis*- Δ^9 -THC**

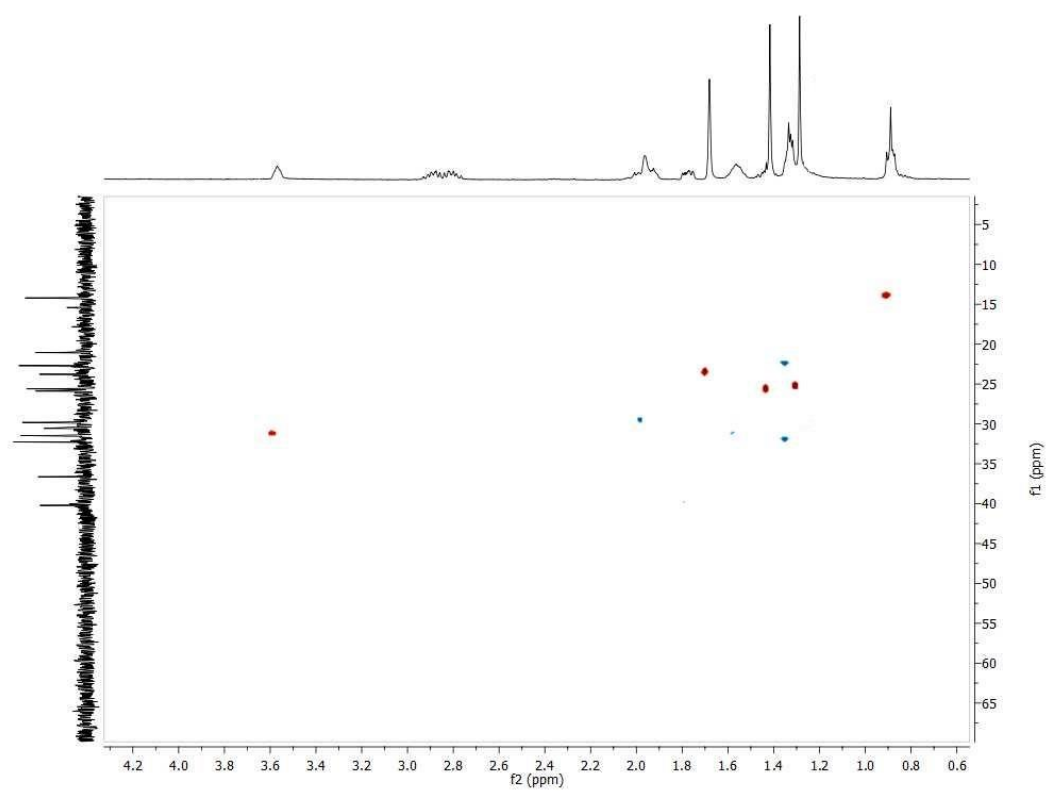
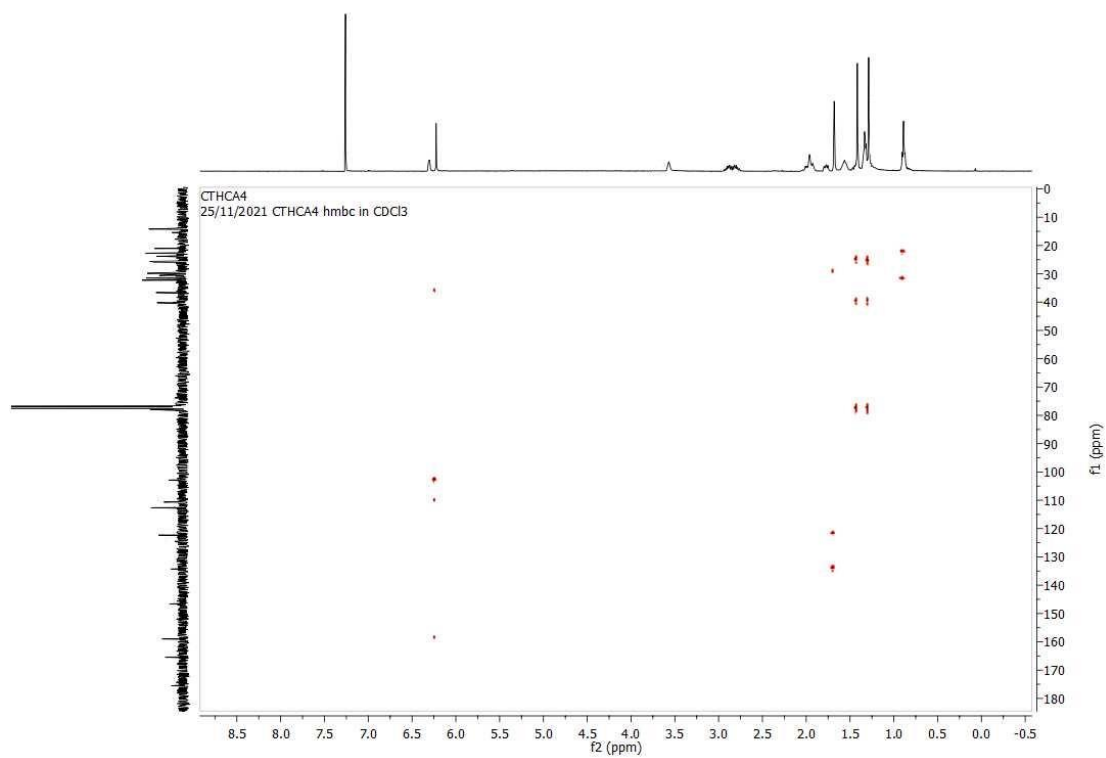
¹H-NMR and ¹³C-NMR of *cis*- Δ^9 -THCATable 1. Characteristic ¹H and ¹³C NMR signals of *cis*- Δ^9 -THC and *cis*- Δ^9 -THCA.


R=H, Δ^9 -THC
R=COOH, Δ^9 -THCA

	¹ H NMR (400 MHz, CDCl ₃)		¹³ C NMR (100 Hz, CDCl ₃)	
	(±)- <i>cis</i> -THC	(±)- <i>cis</i> -THCA	(±)- <i>cis</i> -THC	(±)- <i>cis</i> -THCA
COOH	-	-	-	175.39
10a	3.55 (bt)	3.57 (bt)	31.69	31.45
10	6.23-6.19 (m)	6.30 (bd)	122.14	122.30
9	-	-	135.25	134.28
11	1.69 (s)	1.68 (s)	23.86	23.78
8	1.88-2.03 (m)	1.91-2.03 (m)	29.97	29.81
7	1.88-2.03 (m, 1H) 1.44-1.49 (m, 1H)	1.91-2.03 (m, 1H) 1.43-1.48 (m, 1H)	20.85	21.06
6a	1.70-1.75 (m)	1.74-1.81 (m)	40.24	40.21
6	-	-	76.35	77.96
12	1.27 (s)	1.29 (s)	25.51	25.61
13	1.39 (s)	1.42 (s)	26.11	25.89
10b	-	-	110.21	110.65
1	-	-	154.95	165.47
2	6.13 (d)	-	108.16	102.85
3	-	-	142.64	146.61
4	6.25 (d)	6.22 (s)	110.21	112.64
5	-	-	154.06	158.98
1'	2.42 (t)	2.75-2.94 (m)	35.58	36.63
2'	1.52-1.59 (m)	1.52-1.61 (m)	30.76	31.54
3'-4	1.28-1.32 (m)	1.31-1.35 (m)	31.76-22.73	32.27-22.70
5'	0.88 (t)	0.89 (t)	14.20	14.20
1-OH	4.76 (s)	12.20 (bs)		

¹H NMR of *cis*- Δ^9 -THCA**¹³C NMR of *cis*- Δ^9 -THCA**

1COSY of *cis*- Δ^9 -THCAHSQC of *cis*- Δ^9 -THCA

HSQC of *cis*- Δ^9 -THCA (zoom in)HMBC of *cis*- Δ^9 -THCA

HPLC-HRMS method validation

Table S 4. Linearity parameters for *cis-Δ⁹-THCA* (slope, intercept and R²). Values are expressed as mean±standard error (n=3) and reported for five batches prepared for five consecutive days..

Batch	Slope	Intercept	R ²
1	236430854±4617616	-1816101±622008	0.9970
2	195890084±4780961	599761±644012	0.9953
3	169694594±3726230	2467678±501936	0.9962
4	157518967±1673104	2044471±225373	0.9991
5	170778823±2506501	1061666±337634	0.9983

Table S 5. Intra-day and inter-day accuracy and precision at four concentration levels (LLOQ, LCQ, MQC, and HQC) and recovery and matrix factor of *cis-Δ⁹-THCA* at the QC levels. Values are expressed as mean of three analyses for intra-day accuracy and precision and 15 analyses for inter-day accuracy and precision (n=3 for 5 consecutive days).

Level	Recovery (%)	MF(%)	Accuracy		Precision (RSD%)	
			Intra-day	Inter-day	Intra-day	Inter-day
LLOQ	-	-	110.96	110.99	1.11	5.43
LQC	96.07±1.92	5.99±0.42	105.53	103.01	3.53	7.22
MQC	106.78±5.07	8.24±1.90	95.91	95.42	2.32	7.71
HQC	96.61±2.07	7.84±0.01	100.06	98.36	0.98	4.92

Table S 6. Stability data (short-term, freeze-thaw cycles, and long-term) for *cis-Δ⁹-THCA* calculated as mean of three analyses (n=3) compared to nominal concentration of freshly prepared calibration curves.

Conditions		LLOQ	LQC	MQC	HQC
Short-term (24 h)	Bench-top (20 °C)	112.8	91.70	88.87	85.36
	Fridge (4 °C)	99.62	88.12	93.92	105.3
	Freeze-thaw stability (3 cycles)	10.60	11.51	6.21	3.14
	Freezer (-20 °C)	-	101.4	94.23	103.1
Long-term (45 days)	Fridge (4 °C)	-	113.5	92.69	109.0
	Bench-top (20 °C)	-	107.8	94.36	99.09

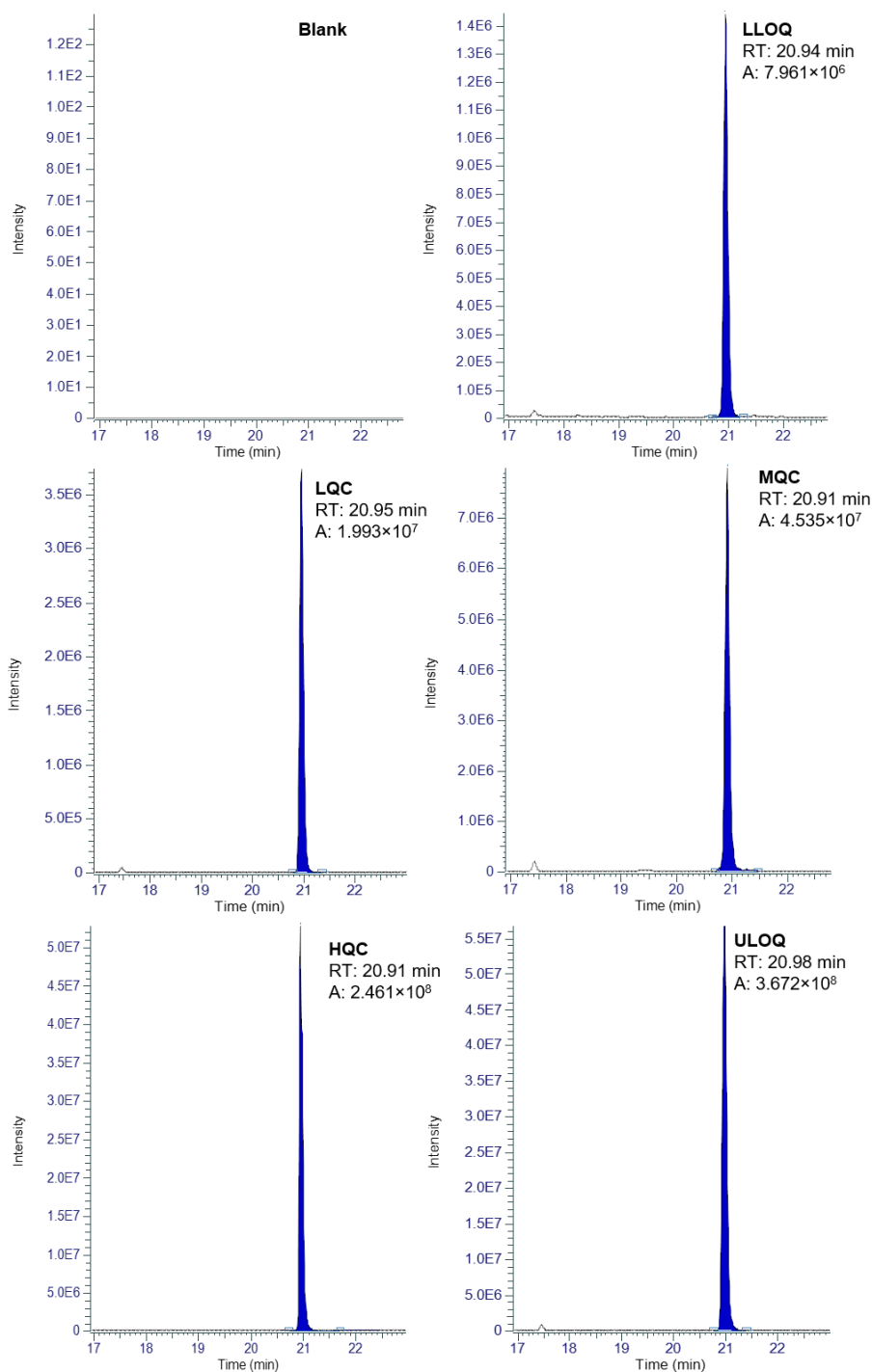


Figure S 10. HPLC-HRMS traces of *cis*- Δ^9 -THCA in HESI- *t*-SIM mode obtained in the validation process (in order: blank, LLOQ, LQC, MQC, HQC, ULOQ).

Bibliography

- [1] M.A. Schafroth, G. Mazzocanti, I. Reynoso-Moreno, R. Erni, F. Pollastro, D. Caprioglio, B. Botta, G. Allegrone, G. Grassi, A. Chicca, F. Gasparrini, J. Gertsch, E.M. Carreira, G. Appendino, Δ^9 -*cis*-Tetrahydrocannabinol: Natural Occurrence, Chirality, and Pharmacology, *J. Nat. Prod.* 84(9) (2021) 2502-2510.
- [2] P. Linciano, F. Russo, C. Citti, F. Tolomeo, R. Paris, F. Fulvio, N. Pecchioni, M.A. Vandelli, A. Laganà, A.L. Capriotti, G. Biagini, L. Carbone, G. Gigli, G. Cannazza, The novel heptyl phorolic acid cannabinoids content in different *Cannabis sativa* L. accessions, *Talanta* 235 (2021) 122704.

ENANTIOSEPARATION OF CHIRAL PHYTOCANNABINOIDS IN MEDICINAL CANNABIS

Fabiana Russo^{a, b}, Francesco Tolomeo^c, Maria Angela Vandelli^d, Giuseppe Biagini^b, Aldo Laganà^e, Anna Laura Capriotti^e, Andrea Cerrato^e, Luigi Carbone^c, Elisabetta Perrone^c, Alberto Cavazzini^f, Vincenzo Maiorano^c, Giuseppe Gigli^c, Giuseppe Cannazza^{c, d, *}, Cinzia Citti^{c, d, *}

a Clinical and Experimental Medicine PhD Program, University of Modena and Reggio Emilia, 41125 – Modena, Italy

b Department of Biomedical, Metabolic and Neural Sciences, University of Modena and Reggio Emilia, 41125 – Modena, Italy

c Institute of Nanotechnology – CNR NANOTEC, Campus Ecotekne, Via Monteroni, 73100 – Lecce, Italy

d Department of Life Sciences, University of Modena and Reggio Emilia, Via Campi 103, 41125 – Modena, Italy

e Department of Chemistry, Sapienza University of Rome, Piazzale Aldo Moro 5, 00185 – Rome, Italy

f Department of Chemical, Pharmaceutical and Agricultural Sciences, University of Ferrara, Via L. Borsari 46, 44121 – Ferrara, Italy

Published in: *J Chromatogr B Analyt Technol Biomed Life Sci.* (2023).

doi: 10.1016/j.jchromb.2023.123682

* Corresponding authors at: Institute of Nanotechnology – CNR NANOTEC, Campus Ecotekne, Via Monteroni, 73100 – Lecce, Italy.

E-mail addresses: giuseppe.cannazza@unimore.it (G. Cannazza), cinzia.citti@unimore.it (C. Citti).

Abstract

The evaluation of the chiral composition of phytocannabinoids in the cannabis plant is particularly important as the pharmacological effects of the (+) and (-) enantiomers of these compounds are completely different. Chromatographic attempts to assess the presence of the minor (+) enantiomers of the main phytocannabinoids, cannabidiolic acid (CBDA) and *trans*- Δ^9 -tetrahydrocannabinolic acid (*trans*- Δ^9 -THCA), were carried out on heated plant extracts for the determination of the corresponding decarboxylated species, cannabidiol (CBD) and *trans*- Δ^9 -tetrahydrocannabinol (*trans*- Δ^9 -THC), respectively. This process produces an altered phytocannabinoid composition with several new and unknown decomposition products. The present work reports for the first time the stereoselective synthesis of the pure (+) enantiomers of the main phytocannabinoids, *trans*-CBDA, *trans*- Δ^9 -THCA, *trans*-CBD and *trans*- Δ^9 -THC, and the development and optimization of an achiral-chiral liquid chromatography method coupled to UV and high-resolution mass spectrometry detection in reversed phase conditions (RP-HPLC-UV-HRMS) for the isolation of the single compounds and evaluation of their actual enantiomeric composition in plant. The isolation of the peaks with the achiral stationary phase ensured the absence of interferences that could potentially co-elute with the analytes of interest in the chiral analysis. The method applied to the Italian medicinal cannabis variety FM2 revealed no trace of the (+) enantiomers for all phytocannabinoids under investigation before and after decarboxylation, thus suggesting that the extraction procedure does not lead to an inversion of configuration.

1. Introduction

Since the discovery of phytocannabinoids and their biological properties, *Cannabis sativa* L. has assumed a key role in a number of scientific areas, especially in the cosmetic [1] and nutraceutical [2] industry with the use of the non-intoxicating species, as well as in the pharmaceutical industry and clinical practice including the adoption of drug-type varieties [3,4]. The latter typically show higher concentration of Δ^9 -tetrahydrocannabinol (Δ^9 -THC), a phytocannabinoid with psychotropic and euphoriant effects [5], while non-intoxicating compounds are generally present in higher levels in fiber-type cannabis varieties. These non-intoxicating compounds include the majority of the members of the phytocannabinoids class since only Δ^9 -THC, its regioisomers and their stereochemical variants have been recognized as responsible for the cannabimimetic and narcotic activity, thus under international control (Schedule I and II of the 1971 Convention on Psychotropic Substances [6]). Notwithstanding the side effects of the use of cannabis, its therapeutic benefits are considerably higher than the potential risks so that the Expert Committee on Drug Dependence (ECDD) of the WHO recommended to remove cannabis from Schedule IV of 1961 Single Convention, which is the most restrictive category for a psychotropic substance, thus recognizing its

medical value [7]. Hence, *Cannabis sativa* L. has become impressively attractive for the vast range of phytocannabinoids produced in the trichomes of the female inflorescences reaching a number as high as 150 and over [8–14] thanks to the great advances in the analytical and software technologies [15,16]. Cannabigerolic acid (CBGA) is the father of the three main phytocannabinoids, namely Δ^9 -tetrahydrocannabinolic acid (Δ^9 -THCA), cannabidiolic acid (CBDA) and cannabichromenic acid (CBCA), so far known to be produced by an enzyme-driven conversion [17]. These carboxylated species are then converted to the well-known cannabigerol (CBG), Δ^9 -THC, cannabidiol (CBD), and cannabichromene (CBC), respectively, via a decarboxylation reaction occurring during heating, drying or storage [18,19]. All other phytocannabinoids originate from either oxidation, cyclization or isomerization reactions of the main phytocannabinoids [20]. Although specific pharmacological properties have been recognized to all phytocannabinoids, only Δ^9 -THC and CBD have been approved for some therapeutic indications [21,22]. These two phytocannabinoids possess two chirality centers, which are responsible for the potential existence of four stereoisomers: (-)-*trans*-, (+)-*trans*-, (-)-*cis*-, and (+)-*cis*-isomer. The *cis* isomers of CBD have never been reported to occur naturally in cannabis, while the *cis* isomers of Δ^9 -THC have been recently found as a scalemic mixture in amounts as high as the (-)-*trans* counterpart in fiber-type cannabis plants [23], meaning that their levels do not exceed 0.3% of the dry weight of the raw material. As regards to CBD, the (-)-*trans* isomer is the one found in the plant, while no literature record mentions the presence of the (+)-*trans* isomer. While nature seems to prefer the (-)-*trans* isomer also for Δ^9 -THC, trace amounts of the (+)-*trans* isomer (0.135% enantiomeric fraction) have been found in the medicinal cannabis variety Bedrocan (Bedrocan B.V., The Netherlands) by Mazzocanti et al. [24]. However, no other studies have been carried out to confirm the presence of this minor stereoisomer in other varieties. From a pharmacological point of view, the stereoisomers of a chiral compound are not equivalent and often show completely different activities [25,26]. With particular attention to *trans*-CBD and *trans*- Δ^9 -THC, the (+)- and (-)- isomers proved to have contrasting biological activities. For example, (-)-*trans*-CBD has no affinity for either CB1 or CB2 receptors, whereas in comparison unnatural (+)-*trans*-CBD showed a strong binding affinity for CB2 and enhanced affinity for CB1 receptors [27], though not as high as (-)-*trans*- Δ^9 -THC [28]. In light of the above, it is extremely important to evaluate the stereoisomeric composition of the phytocannabinoids especially in medicinal cannabis extracts. To this end, a few papers report the development of chiral chromatographic methods for the separation of phytocannabinoids diastereoisomers, in particular by means of liquid chromatography (HPLC) [23,29–31] and supercritical fluid chromatography (SFC) [24] with chiral stationary phases (CSPs). Some authors exploited the advantages of the inverted chirality column approach (ICCA), which proved to be very useful to calculate the enantiomeric excess by both HPLC and SFC [23,24]. In

particular, the ICCA consists of running an enantiomeric pair on two CSPs with the same bound selector but opposite configuration; in this way, the elution order of the given enantiomeric pair is inverted on the two columns according to the reciprocal principle of select and-selector-systems [24,32]. This approach is particularly useful when one enantiomer of the pair is not available as a standard. In order to assess the stereoisomeric composition of phytocannabinoids in cannabis extracts, the original plant material is usually heated to convert the phytocannabinoid precursors (e.g. Δ^9 -THCA) into the corresponding decarboxylated derivatives (e.g. Δ^9 -THC). This procedure is generally undertaken in order to avoid the presence of the carboxylated phytocannabinoids for two main reasons: they are not easy to handle because of their thermal instability and no commercial standard is available for all their diastereoisomers apart from the (-)-*trans*. To the best of the authors' knowledge, no analytical method has been published on the chiral separation of the phytocannabinoid carboxylated precursors, which instead are the real picture of what the plant produces enzymatically. Taking into account that a stereoconversion may occur during the extraction process, including the decarboxylation step, as well as in biological fluids after administration [33], it becomes important to establish whether the enzymatic production of phytocannabinoids in the plant is stereoselective or the minor stereoisomeric forms can be also formed. In order to shed some light on this aspect, which has never been investigated, it is important to work with pure enantiomerically enriched compounds. Since no analytical standard is commercially available for the (+)-*trans* diastereoisomers of Δ^9 -THCA and CBDA, as well as for the decarboxylated counterparts Δ^9 -THC and CBD, a stereoselective synthesis was performed in order to develop and optimize a chiral HPLC method coupled to a diode array detector (DAD) for the separation of all stereoisomers of these carboxylated and decarboxylated analytes. The method was then applied to the Italian medicinal cannabis variety FM2 to evaluate the chiral composition of these main phytocannabinoids. In order to do so, the plant material was extracted without a preventive decarboxylation step and the two phytocannabinoids *trans*- Δ^9 -THCA and *trans*-CBDA were isolated, each in an individual fraction, by achiral reversed phase (RP) HPLC-DAD. After decarboxylation of the starting plant material, the corresponding decarboxylated species *trans*-CBD and *trans*- Δ^9 -THC were isolated and the four phytocannabinoids were analysed by chiral HPLC-DAD. The addition of the high-resolution mass spectrometry (HRMS) detector after the DAD ensured that all analytes were unambiguously identified thus avoiding misinterpretation of the peaks.

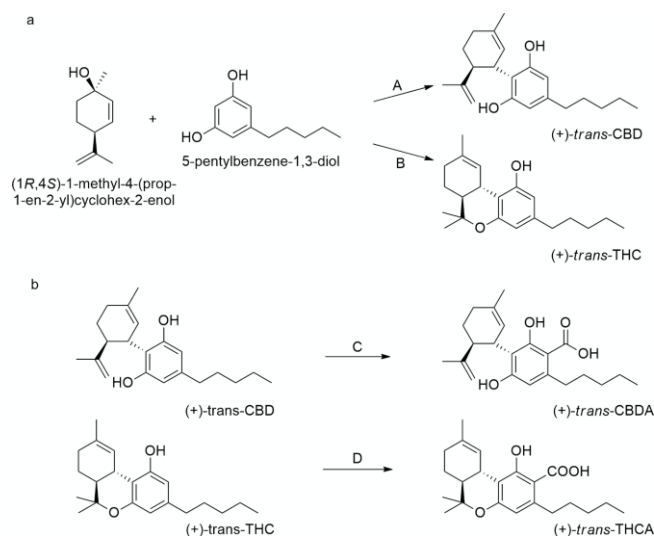


Fig. 1. Synthetic procedure for the (+)-trans enantiomers of CBD, Δ^9 -THC, CBDA and Δ^9 -THCA. a) Synthesis of the decarboxylated forms (+)-trans-CBD and (+)-trans- Δ^9 -THC; b) Synthesis of the carboxylated forms (+)-trans-CBDA and (+)-trans- Δ^9 -THCA. Reagents and conditions: A) pTSA (2%w/w), dry DCM, room temperature, N_2 atmosphere, 4.5 h stirring. B) pTSA (10%mol), dry DCM, room temperature, N_2 atmosphere, 4.5 h stirring. C) MMC (Methyl Magnesium Carbonate) 2 M in DMF, DMF, 120°C stirring for 3 h in a closed vessel. D) MMC, 2 M in DMF, DMF, 120 ° C overnight in a closed vessel.

2. Materials and methods

2.1. Chemicals and reagents

LC-MS grade acetonitrile and formic acid and analytical grade ethanol 96% (v/v) were purchased from Honeywell (Charlotte, North Caroline, USA). Ultrapure water was obtained with a water purification system (Direct-Q 3UV, Merck Millipore, Milan, Italy). Stock solutions of pure certified analytical standards of (-)-trans- Δ^9 -THCA, (-)-trans-CBDA, (-)-trans- Δ^9 -THC, and (-)-trans-CBD, were bought from Cerilliant (Sigma-Aldrich Merck, Milan, Italy), while (+)-trans- Δ^9 -THCA, (+)-trans- Δ^9 -THC, (+)-trans-CBDA and (+)-trans-CBD were synthesized in house. All reagents and solvents for the syntheses were purchased and used without further purification. Reactions were monitored by thin-layer chromatography on silica gel (60F-254, E. Merck) and checked by $KMnO_4$ aqueous solution or UV light. When necessary, reaction products were purified, by normal phase chromatography on silica gel (40–63 μ m) with the solvent system indicated. The chemical structures were ensured through Nuclear Magnetic Resonance (NMR). 1H NMR spectra were recorded on a Bruker 400 spectrometer working at 400.134 MHz. Chemical shifts (δ) are in parts per million (ppm) and they were referenced to the solvent residual peaks ($CDCl_3$ δ = 7.26 ppm). One-dimensional spectra were acquired with a spectral width of 8278 Hz. Optical rotation (α) was measured with a Polarimeter 241 (cell length 100 mm, volume 1 mL) from PerkinElmer (Milan, Italy).

3. Plant material

The FM2 medicinal cannabis variety (batch n. 6A32/1) was supplied by the Military Chemical Pharmaceutical Institute (Florence, Italy) with the authorization of the Italian Ministry of Health (prot. n. SP/062). The raw plant material (100 mg) was finely grinded and a crude extract was obtained following the protocol reported in the German Pharmacopoeia for *Cannabis flos* [34]. Briefly, the plant material was extracted with ethanol 96% (EtOH) in three cycles (5 mL, 2 mL, 2 mL) and the extracts were combined in a volumetric flask and brought to 10 mL final volume with fresh ethanol. A small aliquot (1 mL) was centrifuged at $2000 \times g$ and the pellet removed. After filtration with a 0.45 μm PTFE filter, 10 μL of the sample were injected without further dilution into the achiral RP-HPLC system for the isolation of *trans*-CBDA and *trans*- Δ^9 -THCA. Five injections provided 500 μL of the former and 350 μL of the latter. The solvent was reduced under a gentle stream of nitrogen gas and the residue reconstituted with acetonitrile (ACN) to get the final concentration of 100 $\mu\text{g}/\text{mL}$ of each phytocannabinoid. About 500 mg of the FM2 plant material were placed in a beaker and heated for 2 h at 130 $^\circ\text{C}$. Extraction with ethanol was performed on 100 mg of decarboxylated material as previously described for the crude extract. After filtration with a 0.45 μm PTFE filter, 10 μL of the sample were injected without any further dilution into the achiral RP-HPLC system for the isolation of *trans*-CBD and *trans*- Δ^9 -THC. Five injections provided 350 μL of the former and 250 μL of the latter. The solvent was reduced under a gentle stream of nitrogen gas and the residue reconstituted with ACN to get the final concentration of 100 $\mu\text{g}/\text{mL}$ of each phytocannabinoid.

4. Synthesis and characterization of the (+)-*trans* isomers

(1*S*,2*S*)-5'-methyl-4-pentyl-2'-(prop-1-en-2-yl)-1',2',3',4'-tetrahydro-[1,1'-biphenyl]-2,6-diol, (+)-*trans*-CBD

To a solution of (1*R*,4*S*)-1-methyl-4-(prop-1-en-2-yl)cyclohex-2-enol (0.9 eq., 1.4 mmol) and 5-pentylbenzene-1,3-diol (1 eq., 1.7 mmol) in dry dichloromethane (DCM, 15 mL) at room temperature, in the dark and under nitrogen atmosphere, *p*-toluenesulfonic acid (*p*TSA) (2% w/w of 5-pentylbenzene-1,3-diol) was added. The reaction was stirred in the same conditions for 5 h. After that, the reaction was quenched with 10 mL of a saturated solution of NaHCO_3 . The organic phase was washed with brine, dried over anhydrous Na_2SO_4 and concentrated under vacuum. The obtained crude (500 mg) was chromatographed (crude: silica 1:80, eluent: cyclohexane (CE):DCM, 6:4) to give 150 mg of colourless liquid (40% yield, 92% *ee* by HPLC-UV). ^1H NMR (400 MHz, CDCl_3) δ 6.25 (brs, 1H), 6.18 (brs, 1H), 5.97 (s, 1H), 5.57 (s, 1H), 4.66 (s, 1H), 4.56 (brs, 1H), 3.89–3.77 (m, 1H), 2.47–2.35 (m, 3H), 2.29–2.15 (m, 1H), 2.15–2.03 (m, 1H), 1.88–1.73 (m, 5H), 1.65 (s, 3H), 1.60–1.51 (m, 2H), 1.37–1.22 (m, 4H), 0.88 (t, $J = 7.0$ Hz, 3H) (Figure S1). $[\alpha]_{\text{D}25} = +126$ (*c.* 0.05, 96% EtOH).

5. (6a*S*,10a*S*)-6,6,9-trimethyl-3-pentyl-6a,7,8,10a-tetrahydro- 6*H*-benzo[*c*]chromen-1-ol, (+)-*trans*- Δ^9 -THC

To a solution of resorcinol (1 eq.) and (1*R*,4*S*)-1-methyl-4-(prop-1-en-2-yl)cyclohex-2-enol (0.9 eq.) in dry DCM (10 mL), *p*TSA (10% mol) was added. The reaction was stirred at room temperature and in the dark for 4 h. After that, it was quenched with a saturated solution of NaHCO₃. The organic phase was washed with brine, dried over Na₂SO₄ and concentrated under vacuum. The obtained crude (350 mg) was purified over silica gel (ratio crude:silica 1:100, eluent CE:DCM 6:4) to give 70 mg of colourless liquid. (20% yield, 96% *ee* by HPLC-UV). ¹H NMR (400 MHz, CDCl₃) δ 6.31–6.28 (m, 1H), 6.27 (d, *J* = 1.6 Hz, 1H), 6.14 (d, *J* = 1.6 Hz, 1H), 4.73 (s, 1H), 3.25–3.14 (m, 1H), 2.50–2.37 (m, 2H), 2.23–2.12 (m, 2H), 1.94–1.85 (m, 1H), 1.71–1.64 (m, 4H), 1.59–1.52 (m, 2H), 1.43–1.39 (m, 4H), 1.32–1.28 (m, 4H), 1.09 (s, 3H), 0.88 (t, *J* = 7.0 Hz, 3H) (Figure S2). [α]_{D25} = +160 (*c.* 0.1, CHCl₃).

6. (1'*S*,2'*S*)-2,6-dihydroxy-5'-methyl-4-pentyl-2'-(prop-1-en-2-yl)-1',2',3',4'-tetrahydro-[1,1'-biphenyl]-3-carboxylic acid, (+)-*trans*-CBDA

The conversion of (+)-*trans*-CBD into (+)-*trans*-CBDA has already been in a previous work by our group (39% yield, 99% *ee* by HPLC-UV) [13]. ¹H NMR (400 MHz, CDCl₃) δ 11.93 (brs, 1H), 6.61 (s, 1H), 6.25 (s, 1H), 5.55 (s, 1H), 4.54 (s, 1H), 4.39 (s, 1H), 4.08 (brd, 1H), 2.97–2.87 (m, 1H), 2.87–2.76 (m, 1H), 2.45–2.32 (m, 1H), 2.31–2.20 (m, 1H), 2.16–2.07 (m, 1H), 1.85–1.81 (m, 2H), 1.80 (s, 3H), 1.71 (s, 3H), 1.61–1.53 (m, 2H), 1.36–1.30 (m, 4H), 0.88 (t, *J* = 6.9 Hz, 3H) (Figure S3). [α]_{D20} = +60 (*c.* 0.05, methanol (MeOH)).

7. (6a*S*,10a*S*)-1-hydroxy-6,6,9-trimethyl-3-pentyl-6a,7,8,10a-tetrahydro-6*H*-benzo[*c*]chromene-2-carboxylic acid, (+)-*trans*- Δ^9 -THCA

As for (+)-*trans*-CBDA, (+)-*trans*- Δ^9 -THC was converted into (+)-*trans*-THCA (10% yield, >99% *ee* by HPLC-UV) [13]. ¹H NMR (400 MHz, CDCl₃) δ 12.23 (s, 1H), 6.39 (s, 1H), 6.25 (s, 1H), 3.22 (d, *J* = 7.0 Hz, 1H), 2.97–2.89 (m, 1H), 2.81–2.73 (m, 1H), 2.19–2.15 (m, 2H), 1.94–1.89 (m, 1H), 1.70–1.66 (m, 4H), 1.57 (s, 2H), 1.44 (s, 3H), 1.37–1.31 (m, 5H), 1.11 (s, 3H), 0.90 (t, *J* = 7.0 Hz, 3H) (Figure S4). [α]_{D20} = +206 (*c.* 5.0, chloroform (CHCl₃)).

8. Isolation of phytocannabinoids from FM2 extracts and HPLC-DAD-HRMS/MS analysis

HPLC analyses were performed on a Vanquish Core System equipped with a binary pump, a vacuum degasser, a thermostated autosampler, a thermostated column compartment and a DAD and interfaced to an Exploris 120 Orbitrap HRMS (Thermo Fisher Scientific, Waltham, Massachusetts, USA).

Achiral analysis was carried out with a Poroshell 120 EC-C18 (100 × 3.0 mm I.D., 2.7 μm) with guard (5 × 3 mm I.D., 2.7 μm) (both from Agilent Technologies, Milan, Italy) eluting water and ACN (both with 0.1% formic acid) as mobile phase. The following chromatographic conditions were applied: linear gradient from 60% to 95% ACN (with 0.1% formic acid) in 15 min, followed by isocratic elution at 95% ACN, washing step at 98% ACN for 3 min and re-equilibration with the initial conditions (total run time 26 min), maintaining the flow rate at 0.5 mL/min throughout the entire run. A post-column T-connection was added in order to split the eluent flow (Figure S5). The fractions corresponding to the phytocannabinoids of interest were collected from an output of the T-connection at a flow rate of 0.4 mL/min, while the eluent from the other output flowed at 0.1 mL/min towards the UV and MS detectors. The isolated fractions were then checked for purity under the same chromatographic conditions. The Orbitrap mass analyzer was equipped with a heated electrospray ionization source operating in both positive (HESI⁺) and negative (HESI⁻) mode. The former was employed for the detection of the decarboxylated species, while the latter was applied to the carboxylated compounds based on the best signal response obtained, which was compound-specific [16]. Simultaneous full scan (FS) and data-dependent acquisition (DDA) experiments were run with the parameters optimized by direct infusion of the pure analytes from a syringe pump. For the HESI source: capillary temperature, 390°C; vaporizer temperature, 150°C; electrospray voltage, 4.2 kV (HESI +) and 3.8 kV (HESI-); sheath gas, 70 arbitrary units (au); auxiliary gas, 5 au; sweep gas, 70au; S lens RF level, 70%. For the analyzer: resolution, 60,000 FWHM (full width at half maximum) at *m/z* 200 FS mode and 30,000 FWHM for DDA mode; scan range, *m/z* 75–750; maximum injection time, 54 ms for FS mode and 22 ms for DDA mode; isolation window, *m/z* 0.7 for FS mode and *m/z* 1.2 for DDA mode; stepped NCE (normalized collision energy), 20–40–100. The sample volume injected for the analyses was 5 μL. The analytes precursor ions [M- H]⁻ and [M + H]⁺ were extracted with a 5-ppm mass tolerance from the total ion current. The analyses were acquired with Xcalibur 3.0 (Thermo Fisher Scientific) and processed using FreeStyle 1.7 (Thermo Fisher Scientific).

9. Development and optimization of the chiral HPLC-DAD method

The following CSPs were tested to achieve the optimal chromatographic resolution of the (+) and (-) enantiomers of the four phytocannabinoids under investigation: CHIRALCEL OD-R [cellulose tris (3,5-dimethylphenylcarbamate)] (250 × 4.6 mm I.D., 10 μm), CHIRALCEL OB-H [cellulose tribenzoate] (250 × 4.6 mm I.D., 5 μm), CHIRALCEL OJ-H [cellulose tris (4-methylbenzoate)] (250 × 4.6 mm I. D., 5 μm), CHIRALPAK AD [amylose tris (3,5-dimethylphenylcarbamate)] (250 × 4.6 mm I.D., 10 μm), and CHIRALPAK AD-RH [amylose tris (3,5-dimethylphenylcarbamate)] (150 × 4.6 mm I.D., 5 μm) (all from Daicel supplied by Chiral Technologies Europe S.A.S, France). Also,

the effect of the nature and percentage of the organic modifier, as well as the temperature of the column oven, were screened in order to find the optimal separation conditions. Either ACN, EtOH or 2-propanol (*i*-PrOH) were alternatively tested as organic modifier. The chromatographic output was monitored by DAD at two wavelengths, 274 nm for the decarboxylated species and at 306 nm for the carboxylated ones. During the development and optimization step the chromatographic parameters were calculated for each compound in each analytical run: the retention factors (k_1 and k_2) were calculated as $k_1 = (t_1 - t_0)/t_0$, where t_1 and t_2 are the retention times of the first and second eluted enantiomers, the separation factor (α) was calculated as k_2/k_1 and the resolution factor (R_s) was calculated using the formula $R_s = (t_2 - t_1)/(w_1 + w_2)$, where w_1 and w_2 are the peak widths at the base for the first and second eluted enantiomer.

10. Results and discussion *10.1. Synthesis and characterization of (+)-trans-CBDA, (+)-trans- Δ^9 -THCA, (+)-trans-CBD and (+)-trans- Δ^9 -THC* The evaluation of the chiral composition of phytocannabinoids in plant material requires the use of proper standards for all the stereoisomeric forms of the analytes under investigation. The lack of commercially available standards for the (+) enantiomers has so far limited the extent of such investigation. The ICCA, for example with the Pirkle-type CSPs with both HPLC and SFC, has been explored to evaluate the presence of the (+)-*trans* enantiomer of Δ^9 -THC in the Bedrocan medicinal cannabis variety [24], as well as for the evaluation of the stereoisomeric composition of *cis*- Δ^9 -THC in different plant samples [23]. This approach proved to be useful also when only one enantiomer is available [23,24]. Unfortunately, the studies on the chiral composition of phytocannabinoids in plants are very few and all deal with the decarboxylated forms obtained after heating the samples at high temperatures. As the extraction process could affect the configurational stability, it becomes important to understand the original stereoisomeric composition in the plant material. To this end, the (+) enantiomers of *trans*-CBDA, *trans*- Δ^9 -THCA, *trans*-CBD and *trans*- Δ^9 -THC were obtained by a stereoselective synthetic procedure. In particular, a Friedel-Craft allylation of 5-pentylbenzene-1,3-diol with (1*R*,4*S*)-1-methyl-4-(prop-1-en-2-yl)cyclohex-2-enol, using *p*TSA as catalyst (Fig. 1a) allowed to access the decarboxylated forms, which were then used to obtain the carboxylated ones (Fig. 1b) following a procedure reported in previous works [13,35]. The chemical structure of synthetic standards was confirmed by ^1H NMR spectroscopy and polarimetric analysis. The perfect match between the monodimensional ^1H NMR spectrum of synthetic (+)-*trans*- Δ^9 -THC and the spectroscopic data reported by Schafroth et al. [36], confirmed its chemical structure. Similarly, the comparison of ^1H NMR spectra of (+)-*trans*-CBD, (+)-*trans*-CBDA and (+)-*trans*- Δ^9 -THCA with those of the corresponding (-)-enantiomers reported in the literature [37] ensured their chemical structure

(Supporting information). Lastly, the (+) configuration was confirmed by measuring the optical rotation power for each compound and comparing it to that of the (-) enantiomers.

11. Development and optimization of the chiral HPLC-DAD method

With the pure stereoisomers in hand, we tested various CSPs varying different chromatographic parameters to find the optimal separation conditions. First, both cellulose and amylose based CSPs were employed in the method development step and different column lengths and particle sizes were screened. In general, amylose based CSPs performed better than the cellulose-based ones. Moreover, a smaller particle size (5 μm) guaranteed a better resolution compared to the larger one (10 μm). Therefore, CHIRALPAK AD-RH resulted the optimal solution for all analytes. Several mobile phases were screened for the separation and we could not find one mobile phase optimal for all phytocannabinoids. All chiral chromatographic methods reported in the literature involve only normal phase conditions (NP-HPLC), while RP-HPLC is generally employed for achiral separation of cannabinoids [38]. It is noteworthy that NP conditions can be also used to separate phytocannabinoids with the advantage of using higher flow rates compared to RP conditions thanks to low-viscosity solvents [39]. On the other hand, RP conditions have also been used with CSPs to improve separation of phytocannabinoids and study their retention behaviour on different carbamate polysaccharide-based CSPs [40,41]. Only one record presents a successful chiral resolution of *trans*-CBD enantiomers using RP conditions [42]. The advantage of working in RP conditions is the compatibility of the solvents with the ESI-MS detector, which is particularly useful in the analysis of complex matrices, such as cannabis extracts. In this work, ACN, EtOH and *i*-PrOH (all with 0.1% of formic acid) were used as organic modifier; their percentage with respect to water was decided according to the lipophilicity of the compound: for example, CBD generally elutes earlier than THC, which requires higher percentages of the organic component, and this applies also to their carboxylated counterpart. As a general trend, the decrease in temperature did not improve the enantiomeric resolution. Eventually, the enantiomers of *trans*-CBD and *trans*- Δ^9 -THC were separated with 60% ACN setting the column compartment temperature at 30°C and the flow rate at 1.5 mL/ min. The presence of the additional carboxylic group in CBDA and THCA makes these compounds difficult to separate with ACN, thus shifting the attention to either EtOH or *i*-PrOH. A high percentage of EtOH (80%) gave good results for the separation of the enantiomers of *trans*- Δ^9 -THCA, while it was unable to separate those of *trans*-CBDA. The attempt to use 50% *i*-PrOH instead of EtOH proved to be beneficial for *trans*-CBDA, but was insufficient for *trans*- Δ^9 -THCA, whose enantiomers eluted in the washing step. The optimal conditions were found in 50% *i*-PrOH for *trans*-CBDA and 75% *i*-

PrOH for *trans*- Δ^9 -THCA, both at 30°C and 1 mL/min. All the experimental conditions are reported in Table 1.

12. Evaluation of the enantiomeric composition of *trans*-CBDA and *trans*- Δ^9 -THCA in *cannabis sativa* L.

The assessment of the enantiomeric composition of the main phytocannabinoids *trans*-CBDA and *trans*- Δ^9 -THCA in plants has never been investigated. Attempts were made only on their decarboxylated derivatives and only after a heating step at high temperatures. In order to avoid the variable of the extraction methodology, which could affect the stereostability of the analytes, the analyses in this work were carried out on the unheated ethanol extract of the FM2 variety. Additionally, the chiral evaluation was not performed on the total crude extract since potential interfering compounds could elute at the same retention time of the enantiomers of the analytes. This is particularly important in phytocannabinoids analysis as many compounds are isobaric and present the same MS fragmentation spectrum [43]. Therefore, the compounds of interest *trans*-CBDA and *trans*- Δ^9 -THCA were isolated by analytical achiral chromatography by adding a post-column T-connection, which allowed to collect the pure compounds and bring the eluent at a lower flow rate to the UV and MS detectors. Starting from the unheated and undiluted FM2 extract characterized by 55 mg/g of *trans*-CBDA and 33 mg/g of *trans*- Δ^9 -THCA, five 10 μ L injections were sufficient to obtain 500 μ L of *trans*-CBDA and 350 μ L of *trans*- Δ^9 -THCA. Each phytocannabinoid solution was brought to the final concentration of 100 μ g/mL and checked on the C18 column with both UV and HRMS detectors in order to discard the potential presence of interferences. The purified compounds were then analysed with the CSP using the previously optimized conditions. The corresponding pure enantiomers were always injected for comparison and the match of UV and MS/MS spectra were useful for the unambiguous identification. At the limit of detection of the method (0.005 μ g/mL), both isolated phytocannabinoids resulted enantiomerically pure with the (-)-*trans* being the detected enantiomer (>99% *ee*) (Figs. 2 and 3). In order to understand whether the decarboxylation process could lead to a stereoconversion of the pure enantiomers of *trans*-CBDA and *trans*- Δ^9 -THCA, the plant material was heated at 130 °C for 2 h. The decarboxylated undiluted extract, characterized by 37 mg/g of *trans*-CBD and 24 mg/g of *trans*- Δ^9 -THC, was injected into the achiral chromatographic system to isolate the single peaks of *trans*-CBD and *trans*- Δ^9 -THC as previously done for their carboxylated precursors. The chiral chromatographic analysis was then performed to assess their enantiomeric composition. Both samples containing either *trans*-CBD or *trans*- Δ^9 -THC at the concentration of 100 μ g/mL did not show the presence of the (+) enantiomer at least at the limit of detection of the method (0.05 μ g/mL) (Figs. 4 and 5), suggesting that the decarboxylation in the conditions applied did not affect the stereostability of the investigated compounds.

13. Conclusions

The extent of the evaluation of the chiral composition of phytocannabinoids in the plant material has always been limited due to the unavailability of the analytical standards of the (+) enantiomers of carboxylated phytocannabinoids. This work addresses for the first time the synthesis of the pure (+) enantiomers of the main carboxylated and decarboxylated phytocannabinoids, *trans*-CBDA, *trans*- Δ^9 -THCA, *trans*-CBD and *trans*- Δ^9 -THC. These were used to develop and optimize an HPLC-UV-HRMS/MS method in RP conditions, which allowed convenient coupling with the MS detection. Moreover, the achiral-chiral chromatographic method for the isolation and chiral analysis of the single peak proved to be useful to avoid the presence of interfering compounds co-eluting with the enantiomers peaks that could lead to misinterpretation and erroneous identification. At the limit of the sensitivity of the developed method we found that the main phytocannabinoids, *trans*-CBDA, *trans*- Δ^9 -THCA, *trans*-CBD and *trans*- Δ^9 -THC, are all present as single (-) enantiomers and no trace of the (+) enantiomers was detected in the Italian medicinal cannabis variety FM2. Lastly, the great advantage of the developed achiral-chiral chromatographic method is the possibility to disclose the presence of enantiomeric impurities of single peaks without heating the starting material, which would otherwise lead to an altered phytocannabinoid composition.

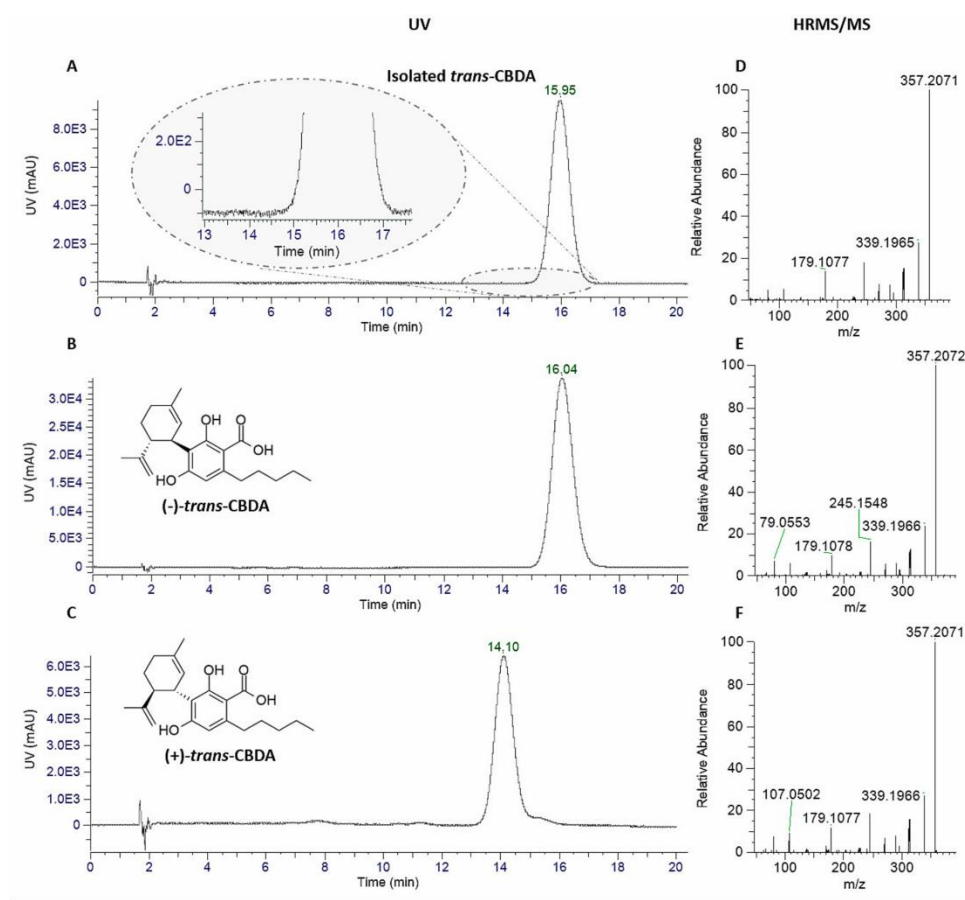


Fig. 2. Comparison of the UV traces and tandem HRMS spectra of the isolated *trans*-CBDA and the pure synthetic (-) and (+) enantiomers of *trans*-CBDA. UV traces at 306 nm of the isolated peak of *trans*-CBDA (A), pure (-)-*trans*-CBDA (B) and pure (+)-*trans*-CBDA (C); HRMS/MS spectra in HESI- mode of the isolated peak of *trans*-CBDA (D), pure (-)-*trans*-CBDA (E) and pure (+)-*trans*-CBDA (F).

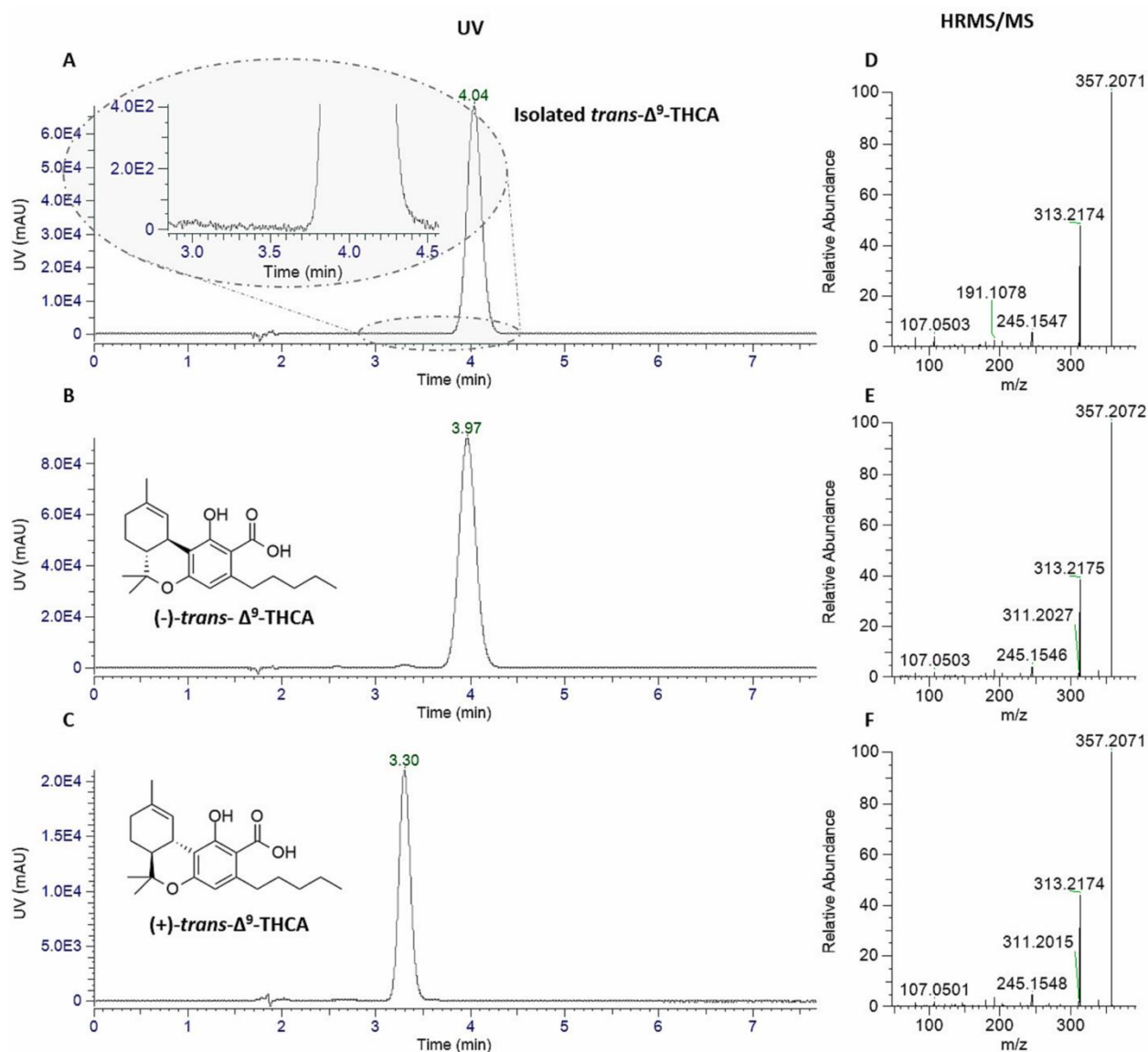


Fig. 3. Comparison of the UV traces and tandem HRMS spectra of the isolated *trans*- Δ^9 -THCA and the pure synthetic (-) and (+) enantiomers of *trans*- Δ^9 -THCA. UV traces at 306 nm of the isolated peak of *trans*- Δ^9 -THCA (A), pure (-)-*trans*- Δ^9 -THCA (B) and pure (+)-*trans*-THCA (C); HRMS/MS spectra in HESI- mode of the isolated peak of *trans*- Δ^9 -THCA (D), pure (-)-*trans*- Δ^9 -THCA (E) and pure (+)-*trans*- Δ^9 -THCA (F).

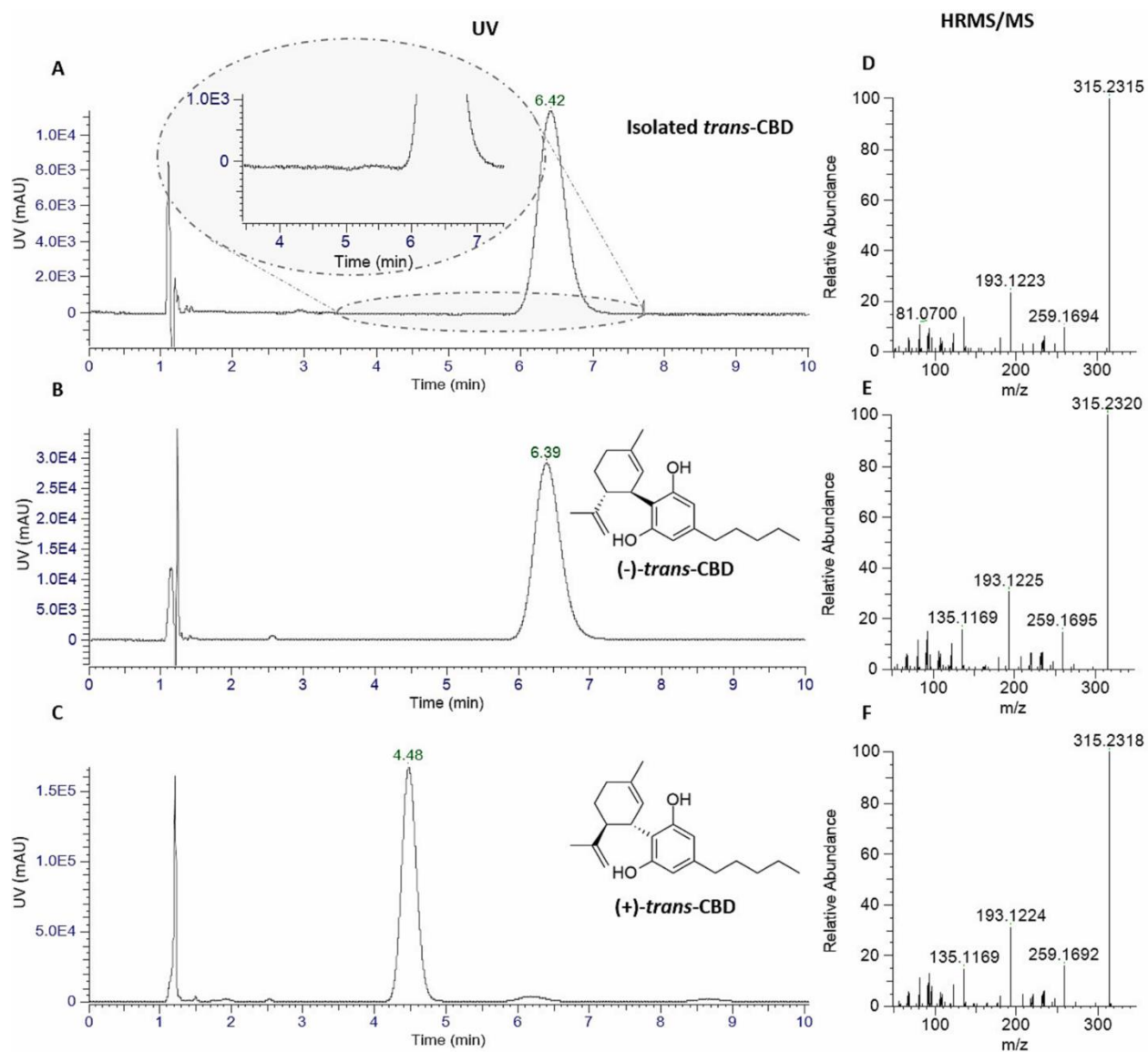


Fig. 4. Comparison of the UV traces and tandem HRMS spectra of the isolated *trans*-CBD and the pure synthetic (-) and (+) enantiomers of *trans*-CBD. UV traces at 270 nm of the isolated peak of *trans*-CBD (A), pure (-)-*trans*-CBD (B) and pure (+)-*trans*-CBD (C); HRMS/MS spectra in HESI + mode of the isolated peak of *trans*-CBD (D), pure (-)-*trans*-CBD (E) and pure (+)-*trans*-CBD (F).

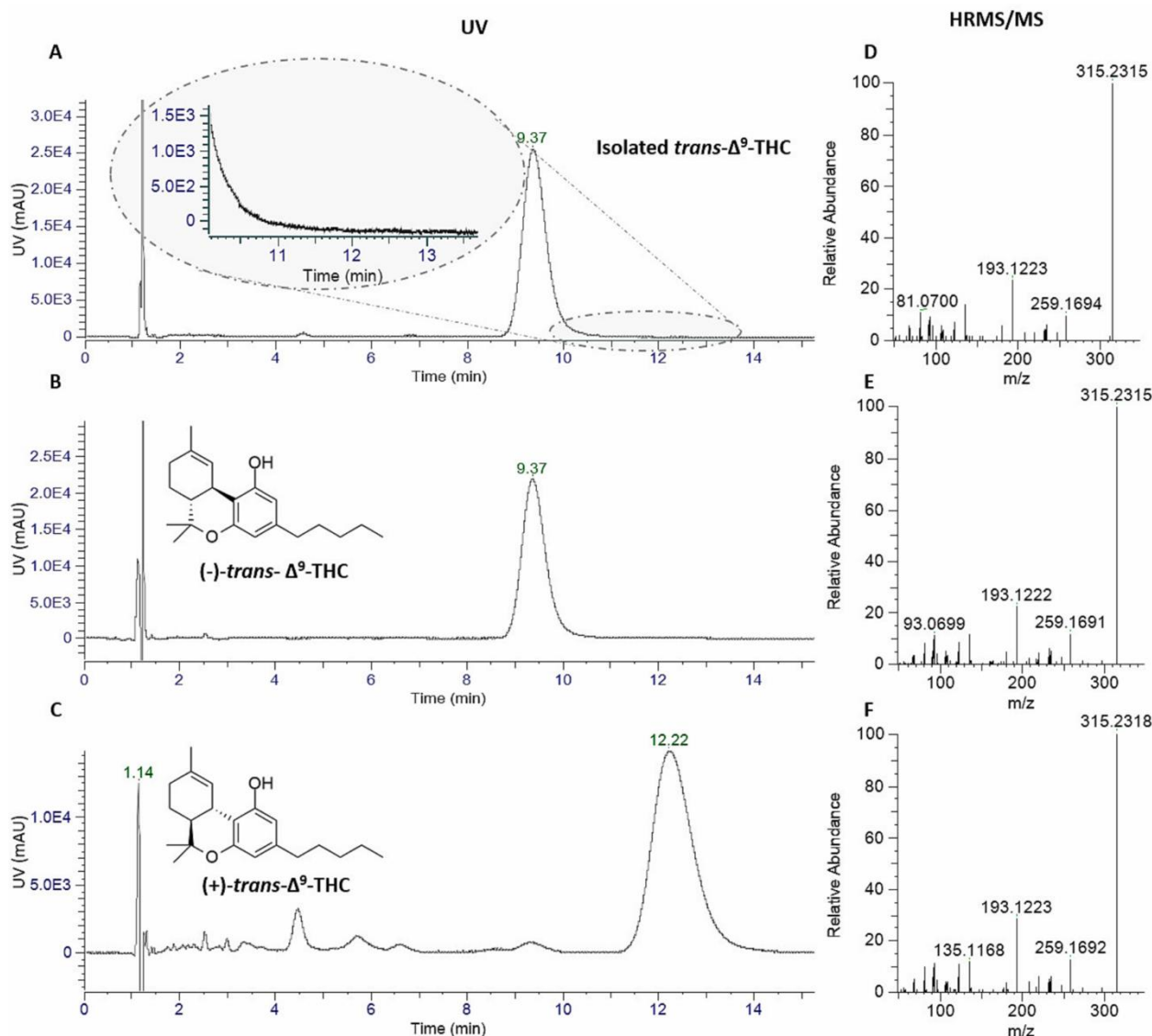


Fig. 5. Comparison of the UV traces and tandem HRMS spectra of the isolated *trans*- Δ^9 -THC and the pure synthetic (-) and (+) enantiomers of *trans*- Δ^9 -THC. UV traces at 270 nm of the isolated peak of *trans*- Δ^9 -THC (A), pure (-)-*trans*- Δ^9 -THC (B) and pure (+)-*trans*- Δ^9 -THC (C); HRMS/MS spectra in HESI + mode of the isolated peak of *trans*- Δ^9 -THC (D), pure (-)-*trans*- Δ^9 -THC (E) and pure (+)-*trans*- Δ^9 -THC (F).

Table

Table 2. Optimization of the chiral chromatographic conditions for the enantiomeric separation of *trans*-CBDA, *trans*- Δ^9 -THCA, *trans*-CBD and *trans*- Δ^9 -THC with different CSPs, organic modifiers, column temperatures and flow rates. For each analysis the retention time (R_T) of the enantiomers (t_1 and t_2), the retention factors (k_1 and k_2), the separation factor (α) and the resolution factor (R_S) were calculated and reported. Best conditions found are reported in bold.

Compound	Column	Organic modifier		T (°C)	Flow rate (mL/min)	R_T (min)		k_1	k_2	α	R_S
		Type	%			t_1	t_2				
<i>trans</i> -CBDA	CHIRALCEL OJ-H	ACN	50	30	0.75	35.9	39.9	8.16	9.18	1.11	0.9
		ACN	50	45	0.75	31.4	34.4	6.92	7.78	1.11	1.0
		ACN	70	30	0.75	7.3	7.7	0.82	0.92	1.05	0.7

	CHIRALCEL AD	ACN	60	30	1.5	9.8	9.8	3.67	3.67	1.00	0.0	
		ACN	60	30	1.5	3.6	3.6	2.00	2.00	1.00	0.0	
		EtOH	80	30	1	3.5	3.8	2.16	0.89	1.08	0.8	
	CHIRALCEL AD- RH	<i>i</i> -PrOH	60	30	1	3.6	4.2	2.16	1.33	1.17	0.6	
		<i>i</i>-PrOH	50	30	1	14.5	16.4	7.43	8.53	1.15	1.3	
		<i>i</i> -PrOH	50	25	1	16.1	17.5	8.20	9.00	1.10	0.9	
		<i>i</i> -PrOH	45	30	1	-	-	-	-	-	-	
<i>trans</i> - Δ^9 -THCA	CHIRALCEL OJ-H	ACN	70	30	0.75	11.3	11.9	1.83	1.98	1.05	0.6	
		ACN	60	30	0.75	20.8	22.6	4.17	4.62	1.09	0.9	
		ACN	60	30	1.5	10.9	10.9	8.08	8.08	1.00	0.0	
	CHIRALCEL AD- RH	EtOH	80	30	0.5	24.5	38.1	1.16	8.52	1.55	4.5	
		EtOH	80	30	1	12.3	19.3	1.16	8.65	1.57	2.9	
		<i>i</i> -PrOH	50	30	1	-	-	-	-	-	-	
		<i>i</i>-PrOH	75	30	1	3.3	4.0	0.9	1.3	1.4	2.3	
<i>trans</i> -CBD	CHIRALCEL OD-R	ACN	70	30	1	7.5	7.5	1.53	1.61	1.03	0.2	
		ACN	70	10	1	7.6	7.9	2.06	2.19	1.04	0.2	
	CHIRALCEL OB-H	ACN	70	10	1	4.9	4.9	1.30	1.30	1.00	0.0	
		ACN	60	30	0.75	9.7	9.7	1.32	1.32	1.00	0.0	
	CHIRALCEL OJ-H	ACN	70	30	0.75	6.4	6.7	1.14	1.19	1.02	0.3	
		ACN	70	10	1	8.7	8.9	1.33	1.44	1.05	0.5	
		ACN	70	30	1	6.9	8.6	1.16	1.69	1.25	1.0	
		ACN	70	30	1.5	4.5	5.6	1.06	1.57	1.24	1.0	
	CHIRALPAK AD	ACN	50	30	1.5	31.0	31.9	13.49	13.91	1.03	0.4	
		EtOH	100	30	0.5	6.8	6.8	0.18	0.18	1.00	0.0	
		EtOH	90	30	0.5	8.8	8.8	0.32	0.32	1.00	0.0	
		EtOH	80	30	0.5	13.4	14.8	1.02	1.23	1.10	0.9	
		CHIRALPAK AD- RH	ACN	70	30	1.5	2.6	3.3	1.16	1.73	1.27	2.3
			ACN	60	30	1.5	5.6	8.0	1.16	1.73	1.27	3.3
<i>trans</i> - Δ^9 -THC	CHIRALCEL OD	ACN	70	10	1	11.5	11.5	1.16	1.73	1.27	0.0	
	CHIRALCEL OB	ACN	70	10	1	6.1	6.5	1.86	2.05	1.07	0.9	
		ACN	60	30	0.75	12.9	13.7	2.09	2.28	1.06	0.9	
	CHIRALCEL OJ-H	ACN	70	30	0.75	11.6	12.5	1.86	2.08	1.08	0.8	
	CHIRALCEL AD	ACN	70	30	1	12.2	14.7	2.81	3.59	1.20	0.9	
		EtOH	100	30	0.5	7.6	9.8	0.32	0.71	1.29	2.1	

		EtOH	90	30	0.5	11.5	16.4	0.73	1.47	1.43	2.9
		EtOH	80	30	0.5	22.2	34.1	2.36	4.16	1.54	3.0
		EtOH	80	30	1	11.2	17.3	2.38	4.23	1.54	2.9
CHIRALCEL RH	AD-	ACN	70	30	1.5	4.9	6.1	1.16	4.08	1.24	1.2
		ACN	60	30	1.5	9.8	12.8	1.158	9.64	1.31	3.0

Funding

This work was partially funded by UNIHEMP research project “Use of iNdustrIal Hemp biomass for Energy and new biocheMicals Production” (ARS01_00668) funded by Ministero dell’Istruzione, dell’Universit`a e della Ricerca (MIUR) and Fondo Europeo di Sviluppo Regionale (FESR) (within the PON R&I 2017–2020 – Axis 2 – Action II – OS 1.b). Grant decree UNIHEMP prot. n. 2016 of 27/07/2018; CUP B76C18000520005. The work was also partially supported by the MIUR project “ECOTEC - ECO-sustainable and intelligent fibers and fabrics for TEChnic clothing”, PON «R&I» 2014–2020, project N° ARS01_00951, CUP B66C18000300005.

CRedit authorship contribution statement

Fabiana Russo: Investigation, Formal analysis. **Francesco Tolomeo:** Investigation, Formal analysis. **Maria Angela Vandelli:** Data curation. **Giuseppe Biagini:** Data curation. **Aldo Lagan`a:** Investigation, Formal analysis. **Anna Laura Capriotti:** Investigation, Formal analysis. **Andrea Cerrato:** Investigation, Formal analysis. **Luigi Carbone:** Data curation. **Elisabetta Perrone:** Data curation. **Alberto Cavazzini:** Investigation, Formal analysis. **Vincenzo Maiorano:** Data curation, Resources. **Giuseppe Gigli:** Resources. **Giuseppe Cannazza:** Conceptualization, Project administration, Methodology, Writing – original draft, Funding acquisition, Writing – review & editing. **Cinzia Citti:** Conceptualization, Project administration, Methodology, Writing – original draft.

Declaration of Competing Interest The authors declare that they have no known competing financial interests or personal relationships that could have appeared to influence the work reported in this paper.

References

- [1] P.R. Cohen, Therapeutic and Cosmetic Uses of Cannabis: Cannabinoids for Acne Treatment and Skin - Rejuvenation, *Skinmed* (2021) 45–47.
- [2] P. Cerino, C. Buonerba, G. Cannazza, J. D’Auria, E. Ottoni, A. Fulgione, A.D. Stasio, B. Pierri, A. Gallo, A Review of Hemp as Food and Nutritional Supplement, *Cannabis and cannabinoid research* 6 (2021) 19–27.
- [3] P. Kumar, D.K. Mahato, M. Kamle, R. Borah, B. Sharma, S. Pandhi, V. Tripathi, H. S. Yadav, S. Devi, U. Patil, J. Xiao, A.K. Mishra, Pharmacological properties, therapeutic potential, and legal status of Cannabis sativa L.: An overview, *Phytother. Res.* 35 (2021) 6010–6029.
- [4] C. Pagano, G. Navarra, L. Coppola, G. Avilia, M. Bifulco, C. Laezza, Cannabinoids: Therapeutic Use in Clinical Practice, *International Journal of Molecular Sciences* 23 (2022) 3344.
- [5] R.G. dos Santos, J.E.C. Hallak, J.A.S. Crippa, Neuropharmacological Effects of the Main Phytocannabinoids: A Narrative Review, in: E. Murillo-Rodriguez, S.R. Pandi- Perumal, J.M. Monti (Eds.), *Cannabinoids and Neuropsychiatric Disorders*, Springer International Publishing, Cham, 2021, pp. 29–45.

- [6] United Nations Convention on Psychotropic Substances, Austria, 1971.
- [7] WHO Expert Committee on Drug Dependence, fortieth report, WHO Technical Report Series, N. 1013, Geneva: World Health Organization, 2018, pp. 25-27.
- [8] C. Citti, P. Linciano, F. Forni, M.A. Vandelli, G. Gigli, A. Lagan`a, G. Cannazza, Analysis of impurities of cannabidiol from hemp. Isolation, characterization and synthesis of cannabidibutol, the novel cannabidiol butyl analog, *J. Pharm. Biomed. Anal.* 175 (2019), 112752.
- [9] C. Citti, P. Linciano, F. Forni, M.A. Vandelli, G. Gigli, A. Lagan`a, G. Cannazza, Chemical and spectroscopic characterization data of ‘cannabidibutol’, a novel cannabidiol butyl analog, *Data in Brief* 26 (2019), 104463.
- [10] F. Tolomeo, F. Russo, M.A. Vandelli, G. Biagini, A.L. Capriotti, A. Lagan`a, L. Carbone, G. Gigli, G. Cannazza, C. Citti, HPLC-UV-HRMS analysis of cannabigerovarín and cannabigerobutol, the two impurities of cannabigerol extracted from hemp, *J. Pharm. Biomed. Anal.* 203 (2021), 114215.
- [11] P. Linciano, C. Citti, F. Russo, F. Tolomeo, A. Lagan`a, A.L. Capriotti, L. Luongo, M. Iannotta, C. Belardo, S. Maione, F. Forni, M.A. Vandelli, G. Gigli, G. Cannazza, Identification of a new cannabidiol n-hexyl homolog in a medicinal cannabis variety with an antinociceptive activity in mice: cannabidihexol, *Sci. Rep.* 10 (2020) 22019.
- [12] P. Linciano, C. Citti, L. Luongo, C. Belardo, S. Maione, M.A. Vandelli, F. Forni, G. Gigli, A. Lagan`a, C.M. Montone, G. Cannazza, Isolation of a high-affinity cannabinoid for the human CB1 receptor from a medicinal Cannabis sativa variety: Δ 9-Tetrahydrocannabutol, the butyl homologue of Δ 9-Tetrahydrocannabinol, *J. Nat. Prod.* 83 (2020) 88–98.
- [13] P. Linciano, F. Russo, C. Citti, F. Tolomeo, R. Paris, F. Fulvio, N. Pecchioni, M. A. Vandelli, A. Lagan`a, A.L. Capriotti, G. Biagini, L. Carbone, G. Gigli, G. Cannazza, The novel heptyl phorolic acid cannabinoids content in different Cannabis sativa L. accessions, *Talanta* 235 (2021), 122704.
- [14] C. Citti, P. Linciano, F. Russo, L. Luongo, M. Iannotta, S. Maione, A. Lagan`a, A. L. Capriotti, F. Forni, M.A. Vandelli, G. Gigli, G. Cannazza, A novel phytocannabinoid isolated from Cannabis sativa L. with an in vivo cannabimimetic activity higher than Δ 9-tetrahydrocannabinol: Δ 9-Tetrahydrocannabiphorol, *Sci. Rep.* 9 (2019) 20335.
- [15] C.M. Montone, A. Cerrato, B. Botta, G. Cannazza, A.L. Capriotti, C. Cavaliere, C. Citti, F. Ghirga, S. Piovesana, A. Lagan`a, Improved identification of phytocannabinoids using a dedicated structure-based workflow, *Talanta* 219 (2020), 121310.
- [16] A. Cerrato, C. Citti, G. Cannazza, A.L. Capriotti, C. Cavaliere, G. Grassi, F. Marini, C.M. Montone, R. Paris, S. Piovesana, A. Lagan`a, Phytocannabinomics: Untargeted metabolomics as a tool for cannabis chemovar differentiation, *Talanta* 230 (2021), 122313.
- [17] M.N. Tahir, F. Shahbazi, S. Rondeau-Gagn`e, J.F. Trant, The biosynthesis of the cannabinoids, *Journal of Cannabis Research* 3 (2021) 7.
- [18] O.-E. Schultz, G. Haffner, Zur Frage der Biosynthese der Cannabinole, *Arch. Pharm.* 293 (1960) 1–8.
- [19] T. Yamauchi, Y. Shoyama, H. Aramaki, T. Azuma, I. Nishioka, Tetrahydrocannabinolic acid, a genuine substance of tetrahydrocannabinol, *Chem. Pharm. Bull. (Tokyo)* 15 (1967) 1075–1076.
- [20] L.O. Hanu`s, S.M. Meyer, E. Mu`noz, O. Tagliatalata-Scafati, G. Appendino, Phytocannabinoids: a unified critical inventory, *Nat. Prod. Rep.* 33 (2016) 1357–1392.
- [21] M. Maccarrone, R. Maldonado, M. Casas, T. Henze, D. Centonze, Cannabinoids therapeutic use: what is our current understanding following the introduction of THC, THC:CBD oromucosal spray and others? *Expert Rev. Clin. Pharmacol.* 10 (2017) 443–455.

- [22] A. Talwar, E. Estes, R. Aparasu, D.S. Reddy, Clinical efficacy and safety of cannabidiol for pediatric refractory epilepsy indications: A systematic review and meta-analysis, *Exp. Neurol.*, DOI [https://doi.org/10.1016/j.expneurol.2022.114238\(2022\)114238](https://doi.org/10.1016/j.expneurol.2022.114238(2022)114238).
- [23] M.A. Schafroth, G. Mazzocanti, I. Reynoso-Moreno, R. Erni, F. Pollastro, D. Caprioglio, B. Botta, G. Allegrone, G. Grassi, A. Chicca, F. Gasparrini, J. Gertsch, E.M. Carreira, G. Appendino, Δ^9 -cis-Tetrahydrocannabinol: Natural Occurrence, Chirality, and Pharmacology, *J. Nat. Prod.* 84 (2021) 2502–2510.
- [24] G. Mazzocanti, O.H. Ismail, I. D'Acquarica, C. Villani, C. Manzo, M. Wilcox, A. Cavazzini, F. Gasparrini, Cannabis through the looking glass: chemo- and enantio-selective separation of phytocannabinoids by enantioselective ultra high performance supercritical fluid chromatography, *Chemical Communications* 53 (2017) 12262–12265.
- [25] U.M. Battisti, C. Citti, M. Larini, G. Ciccarella, N. Stasiak, L. Troisi, D. Braghiroli, C. Parenti, M. Zoli, G. Cannazza, “Heart-cut” bidimensional achiral-chiral liquid chromatography applied to the evaluation of stereoselective metabolism, in vivo biological activity and brain response to chiral drug candidates targeting the central nervous system, *J. Chromatogr. A* 1443 (2016) 152–161.
- [26] U.M. Battisti, C. Citti, G. Rastelli, L. Pinzi, G. Puja, F. Ravazzini, G. Ciccarella, D. Braghiroli, G. Cannazza, An unexpected reversal in the pharmacological stereoselectivity of benzothiadiazine AMPA positive allosteric modulators, *MedChemComm* 7 (2016) 2410–2417.
- [27] I. Gonz'alez-Mariscal, B. Carmona-Hidalgo, M. Winkler, J.D. Unciti-Broceta, A. Escamilla, M. G'omez-Cañas, J. Fern'andez-Ruiz, B.L. Fiebich, S.-Y. Romero-Zerbo, F.J. Bermúdez-Silva, J.A. Collado, E. Muñoz, (+)-trans-Cannabidiol-2-hydroxy pentyl is a dual CB1R antagonist/CB2R agonist that prevents diabetic nephropathy in mice, *Pharmacological Research* 169 (2021), 105492.
- [28] A.C. Howlett, F. Barth, T.I. Bonner, G. Cabral, P. Casellas, W.A. Devane, C. C. Felder, M. Herkenham, K. Mackie, B.R. Martin, R. Mechoulam, R.G. Pertwee, International Union of Pharmacology. XXVII. Classification of Cannabinoid Receptors, *Pharmacol. Rev.* 54 (2002) 161–202.
- [29] S. Levin, S. Abu-Lafi, J. Zahalka, R. Mechoulam, Resolution of chiral cannabinoids on amylose tris (3, 5-dimethylphenylcarbamate) chiral stationary phase: Effects of structural features and mobile phase additives, *J. Chromatogr. A* 654 (1993) 53–64.
- [30] S. Levin, M. Sterin, S. Abu-lafi, Structural features affecting chiral resolution of cannabimimetic enantiomers by amylose 3, 5-dimethylphenylcarbamate chiral stationary phase, *Chirality* 7 (1995) 140–146.
- [31] S. Abu-Lafi, M. Sterin, S. Levin, Role of hydroxyl groups in chiral recognition of cannabinoids by carbamated amylose, *J. Chromatogr. A* 679 (1994) 47–58.
- [32] V. Schurig, The Reciprocal Principle of Selectand-Selector-Systems in Supramolecular Chromatography †, *Molecules* 21 (2016) 1535.
- [33] C. Citti, D. Braghiroli, M.A. Vandelli, G. Cannazza, Pharmaceutical and biomedical analysis of cannabinoids: A critical review, *J. Pharm. Biomed. Anal.* 147 (2018) 565–579.
- [34] Cannabis Flos; New Text of the German Pharmacopoeia, Bonn, Germany, 2018.
- [35] R. Mechoulam, Z. Ben-Zvi, Carboxylation of resorcinols with methylmagnesium carbonate. Synthesis of cannabinoid acids, *J. Chem. Soc., Chem. Commun.*, DOI 10.1039/C29690000343(1969) 343-344.
- [36] M.A. Schafroth, G. Zuccarello, S. Krautwald, D. Sarlah, E.M. Carreira, Stereodivergent Total Synthesis of Δ^9 -Tetrahydrocannabinols, *Angewandte Chemie International Edition* 53 (2014) 13898–13901.
- [37] Y.H. Choi, A. Hazekamp, A.M.G. Peltenburg-Looman, M. Fr'ed'erich, C. Erkelens, A. W.M. Lefeber, R. Verpoorte, NMR assignments of the major cannabinoids and cannabiflavonoids isolated from flowers of *Cannabis sativa*, *Phytochem. Anal.* 15 (2004) 345–354.

- [38] W.J. Umstead, Polysaccharide Chiral Stationary Phases for the Achiral and Chiral Separation of Cannabinoids, DOI.
- [39] C. De Luca, A. Buratti, Y. Krauke, S. Stephan, K. Monks, V. Brighenti, F. Pellati, A. Cavazzini, M. Catani, S. Felletti, Investigating the effect of polarity of stationary and mobile phases on retention of cannabinoids in normal phase liquid chromatography, *Anal. Bioanal. Chem.* 414 (2022) 5385–5395.
- [40] C. De Luca, A. Buratti, W. Umstead, P. Franco, A. Cavazzini, S. Felletti, M. Catani, Investigation of retention behavior of natural cannabinoids on differently substituted polysaccharide-based chiral stationary phases under reversed-phase liquid chromatographic conditions, *J. Chromatogr. A* 1672 (2022), 463076.
- [41] T. Onishi, W.J. Umstead, The Separation of Cannabinoids on Sub-2 μm Immobilized Polysaccharide Chiral Stationary Phases, *Pharmaceuticals (Basel)* 14 (2021).
- [42] J.U. Weston, The Chiral Separation of the (+) and (-) Enantiomers of Cannabidiol, *Cannabis, Science and Technology* 5 (2022) 30–34.
- [43] A.L. Capriotti, G. Cannazza, M. Catani, C. Cavaliere, A. Cavazzini, A. Cerrato, C. Citti, S. Felletti, C.M. Montone, S. Piovesana, A. Lagan`a, Recent applications of mass spectrometry for the characterization of cannabis and hemp phytocannabinoids: From targeted to untargeted analysis, *J. Chromatogr. A* 1655 (2021), 462492.

Supplementary Material

Enantioseparation of chiral phytocannabinoids in medicinal cannabis

Fabiana Russo^{a,b}, Francesco Tolomeo^c, Maria Angela Vandelli^d, Giuseppe Biagini^b, Aldo Laganà^{c,e}, Anna Laura Capriotti^e, Andrea Cerrato^e, Luigi Carbone^c, Elisabetta Perrone^e, Alberto Cavazzini^f, Giuseppe Gigli^c, Giuseppe Cannazza^{c,d,*}, Cinzia Citti^{c,d,*}

^a Clinical and Experimental Medicine PhD Program, University of Modena and Reggio Emilia, 41125 – Modena, Italy

^b Department of Biomedical, Metabolic and Neural Sciences, University of Modena and Reggio Emilia, 41125 – Modena, Italy

^c Institute of Nanotechnology – CNR NANOTEC, Campus Ecotekne, Via Monteroni, 73100 – Lecce, Italy

^d Department of Life Sciences, University of Modena and Reggio Emilia, Via Campi 103, 41125 – Modena, Italy

^e Department of Chemistry, Sapienza University of Rome, Piazzale Aldo Moro 5, 00185 – Rome, Italy

^f Department of Chemical, Pharmaceutical and Agricultural Sciences, University of Ferrara, Via L. Borsari 46, 44121 – Ferrara, Italy

Table of contents

¹ H NMR of (+)- <i>trans</i> -CBD	---SI-2
¹ H NMR of (+)- <i>trans</i> - Δ^9 -THC	---SI-3
¹ H NMR of (+)- <i>trans</i> -CBDA	---SI-4
¹ H NMR of (+)- <i>trans</i> - Δ^9 -THCA	---SI-5
Comparison of ¹ H NMR assignments of (+)- and (-)- <i>trans</i> enantiomers of CBDA and CBD	---SI-6
Comparison of ¹ H NMR assignments of (+)- and (-)- <i>trans</i> enantiomers of Δ^9 -THCA and Δ^9 -THC	---SI-7
Isolation of phytocannabinoids	---SI-8

* Corresponding authors:

Giuseppe Cannazza, Ph.D., Email: giuseppe.cannazza@unimore.it; Tel.: +39 059 2055013.; Fax: +39 059 2055750.

Cinzia Citti, Ph.D., Email: cinzia.citti@unimore.it; Tel.: +39 0832 319206.

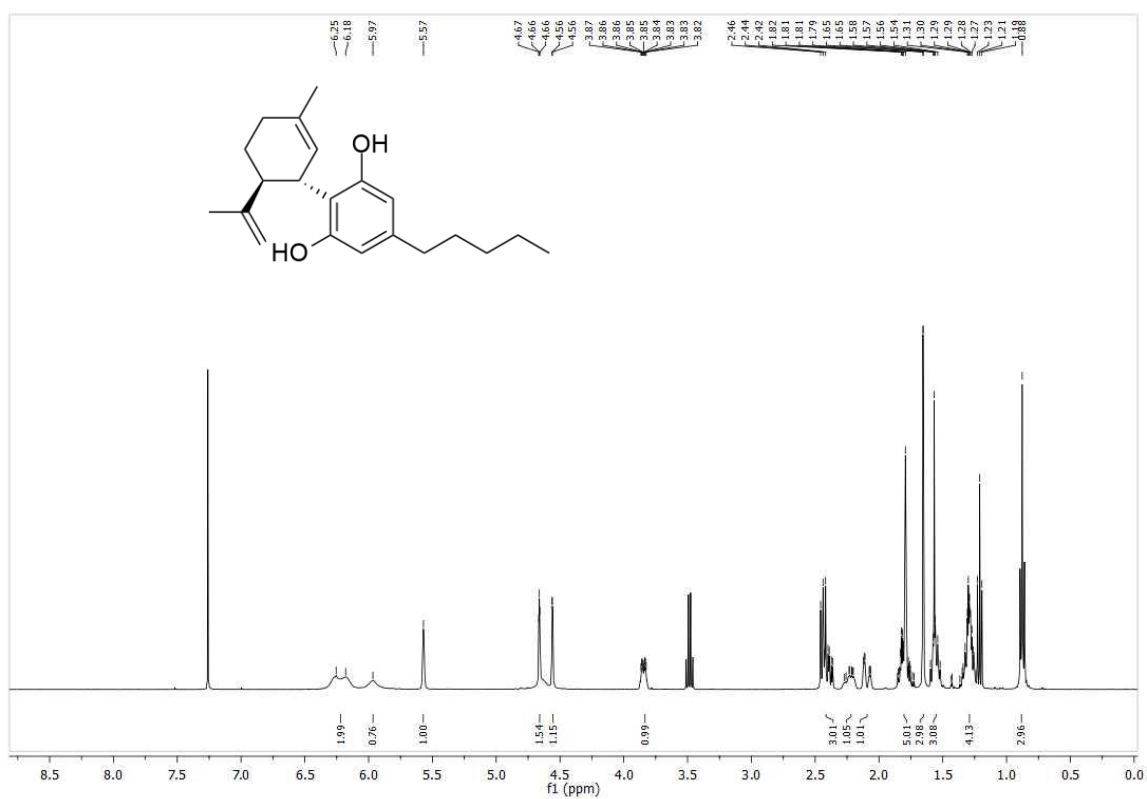


Figure S 11. ¹H NMR of (+)-trans-CBD.

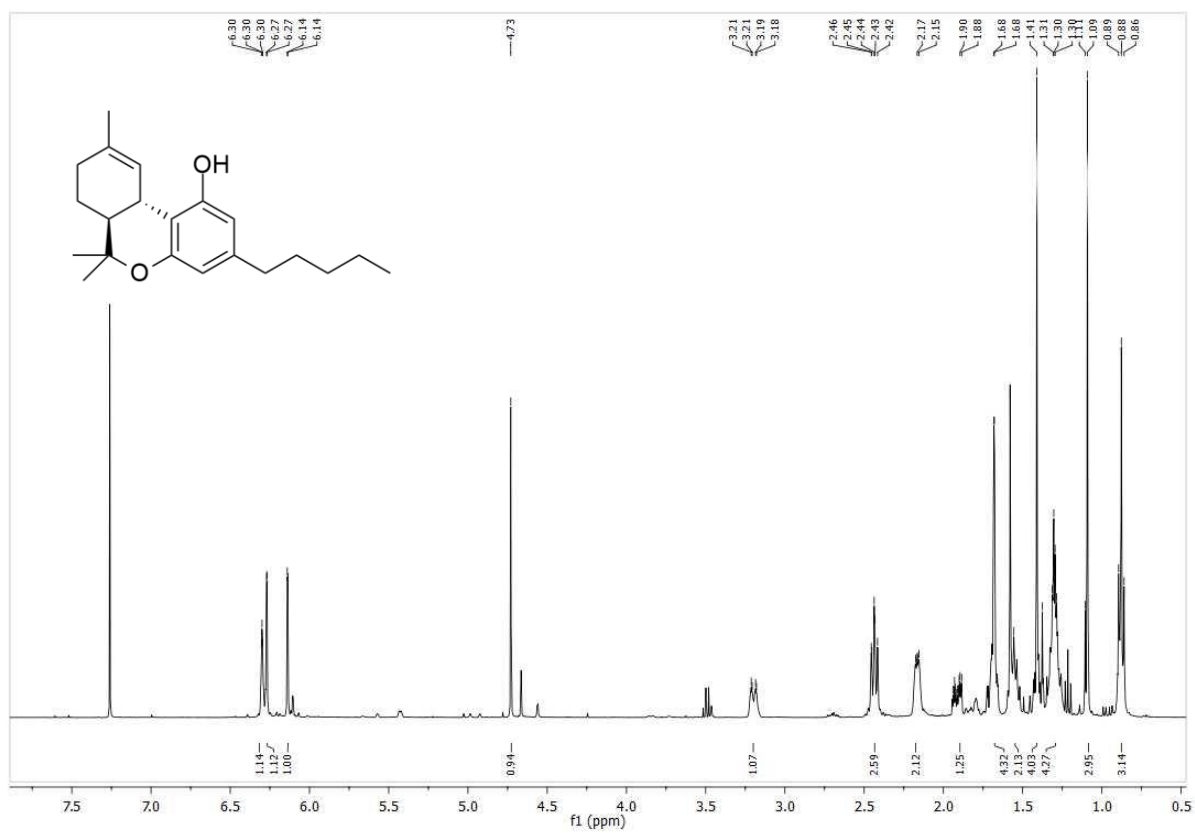


Figure S 12. ¹H NMR of (+)-trans- Δ^9 -THC.

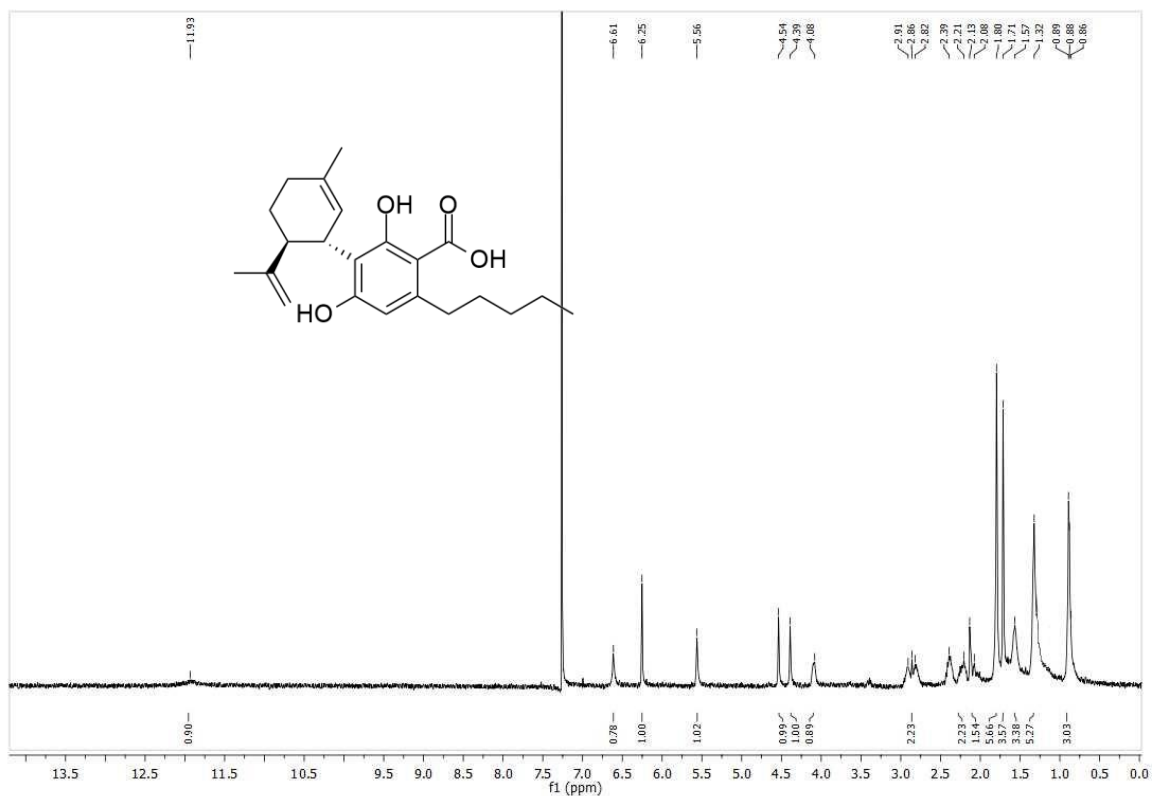


Figure S 13. ^1H NMR of (+)-trans-CBDA.

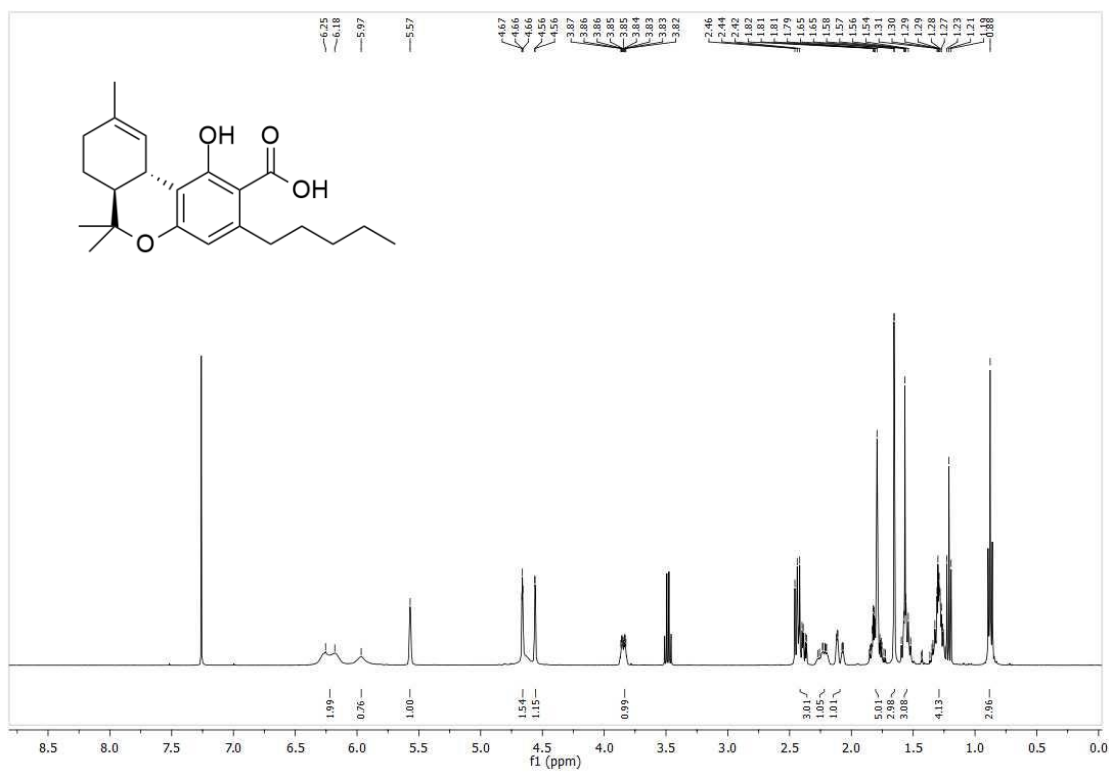
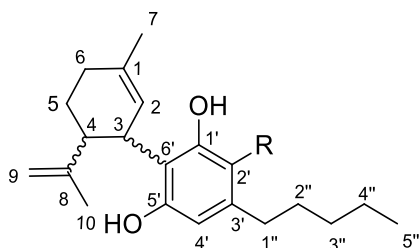


Figure S 14. ^1H NMR of (+)-trans- Δ^9 -THCA.

Table S 7. Comparison of ^1H NMR assignments of (+)- and (-)-*trans* enantiomers of *trans*-CBDA and *trans*-CBD.

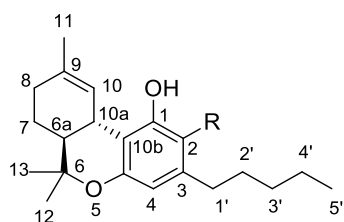


R=H (+)-*trans*-CBD

R=COOH (+)-*trans*-CBDA

Position	(+)- <i>trans</i> -CBD	(-)- <i>trans</i> -CBD	(+)- <i>trans</i> -CBDA	(-)- <i>trans</i> -CBDA
2	5.57 (s, 1H)	5.57 (s, 1H)	5.56 (brs, 1H)	5.55 (s, 1H)
3	3.89-3.77 (m, 1H)	3.88-3.78 (m, 1H)	4.08 (brd, 1H)	4.08 (brd, 1H)
4	2.47-2.35 (m, 3H)	2.48-2.35 (m, 3H)	2.45-2.33 (m, 1H)	2.45-2.32 (m, 1H)
5	1.88-1.73 (m, 5H)	1.87-1.75 (m, 5H)	1.85-1.81 (m, 2H)	1.85-1.81 (m, 2H)
6	2.29-2.15 (m, 1H)	2.30-2.17 (m, 1H)	2.29-2.17 (m, 1H)	2.31-2.20 (m, 1H)
	2.15-2.03 (m, 1H)	2.14-2.05 (m, 1H)	2.15-2.06 (m, 1H)	2.16-2.07 (m, 1H)
7	1.88-1.73 (m, 5H)	1.87-1.74 (m, 5H)	1.80 (s, 3H)	1.80 (s, 3H)
9	4.66 (s, 1H)	4.66 (s, 1H)	4.54 (s, 1H)	4.54 (s, 1H)
	4.56 (s, 1H)	4.56 (s, 1H)	4.39 (s, 1H)	4.39 (s, 1H)
10	1.65 (s, 3H)	1.65 (s, 3H)	1.71 (s, 3H)	1.71 (s, 3H)
2'	6.25 (brs, 1H)	6.27 (brs, 1H)	-	-
4'	6.18 (brs, 1H)	6.18 (brs, 1H)	6.25 (s, 1H)	6.25 (s, 1H)
1''	2.47-2.35 (m, 3H)	2.48-2.35 (m, 3H)	2.97-2.87 (m, 1H)	2.97-2.87 (m, 1H)
			2.87-2.76 (m, 1H)	2.87-2.76 (m, 1H)
2''	1.60-1.51 (m, 2H)	1.60-1.51 (m, 2H)	1.61-1.53 (m, 2H)	1.61-1.53 (m, 2H)
3''	1.37-1.22 (m, 4H)	1.37-1.22 (m, 4H)	1.35-1.31 (m, 4H)	1.36-1.30 (m, 4H)
4''	1.37-1.22 (m, 4H)	1.37-1.22 (m, 4H)	1.35-1.31 (m, 4H)	1.36-1.30 (m, 4H)
5''	0.88 (t, $J = 7.0$ Hz, 3H)	0.88 (t, $J = 7.0$ Hz, 3H)	0.88 (t, $J = 6.9$ Hz, 3H)	0.88 (t, $J = 6.9$ Hz, 3H)
1'-OH	5.97 (s, 1H)	5.96 (s, 1H)	11.93 (brs, 1H)	11.93 (brs, 1H)
5'-OH	-	-	6.61 (s, 1H)	6.61 (s, 1H)

Table S 8. Comparison of ^1H NMR assignments of (+)- and (-)-trans enantiomers of trans- Δ^9 -THCA and trans- Δ^9 -THC.



R = H (+)-trans- Δ^9 -THC

R = COOH (+)-trans- Δ^9 -THCA

Position	(+)-trans-THC	(-)-trans-THC	(+)-trans-THCA	(-)-trans-THCA
2	6.14 (d, $J = 1.6$ Hz, 1H)	6.14 (d, $J = 1.6$ Hz, 1H)	-	-
4	6.27 (d, $J = 1.6$ Hz, 1H)	6.27 (d, $J = 1.6$ Hz, 1H)	6.25 (s, 1H)	6.26 (s, 1H)
6a	1.71-1.64 (m, 4H)	1.71-1.67 (m, 4H)	1.70-1.66 (m, 4H)	1.70-1.66 (m, 4H)
7	1.94-1.85 (m, 1H)	1.95-1.85 (m, 1H)	1.94-1.89 (m, 1H)	1.94-1.89 (m, 1H)
	1.43-1.39 (m, 4H)	1.44-1.40 (m, 4H)	1.37-1.31 (m, 5H)	1.37-1.31 (m, 5H)
8	2.23-2.12 (m, 2H)	2.21-2.11 (m, 2H)	2.19-2.15 (m, 2H)	2.19-2.15 (m, 2H)
10	6.31-6.28 (m, 1H)	6.32-6.28 (m, 1H)	6.39 (s, 1H)	6.39 (1H, brs)
10a	3.25-3.14 (m, 1H)	3.25-3.15 (m, 1H)	3.22 (d, $J = 7.0$ Hz, 1H)	3.23 (d, $J = 7.0$ Hz, 1H)
11	1.71-1.64 (m, 4H)	1.71-1.67 (m, 4H)	1.70-1.66 (m, 4H)	1.70-1.66 (m, 4H)
12	1.43-1.39 (m, 4H)	1.44-1.40 (m, 4H)	1.44 (s, 3H)	1.44 (s, 3H)
13	1.09 (s, 3H)	1.09 (s, 3H)	1.11 (s, 3H)	1.11 (s, 3H)
1'	2.50-2.37 (m, 2H)	2.48-2.38 (m, 2H),	2.97-2.89 (m, 1H)	2.97-2.89 (m, 1H)
			2.81-2.73 (m, 1H)	2.81-2.73 (m, 1H)
2'	1.59-1.52 (m, 2H)	1.60-1.51 (m, 2H)	1.61-1.50 (m, 2H)	1.61-1.50 (m, 2H)
3'	1.32-1.28 (m, 4H)	1.33-1.24 (m, 4H)	1.37-1.31 (m, 5H)	1.37-1.32 (m, 5H)
4'	1.32-1.28 (m, 4H)	1.33-1.24 (m, 4H)	1.37-1.31 (m, 5H)	1.37-1.32 (m, 5H)
5'	0.88 (t, $J = 7.0$ Hz, 3H)	0.88 (t, $J = 7.0$ Hz, 3H)	0.90 (t, $J = 7.0$ Hz, 3H)	0.90 (t, $J = 7.0$ Hz, 3H)
1-OH	4.73 (s, 1H)	4.71 (s, 1H)	12.23 (s, 1H)	12.19 (s, 1H)

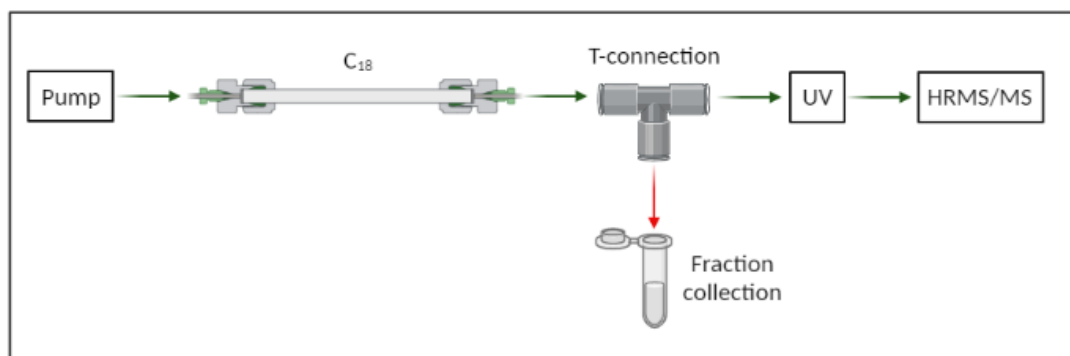


Figure S 15. Scheme of the eluent flow for the isolation of phytocannabinoids on the C₁₈ column.

BIDIMENSIONAL HEART-CUT ACHIRAL-CHIRAL LIQUID CHROMATOGRAPHY COUPLED TO HIGH-RESOLUTION MASS SPECTROMETRY FOR THE SEPARATION OF THE MAIN CHIRAL PHYTOCANNABINOIDS AND ENANTIOMERIZATION STUDIES OF CANNABICHROMENE AND CANNABICHROMENIC ACID

Fabiana Russo ^{a,b}, Elena Ferri ^b, Diego Pinetti ^c, Maria Angela Vandelli ^b, Aldo Lagana ^d, Anna Laura Capriotti ^d, Alberto Cavazzini ^e, Giuseppe Gigli ^f, Cinzia Citti ^{b,f,*}, Giuseppe Cannazza ^{b,f}

a Clinical and Experimental Medicine PhD Program, University of Modena and Reggio Emilia, 41125, Modena, Italy

b Department of Life Sciences, University of Modena and Reggio Emilia, Via Campi 103, 41125, Modena, Italy

c Centro Interdipartimentale Grandi Strumenti (CIGS), University of Modena and Reggio Emilia, Via Campi 213/A, Modena, 41125, Italy

d Department of Chemistry, Sapienza University of Rome, Piazzale Aldo Moro 5, 00185, Rome, Italy

e Department of Chemical, Pharmaceutical and Agricultural Sciences, University of Ferrara, Via L. Borsari 46, 44121, Ferrara, Italy

f Institute of Nanotechnology – CNR NANOTEC, Campus Ecotekne, Via Monteroni, 73100, Lecce, Italy

Published in: *Talanta*. (2024)

doi: 10.1016/j.talanta.2023.125161

* Corresponding author. Department of Life Sciences, University of Modena and Reggio Emilia, Via Campi 103, 41125, Modena, Italy.

E-mail address: cinzia.citti@unimore.it (C. Citti).

Abstract

In this work, a heart-cut bidimensional achiral-chiral liquid chromatography method coupled to high-resolution mass spectrometry was developed for the separation of the main carboxylated phytocannabinoids, namely cannabidiolic acid (CBDA), tetrahydrocannabinolic acid (THCA), cannabichromenic acid (CBCA), and cannabicyclolic acid (CBLA), and decarboxylated derivatives, namely cannabidiol (CBD), Δ^9 -tetrahydrocannabinol (Δ^9 -THC), cannabichromene (CBC), and cannabicyclol (CBL), and the evaluation of their enantiomeric composition in extracts of different *Cannabis sativa* L. varieties. Optimal conditions for the chiral analysis of CBC- and CBL-type compounds were found with methanol and water (95:5, v/v, with 0.1% formic acid, 1.5 mL/min) on an amylose-based chiral stationary phase. These settings also allowed to evaluate the parameters responsible for CBC and CBCA racemization.

1. Introduction

Phytocannabinoids derived from *Cannabis sativa* L. have garnered significant attention from the scientific community due to their pharmacological value. Tetrahydrocannabinol (THC) and cannabidiol (CBD) have been extensively studied both chemically and pharmacologically, making them the most well-known members of this class. While cannabichromene (CBC) has received less investigation, it is considered one of the “big four” phytocannabinoids alongside THC, CBD, and cannabigerol (CBG). The production and storage of THC and CBD occur in the capitate stalked trichomes of cannabis inflorescence, with their concentration increasing during maturation and flowering. In contrast, CBC appears to reach peak production shortly after seedling formation, decrease during development, and stabilize at a low level during maturation [1]. All phytocannabinoids are initially synthesized in their carboxylic acid forms, such as cannabigerolic acid (CBGA), tetrahydrocannabinolic acid (THCA), cannabidiolic acid (CBDA), and cannabichromenic acid (CBCA). These acids undergo decarboxylation into their corresponding neutral derivatives when exposed to heat and light. The enzymatic conversion of CBGA into the three primary phytocannabinoids (THCA, CBDA, and CBCA) is facilitated by different oxydacyclases: THCA synthase (THCAS), CBDAS (CBDA synthase), and CBCAS (CBCA synthase) [2]. Notably, CBCAS operates differently from THCAS and CBDAS. Following FAD-promoted hydride abstraction from the benzallylic carbon and subsequent oxidation, the resulting quinone methide cyclizes to form a chromene structure [1,3]. Conversely, THCAS and CBDAS catalyze intramolecular cyclization through electrophilic addition, leading to THCA formation, or proton loss, resulting in CBDA formation, respectively [1]. THCA and CBDA have been found to exist as enantiopure (-)-*trans* isomers in *Cannabis sativa* L. However, one study reports the presence of a trace amount of the (+)-*trans* isomer of the decarboxylated derivative of THCA, Δ^9 -THC, in a medicinal cannabis extract [4]. Regarding CBCA, there are reports of a racemic mixture of the decarboxylated derivative CBC [5,6], as well as a scalemic mixture of the compound found in a plant sample [4]. Notably, Morimoto et al. conducted interesting research where they isolated and partially purified CBDAS from young leaves of a CBDA-rich variety [2]. They incubated the isolated enzyme with the substrate CBGA and analyzed the decarboxylated product (obtained at 120 °C for 5

min) using chiral high-performance liquid chromatography coupled with UV detection (HPLC-UV) [2]. The resulting CBC was found to exist as two enantiomers in a 1:5 ratio based on the elution order [2]. The authors concluded that this enantiomeric ratio is inherited from the precursor CBCA, which must be synthesized with this stereoselectivity, as the decarboxylation process did not cause erosion of the enantiopurity [2]. As the quinone methide intermediate in the biosynthesis of CBCA is achiral, the resulting product must retain the stereochemistry imparted by the enzyme. Recent experiments conducted by Agua et al. demonstrated that the major enantiomer in the scalemic mixture is the (-) isomer corresponding to the *R* configuration [7]. In the same study, racemization experiments of CBC were conducted under strict laboratory conditions, but only minimal erosion of enantiopurity was observed, suggesting that other factors during handling and storage may promote racemization [7]. Due to the challenges in resolving CBCA enantiomers using chiral HPLC, the direct evaluation of the enantiomeric composition of CBCA has not been attempted. Instead, it is analyzed indirectly after decarboxylation into CBC. Although the heating process has been shown not to affect the stereostability of the chiral center, indirect analysis has limitations and may result in the detection of other decomposition products. It is well-known from previous studies that exposure to light leads to further cyclization of CBC into CBL, as well as photooxidation and conversion of its carboxylated precursor CBCA into CBLA [6,8]. Therefore, chiral analysis should be conducted directly on the carboxylated precursor, and suitable conditions need to be established for the separation of both CBCA and CBLA enantiomers. The chiral analysis of CBCA and CBC is crucial considering the growing interest in their therapeutic potential. CBC has shown promising anti-inflammatory [9], anticonvulsant [10], anticancer [11], and antidepressant activities [12]. CBCA also possesses anticonvulsant properties [10] and exhibits significant antibacterial effects against methicillin-resistant *Staphylococcus aureus* (MRSA), surpassing the potency of vancomycin [13]. This study aims to develop a chromatographic system capable of separating the enantiomers of major chiral phytocannabinoids, including CBDA, THCA, and CBCA, in cannabis full extracts. For this purpose, a two-dimensional achiral-chiral liquid chromatography method coupled with high-resolution mass spectrometry detection (2D-AC-HPLC-HRMS) was developed, utilizing previously optimized conditions [14]. To gain insights into the enantiomerization process of CBCA and CBC, the effects of temperature and UV light were investigated.

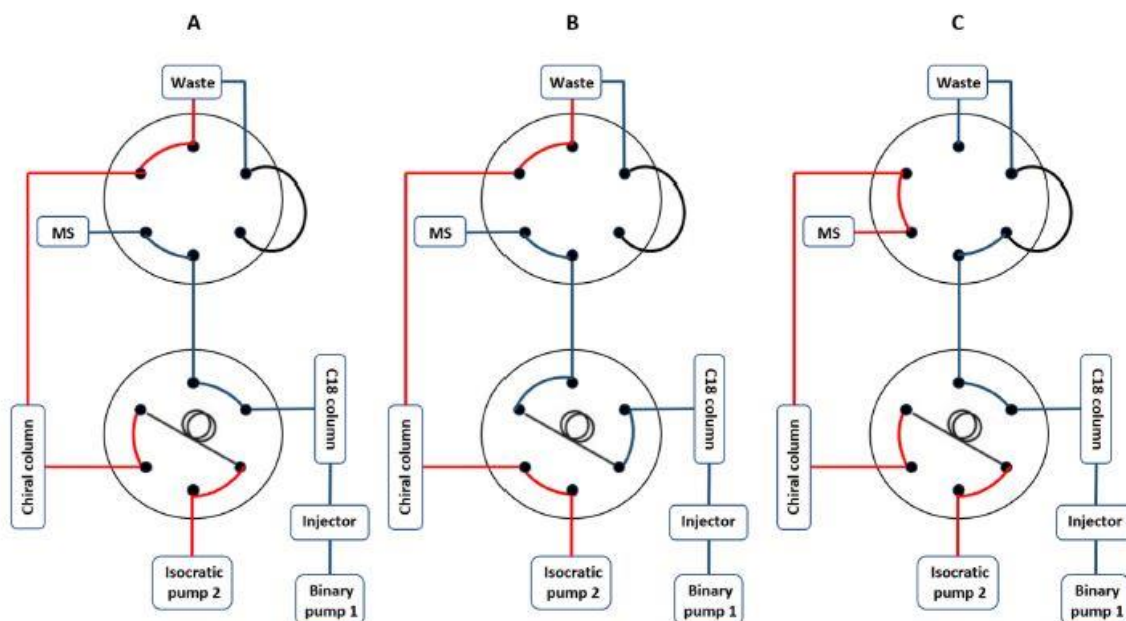


Fig. 1. Heart-cut 2D-AC-HPLC-HRMS method. Schematic representation of the heart-cut 2D-AC-HPLC system.

2. Materials and methods

2.1. Chemicals and reagents

Acetonitrile (ACN) and formic acid (FA) were LC-MS grade, while ethanol 96% (v/v) was analytical grade. Organic solvents were purchased from Honeywell (Charlotte, North Carolina, USA), while ultrapure water was obtained with a water purification system (Direct-Q 3UV, Merck Millipore, Milan, Italy). Stock solutions of pure certified analytical standards of (-)-*trans*-CBDA, (-)-*trans*-THCA, CBCA, CBLA, (-)-*trans*-CBD, (-)-*trans*- Δ^9 -THC, CBC and CBL were bought from Cerilliant (Sigma-Aldrich Merck, Milan, Italy). Minor (+)-*trans* enantiomers of CBDA (99% *ee*), THCA (99% *ee*), CBD (92% *ee*), and Δ^9 -THC (96% *ee*) were available *in house* from previous syntheses [14]. Their purity was checked before use confirming their high stability after six months at -20°C.

2.2. Plant material

Cannabis sativa L. samples from different varieties including Carmagnola (one sample), CS Fibrante (one sample), Codimono (one sample), Eletta Campana Silvana (five samples), Ferimon (one sample), and Kompolti (one sample) were kindly provided by local growers. These varieties are registered in the Italian/EU Catalogue of the industrial hemp varieties grown from certified seeds (Common Catalogue of Varieties of Agricultural Plant Species) and showed a prevalence of CBDA with THCA levels below 0.3% (chemotype III). The FM2 medicinal cannabis variety (batch n. 6A32/1) was supplied by the Military Chemical Pharmaceutical Institute (Florence, Italy) with the authorization of the Italian Ministry of Health (prot. 136 n. SP/062). The crude extracts were obtained following the protocol reported in the German Pharmacopoeia for *Cannabis flos* [15]. Briefly, 500 mg of the raw material were finely grinded and extracted in three cycles with decreasing volumes (20 mL, 15 mL, 10 mL) of ethanol 96% (EtOH). The combined ethanol extracts were

brought to 50 mL fresh ethanol in a volumetric flask. After centrifugation of a small aliquot (1 mL) at 2000×g, the supernatant was filtered through a 0.45 µm PTFE filter and injected after a 10 × dilution with mobile phase into the HPLC system. Decarboxylation of the FM2 inflorescence was carried out at 120°C for 2 h.

2.3. Bidimensional heart-cut achiral-chiral HPLC-HRMS analysis

HPLC analysis was performed on an Ultimate 3000 LC system (ThermoFisher Scientific, Waltham, Massachusetts, USA) equipped with a binary pump, a vacuum degasser, a thermostated autosampler set at 4°C, and a thermostated column compartment set at 30 °C. Achiral analysis was performed on a Poroshell 120 EC-C18 column (100 × 3.0 mm I.D., 2.7 µm) with guard (5 × 3 mm I.D., 2.7 µm) (both from Agilent Technologies, Milan, Italy) eluting water and ACN (both with 0.1% formic acid) as mobile phase from the binary pump 1 through the six-port valve 1 (Fig. 1). The elution program employed was slightly modified from previous works using water and acetonitrile (both with 0.1% formic acid (FA)) as mobile phase [16,17]. Briefly, the ACN gradient increased from 5% to 95% ACN from 2.0 to 20.0 min, held at 95% for 5 min and decreased back to 5% at 25.1 min. The column was re-equilibrated back to 5% ACN for 5 min and the run was stopped at 40 min. The flow rate was maintained at 0.5 mL/min. The eluent was directed through the six-port valve 2 to the HRMS detector as shown in Fig. 1A. At the retention time of a selected compound the position of valve 1 was changed from “load” to “inject” to trap the peak into the 100-µL loop (Fig. 1B). After a customized interval, which was different for each phytocannabinoid (Table S1, Supplementary Material), valve 1 was switched back to “load” to connect the loop to the isocratic pump 2 (Fig. 1C). Simultaneously valve 2 was switched to carry the eluent from the chiral column to the HRMS detector and that from the C18 column to the waste (Fig. 1C). The mobile phase for the chiral analysis was changed for each enantiomeric pair (Table S2, Supplementary Material). Chiral separation of phytocannabinoids was achieved on a Chiralpack AD-RH [amylose tris (3,5-dimethylphenylcarbamate)] (150 × 4.6 mm I. D., 5 µm) (Daicel Chiral Technologies Europe S.A.S, France). Since CBD and THC enantiomers could be separated with the same mobile phase and had reasonably different retention times, they could be resolved within the same analytical run by switching only valve 1 at the selected retention times. The chromatographic apparatus was interfaced to a heated electrospray ionization source and a Q-Exactive Orbitrap high-resolution mass spectrometer (HESI-HRMS) utilizing simultaneously positive (HESI+) and negative (HESI-) polarity mode. Carboxylated species were analyzed in HESI- mode, while decarboxylated species better performed with HESI+ mode [18]. Simultaneous full scan (FS) and data-dependent acquisition (DDA) experiments were run for the achiral analysis with the parameters optimized in previous works (see also Table S3, Supplementary Material) [18–21]. For the chiral analysis the Orbitrap mass analyzer was switched to SIM (single ion monitoring) mode with an inclusion list of two precursor ions at m/z 357.2071 in HESI⁻ mode and 315.2319 in HESI⁺ mode in order to detect only the analytes under investigation. To further improve the sensitivity of the SIM detection, a PRM (parallel reaction monitoring) experiment was added simultaneously, which enabled the fragmentation of the selected ions. The sample volume injected for the analyses was 5 µL. The analytes precursor ions [M-H]⁻ and [M+H]⁺ were extracted with a 5-ppm mass tolerance from the total ion current. The analyses were acquired with Xcalibur 3.0 (ThermoFisher Scientific) and processed using FreeStyle 1.7 (ThermoFisher Scientific). The separation of

phytocannabinoids in standard racemates achieved by the developed heart-cut bidimensional method is reported in Figure S1 (Supplementary Material).

2.4. Circular dichroism analysis

Circular dichroism (CD) analysis was performed on a Jasco CD-2095 Plus chiral detector interfaced to the HPLC system through a JMBS Hercule Lite interface (Jasco Europe, Italy). Spectra of CBCA and CBC enantiomers were acquired online and processed using Borwin software 1.5 (Jasco Europe, Italy). Individual enantiomers (100 µg/mL, 10 µL) were analyzed eluting 95% MeOH with 0.1% FA at 1.5 mL/min on the Chiralpack AD-RH. CD was set at 258 nm and 280 nm for the detection of CBCA and CBC, respectively. *2.5. CBCA and CBC enantiomerization studies* A Vanquish Core System (ThermoFisher Scientific, Waltham, Massachusetts, USA) equipped with a binary pump, a vacuum degasser, a thermostated autosampler set at 4 °C, a thermostated column compartment set at 30 °C, and a diode array detector (HPLC-DAD) was employed to isolate CBCA and CBC enantiomers from the corresponding racemate. The UV trace was analyzed at 270 nm, which provided the best detector response in terms of signal intensity. The pure analytical standard (1 mg/mL) was injected on the Chiralpack AD-RH and the enantiomers of either CBCA or CBC were separated with 95% MeOH with 0.1% FA at 1.5 mL/min using the chromatographic settings developed in a previous work [14]. A 10-µL injection was repeated thirty times in order to collect thirty 100-µL samples of each enantiomer for all the enantiomerization experiments. The isolated fractions were first checked for purity under the same chromatographic conditions.

2.5.1. Heat-driven enantiomerization

Enantiomerization studies of CBCA were first performed under controlled conditions in a bench oven at different temperatures, 60°C, 120°C and 130°C, and the isolated enantiomers were placed in 1-mL amber glass vials (ThermoFisher Scientific, Waltham, Massachusetts, USA). Each aliquot was dissolved in 50 µL of ACN and analyzed at a fixed time point for a total of 120 min. CBC enantiomers were evaluated only at 120 °C for 120 min. *2.5.2. UV light-driven enantiomerization* Either CBCA or CBC enantiomers were placed in a 1-mL clear glass vial (ThermoFisher Scientific, Waltham, Massachusetts, USA) under a 254 nm UV lamp and checked by chiral HPLC-DAD to observe erosion of the enantiopurity. The experiment was followed for 120 min. Lastly, 500 µL of CBCA enantiomers were placed under natural sunlight and checked for erosion of the enantiopurity at the end of each day for five consecutive days.

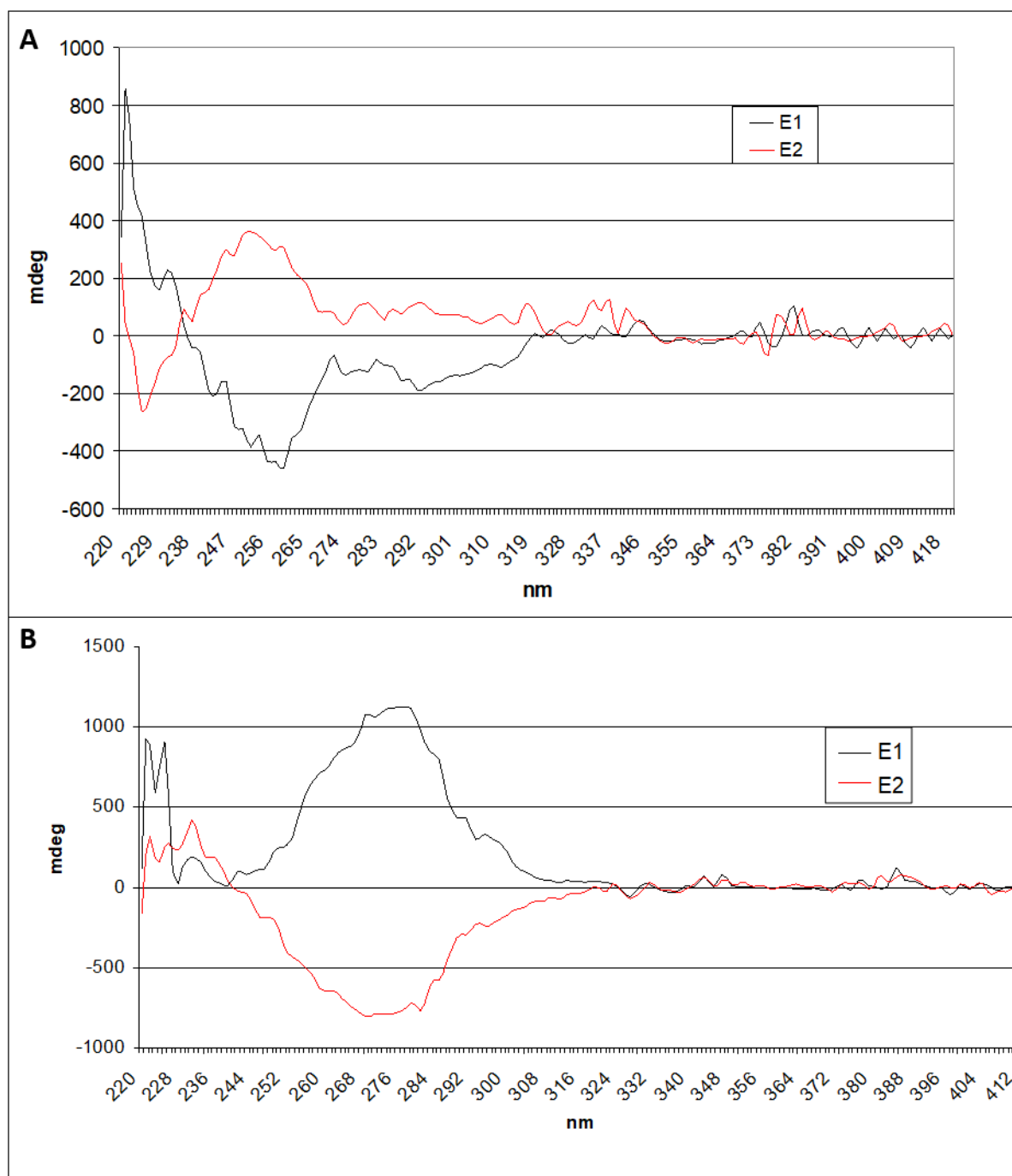


Fig. 2. Online CD spectra of CBCA and CBC enantiomers. Online CD analysis of isolated CBCA (A) and CBC (B) enantiomers eluting with 95% methanol on Chiralpack AD-RH (150 × 4.6 mm I.D., 5 μ m). The blue trace corresponds to the first eluted enantiomer (E1), while the red trace corresponds to the second eluted enantiomer (E2)

3. Results and discussion

3.1. Development of the heart-cut 2D-AC-HPLC-HRMS

In a previous study [14], enantiomers of the main carboxylated and decarboxylated phytocannabinoids (CBDA, THCA, CBD, and Δ^9 -THC) were successfully separated using an amylose-based chiral stationary phase (CSP) (Chiralpack AD-RH) in reversed-phase (RP) mode. However, the process of isolating compounds on the achiral column, drying the solvent, resuspending the samples, and conducting single peak chiral analysis can be labor-intensive. To address this, a heart-cut bidimensional liquid chromatography approach is a more

convenient technique. This strategy involves trapping a single peak from the achiral column in the first dimension and diverting the flow to a second column with a post-column divert valve [22,23]. The trapped compound can then be evaluated for its enantiomeric composition using a chiral column in the second dimension, eliminating the influence of external factors. However, one challenge with this approach is the compatibility of the mobile phases used in the two dimensions. While normal phase conditions are generally preferred for chiral separation of phytocannabinoids due to better peak shape, they are not compatible with the aqueous mobile phases (RP conditions) used in the first dimension. As a result, online coupling of the two dimensions is not possible, thus fraction collection and off-line chiral analysis are required. Alternatively, direct analysis of the cannabis full extract on the chiral column can be performed [4], but this may present difficulties in unambiguously identifying peaks due to potential co-eluting species [14]. The separation of the target phytocannabinoids was achieved by combining two methods: achiral analysis and off-line chiral analysis, which were optimized in a previous study [14]. In the first dimension, a gradient elution of acetonitrile from 5% to 95% was performed in RP conditions using a C18 core-shell stationary phase. By utilizing the previously optimized enantioseparation conditions for THCA, CBDA, Δ^9 -THC, and CBD in reversed-phase (RP) conditions [14], it was feasible to integrate the achiral separation with the chiral analysis. The mobile phase composition was adjusted individually for each phytocannabinoid in the second dimension since it was challenging to find a single optimal solvent combination for the separation of all enantiomeric pairs. The use of RP conditions in the second dimension facilitated compatibility with the HESI-HRMS detection. A scheme representative of the chromatographic settings employed is pictured in Fig. 1. In contrast, the separation of CBCA enantiomers has proven challenging, and the optimal chromatographic conditions have not yet been identified. However, CBC enantiomers have been successfully resolved using various CSPs in normal phase conditions, including Chiralcel OD-R [2], Lux Amylose-1 [7], and Chiralpack IB N-3 [24]. One study achieved satisfactory separation of CBC enantiomers in reversed-phase conditions using sub-2 μm immobilized CSPs such as Chiralpack ID-U, IG-U, and ID-U coupled to IC-U [25]. More recently, both cellulose-based (Chiralpack IC) and amylose-based (Chiralpack IF) CSPs have demonstrated good baseline resolution of CBC enantiomers under reversed-phase conditions [26]. To optimize the chromatographic conditions for the chiral separation of CBCA and CBC enantiomers, the Chiralpack AD-RH column that had previously shown promising results for the separation of THCA, CBDA, Δ^9 -THC, and CBD enantiomers was initially selected [14]. The optimization process was conducted offline. A mobile phase consisting of water and ACN (with 0.1% FA) was initially used, and satisfactory resolution of the two CBCA enantiomers was achieved with 95% of the organic modifier. However, the second eluted enantiomer (E2) exhibited a broad peak shape. Considering the likelihood of isomerization of CBCA to CBLA and CBC to CBL, pure standards of all four phytocannabinoids were analyzed under the same conditions. While good separation of CBLA enantiomers was achieved, the resolution between E2 of CBCA and CBLA was poor due to their broad peak shapes. Additionally, CBC and CBL could not be distinguished from their carboxylated precursors, and baseline resolution of CBC enantiomers was not achieved. To address these challenges, ACN was replaced with MeOH, and various percentages of MeOH (ranging from 80% to 98%) were tested. The optimal conditions were

determined to be 95% MeOH, despite the poor resolution between the first eluted enantiomers of CBLA and CBL, as well as between the second eluted enantiomers of CBC and CBL. It is important to note that the elution order of CBCA and CBLA enantiomers was inverted when ACN was substituted with MeOH, but the peak shape was significantly improved. Therefore, this mobile phase composition was selected for the chiral analysis of the targeted phytocannabinoids (Figure S2, Supplementary Material). Due to partial peak overlapping, the use of high-resolution mass spectrometry (HRMS) was necessary to provide distinctive fragments for the identification of each phytocannabinoid under investigation. This allowed for better differentiation and characterization of the compounds (Figure S3, Supplementary Material). In this study, circular dichroism (CD) analysis was conducted on pure standards of CBCA and CBC to determine their enantiomeric properties. The CD analysis performed on CBCA at 258 nm showed a negative Cotton effect for the first eluted enantiomer (CBCA-E1) and a positive Cotton effect for the second eluted enantiomer (CBCA-E2) (Fig. 2A). Conversely, CD analysis of CBC at 280 nm revealed a positive Cotton effect for the first eluted enantiomer (CBC-E1) and a negative Cotton effect for the second eluted enantiomer (CBC-E2) (Fig. 2B). Based on these CD results, the enantiomers of CBCA were designated as [CD(-) 258]-CBCA for the first eluted enantiomer (CBCA-E1) with a negative Cotton effect at 258 nm, and [CD(+)258]-CBCA for the second eluted enantiomer (CBCA-E2) with a positive Cotton effect at 258 nm. Similarly, the enantiomers of CBC were labeled as [CD(+)280]-CBC for the first eluted enantiomer (CBC-E1) with a positive Cotton effect at 280 nm, and [CD(-)280]-CBC for the second eluted enantiomer (CBC-E2) with a negative Cotton effect at 280 nm.

Table

1. Enantiomeric composition of CBCA in the tested cannabis extracts using the heart-cut 2D-AC-HPLC-HRMS method.

Sample	[CD(-)258]-CBCA:[CD(+)258]-CBCA (<i>er</i>)
Carmagnola	41:59
CS	44:56
Fibrante	42:58
Codimono	48:52
Eletta Campana_1	46:54
Eletta Campana_2	43:57
Eletta Campana_3	41:59
Eletta Campana_4	45:55
Eletta Campana_5	32:68
Silvana	50:50
Ferimon	76:24
Kompolti	42:58
FM2	45:55

3.2. Chiral analysis of phytocannabinoids in *Cannabis sativa* L. Samples

The analysis of various *Cannabis sativa* L. samples using the developed heart-cut 2D-AC-HPLC-HRMS method confirmed previous results reported for CBDA and THCA [14]. but, at the same time, revealed interesting findings regarding the enantiomeric composition of CBCA. No trace of the (+) enantiomers of CBDA and THCA was present in the cannabis extracts, which showed only the presence of the (-) enantiomer. On the other hand, in most samples CBCA was found to be nearly racemic, with only a slight enantiomeric excess of [CD(+)]258]-CBCA, as indicated in Table 1. Only two samples exhibited CBCA as a scalemic mixture, with enantiomeric ratios of 76:24 and 32:68 in the Eletta Campana and Ferimon varieties, respectively. These results align with previous reports on CBC, which also demonstrated a similar pattern of enantiomeric composition [4–6]. In order to understand the effects of decarboxylation on CBCA, the FM2 plant material was heated at 120°C for 2 h. A representative trace obtained with the heart-cut 2D-AC-HPLC-HRMS method is shown in Fig. 3. Fig. 3A and B displays the achiral separation of carboxylated phytocannabinoids and the determination of their enantiomeric composition in the FM2 cannabis extract, respectively. The same separation is shown in Fig. 3C and D following the decarboxylation of the initial inflorescence. While the CBD and Δ^9 -THC generated by decarboxylation retained the same stereochemistry of their native precursors with no erosion of the enantiopurity as recently reported [14], a slight decrease of the enantiomeric ratio was observed for CBC enantiomers compared to the starting CBCA. It is noteworthy that [CD(+)]258]-CBCA was typically the dominant enantiomer in the investigated varieties, except for the CBD-rich Ferimon variety, where [CD(-)]258]-CBCA was the dominant enantiomer within the scalemic mixture. In a separate study, Calcaterra et al. observed the phenomenon of opposite enantiomeric dominance in the chiral analysis of CBC in two cannabis varieties: the CBD-rich Carmagnola variety and a CBG-rich accession, with the latter obtained from both indoor and outdoor cultivation [27]. Additionally, Agua et al. conducted research on the absolute configuration assignment of CBC enantiomers by synthesizing a CBL derivative, and their findings indicated that (*R*)-CBC, corresponding to (-)-CBC, was the dominant enantiomer [7]. The different enantiomeric dominance observed in the literature and in the present study may be attributed to strain-specific characteristics, potentially stemming from enzymatic factors, as suggested by Calcaterra et al. [27].

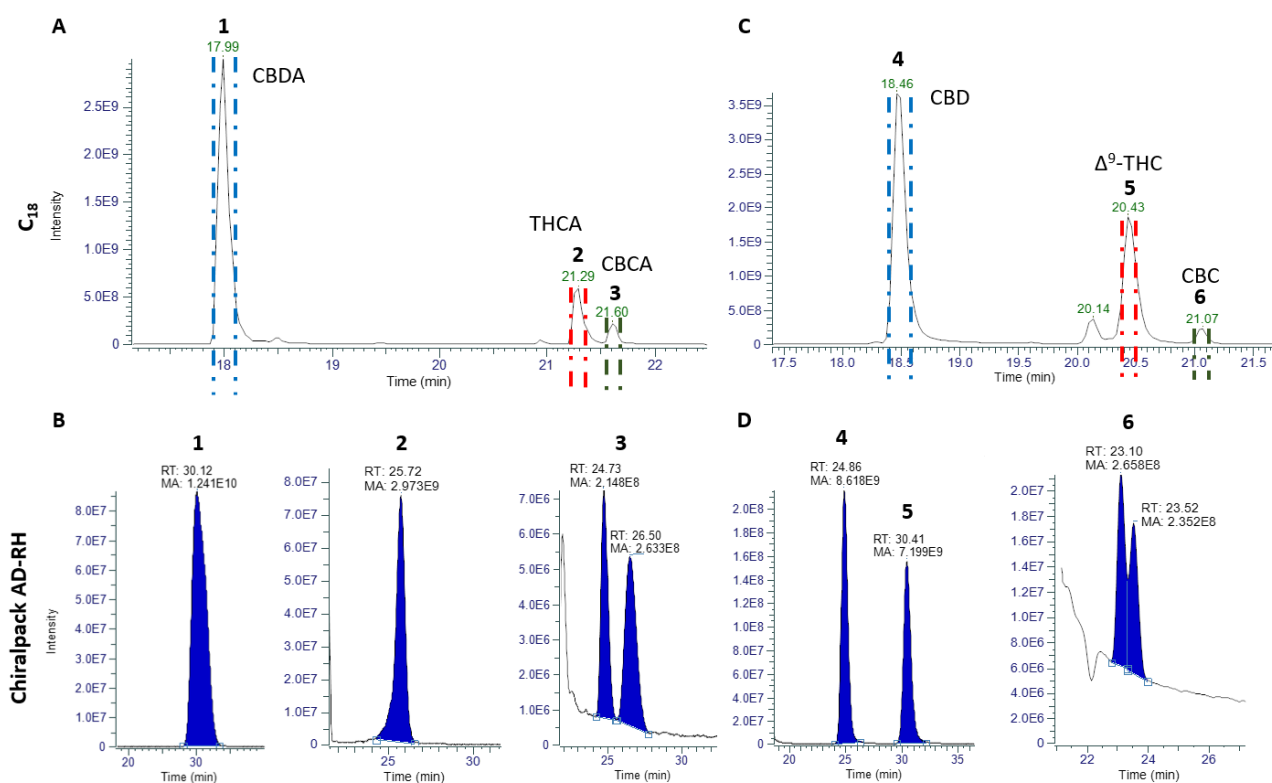


Fig. 3. Heart-cut 2D-AC-HPLC-HRMS analysis of FM2 extract. Achiral analysis of the native (A) and decarboxylated (C) FM2 extract on Poroshell 120 EC-C18 (100 × 3.0 mm I.D., 2.7 μm) with guard (5 × 3 mm I.D., 2.7 μm) and enantiomeric resolution of the carboxylated phytocannabinoids CBDA (1), THCA (2), and CBCA (3) (B) and decarboxylated derivatives CBD, Δ⁹-THC, and CBC (D) on Chiralpack AD-RH (150 × 4.6 mm I.D., 5 μm).

Table 2

Enantiomerization studies on isolated [CD(+)]258]-CBCA at 130 °C.

130 °C						
CBCA			CBC			
Time (min)	Relative area (%)	<i>er</i>	Relative area (%)	<i>er</i>	Relative area (%)	<i>er</i>
		[CD(-)]258]-CBCA	[CD(+)]258]-CBCA		[CD(+)]280]-CBC	[CD(-)]280]-CBC
0	100	0	100	0	-	-
30	8	1	99	92	96	4
60	0	-	-	100	90	10
120	0	-	-	100	78	22
180	0	-	-	100	69	31
240	0	-	-	100	67	33
300	0	-	-	100	65	35

3.3. Enantiomerization studies

The peak isolation method developed in a previous study [14] was successfully employed for the isolation of individual enantiomers of CBCA and CBC from the corresponding racemic analytical standards. These isolated

enantiomers were utilized for the enantiomerization studies, which were conducted on the chiral column under the optimized conditions. Initially, [CD(+)]258]-CBCA was subjected to heating at 60°C for 4 h, and samples were analyzed at various time intervals (Table S2, Supplementary Material). It is established in the literature that the isomerization of CBCA to CBLA does not alter the stereochemistry at the C2 chiral center [28]. Therefore, it was assumed that the formed CBLA isomer would possess the same optical rotation as the starting material CBCA. The formation of CBLA was observed after 30 min and gradually increased from 2% to 5% based on the relative peak area over the course of 4 h. No decarboxylation products were detected during the process. When the sample was left in the oven for 24 h, the chromatogram exhibited the presence of 6% CBLA and 5% CBC. Until the 24-h mark, CBLA was observed as a single enantiomer. However, after 24 h, 10% of the minor stereoisomer appeared. On the other hand, the small amount of CBC detected was found as a single enantiomer, specifically [CD(+)]280]-CBC. In an attempt to trigger isomerization, enantiomerization, or decarboxylation reactions, the temperature was increased to 130°C, which mimicked commonly employed conditions for inflorescence decarboxylation [29] (Table 2). However, no isomerization to CBLA or enantiomerization was observed, except for a slight decrease in enantiomeric purity after 30 min. At this high temperature, CBCA was rapidly and completely converted to CBC, which was unexpectedly found to undergo almost complete racemization after 5 h (Fig. 4). This finding contrasts with the results reported by Morimoto et al., who observed no enantiomerization following decarboxylation [2]. To further investigate this phenomenon, the temperature was lowered by 10°C, resulting in a slower rate of enantiomerization (Table 3). Similar results were obtained when pure isolated CBC enantiomers were subjected to heating at 120°C for 4 h (Table 4). The analysis revealed an enantiomeric ratio of 80:20, indicating that heat plays a significant role in the racemization of CBC, starting from a pure single enantiomer of CBCA. It should be noted that Morimoto et al. heated CBCA at 120°C for only 5 min, which may have been insufficient to observe a decrease in enantiopurity of the decarboxylation product CBC [2]. Similarly, Agua et al. investigated the racemization of CBC under stringent and controlled laboratory conditions, but they reported minimal or undetectable racemization [7]. In the present study, CBC racemization was studied in a solvent-free environment and at high temperatures, which likely played a crucial role in initiating the enantiomerization process. The wide range of enantiomeric ratios (*ers*) observed for CBCA in the tested samples indicates that factors other than the ones investigated in the study are responsible for the erosion of enantiomeric purity. While none of the conditions employed resulted in CBCA racemization, only CBC racemization was observed, which could explain why CBC was found as either a racemic or a scalemic mixture. Another factor that can influence the stability of phytocannabinoids is light exposure, which occurs during the handling and storage of cannabis biomass. To investigate this, isolated [CD(+)]280]-CBC and [CD(+)]258]-CBCA were exposed to a 254 nm UV lamp for 2 h and analyzed at specific time points (Tables 5 and 6, respectively). Surprisingly, CBC exhibited rapid racemization within 2 h (58:42 *er*), while no isomerization product (CBL) was detected (Fig. 5). On the other hand, CBCA showed slower enantioconversion, resulting in a 95:5 *er* after 2 h (Fig. 6). As expected, a significant amount of CBLA was formed, indicating that isomerization occurs at a faster rate than racemization. Additionally, no CBC formation was observed, suggesting that decarboxylation occurs only upon heating.

When left under direct sunlight for 5 days, the enantiomeric excess (*ee*) of CBCA was eroded up to 34% (Table 7). These findings highlight the impact of light exposure on the stability and enantiomeric purity of phytocannabinoids. Indeed, the results obtained in this study, although not entirely consistent with previous literature findings [2,7], provide valuable insights into the factors that can contribute to the presence of scalemic or racemic mixtures of CBCA and CBC. The findings highlight the significant influence of UV light and heat on the erosion of the enantiomeric purity that is initially present in the cannabis plant. The observed racemization of CBC under high temperature conditions and the enantioconversion of CBCA under UV light exposure emphasize the susceptibility of these compounds to undergo stereochemical changes. These factors, along with other environmental and handling conditions, may explain the variability in the enantiomeric composition of CBCA and CBC found in different cannabis samples. Further research and understanding of the underlying mechanisms will contribute to a comprehensive understanding of the stability and enantiomeric behavior of phytocannabinoids.

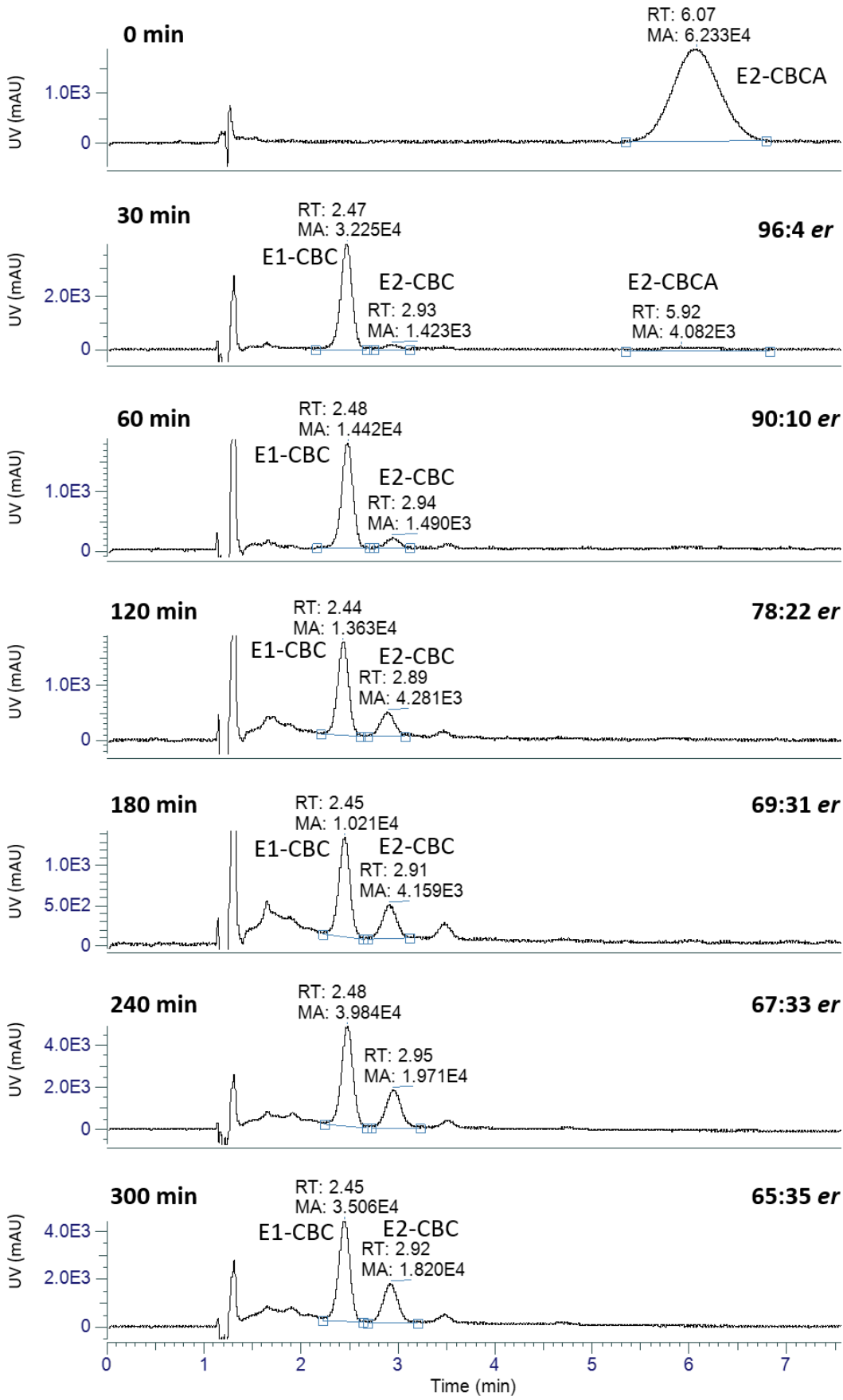


Fig. 4. Enantiomerization studies of CBCA at 130 °C. HPLC-UV chromatograms of [CD(+)-258]-CBCA after incubation at 130 °C in oven at fixed time points.

Table 3. Enantiomerization studies on isolated [CD(+)-280]-CBC at 120 °C.

Time (min)	120 °C					
	CBCA			CBC		
	Relative area (%)	<i>er</i>		Relative area (%)	<i>er</i>	
		[CD(-)-258]-CBCA	[CD(+)-258]-CBCA		[CD(-)-280]-CBC	[CD(+)-280]-CBC
0	100	0	100	0	-	-
30	24	4	96	76	98	2
60	6	<LOD	100	94	95	5
120	0	-	-	100	88	12
180	0	-	-	100	80	20
240	0	-	-	100	76	24
300	0	-	-	100	72	28

Table 4 Enantiomerization studies on isolated [CD(+)-280]-CBC at 120 °C.

Time (min)	120°C	
	CBC	
	<i>er</i>	
	[CD(+)-280]-CBC	[CD(-)-280]-CBC
0	100	-
30	99	1
75	96	4
120	90	10
180	85	15
240	80	20

Table 5. Enantiomerization studies on isolated [CD(+)-280]-CBC under UV light (254 nm).

Time (min)	UV (254 nm)	
	CBC	
	<i>er</i>	
	[CD(+)-280]-CBC	[CD(-)-280]-CBC
0	100	-
30	94	6

75	81	19
120	58	42

Table 6. Enantiomerization studies on isolated [CD(+)-258]-CBCA under UV light (254 nm) for 2 h.

Time (min)	UV (254 nm)					
	CBCA			CBLA		
	Relative area (%)	<i>er</i> [CD(-)258]- CBCA	[CD(+)-258]- CBCA	Relative area (%)	<i>er</i> [CD(-)258]- CBLA	[CD(+)-258]- CBLA
0	100	-	100	-	-	-
30	94	1	99	6	100	<LOD
75	83	2	98	17	100	<LOD
120	73	3	97	27	100	<LOD

4. Conclusions

The development of the heart-cut bidimensional achiral-chiral liquid chromatography method coupled to high-resolution mass spectrometry presented in this work has provided a valuable tool for the separation and analysis of the main phytocannabinoids in *Cannabis sativa* L. extracts. This method has enabled for the first time the successful separation of all the main chiral carboxylated phytocannabinoids on the chiral dimension, which is a significant advancement in the field. The investigation into the parameters responsible for the racemization of CBC and CBCA has shed light on the variability of results reported in previous independent studies. By understanding the factors contributing to the erosion of enantiomeric purity, this work contributes to a better understanding of the stability and behavior of these compounds, which is crucial for accurate analysis and interpretation of phytocannabinoid enantiomeric profiles. From a therapeutic perspective, both CBC and CBCA have exhibited promising pharmacological properties. CBC has shown anti-inflammatory, anticonvulsant, anticancer, and antidepressant activity, while CBCA has demonstrated potent antibacterial properties against methicillin-resistant *Staphylococcus aureus* (MRSA) and anticonvulsant activity. However, all biological assays have been conducted using racemic mixtures of these compounds. It is important to evaluate the pharmacological activity of individual enantiomers since different enantiomers often exhibit different pharmacological profiles. Therefore, future research should focus on assessing the stereochemical stability of CBC and CBCA under conditions that mimic *in vitro* and *in vivo* environments. This knowledge will facilitate the design of stereoselective pharmacological experiments and enhance our understanding of the therapeutic potential of these phytocannabinoids.

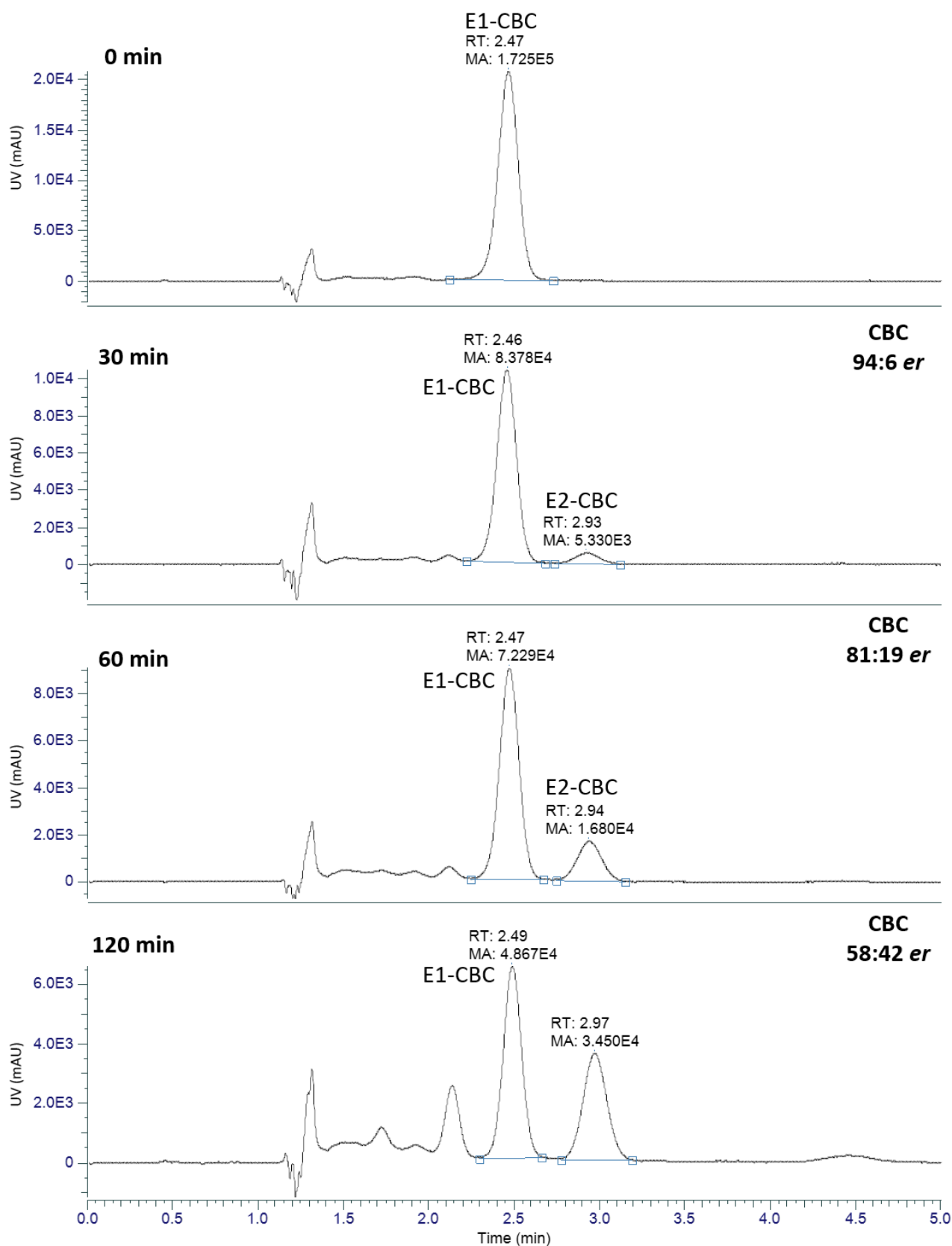


Fig. 5. Enantiomerization studies of CBC at 120 ° C. HPLC-UV chromatograms of [CD(+)-280]-CBC after incubation at 120 ° C in oven at fixed time points.

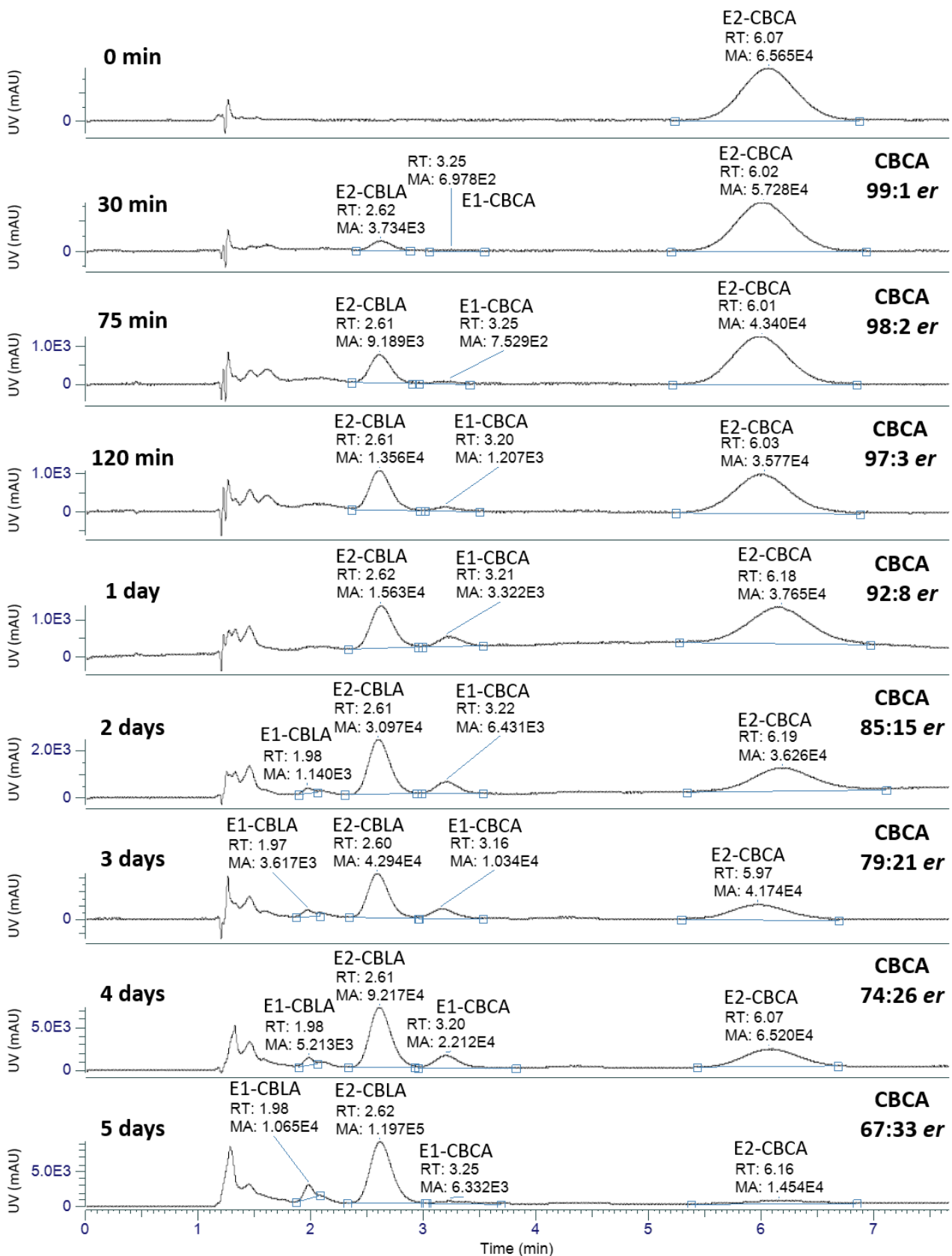


Fig. 6. Enantiomerization studies of CBCA under UV light. HPLC-UV chromatograms of [CD(+)]258]-CBCA after incubation under the UV light (254 nm) at fixed time points up to 2 h and under the direct sunlight for 5 days.

Table 7. Enantiomerization studies on isolated [CD(+)-258]-CBCA under UV light (254 nm) for 5 days.

Time (days)	Relative area (%)	UV (254 nm)					
		CBCA			CBLA		
		<i>er</i>		Relative area (%)	<i>er</i>		Relative area (%)
	[CD(-)-258]-CBCA	[CD(+)-258]-CBCA		[CD(-)-258]-CBLA	[CD(-)-258]-CBCA		
0	100	-	100	-	-	-	
1	72	8	92	28	100	-	
2	57	15	85	43	97	3	
3	52	21	79	48	95	5	
4	47	26	74	53	95	5	
5	14	33	67	86	92	8	

Credit author statement

Cinzia Citti, Giuseppe Cannazza: Conceptualization, Methodology, Formal analysis (method development), Writing – original draft preparation. Fabiana Russo, Elena Ferri, Diego Pinetti: Formal analysis (enantiomerization studies). Aldo Lagan`a, Anna Laura Capriotti, Alberto Cavazzini: Data curation, Methodology, Validation, Writing - Reviewing and Editing. Giuseppe Gigli, Giuseppe Cannazza: Funding acquisition, Resources.

Funding

This work was funded by UNIHEMP research project “Use of iNdustrIal Hemp biomass for Energy and new biocheMicals Production” (ARS01_00668) funded by Fondo Europeo di Sviluppo Regionale (FESR) (within the PON R&I 2017–2020 – Axis 2 – Action II – OS 1.b). Grant decree UNIHEMP prot. n. 2016 of July 27, 2018; CUP B76C18000520005.

References

- [1] F. Pollastro, D. Caprioglio, D. Del Prete, F. Rogati, A. Minassi, O. Tagliatela-Scafati, E. Munoz, G. Appendino, Cannabichromene, *Nat. Prod. Commun.* 13(9) (2018) 1934578X1801300922.
- [2] S. Morimoto, K. Komatsu, F. Taura, Y. Shoyama, Enzymological Evidence for Cannabichromenic Acid Biosynthesis, *J. Nat. Prod.* 60(8) (1997) 854-857.
- [3] E.P.M. de Meijer, K.M. Hammond, M. Micheler, The inheritance of chemical phenotype in *Cannabis sativa* L. (III): variation in cannabichromene proportion, *Euphytica* 165(2) (2009) 293-311.
- [4] G. Mazzocanti, O.H. Ismail, I. D’Acquarica, C. Villani, C. Manzo, M. Wilcox, A. Cavazzini, F. Gasparrini, Cannabis through the looking glass: chemo- and enantio-selective separation of phytocannabinoids by enantioselective ultra high performance supercritical fluid chromatography, *Chemical Communications* 53(91) (2017) 12262-12265.
- [5] Y. Gaoni, R. Mechoulam, Isolation and structure of Δ^9 -tetrahydrocannabinol and other neutral cannabinoids from hashish, *J. Am. Chem. Soc.* 93(1) (1971) 217-224.
- [6] M.A. Elsohly, D. Slade, Chemical constituents of marijuana: the complex mixture of natural cannabinoids, *Life Sci.* 78(5) (2005) 539-48.
- [7] A.R. Agua, P.J. Barr, C.K. Marlowe, M.C. Pirrung, Cannabichromene Racemization and Absolute Stereochemistry Based on a Cannabicyclol Analog, *The Journal of Organic Chemistry* 86(12) (2021) 8036-8040.
- [8] Y. Shoyama, T. Fujita, T. Yamauchi, I. Nishioka, Cannabichromenic acid, a genuine substance of cannabichromene, *Chem. Pharm. Bull. (Tokyo)* 16(6) (1968) 1157-8.
- [9] B. Romano, F. Borrelli, I. Fasolino, R. Capasso, F. Piscitelli, M. Cascio, R. Pertwee, D. Coppola, L. Vassallo, P. Orlando, V. Di Marzo, A. Izzo, The cannabinoid TRPA1 agonist cannabichromene inhibits nitric oxide production in macrophages and ameliorates murine colitis, *Br. J. Pharmacol.* 169(1) (2013) 213-229.
- [10] L.L. Anderson, A. Ametovski, J. Lin Luo, D. Everett-Morgan, I.S. McGregor, S.D. Banister, J.C. Arnold, Cannabichromene, related phytocannabinoids, and 5-fluoro-cannabichromene have anticonvulsant properties in a mouse model of Dravet Syndrome, *ACS Chem. Neurosci.* 12(2) (2021) 330-339.

- [11] O. Anis, A.C. Vinayaka, N. Shalev, D. Namdar, S. Nadarajan, S.M. Anil, O. Cohen, E. Belausov, J. Ramon, E. Mayzlish Gati, Cannabis-derived compounds cannabichromene and Δ^9 -tetrahydrocannabinol interact and exhibit cytotoxic activity against urothelial cell carcinoma correlated with inhibition of cell migration and cytoskeleton organization, *Molecules* 26(2) (2021) 465.
- [12] A.T. El-Alfy, K. Ivey, K. Robinson, S. Ahmed, M. Radwan, D. Slade, I. Khan, M. ElSohly, S. Ross, Antidepressant-like effect of Δ^9 -tetrahydrocannabinol and other cannabinoids isolated from *Cannabis sativa* L, *Pharmacology Biochemistry and Behavior* 95(4) (2010) 434-442.
- [13] M. Galletta, T.A. Reekie, G. Nagalingam, A.L. Bottomley, E.J. Harry, M. Kassiou, J.A. Triccas, Rapid Antibacterial Activity of Cannabichromenic Acid against Methicillin-Resistant *Staphylococcus aureus*, *Antibiotics* 9(8) (2020) 523.
- [14] F. Russo, F. Tolomeo, M. Angela Vandelli, G. Biagini, A. Laganà, A. Laura Capriotti, A. Cerrato, L. Carbone, E. Perrone, A. Cavazzini, V. Maiorano, G. Gigli, G. Cannazza, C. Citti, Enantioseparation of chiral phytocannabinoids in medicinal cannabis, *J. Chromatogr. B* 1221 (2023) 123682.
- [15] *Cannabis Flos*; New Text of the German Pharmacopoeia, Bonn, Germany, 2018.
- [16] A. Cerrato, C. Citti, G. Cannazza, A.L. Capriotti, C. Cavaliere, G. Grassi, F. Marini, C.M. Montone, R. Paris, S. Piovesana, A. Laganà, Phytocannabinomics: Untargeted metabolomics as a tool for cannabis chemovar differentiation, *Talanta* 230 (2021) 122313.
- [17] C. Citti, P. Linciano, F. Russo, L. Luongo, M. Iannotta, S. Maione, A. Laganà, A.L. Capriotti, F. Forni, M.A. Vandelli, G. Gigli, G. Cannazza, A novel phytocannabinoid isolated from *Cannabis sativa* L. with an in vivo cannabimimetic activity higher than Δ^9 -tetrahydrocannabinol: Δ^9 -Tetrahydrocannabiphorol, *Sci. Rep.* 9(1) (2019) 20335.
- [18] P. Linciano, C. Citti, L. Luongo, C. Belardo, S. Maione, M.A. Vandelli, F. Forni, G. Gigli, A. Laganà, C.M. Montone, G. Cannazza, Isolation of a high-affinity cannabinoid for the human CB1 receptor from a medicinal *Cannabis sativa* variety: Δ^9 -Tetrahydrocannabitol, the butyl homologue of Δ^9 -Tetrahydrocannabinol, *J. Nat. Prod.* 83(1) (2020) 88-98.
- [19] P. Linciano, C. Citti, F. Russo, F. Tolomeo, A. Laganà, A.L. Capriotti, L. Luongo, M. Iannotta, C. Belardo, S. Maione, F. Forni, M.A. Vandelli, G. Gigli, G. Cannazza, Identification of a new cannabidiol n-hexyl homolog in a medicinal cannabis variety with an antinociceptive activity in mice: cannabidihexol, *Sci. Rep.* 10(1) (2020) 22019.
- [20] U.M. Battisti, C. Citti, M. Larini, G. Ciccarella, N. Stasiak, L. Troisi, D. Braghiroli, C. Parenti, M. Zoli, G. Cannazza, "Heart-cut" bidimensional achiral-chiral liquid chromatography applied to the evaluation of stereoselective metabolism, in vivo biological activity and brain response to chiral drug candidates targeting the central nervous system, *J. Chromatogr. A* 1443 (2016) 152-161.
- [21] G. Cannazza, U. Battisti, M.M. Carrozzo, L. Brasili, D. Braghiroli, C. Parenti, Evaluation of stereo and chemical stability of chiral compounds, *Chirality* 23(10) (2011) 851-859.
- [22] W.J. Umstead, Polysaccharide Chiral Stationary Phases for the Achiral and Chiral Separation of Cannabinoids.
- [23] T. Onishi, W.J. Umstead, The Separation of Cannabinoids on Sub-2 μm Immobilized Polysaccharide Chiral Stationary Phases, *Pharmaceuticals (Basel)* 14(12) (2021).
- [24] C. De Luca, A. Buratti, W. Umstead, P. Franco, A. Cavazzini, S. Felletti, M. Catani, Investigation of retention behavior of natural cannabinoids on differently substituted polysaccharide-based chiral stationary phases under reversed-phase liquid chromatographic conditions, *J. Chromatogr. A* 1672 (2022) 463076.
- [25] A. Calcaterra, G. Cianfoni, C. Tortora, S. Manetto, G. Grassi, B. Botta, F. Gasparrini, G. Mazzocanti, G. Appendino, Natural Cannabichromene (CBC) Shows Distinct Scalemicity Grades and Enantiomeric Dominance in *Cannabis sativa* Strains, *J. Nat. Prod.* 86(4) (2023) 909-914.
- [26] H. Jeon, G. Kang, M.J. Kim, J.S. Shin, S. Han, H.-Y. Lee, On the Erosion of Enantiopurity of Rhodonoids via Their Asymmetric Total Synthesis, *Organic Letters* 24(11) (2022) 2181-2185.
- [27] M.A. Schafroth, G. Mazzocanti, I. Reynoso-Moreno, R. Erni, F. Pollastro, D. Caprioglio, B. Botta, G. Allegrone, G. Grassi, A. Chicca, F. Gasparrini, J. Gertsch, E.M. Carreira, G. Appendino, Δ^9 -cis-Tetrahydrocannabinol: Natural Occurrence, Chirality, and Pharmacology, *J. Nat. Prod.* 84(9) (2021) 2502-2510.

Supplementary material

Bidimensional heart-cut achiral-chiral liquid chromatography coupled to high-resolution mass spectrometry for the separation of the main chiral phytocannabinoids and enantiomerization studies of cannabichromene and cannabichromenic acid

Fabiana Russo^{a,b}, Elena Ferri^b, Maria Angela Vandelli^c, Giuseppe Biagini^b, Aldo Laganà^d, Anna Laura Capriotti^d, Alberto Cavazzini^e, Giuseppe Gigli^f, Giuseppe Cannazza^{c,f,*}, Cinzia Citti^{c,f,*}

^a Clinical and Experimental Medicine PhD Program, University of Modena and Reggio Emilia, 41125 – Modena, Italy

^b Department of Biomedical, Metabolic and Neural Sciences, University of Modena and Reggio Emilia, 41125 – Modena, Italy

^c Department of Life Sciences, University of Modena and Reggio Emilia, Via Campi 103, 41125 – Modena, Italy

^d Department of Chemistry, Sapienza University of Rome, Piazzale Aldo Moro 5, 00185 – Rome, Italy

^e Department of Chemical, Pharmaceutical and Agricultural Sciences, University of Ferrara, Via L. Borsari 46, 44121 – Ferrara, Italy

^f Institute of Nanotechnology – CNR NANOTEC, Campus Ecotekne, Via Monteroni, 73100 – Lecce, Italy

Table of Content

Table S1. Retention time interval for valve position change	... SI-2
Table S2. Mobile phases for chiral analysis	... SI-2
Table S3. HESI and Orbitrap parameters	... SI-2
Figure S1. Separation of phytocannabinoids enantiomers by heart-cut 2D-AC-HPLC-HRMS in standard mixtures	... SI-3
Figure S2. Optimization of the chromatographic conditions for the chiral analysis of CBCA, CBLA, CBC, and CBL	... SI-4
Figure S3. UV and MS/MS characterization of CBCA, CBLA, CBC, and CBL	... SI-5
Table S4. Enantiomerization studies on isolated [CD(+)] ₂₅₈ -CBCA at 60 °C	... SI-6

* Corresponding authors:

Giuseppe Cannazza, Ph.D., Email: giuseppe.cannazza@unimore.it; Tel.: +39 059 2055013.; Fax: +39 059 2055750.

Cinzia Citti, Ph.D., Email: cinzia.citti@unimore.it; Tel.: +39 0832 319206.

Table S 9. Retention time (R_T) interval for valve position change from “inject” to “load” for peak trapping in the 100- μ L sample loop.

Compound	Loop load R_T (min)
CBDA	17.85-18.05
CBD	18.41-18.55
Δ^9 -THC	20.39-20.48
CBC	21.02-21.21
THCA	21.20-21.40
CBCA	21.55-21.70

Table S 10. Chromatographic conditions for the chiral analysis of each phytocannabinoid. All mobile phases contained 0.1% FA.

Compound	Eluent (v/v)	Flow rate (mL/min)
CBDA	50% <i>i</i> PrOH	1
CBD	60% ACN	1.5
Δ^9 -THC	60% ACN	1.5
CBC	95% MeOH	1.5
THCA	75% <i>i</i> PrOH	1
CBCA	95% MeOH	1.5

Table S 11. Optimized parameters of HESI source and Orbitrap mass analyzer.

MS part	Parameter	FS	DDA	SIM	PRM
HESI	capillary temp.	320 °C	320 °C	320 °C	320 °C
	vaporizer temp.	280 °C	280 °C	280 °C	280 °C
	electrospray voltage	4.2 kV (HESI+)	4.2 kV (HESI+)	4.2 kV (HESI+)	4.2 kV (HESI+)
		3.8 kV (HESI-)	3.8 kV (HESI-)	3.8 kV (HESI-)	3.8 kV (HESI-)
	sheath gas	55 au	55 au	55 au	55 au
	auxiliary gas	30 au	30 au	30 au	30 au
	S lens RF level	45%	45%	45%	45%
Orbitrap	Resolution	35,000 FWHM	17,500 FWHM	35,000 FWHM	17,500 FWHM
	Scan range	m/z 75-750	m/z 75-750	m/z 75-750	m/z 75-750
	AGC target	5E05	2E5	5E05	2E5
	Max injection time	123 ms	100 ms	123 ms	100 ms
	Isolation window	1 m/z	1 m/z	1 m/z	1 m/z
	CE	-	20 eV	-	20 eV

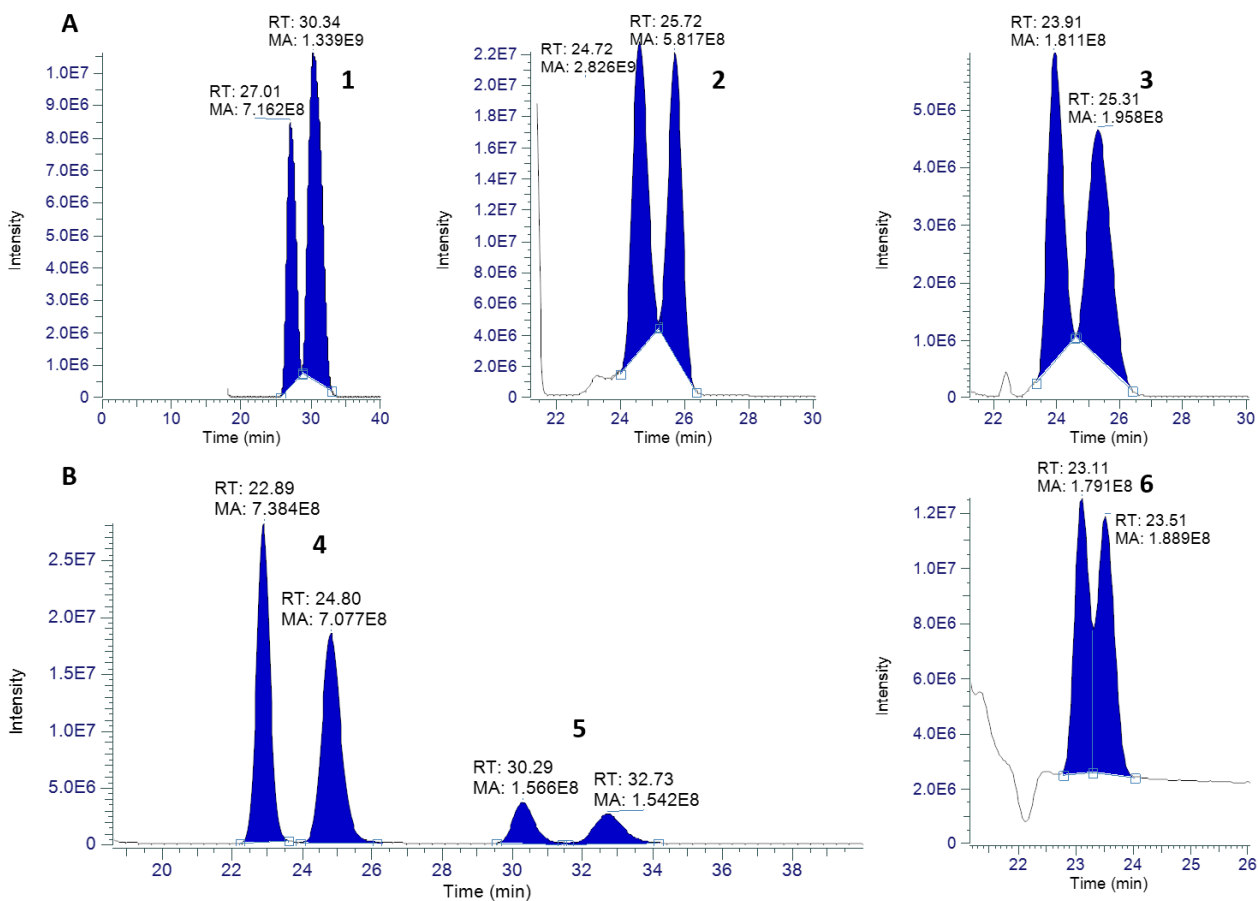


Figure S 16. Heart-cut bidimensional acihiral-chiral liquid chromatography coupled to high-resolution mass spectrometry (2D-AC-HPLC-HRMS) analysis of both carboxylated (**A**) (CBDA, **1**; THCA, **2**; CBCA, **3**) and decarboxylated (**B**) (CBD, **4**; Δ^9 -THC, **5**; CBC, **6**) phytocannabinoid enantiomers (as they appear in the second chiral dimension) in standard mixtures.

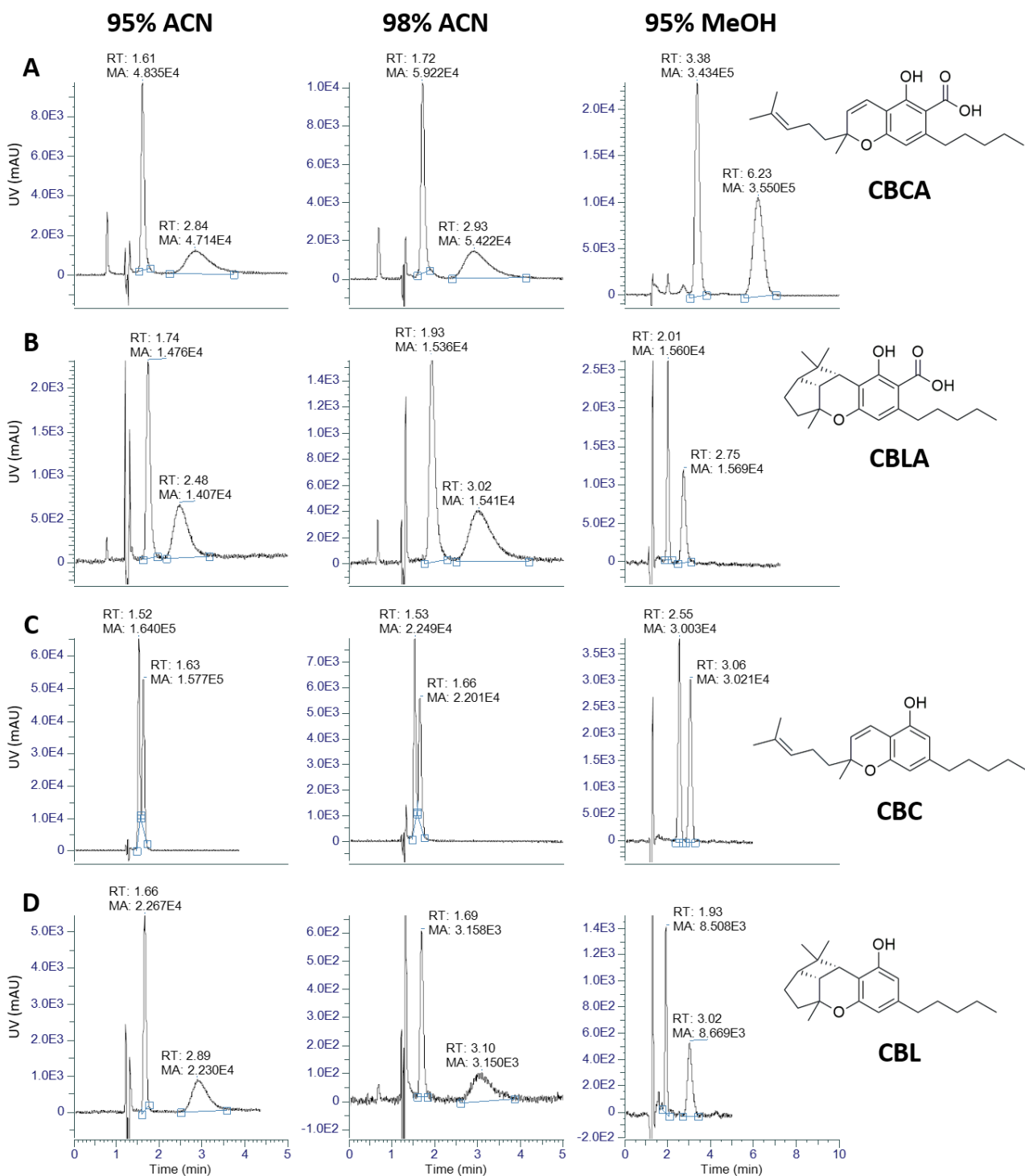


Figure S 17. Optimization of the chromatographic conditions for the chiral analysis of CBCA, CBLA, CBC, and CBL.

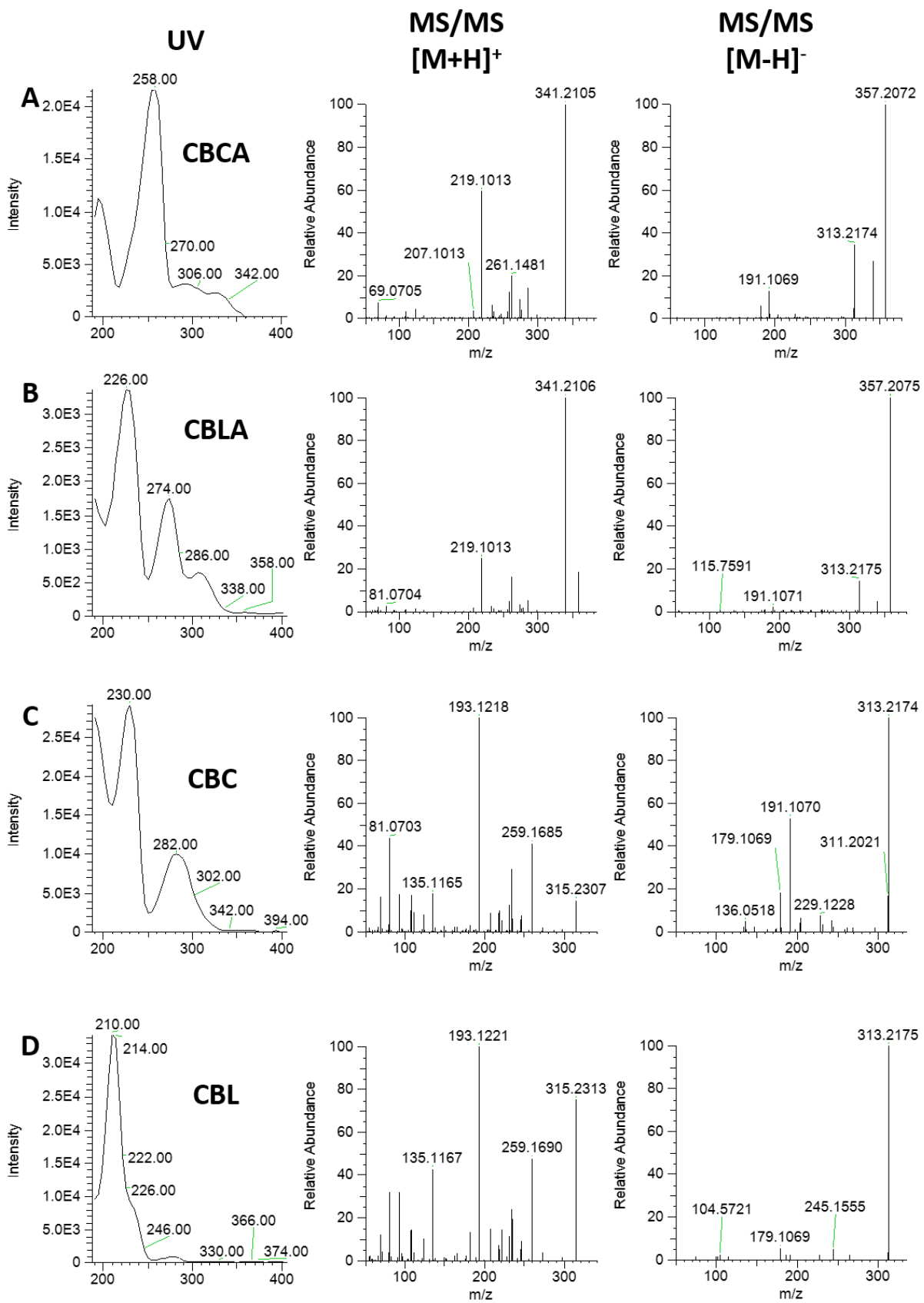


Figure S 18. UV and MS/MS characterization of CBCA, CBLA, CBC, and CBL.

Table S 12. Enantiomerization studies on isolated [CD(+)₂₅₈]-CBCA at 60 °C.

60 °C									
CBCA				CBLA			CBC		
Time (min)	Relative area (%)	<i>er</i>		Relative area (%)	<i>er</i>		Relative area (%)	<i>er</i>	
		[CD(-) ₂₅₈]-CBCA	[CD(+) ₂₅₈]-CBCA		[CD(-) ₂₅₈]-CBLA	[CD(+) ₂₅₈]-CBLA		[CD(+) ₂₈₀]-CBC	[CD(-) ₂₈₀]-CBC
0	100	0	100	0	0	100	0	-	-
30	98	0	100	2	0	100	0	-	-
60	98	0	100	2	0	100	0	-	-
90	97	0	100	3	0	100	0	-	-
150	96	0	100	4	0	100	0	-	-
240	95	0	100	5	0	100	0	-	-
1440	89	0	100	6	10	90	5	100	0

CHAPTER 3

IDENTIFICATION OF PHYTOCANNABINOID DERIVATIVES AS NEW PSYCHOACTIVE SUBSTANCES (NPS)

***SYNTHESIS AND PHARMACOLOGICAL ACTIVITY OF THE EPIMERS OF
HEXAHYDROCANNABINOL (HHC)***

Fabiana Russo^{1,2}, Maria Angela Vandelli³, Giuseppe Biagini², Martin Schmid⁴, Livio Luongo⁵, Michela Perrone⁵, Federica Ricciardi⁵, Sabatino Maione⁵, Aldo Laganà⁶, Anna Laura Capriotti⁶, Alfonso Gallo⁷, Luigi Carbone⁸, Elisabetta Perrone⁸, Giuseppe Gigli⁸, Giuseppe Cannazza^{3,8*} & Cinzia Citti^{3,8*}

1 Clinical and Experimental Medicine PhD Program, University of Modena and Reggio Emilia, 41125 Modena, Italy.

2 Department of Biomedical, Metabolic and Neural Sciences, University of Modena and Reggio Emilia, 41125 Modena, Italy.

3 Department of Life Sciences, University of Modena and Reggio Emilia, Via Campi 103, 41125 Modena, Italy.

4 Department of Pharmaceutical Chemistry, Institute of Pharmaceutical Sciences, University of Graz, Schubertstraße 1, 8010 Graz, Austria.

5 Division of Pharmacology, Department of Experimental Medicine, Università Della Campania “L. Vanvitelli”, Via Santa Maria di Costantinopoli 16, 80138 Naples, Italy.

6 Department of Chemistry, Sapienza University of Rome, Piazzale Aldo Moro 5, 00185 Rome, Italy.

7 Department of Chemistry, Istituto Zooprofilattico Sperimentale del Mezzogiorno, Via Salute 2, 80055 Portici, Italy.

8 Institute of Nanotechnology – CNR NANOTEC, Campus Ecotekne, Via Monteroni, 73100 Lecce, Italy.

Published in: *Scientific Report* 13, 11061 (2023).

<https://doi.org/10.1038/s41598-023-38188-5>

*email: giuseppe.cannazza@unimore.it; cinzia.citti@unimore.it

Abstract

Cannabis is a multifaceted plant with numerous therapeutic properties on one hand, and controversial psychotropic activities on the other hand, which are modulated by CB1 endocannabinoid receptors. Δ^9 -Tetrahydrocannabinol (Δ^9 -THC) has been identified as the main component responsible for the psychotropic effects, while its constitutional isomer cannabidiol (CBD) has shown completely different pharmacological properties. Due to its reported beneficial effects, Cannabis has gained global popularity and is openly sold in shops and online. To circumvent legal restrictions, semisynthetic derivatives of CBD are now frequently added to cannabis products, producing "high" effects similar to those induced by Δ^9 -THC. The first semi-synthetic cannabinoid to appear in the EU was obtained through cyclization and hydrogenation of CBD, and is known as hexahydrocannabinol (HHC). Currently, there is limited knowledge regarding HHC, its pharmacological properties, and its prevalence, as it is not commonly investigated in routine toxicological assays. In this study, synthetic strategies were explored to obtain an excess of the active epimer of HHC. Furthermore, the two epimers were purified and individually tested for their cannabinomimetic activity. Lastly, a simple and rapid chromatographic method employing a UV detector and a high-resolution mass spectrometer was applied to identify and quantify up to ten major phytocannabinoids, as well as the HHC epimers, in commercial cannabis samples.

Introduction

Cannabis is the most widely used illicit drug, with an estimated 4% of the population (15–64 years old) in 2019 reported to have used it, according to the World Drug Report 2021¹. Δ^9 -Tetrahydrocannabinol (Δ^9 -THC), which was identified by Raphael Mechoulam in the early 1960s, is the primary phytocannabinoid responsible for the psychotropic effects of cannabis. The constitutional isomer of Δ^9 -THC, cannabidiol (CBD), is the second most abundant phytocannabinoid found in cannabis and does not exhibit any narcotic activity. CBD is predominantly present in cannabis cultivated for industrial purposes, commonly referred to as hemp varieties. Other so-called "minor" phytocannabinoids have been isolated and characterized, and some of them have demonstrated euphoriant activity similar to Δ^9 -THC. Among the recently discovered THC-type phytocannabinoids, such as Δ^9 -tetrahydrocannabiphorol (Δ^9 -THCP)², Δ^9 -tetrahydrocannabihexol (Δ^9 -THCH)³, and Δ^9 -tetrahydrocannabibutolm (Δ^9 -THCB)⁴, the heptyl homologue has exhibited an unequivocal cannabinomimetic activity even higher than Δ^9 -THC in animal experiments². After the identification of Δ^9 -THC as the main psychotropic component of cannabis, chemical and pharmaceutical research

focused on modifying the lead compound to obtain more potent analogues⁵. Additionally, the discovery of the endocannabinoid receptors CB1 and CB2 has led to the identification of new scaffolds, enabling the development of increasingly potent synthetic cannabinoids (SCs). However, such compounds, which have limited therapeutic utility, are generally synthesized in illegal laboratories and sold for recreational use. Recently, over 250 synthetic compounds targeting the endocannabinoid system have been developed in clandestine laboratories⁶. These compounds are typically added to products often referred to as “Spice” or “K2” and distributed to end-users⁷. In contrast to THC, which has a relatively large safety margin when used recreationally and requires higher doses to cause serious adverse effects⁸, the use of SCs has been documented as completely unsafe, with a range of dangerous side effects⁹. Low-THC cannabis varieties (containing up to 0.3% THC) have recently been legalized in the USA¹⁰. These varieties can have high levels of CBD, which lacks cannabinomimetic properties and has been recognized as a potent antiepileptic drug¹¹. However, when CBD is treated with acids, it cyclizes to form Δ^9 -THC and Δ^8 -THC¹². Both THC isomers are subject to international restrictions and are scheduled under Schedule II of the United Nations Convention on Psychotropic Substances¹³. To address the marketing of controlled substances, the development of semi-synthetic derivatives of CBD has become a widely employed strategy in the USA. The first semi-synthetic cannabinoid (SSC) reported in the EU and monitored as a novel psychoactive substance (NPS) by the EU Early Warning System since October 21, 2022, is hexahydrocannabinol, better known as HHC¹⁴. HHC (hexahydrocannabinol) was first described in 1940 by Adams¹⁵, but it has only recently gained attention from toxicologists and analysts¹⁶. Despite its long history, few experimental studies have investigated its effects, particularly in humans. HHC is often sold as a “legal” alternative to illegal THC, and it is commonly sprayed onto or mixed with cannabis products marketed as “legal highs”¹⁴. HHC has three stereogenic centres, which theoretically give rise to eight stereoisomers. However, in practice, HHC is consistently found as two epimers: 9*R* and 9*S*, while the configuration at C10*a* and C6*a* remains unchanged. Early studies on HHC’s biological activity in animals, although compromised by the low purity of the material used, indicated that HHC exhibited lower marijuana-like activity compared to THC^{17,18}. Subsequent studies using better-characterized material revealed that the R epimer is the one responsible for cannabinomimetic activity, while the S epimer is either devoid of or has less psychotropic effect¹⁹. The psychotropic activity of HHC epimers was evaluated in a study by Mechoulam et al. in 1980, which involved administering the individual epimers of HHC to rhesus monkeys²⁰. The study found that the epimer with the equatorial methyl substituent ((*R*)-HHC) induced severe stupor, ataxia, immobility, and other effects indicative of high potency, even at low doses. The epimer with the axial methyl group ((*S*)-HHC) induced drowsiness and decreased motor activity at higher doses²⁰. However, the

authors noted that the compound used was not pure, and impurities of the other epimer could have influenced the results²⁰. The potency of a cannabis product containing HHC depends on the abundance of one epimer relative to the other. Recent studies have reported an excess of the 9*R* epimer in certain industrial hemp products¹⁶. Therefore, it is important to investigate the formation of one epimer over the other starting from CBD and analyze the epimeric ratio in HHC-containing cannabis products. The present study aims to evaluate the epimeric excess resulting from different synthetic strategies and determine the concentrations of both epimers in commercial HHC-containing cannabis products. To achieve these goals, high-performance liquid chromatography coupled with a diode array detector and high-resolution mass spectrometry (HPLC–DAD–HRMS) was employed. In addition to HHC epimers, ten other phytocannabinoids commonly found in cannabis extracts were analyzed, including CBD, Δ^9 -THC, Δ^8 -THC, CBG, CBC, their corresponding carboxylated native precursors (cannabidiolic acid (CBDA), tetrahydrocannabinolic acid (THCA), cannabigerolic acid (CBGA), and cannabichromenic acid (CBCA)), and the THC oxidation product cannabinol (CBN) (Fig. 1). Lastly, the tetrad test, a behavioral assay, was performed on mice after administering the individual HHC epimers, and the results were compared to those reported for Δ^9 -THC. This test helps evaluate the psychoactive effects of substances.

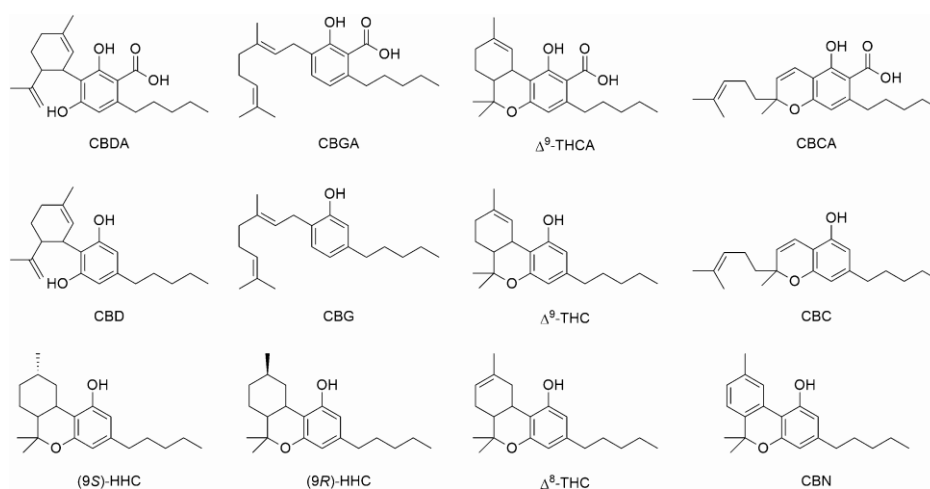


Figure 1. Chemical structure of the analyzed cannabinoids

Results

Synthesis of HHC epimers.

The synthesis of HHC epimers was carried out by subjecting CBD to acidic treatment. Depending on the reaction conditions, cyclization and hydrogenation of CBD can lead to the formation of either Δ^9 -THC or Δ^8 -THC as reaction intermediates. Gaoni and Mechoulam, in particular, obtained Δ^9 -THC by treating CBD with HCl as a catalyst for a short time (2 h), while Δ^8 -THC was obtained when CBD

was treated with *p*-toluenesulfonic acid (*p*TSA) for a longer duration (18 h)²¹. Subsequent reduction of the double bond on the terpene group resulted in a mixture of the two HHC epimers. Hydrogenation of Δ^9 -THC yielded an excess of the *S* epimer compared to the *R* epimer (approximately 2:1 ratio), whereas hydrogenation of Δ^8 -THC gave a 3:1 epimeric ratio in favour of the *R* epimer²¹. Based on this knowledge, CBD was treated with either HCl or *p*TSA for specific durations, followed by hydrogenation without purification of the intermediates. HHC was obtained as the product in both reactions, but with different epimeric ratios depending on the reaction conditions. Specifically, the reaction with HCl for 2 h resulted in a 57:43 *S/R* ratio, while the reaction with *p*TSA for 18 h yielded a 61:39 *R/S* ratio (Fig. 2). The individual HHC epimers, (9*S*)-HHC and (9*R*)-HHC, were isolated using semi-preparative HPLC, achieving purity grades exceeding 95% and 99%, respectively, which were sufficient for conducting the biological tests. UV, MS, and NMR analyses were performed to characterize both epimers. The UV spectra were found to be superimposable (Fig. 3a, b), while the MS2 dimension showed similar patterns, distinguished only by the relative abundance (RA) of a fragment at *m/z* 193.1223 in HESI⁺ mode. This fragment likely corresponds to the resorcinol group attached to one carbon atom of the reduced terpene moiety, with the oxygen atom no longer included in the pyran ring (Fig. 3c, d). In the mass fragmentation spectrum, the *S* epimer had an RA of 83% for this fragment, whereas the *R* epimer had an RA of 20%. In contrast, the HESI⁻ mode produced identical fragmentation patterns (Fig. 3e, f). Furthermore, the ¹H NMR analysis revealed distinctive differences, indicating that the first eluted epimer on reversed-phase HPLC corresponds to (9*S*)-HHC, while the second eluted epimer corresponds to (9*R*)-HHC (Fig. 3g). The stereochemistry at C9 was determined by comparing the NMR data obtained in this study with those reported in the literature by Archer et al.²² and Gaoni et al.²¹. Archer et al. provided a partial spectrum of a (*S*)-HHC/(*R*)-HHC mixture with a 3:1 ratio, demonstrating that the signals indicated as “major” corresponded to the *S* isomer, while those indicated as “minor” corresponded to the *R* isomer²². The findings of Gaoni et al. and Archer’s work support the characterization of the HHC epimers based on the NMR spectra. Gaoni et al. suggested that the isomer labeled as VIa, which exhibited a proton signal at C10 α (C3 in the old numbering system) appearing “as a broad doublet centered at 2.85 ppm”, corresponded to the isomer with the methyl group at C9 (C1 in the old numbering system) in the axial position ((*S*)-HHC). Conversely, the “broad doublet centered at 3.05 ppm” in structure VIb corresponded to the isomer with the methyl group at C9 in the equatorial position ((*R*)-HHC)²¹. In the current study, a peculiar shift in the NMR spectrum was observed for the hydrogen attached to C10 α , with a change from 2.85 ppm in (*S*)-HHC to 3.03 ppm in (*R*)-HHC. Additionally, the hydrogen atom of C10 α exhibited a shift from 2.67 ppm in the *S* epimer to 2.49–2.37 ppm in the *R* epimer. These observed shifts are consistent

with the data reported in the previously mentioned works^{21,22}, further confirming the assignment of the stereochemistry of the HHC epimers in this study.

HPLC-UV-HRMS analysis.

A previously reported and validated HPLC–UV-HRMS method²³ was adapted for the determination of ten phytocannabinoids and the HHC epimers. A C18 stationary phase with core–shell technology was utilized for the separation of all phytocannabinoids, and an isocratic elution program with 70% ACN for 20 min provided good baseline resolution of all peaks. Figure 4 displays the UV traces of all cannabinoid standards at a concentration of 10 µg/mL at 228 nm.

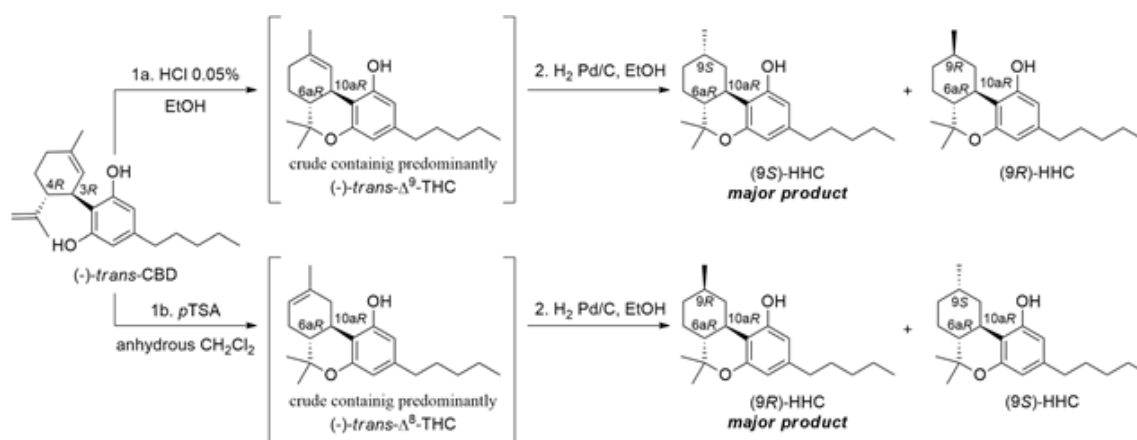


Figure 2. Synthesis of HHC. Step 1a-b: Cyclization of CBD. Step 2: Hydrogenation of the crude reaction mixture.

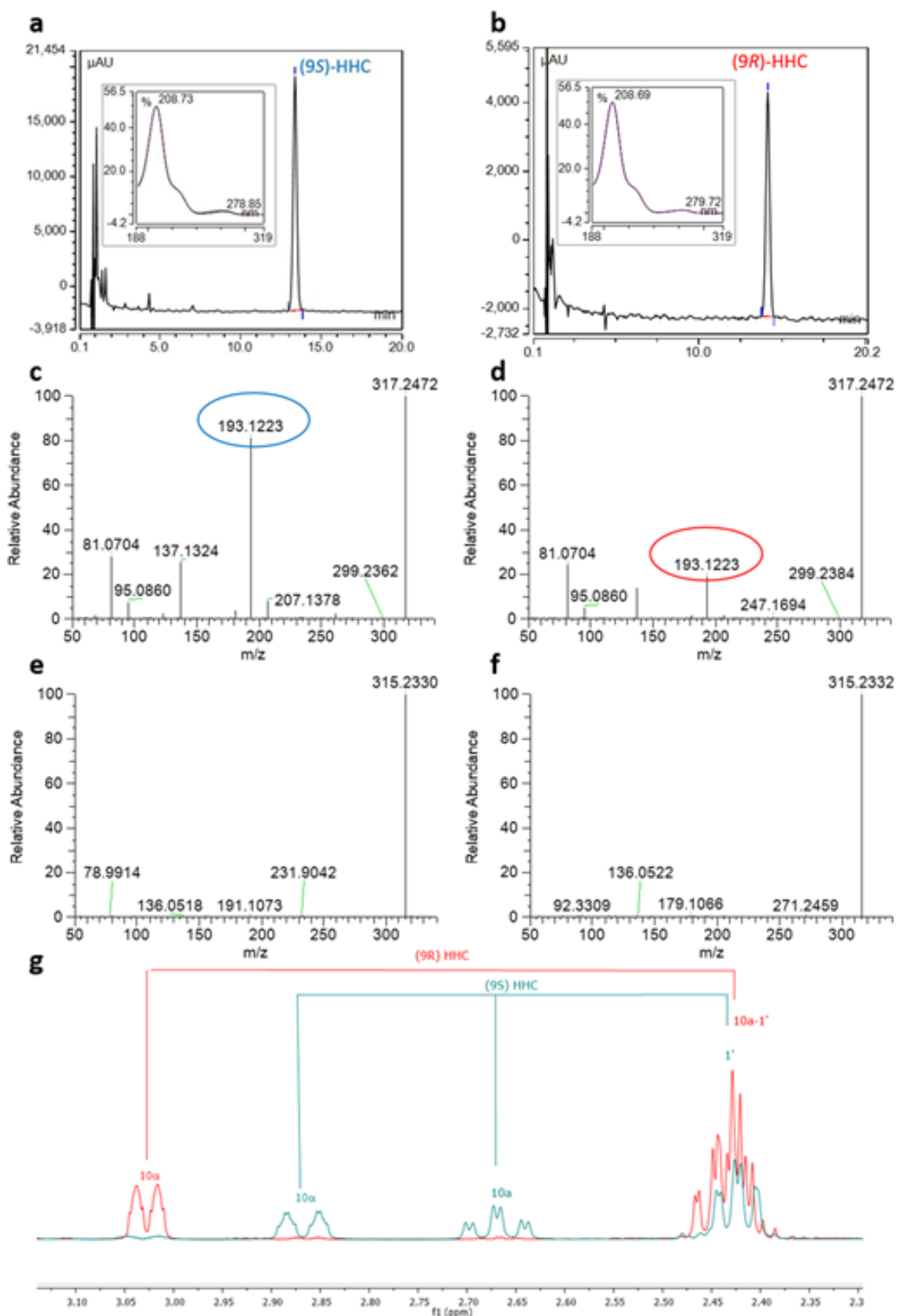


Figure 3. HPLC–UV–HRMS/MS and NMR characterization of the isolated (9S)-HHC and (9R)-HHC. HPLC–UV trace of (9S)-HHC (a) and (9R)-HHC (b) with the respective UV spectrum in the boxes; HRMS/MS pattern in HESI+ mode of (9S)-HHC (c) and (9R)-HHC (d) (the discriminant fragment is circled in blue and red for (9S)-HHC and (9R)-HHC respectively); HRMS/MS pattern in HESI- mode of (9S)-HHC (e) and (9R)-HHC (f); discriminant chemical shifts in the ^1H NMR spectra of (9S)-HHC (blue) and (9R)-HHC (red) (g).

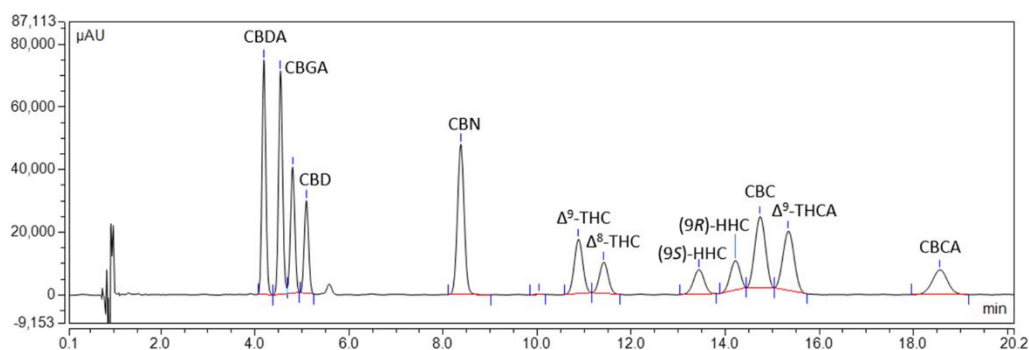


Figure 4. HPLC–UV chromatogram of a cannabinoid standard mixture. HPLC–UV chromatogram of a standard mixture containing ten phytocannabinoids (CBDA, CBGA, CBG, CBD, CBN, Δ^9 -THC, Δ^8 -THC, CBC, THCA, and CBCA) and the two HHC epimers at the concentration of 10 $\mu\text{g}/\text{mL}$.

The method was applied to analyze all phytocannabinoids and HHC epimers in ethanolic extracts of two hemp biomass samples (HHC-1 and HHC-2), one HHC hashish sample (HHC-3), and a pure HHC sample (HHC-4) (Figure S5, Supporting Information). Extraction of the analytes was performed using ethanol, as previous studies have demonstrated its superior ability to extract this class of compounds^{2–4,24–26}. The chromatograms of the extracts were examined for interfering compounds using HRMS, which confirmed the absence of other cannabinoids at the retention time of the analytes. All extracts were found to contain both epimers, with the *R* form being approximately twice as abundant as the *S* form. In the sample claimed to be pure HHC, the two epimers were present in a 58:42 mixture. In the three analyzed extracts, the amount of the *S* epimer ranged from 8.40 to 11.66% (on dry weight), while the *R* epimer was found in the range of 17.13% to 26.46%. All extracts exhibited a prominent presence of CBDA and CBD, along with lower amounts of CBGA, indicating that the inflorescence originated from industrial hemp varieties. Specifically, CBDA ranged from 2.8 to 7.18%, and CBD ranged from 1.20 to 2.60%. CBGA was also detected in low concentrations, ranging from 0.06 to 0.26%. Additionally, CBN was consistently present in all samples, with concentrations ranging from 0.05 to 0.21%. All samples showed the presence of both Δ^9 -THC and Δ^8 -THC, with the former being predominant. On the other hand, THCA and CBCA were present in trace amounts. The cannabinoid concentrations in the analyzed samples are reported in Table 1. Isomers of HHC could be tentatively identified in all extracts by HRMS, along with other oxidation derivatives of HHC. Since no standard was available for these compounds, only the molecular formula could be hypothesized (Figure S6). Interestingly, the sample of pure HHC exhibited a unique peak at 12.96 min with a precursor ion $[\text{M} + \text{H}]^+$ at m/z 319.2629 and $[\text{M}-\text{H}]^-$ at m/z 317.2488, displaying higher intensity in positive ionization mode (Figure S6). This compound, with a predicted molecular formula of $\text{C}_{21}\text{H}_{34}\text{O}_2$, presented a characteristic fragment at m/z 139.1480, which differed by two hydrogen atoms from that of HHC (137.1324) and by four hydrogen atoms from CBD- and

THC-like cannabinoids (135.1174). This fragment could likely be attributed to the terpene moiety. Based on the chromatographic data, which showed a longer retention time compared to CBD, and the HRMS fragmentation pattern, a CBD-like structure with all saturated C–C bonds on the terpene moiety could be proposed. As its retention time fell between THC and HHC species, the presence of an additional free hydroxyl group could explain its higher hydrophilicity compared to HHC, while the complete saturation of the terpene moiety could account for its higher lipophilicity compared to THC. This compound is likely to derive from the hydrogenation of residual CBD starting material in the reaction mixture, known as H4CBD. The spectroscopic data aligns with the findings reported by Collins et al., who synthesized and characterized both HHC and H4CBD.

	HHC-1	HHC-2	HHC-3	HHC-4
CBDA	7.54 ± 0.51	4.38 ± 0.26	2.91 ± 0.13	< LOD
CBGA	0.12 ± 0.03	0.29 ± 0.04	0.11 ± 0.07	< LOD
CBG	< LOQ	< LOQ	< LOQ	< LOD
CBD	1.25 ± 0.07	1.51 ± 0.12	2.83 ± 0.33	< LOD
CBN	< LOQ	< LOQ	0.22 ± 0.01	0.13
Δ ⁹ -THC	0.35 ± 0.02	0.26 ± 0.01	1.97 ± 0.12	0.29 ± 0.00
Δ ⁸ -THC	0.12 ± 0.04	< LOD	0.24 ± 0.01	0.16 ± 0.03
CBC	< LOD	< LOD	< LOD	< LOD
(9 <i>S</i>)-HHC	9.36 ± 0.43	8.78 ± 0.54	11.61 ± 0.08	4.15 ± 0.07
(9 <i>R</i>)-HHC	18.71 ± 0.97	17.73 ± 0.86	26.50 ± 0.07	5.60 ± 0.28
Δ ⁹ -THCA	0.15 ± 0.05	< LOQ	< LOD	< LOD
CBCA	< LOD	< LOD	< LOD	< LOD

Table 1. Concentration of phytocannabinoids and HHC epimers in the three extracts and in the commercial HHC mixture. Values are expressed in % (w/w) as mean ± SD (n = 3)

In vivo determination of the cannabinoid profile of (9*R*)-HHC and (9*S*)-HHC.

The cannabimimetic activity of (9*R*)-HHC and (9*S*)-HHC was evaluated using a tetrad of behavioral tests on mice. These tests assess spontaneous activity, catalepsy (immobility index), analgesia, and changes in rectal temperature (Fig. 5a), which are physiological manifestations of cannabinoid activity²². After intraperitoneal administration, (9*R*)-HHC at a dose of 10 mg/kg significantly reduced the spontaneous activity of mice in the open field test compared to the vehicle-treated group. The distance covered by mice in the open field was significantly decreased by (9*R*)-HHC (1476.750 ± 159.842 cm, *p* = 0.0183), whereas (9*S*)-HHC did not affect locomotion (3469.750 ± 833.532 cm, *p* = 0.7392) (Figs. 5b and 5f). In the catalepsy test, (9*R*)-HHC administration increased the latency of moving from the catalepsy bar, indicating a decrease in cataleptic behaviour. Although the difference

was not statistically significant compared to the vehicle-treated group, there was a trend towards reduced catalepsy (14.250 ± 7.642 s, $p = 0.3097$) for (9*R*)-HHC (Fig. 5c). In the hot plate test, (9*R*)-HHC demonstrated a significant antinociceptive effect, indicating analgesic properties. The latency to respond to the hot plate stimulus was significantly increased by (9*R*)-HHC (22.200 ± 3.040 s, $p = 0.0204$) compared to the vehicle-treated group (13.768 ± 2.367 s) (Fig. 5d). In contrast, (9*S*)-HHC did not induce catalepsy (0.500 ± 0.289 s, $p = 0.6259$) or analgesia (13.250 ± 3.146 s, $p = 0.9934$).

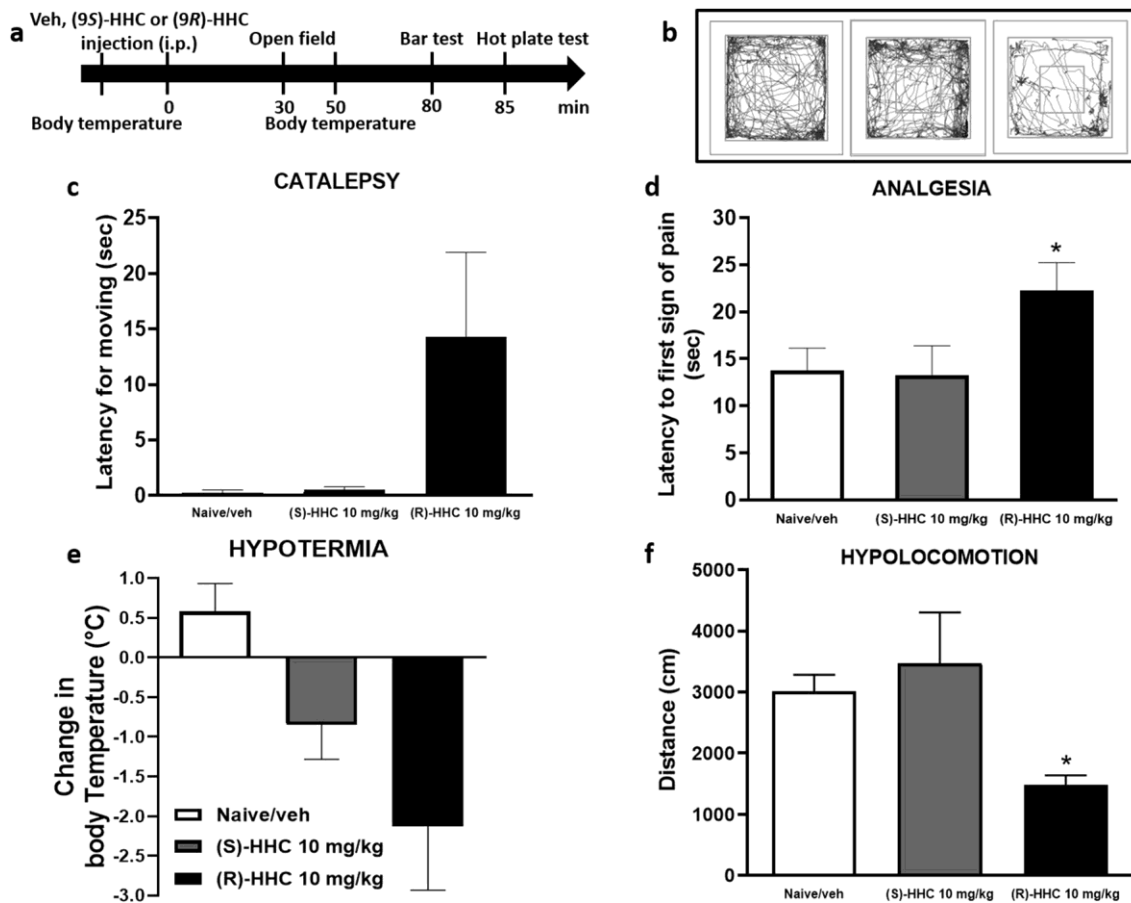


Figure 5. Dose-dependent effects of (9*R*)-HHC and (9*S*)-HHC administration (10 mg/kg, i.p.) on the tetrad behavioural tests in mice in comparison to vehicle. Time schedule of the tetrad tests in min from (9*R*)-HHC, (9*S*)-HHC or vehicle administration (a). Locomotion decrease induced by (9*R*)-HHC administration in the open field test (b, f). Decrease of body temperature after (9*R*)-HHC administration (e); the values are expressed as the difference between the basal temperature (i.e., taken before (9*R*)-HHC or vehicle administration) and the temperature measured after (9*R*)-HHC or vehicle administration. Increase in the latency for moving from the catalepsy bar after (9*R*)-HHC administration (c). Increase in the latency after the first sign of pain shown by the mouse in the hot plate test following (9*R*)-HHC administration (d). Data are represented as the mean \pm SEM of 4 mice per group. * indicates significant differences compared to vehicle injection, * $p < 0.05$ Tukey's test

Lastly, both (9*R*)-HHC and (9*S*)-HHC showed a trend towards decreasing body temperature, indicating hypothermic effects. However, the difference was not statistically significant compared to the vehicle-treated mice. (9*R*)-HHC exhibited a greater trend towards decreasing body temperature (-2.125 ± 0.808 °C, $p = 0.1553$) compared to (9*S*)-HHC (-0.850 ± 0.435 °C, $p = 0.1137$), but further analysis is needed to establish statistical significance (Fig. 5e). These results suggest that (9*R*)-HHC

possesses cannabimimetic activity, as evidenced by decreased locomotor activity, decreased catalepsy, increased analgesia, and a trend towards hypothermia. In contrast, (9*S*)-HHC did not significantly affect these behavioural parameters.

Discussion

Since the discovery of Δ^9 -THC as the main psychoactive compound in cannabis, efforts have been made by medicinal chemists to modify its chemical structure in order to improve its pharmacological properties. However, very few, if any, of these derivatives have successfully reached the market as approved drugs. On the other hand, over the past fifteen years, a large number of synthetic cannabinoids (SCs) or “spice” have emerged as illegal drugs. These SCs are structurally distinct from Δ^9 -THC and have been marketed as alternatives to cannabis. In recent years, there has been a resurgence in the cultivation of cannabis for industrial purposes, particularly due to the high concentrations of CBD, which is non-psychoactive and possesses various therapeutic properties. CBD is used in medicinal products for the treatment of certain types of childhood epilepsy¹¹. The World Health Organization (WHO) has suggested that CBD should not be classified as a scheduled substance, as it lacks the intoxicating properties associated with THC or other SCs²⁷. In some European countries, the recreational use of industrial hemp inflorescence as a substitute for high-THC cannabis has become a widespread phenomenon known as “light cannabis”. However, the legal status of such products remains unclear in European legislation. In parallel, the USA have allowed the legal marketing of all cannabis products with THC levels below 0.3% with the Farm Bill Act in 2018. Alongside the emergence of SCs, there has been the appearance of semi-synthetic cannabinoids (SSCs) in the United States. These compounds are derived from chemical modifications of cannabinoids extracted from cannabis. One such compound, HHC, is the hydrogenation product of Δ^9 -THC and Δ^8 -THC. By removing the double bond at either the C9 or C8 position, a new stereogenic center is generated, resulting in either the *R* or *S* epimer. Mechoulam had suggested that it is possible to obtain an excess of the *R* epimer from Δ^8 -THC and an excess of the *S* epimer from Δ^9 -THC²¹. In vitro studies have indicated that the *R* epimer has a higher affinity for the CB1 receptor, while the *S* epimer has poor affinity¹⁹. This suggests that different epimeric mixtures with varying intensities of biological effects can be obtained based on the synthetic procedure. CBD has been shown to isomerize to either Δ^9 -THC or Δ^8 -THC under acidic conditions, depending on factors such as reaction time, catalyst type, and reaction conditions^{2,12,21}. As a result, the production of Δ^8 -THC and Δ^9 -THC as semi-synthetic products from CBD extracted from hemp has increased¹⁴. However, both Δ^8 -THC and Δ^9 -THC are controlled substances and not legally marketed. Therefore, the subsequent reduction of the double bond to form semi-synthetic HHC has allowed for a legal alternative that offers similar

psychoactive effects to THC. HHC is currently being sprayed onto hemp products and openly sold to provide the desired “high” effects of cannabis. The scientific studies on HHC are limited, highlighting the need for further investigation. The researchers’ work demonstrates that HHC can be obtained from CBD, and the reaction conditions can selectively favour the production of one epimer over the other. Using a validated analytical method, the presence of HHC was identified in two commercial samples of hemp biomass (HHC-1 and HHC-2) and one hemp hashish sample (HHC-3). The concentrations of the *R* epimer were consistently higher than those of the *S* epimer in all samples. The hemp biomass samples also contained significant concentrations of other phytocannabinoids, particularly CBDA and CBD, indicating that they were derived from industrial hemp. The levels of Δ^9 -THC and Δ^8 -THC in the biomass extracts and pure HHC mixture were below 0.5%, while the HHC hashish sample contained around 2% of these phytocannabinoids. The presence of Δ^9 -THC and Δ^8 -THC could be attributed to residues from the HHC synthesis process, although a natural origin cannot be ruled out. The relatively high levels of HHC compared to CBD and THC in the samples suggest its exogenous origin rather than being naturally occurring²⁸. Furthermore, since the *R* epimer was consistently found in excess of the *S* epimer, it is likely that HHC was synthesized starting from CBD with Δ^8 -THC as the reaction intermediate, rather than using Δ^9 -THC. Analysis of the pure HHC sample (HHC-4) revealed the absence of CBDA and CBD, but the presence of CBN, Δ^8 -THC, and Δ^9 -THC as impurities alongside the main component HHC. The *R* epimer was slightly in excess, indicating a similar synthetic route.

Methods

Chemicals and reagents.

Ethanol 96%, acetonitrile (ACN), and formic acid (FA) were all LC–MS grade and were bought from Sigma Aldrich (USA). Ultrapure water was obtained with a water purification system (Direct-Q 3UV, Merck Millipore, Milan, Italy). Chemicals and solvents employed in the synthetic process were reagent grade and used without further purification. The following abbreviations for common organic solvents were adopted: diethyl ether (Et₂O); dichloromethane (CH₂Cl₂); cyclohexane (CE); chloroform (CDCl₃); ethanol (EtOH). Stock solutions (1 mg/mL) of certified reference cannabinoid standards of CBDA, Δ^9 -THCA, CBGA, CBCA, CBD, CBG, CBC, CBN, as well as of Δ^9 -THC and Δ^8 -THC (500 μ g/mL) were bought from Cayman Chemical (Ann Arbor, Michigan, USA). Stock solutions (1 mg/mL) of CBDH, Δ^9 -THCH, (9*R*)-HHC and (9*S*)-HHC were obtained by properly diluting the pure compounds in-house synthesized.

Plant material.

Samples of hemp biomass (HHC-1 and HHC-2), HHC hashish (HHC-3) and pure HHC were purchased from Baked Bologna (Bologna, Italy). The use of *Cannabis sativa* L. plants with THC levels below 0.5% in the present study complies with the Italian guidelines according to the Law 242/2016 and to the common agricultural policy (art. 38–44) of the European Union Treaty (GUCE 26/10/2012).

Synthetic procedure a for HHC.

CBD (0.7 mmol) was dissolved in 20 mL of absolute EtOH containing 0.05% HCl and refluxed for 2 h. The resulting crude was neutralized with a saturated solution of Na₂CO₃ and subject to hydrogenation with an H-Cube ThalesNano flow reactor (Budapest, Hungary) according to the following experimental conditions: 3 mm 10% Pd/C cartridge, 30 °C, 20 bar, 1 mL/min. The crude product mixture showed a 57:43 *S/R* HHC mixture along with other by-products. The solvent was evaporated and the crude of the reaction was purified with semipreparative HPLC–UV (Column Luna 5 µm C18, 100 Å, 250 × 10 mm- Phenomenex, Bologna, Italy). An isocratic elution was employed with mobile phase 80% ACN (with 0.1% FA) and 20% MilliQ water (with 0.1% FA) at a flow rate of 7.5 mL/min. The UV trace was followed at 228 nm and the compounds of interest were obtained with a purity higher than 95% (12 mg for (9*R*)-HHC and 8 mg for (9*S*)-HHC).

Synthetic procedure b for HHC.

To a solution of CBD (0.7 mmol) in 15 mL of anhydrous CH₂Cl₂, *p*TSA (10 mg, 10% mol) was added at room temperature, under a nitrogen atmosphere. The reaction was stirred in the same conditions for 48 h. After that, the mixture was diluted with Et₂O and washed with a saturated solution of NaHCO₃. The organic layer was collected, washed with brine, dried over anhydrous Na₂SO₄ and concentrated. The obtained crude was subject to hydrogenation as described for the synthetic procedure *b* to give a crude product with a 61:39 *R/S* HHC mixture. The two epimers were purified with semi-preparative HPLC as reported above (11 mg for (9*S*)-HHC and 8 mg for (9*R*)-HHC).

NMR characterization of HHC.

NMR spectra were recorded either on a Bruker 400 (working at 400.134 MHz for ¹H and 100.62 MHz for ¹³C) or a Bruker 600 spectrometer (working at 600.130 MHz for ¹H and 150.902 MHz for ¹³C). Monodimensional spectra were acquired with a spectral width of 8278 Hz (for ¹H NMR) and 23.9 kHz (for ¹³C NMR), a relaxation delay of 1 s and a number of transients of 32 and 1024 for ¹H NMR and ¹³C NMR, respectively. NMR spectra were acquired in CDCl₃ and chemical shifts (δ) were

registered in ppm with respect to that of the residual solvent ($\delta = 7.26$ ppm for 1H and $\delta = 77.20$ ppm for 13C); coupling constants are reported in Hz, splitting patterns are expressed as singlet (s), doublet (d), triplet (t), quartet (q), double doublet (dd), quintet (qnt), multiplet (m), broad signal (b).

(9S)-6,6,9-trimethyl-3-pentyl-6a,7,8,9,10,10a-hexahydro-6H-benzo[c]chromen-1-ol
((9S)-HHC).

¹H NMR (400 MHz, CDCl₃) δ 6.25 (s, 1H, C4), 6.07 (s, 1H, C2), 4.61 (s, 1H, OH), 2.92–2.79 (m, 1H, C10 α), 2.67 (td, $J = 11.4, 2.9$ Hz, 1H, C10 α), 2.46–2.38 (m, 2H, C1'), 2.11 (m, 1H, C9), 1.68–1.61 (m, 2H, C8-C7), 1.58–1.52 (m, 2H, C2'), 1.46–1.44 (m, 1H, C6a) 1.36 (s, 3H, C12), 1.33–1.28 (s, 6H, C4'-C3'-C10 β), 1.13 (d, $J = 7.2$ Hz, 3H, C11), 1.09 (s, 3H, C13), 0.88 (t, $J = 7.0$ Hz, 3H, C5'). ¹³C NMR (101 MHz, CDCl₃) δ 155.38, 154.77, 142.65, 110.63, 110.19, 107.79, 77.03, 50.09, 36.33, 35.59, 32.40, 31.77, 30.76, 29.49, 28.06, 27.76, 27.10, 23.26, 22.73, 19.30, 18.98, 14.20.

(9R)-6,6,9-trimethyl-3-pentyl-6a,7,8,9,10,10a-hexahydro-6H-benzo[c]chromen-1-ol
((9R)-HHC).

¹H NMR (600 MHz, CDCl₃) δ 6.25 (s, 1H, C4), 6.08 (s, 1H, C2), 4.64 (s, 1H, OH), 3.03 (d, $J = 12.9$ Hz, 1H, C10 α), 2.49–2.37 (m, 3H, C1'-C10 α), 1.87–1.80 (m, 2H, C8-1H, C7-1H), 1.67–1.60 (m, 1H, C9), 1.59–1.52 (m, 2H, C2'), 1.46–1.44 (m, 1H, C6a), 1.36 (s, 3H, C12), 1.34–1.24 (m, 4H, C4'-C3'), 1.16–1.07 (m, 2H, C8-1H, C7-1H), 1.06 (s, 3H, C13) 0.94 (d, $J = 6.6$ Hz, 3H, C11), 0.88 (t, $J = 7.0$ Hz, 3H, C5'), 0.78 (m, 1H, C10 β). ¹³C NMR (151 MHz, CDCl₃) δ 155.15, 154.83, 142.74, 110.44, 110.23, 107.77, 77.14, 49.30, 39.16, 35.71, 35.58, 33.03, 31.75, 30.76, 28.24, 27.94, 22.78, 22.73, 19.22, 14.21.

HPLC-UV-HRMS analysis.

A Vanquish Core system (Thermo Fisher Scientific, Waltham, Massachusetts, USA) with binary pump, vacuum degasser, thermostated autosampler and column compartment, and diode array detector (DAD) was interfaced to an Exploris 120 Orbitrap mass analyzer with a heated electrospray ionization source (HESI). The chromatographic separation was achieved on a Poroshell 120 EC C18 (100 . 3.0 mm, 2.7 μ m) (Agilent, Milan, Italy) with an isocratic elution at 70% ACN for 20 min and a washing step at 98% ACN for 3 min. The column was re-equilibrated at 70% ACN for further 3 min for a total run time of 26 min at a constant flow rate of 0.5 mL/min. To assess the cannabimimetic activity of HHC, the tetrad test in mice was conducted. Due to the limited availability of the two epimers, only one dose (10 mg/kg) was tested, similar to the dose used for THC in the tetrad test. The results showed that (9R)-HHC significantly affected two out of the four behaviours in the tetrad test: hypolocomotion (reduced spontaneous activity) and analgesia (pain relief). These findings suggest a partial CB1-mediated psychotropic effect. However, the potency of HHC in inducing the tetrad effects was lower than that of Δ^9 -THC and Δ^9 -THCP, a recently discovered THC analog. In summary, a likely origin for the first SSC that appeared in the European market has been proposed in this work, and the biological tests confirmed that the cannabimimetic activity of HHC resides in the *R* epimer, while the

S epimer has minimal activity, consistent with the in vitro binding studies on the CB1 receptor. Further evaluation is needed to determine whether HHC should be classified as a scheduled narcotic substance. The HESI parameters were optimized in previous works for cannabinoids: spray voltage 4200 kV and 3800 kV for HESI⁺ and HESI⁻ mode respectively, sheath gas 70 au, auxiliary gas 5 au, sweep gas 0.5 au, ion transfer tube temperature 390 °C and vaporizer temperature 150°C^{26,29}. The mass analyzer was operated in both full scan (FS) and data-dependent acquisition (DDA) mode. In FS mode the resolution was set at 60,000 FWHM (full width at half maximum), the RF lens level at 70%, the maximum injection time 54 ms, the *m/z* range at 150–750, and the isolation window at *m/z* 1.2. In DDA mode the resolution was set at 30,000 FWHM, the maximum injection time at 22 ms, the *m/z* range at 50–750, the isolation window at *m/z* 1.2, and the stepped normalized collision energy (NCE) at 20–40-100^{26,29}. The injection volume was 5 µL. The analyses were acquired with Xcalibur 3.0 and processed using Chromeleon 7 for the UV traces and TraceFinder 54.0 for the MS traces (all from Thermo Fisher Scientific).

Calibration standards and sample preparation and cannabinoids quantification.

Calibration solutions of all phytocannabinoid standards were prepared by diluting the stock solutions with ACN to get the final concentrations indicated in Table S1. Each dilution was run in triplicate and the calibration curves were built using both UV and MS data. Area of the peaks for each analyte was plotted against nominal concentration and the back-calculated concentration was checked to be within 15% of the nominal value. Samples of hemp inflorescence and HHC hashish were extracted using the method reported in the German Pharmacopoeia for the extraction of phytocannabinoids from cannabis inflorescence²⁴. The extracts HHC-1 and HHC-2 from hemp inflorescence were analysed after 100 . dilution with mobile phase, while the extract HHC-3 from HHC hashish was 1000 . diluted. The sample of pure HHC (HHC-4) was injected at the concentration of 10 µg/mL obtained by dissolving 10 mg of the sample in 1 mL of ACN and preparing serial 10 . dilutions with mobile phase up to the desired concentration. Quantification of cannabinoids was accomplished with both UV and MS data. The UV chromatograms were extracted at 228 nm. The exact *m/z* of the precursor ion in both HESI⁺ and HESI⁻ mode was extracted with a 5-ppm error from the HRMS TIC and used for calibration.

Tetrad test.

In the experiment, male C57BL6/J mice at 7 weeks old were used (*n* = 4). They were divided into two groups: one group received (9*R*)-HHC at a dose of 10 mg/kg dissolved in a vehicle (1:1:18; EtOH:Kolliphor EL:0.9% saline) via intraperitoneal (i.p.) administration, and the other group received only the vehicle as a control. The same animals were used for all four behavioural tests. The

effects of (9R)-HHC on hypomotility (measured using the open field test), hypothermia (measured by monitoring body temperature), antinociception (evaluated using the hot plate test), and catalepsy (assessed through the bar test) were assessed. These tests were performed following the procedures described by Metna- Laurent et al.³⁰. Statistical analysis of the data was conducted using the one-way analysis of variance (ANOVA) followed by Tukey's multiple comparisons test.

Body temperature. The measurement of body temperature was performed after immobilizing the mouse. A probe was gently inserted 1 cm into the rectum, and the temperature was recorded once it stabilized. The probe was cleaned with 70% ethanol and dried with a paper towel between each mouse to prevent cross-contamination.

Open field. The open field test was conducted 30 min after administering the drug (or vehicle). The apparatus used for the test was cleaned with a 70% ethanol solution before each behavioural session. Naive mice were randomly assigned to different treatment groups. The mice were placed in an open field arena (dimensions: length . width . height: 44 . 44 . 30 cm), and their ambulatory activity (total distance travelled in cm) was recorded and analyzed for a duration of 15 min. An automated behavioural tracking system called Any-maze, specifically the Video-tracking software by Ugo Basile, was used to record and analyze the behaviours.

Bar test. The bar test was conducted to assess catalepsy. A glass rod measuring 40 cm in length and 0.4 cm in diameter was horizontally elevated 5 cm above the surface. The mouse's forelimbs were positioned on the bar while the hind legs remained on the floor of the cage, ensuring that the mouse was not lying down on the floor. The chronometer was started when the mouse held onto the bar with both forelimbs, and it was stopped when the mouse descended from the bar (i.e., when the two forepaws touched the floor) or after 5 min (cut-off time). Catalepsy was measured as the duration in seconds that the mouse held the elevated bar.

Hot plate. Each mouse was placed on a hot plate (Ugo Basile), which was kept at the constant temperature of 52 °C. Licking of the hind paws or jumping were considered as a nociceptive response (NR) and the latency was measured in s 85 min after drug or vehicle administration, taking a cut-off time of 30 s to prevent tissue damage. The hot plate test was performed to evaluate antinociceptive effects. Each mouse was placed on a hot plate set at a constant temperature of 52 °C. The licking of hind paws or jumping were considered nociceptive responses (NR), and the latency to respond was measured in seconds. The measurement was taken 85 min after drug or vehicle administration, with a cut-off time of 30 s to prevent tissue damage.

Animals

In the described experiments, male C57BL/6 mice from Charles River (Italy) were used. The mice weighed between 18 and 20 g. The mice were acclimated to the laboratory conditions for at least 1 week before the start of the experiments. The laboratory maintained a 12-h light/dark cycle with the lights turning on at 6:00 A.M. The temperature in the facility was maintained at 20–22 °C, and the humidity was kept at 55–60%. The mice were housed in cages with three mice per cage. They had access to standard chow and tap water *ad libitum*, meaning they could eat and drink freely. The experimental procedures conducted in this study received ethical approval from the Animal Ethics Committee of the University of Campania “L. Vanvitelli” in Naples, Italy. The specific protocol number for the experiments was 24/2023-PR. All the experiments were conducted in accordance with the regulations outlined by the Italian law (D.L. 116/92) and the European Commission (O.J. of E.C. L358/1, 18/12/86) regarding the protection of animals used for research purposes. The experimental methods described in the study also followed the ARRIVE guidelines, which provide recommendations for reporting animal research³¹. Animal care and welfare were the responsibility of trained personnel who adhered to the relevant Italian and European regulations. Every effort was made to minimize the number of animals used in the experiments and to prevent any unnecessary suffering or harm to the animals during the course of the study. (Fig. S1).

Acknowledgements

The authors acknowledge Giovanna Negro and Giulio Guarini for their help in the extraction and sample analysis.

Author contributions

G.C. and C.C. developed and supervised the project, conceived the experiments plan and drafted the manuscript; M.S. carried out the synthesis and purification of HHC epimers; F.Russo carried out the spectroscopic characterization of HHC epimers and optimized the HPLC–UV–HRMS method; L.L., M.P., F.Ricciardi and S.M. performed the *in vivo* tetrad tests; A.G., A.L. and A.L.C. performed the HPLC–UV–HRMS analyses, M.A.V. and G.B. performed the statistical analysis; L.C. and E.P. performed the extraction of the samples; G.G. provided the instrumental and material resources. All authors reviewed the manuscript.

References

1. UNODC. World Drug Report 2021. (United Nations Office on Drugs and Crime, 2021).

2. Citti, C. *et al.* A novel phytocannabinoid isolated from *Cannabis sativa* L. with an in vivo cannabimimetic activity higher than Δ^9 -tetrahydrocannabinol: Δ^9 -Tetrahydrocannabiphorol. *Sci. Rep.* **9**, 20335. <https://doi.org/10.1038/s41598-019-56785-1> (2019).
3. Linciano, P. *et al.* Identification of a new cannabidiol n-hexyl homolog in a medicinal cannabis variety with an antinociceptive activity in mice: cannabidihexol. *Sci. Rep.* **10**, 22019. <https://doi.org/10.1038/s41598-020-79042-2> (2020).
4. Linciano, P. *et al.* Isolation of a high-affinity cannabinoid for the human CB1 receptor from a medicinal *Cannabis sativa* variety: Δ^9 -tetrahydrocannabutol, the butyl homologue of Δ^9 -tetrahydrocannabinol. *J. Nat. Prod.* **83**, 88–98. <https://doi.org/10.1021/acs.jnatprod.9b00876> (2020).
5. Bow, E. W. & Rimoldi, J. M. The structure-function relationships of classical cannabinoids: CB1/CB2 modulation. *Perspect. Med. Chem.* **8**, PMC.S32171. <https://doi.org/10.4137/pmc.s32171> (2016).
6. UNODC. Early warning advisory (EWA) on new psychoactive substances (NPS). (United Nations Office on Drugs and Crime 2017).
7. Musselman, M. E. & Hampton, J. P. “Not for human consumption”: A review of emerging designer drugs. *Pharmacotherapy* **34**, 745–757. <https://doi.org/10.1002/phar.1424> (2014).
8. Jiang, H.-E. *et al.* A new insight into *Cannabis sativa* (Cannabaceae) utilization from 2500-year-old Yanghai Tombs, Xinjiang, China. *J. Ethnopharmacol.* **108**, 414–422. <https://doi.org/10.1016/j.jep.2006.05.034> (2006).
9. Schifano, F., Orsolini, L., Papanti, D. & Corkery, J. NPS: Medical consequences associated with their intake. *Curr. Top. Behav. Neurosci.* **32**, 351–380. https://doi.org/10.1007/7854_2016_15 (2017).
10. Leas, E. C. The hemp loophole: A need to clarify the legality of delta-8-THC and other hemp-derived tetrahydrocannabinol compounds. *Am. J. Public Health* **111**, 1927–1931. <https://doi.org/10.2105/ajph.2021.306499> (2021).
11. EPIDIOLEX, <https://www.accessdata.fda.gov/drugsatfda_docs/label/2018/210365lbl.pdf> (
12. Citti, C. *et al.* Origin of Δ^9 -tetrahydrocannabinol impurity in synthetic cannabidiol. *Cannabis Cannabinoid Res.* **6**, 28–39. <https://doi.org/10.1089/can.2020.0021> (2020).
13. (Austria, 1971).
14. EMCDDA. (European Monitoring Centre for Drugs and Drug Addiction, Lisbon, 2022).
15. Adams, R., Hunt, M. & Clark, J. H. Structure of cannabidiol, a product isolated from the marijuana extract of Minnesota wild hemp I.. *J. Am. Chem. Soc.* **62**, 196–200. <https://doi.org/10.1021/ja01858a058> (1940).
16. Casati, S. *et al.* Hexahydrocannabinol on the light cannabis market: The latest “new” entry. *Cannabis Cannabinoid Res.* <https://doi.org/10.1089/can.2022.0253> (2022).
17. Adams, R., Pease, D., Cain, C. & Clark, J. Structure of cannabidiol. VI. Isomerization of cannabidiol to tetrahydrocannabinol, a physiologically active product. Conversion of cannabidiol to cannabinol. *J. Am. Chem. Soc.* **62**, 2402–2405 (1940).
18. Adams, R. *et al.* Structure of cannabidiol. VIII. Position of the double bonds in cannabidiol. Marijuana activity of tetrahydrocannabinols. *J. Am. Chem. Soc.* **62**, 2566–2567. <https://doi.org/10.1021/ja01866a510> (1940).

19. Reggio, P. H., Greer, K. V. & Cox, S. M. The importance of the orientation of the C9 substituent to cannabinoid activity. *J. Med. Chem.* **32**, 1630–1635. <https://doi.org/10.1021/jm00127a038> (1989).
20. Mechoulam, R. *et al.* Stereochemical requirements for cannabinoid activity. *J. Med. Chem.* **23**, 1068–1072. <https://doi.org/10.1021/jm00184a002> (1980).
21. Gaoni, Y. & Mechoulam, R. Hashish—VII: The isomerization of cannabidiol to tetrahydrocannabinols. *Tetrahedron* **22**, 1481–1488. [https://doi.org/10.1016/S0040-4020\(01\)99446-3](https://doi.org/10.1016/S0040-4020(01)99446-3) (1966).
22. Archer, R. A., Boyd, D. B., Demarco, P. V., Tyminski, I. J. & Allinger, N. L. Structural studies of cannabinoids. Theoretical and proton magnetic resonance analysis. *J. Am. Chem. Soc.* **92**, 5200–5206. <https://doi.org/10.1021/ja00720a033> (1970).
23. Citti, C. *et al.* Medicinal cannabis: Principal cannabinoids concentration and their stability evaluated by a high performance liquid chromatography coupled to diode array and quadrupole time of flight mass spectrometry method. *J. Pharm. Biomed. Anal.* **128**, 201–209. <https://doi.org/10.1016/j.jpba.2016.05.033> (2016).
24. *Cannabis Flos; New text of the german pharmacopoeia.* (2018).
25. Brighenti, V., Pellati, F., Steinbach, M., Maran, D. & Benvenuti, S. Development of a new extraction technique and HPLC method for the analysis of non-psychoactive cannabinoids in fibre-type *Cannabis sativa* L. (hemp). *J. Pharm. Biomed. Anal.* **143**, 228–236. <https://doi.org/10.1016/j.jpba.2017.05.049> (2017).
26. Tolomeo, F. *et al.* Cis- Δ^9 -tetrahydrocannabinolic acid occurrence in *Cannabis sativa* L.. *J. Pharm. Biomed. Anal.* **219**, 114958. <https://doi.org/10.1016/j.jpba.2022.114958> (2022).
27. WHO Expert Committee on Drug Dependence, fortieth report. 25–27 (Geneva: World Health Organization, 2018).
28. Ujvary, I. Hexahydrocannabinol and closely related semi-synthetic cannabinoids: A comprehensive review. *Drug Test. Anal.* <https://doi.org/10.1002/dta.3519> (2023).
29. Tolomeo, F. *et al.* HPLC-UV-HRMS analysis of cannabigerovarin and cannabigerobutol, the two impurities of cannabigerol extracted from hemp. *J. Pharm. Biomed. Anal.* **203**, 114215. <https://doi.org/10.1016/j.jpba.2021.114215> (2021).
30. Metna-Laurent, M., Mondesir, M., Grel, A., Vallee, M. & Piazza, P.-V. Cannabinoid-induced tetrad in mice. *Curr. Protoc. Neurosci.* <https://doi.org/10.1002/cpns.31> (2017).
31. Percie du Sert, N. *et al.* The ARRIVE guidelines 2.0: Updated guidelines for reporting animal research. *PLoS Biol.* **18**, 3000410. <https://doi.org/10.1371/journal.pbio.3000410> (2020).

Supplementary material

Synthesis and pharmacological activity of the epimers of hexahydrocannabinol (HHC)

Fabiana Russo^{a,b}, Maria Angela Vandelli^c, Giuseppe Biagini^b, Martin Schmid^d, Livio Luongo^e, Michela Perrone^e, Federica Ricciardi^e, Sabatino Maione^e, Aldo Laganà^f, Anna Laura Capriotti^f, Alfonso Gallo^g, Luigi Carbone^h, Elisabetta Perrone^h, Giuseppe Gigli^h, Giuseppe Cannazza^{c,h,*}, Cinzia Citti^{h,c,*}

^a Clinical and Experimental Medicine PhD Program, University of Modena and Reggio Emilia, 41125 – Modena, Italy

^b Department of Biomedical, Metabolic and Neural Sciences, University of Modena and Reggio Emilia, 41125 – Modena, Italy

^c Department of Life Sciences, University of Modena and Reggio Emilia, Via Campi 103, 41125 – Modena, Italy

^d Institute of Pharmaceutical Sciences, Department of Pharmaceutical Chemistry, University of Graz, Schubertstraße 1, Graz, A-8010, Austria

^e Department of Experimental Medicine, Division of Pharmacology, Università della Campania “L. Vanvitelli”, Via Santa Maria di Costantinopoli 16, 80138, Naples, Italy.

^f Department of Chemistry, Sapienza University of Rome, Piazzale Aldo Moro 5, 00185 – Rome, Italy

^g Department of Chemistry, Istituto Zooprofilattico Sperimentale del Mezzogiorno, Via Salute 2, 80055 Portici, Italy

^h Institute of Nanotechnology – CNR NANOTEC, Campus Ecotekne, Via Monteroni, 73100 – Lecce, Italy

Table of Content

Table S1. ¹ H NMR assignments (δ) of (9 <i>S</i>)-HHC and (9 <i>R</i>)-HHC	... SI-2
Figure S1. ¹ H NMR spectroscopic characterization of (9 <i>S</i>)-HHC	... SI-3
Figure S2. ¹³ C NMR spectroscopic characterization of (9 <i>S</i>)-HHC	... SI-3
Figure S3. ¹ H NMR spectroscopic characterization of (9 <i>R</i>)-HHC	... SI-4
Figure S4. ¹³ C NMR spectroscopic characterization of (9 <i>R</i>)-HHC	... SI-4
Figure S5. HPLC-UV chromatograms of the analysed samples	... SI-5
Figure S6. MS data of the unknown impurity in sample HHC-4	... SI-6
Table S2. Calibration parameters of the analytes	... SI-7

* Corresponding authors:

Giuseppe Cannazza, Ph.D., Email: giuseppe.cannazza@unimore.it; Tel.: +39 059 2055013.; Fax: +39 059 2055750.

Cinzia Citti, Ph.D., Email: cinzia.citti@unimore.it; Tel.: +39 0832 319206.

Table S3. ¹H NMR assignments for (9*S*)-HHC and (9*R*)-HHC. In bold the discriminant signals.

¹H chemical shifts (ppm)

Atom number	(9<i>S</i>)-HHC	(9<i>R</i>)-HHC
2	6.07	6.07
4	6.25	6.25
6a	1.46-1.44	1.46-1.44
7	1.68-1.61	1.87-1.80 1.16-1.07
8	1.68-1.61	1.87-1.80 1.16-1.07
9	2.11	1.67-1.60
10a	2.67	2.49-2.37
10α	2.92-2.79	3.03
10β	1.33-1.28	0.78
11	1.13	0.94
12	1.36	1.36
13	1.09	1.06
-OH	4.61	4.64
1'	2.46-2.38	2.49-2.37
2'	1.58-1.52	1.59-1.52
3'	1.33-1.28	1.34-1.24
4'	1.33-1.28	1.34-1.24
5'	0.88	0.88

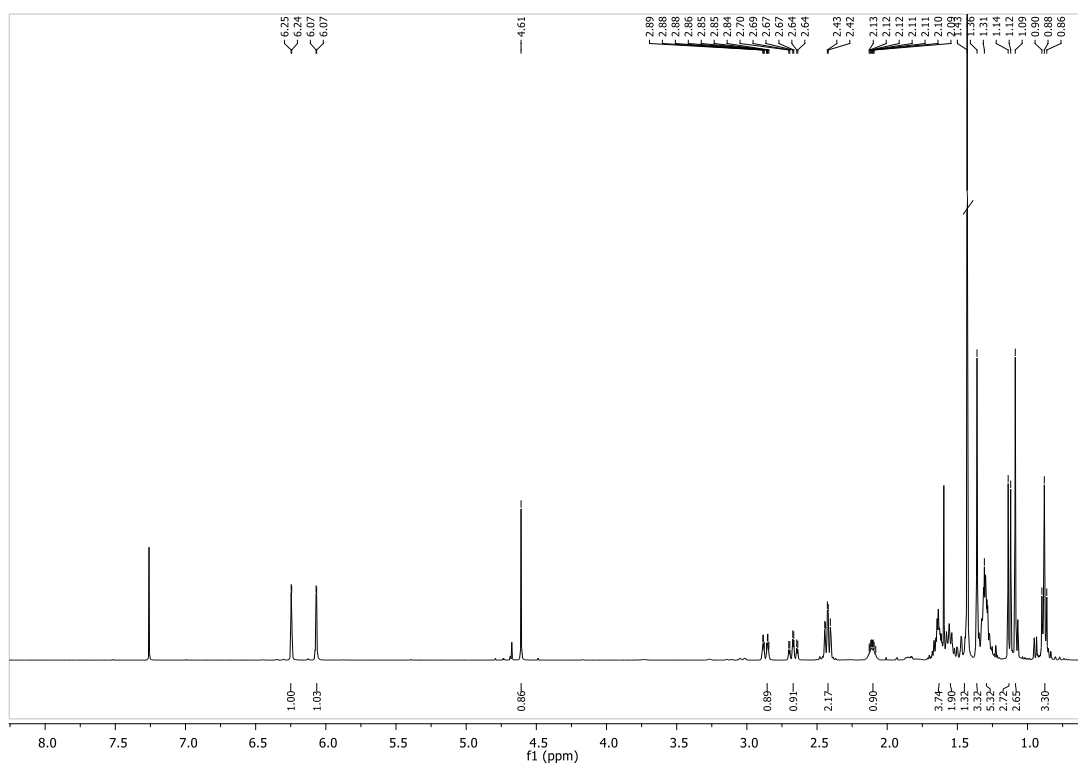


Figure S1. ^1H NMR of (9S)-HHC

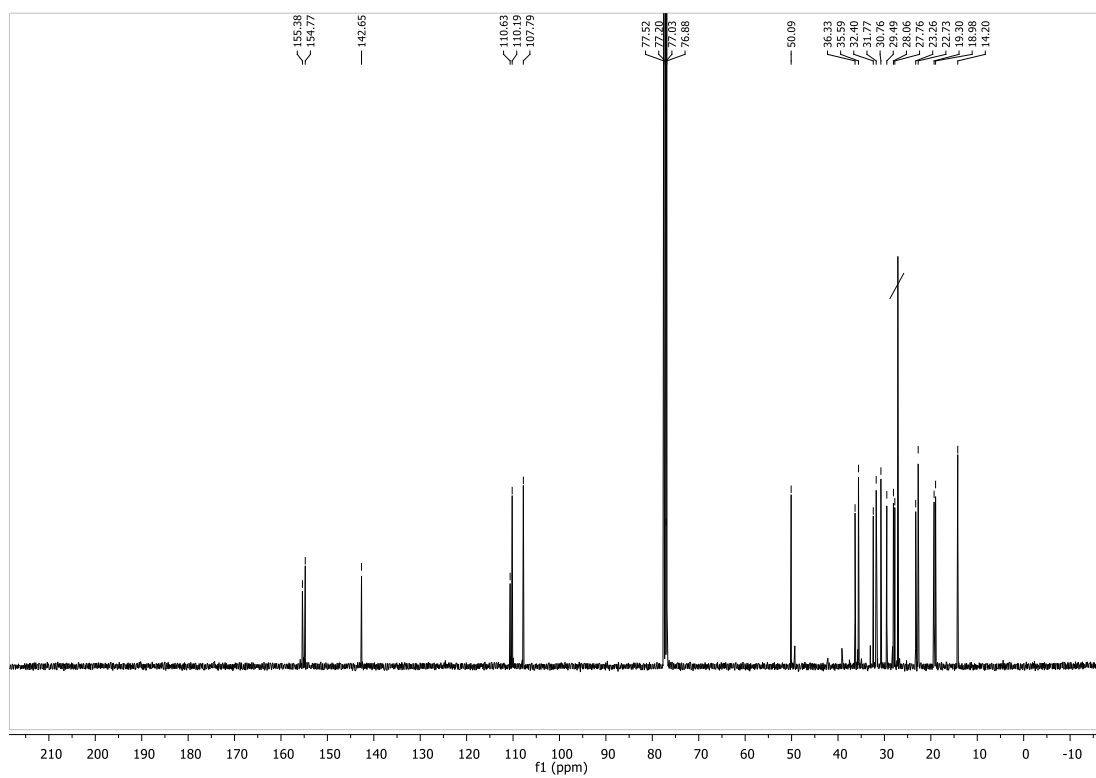


Figure S2. ^{13}C NMR of (9S)-HHC

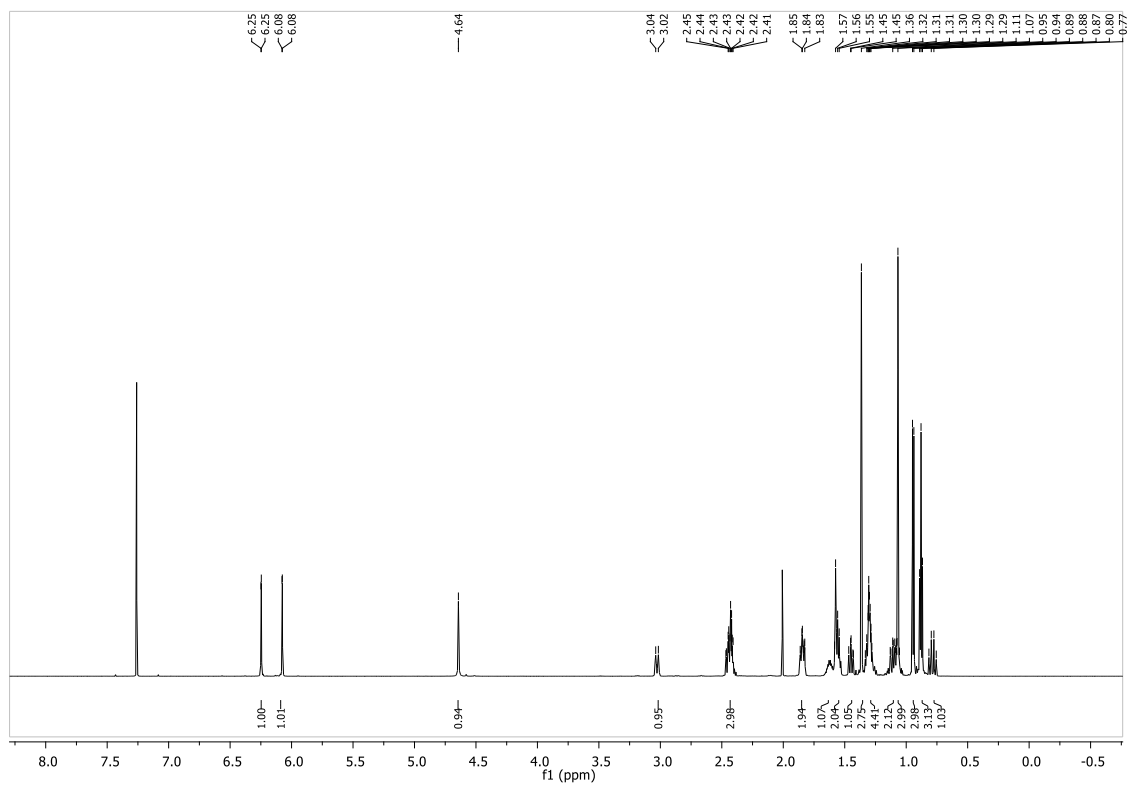


Figure S3. ¹H NMR of (9R)-HHC

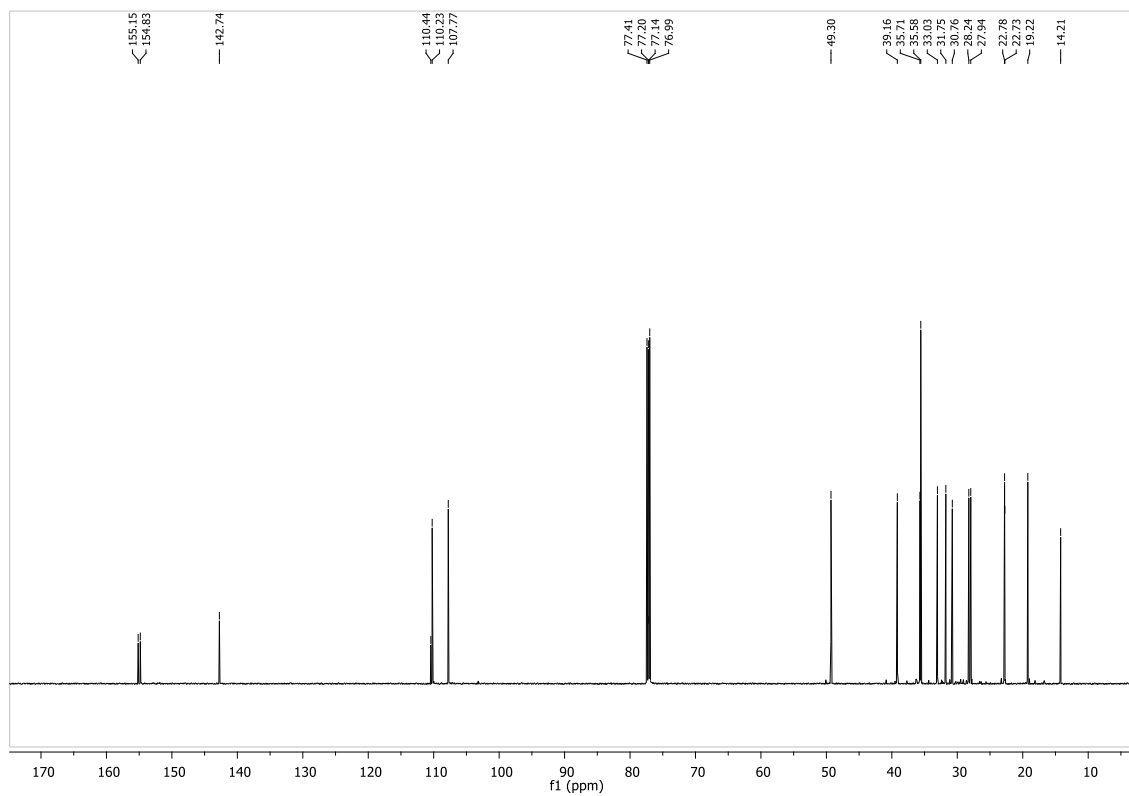


Figure S4. ¹³C NMR of (9S)-HHC

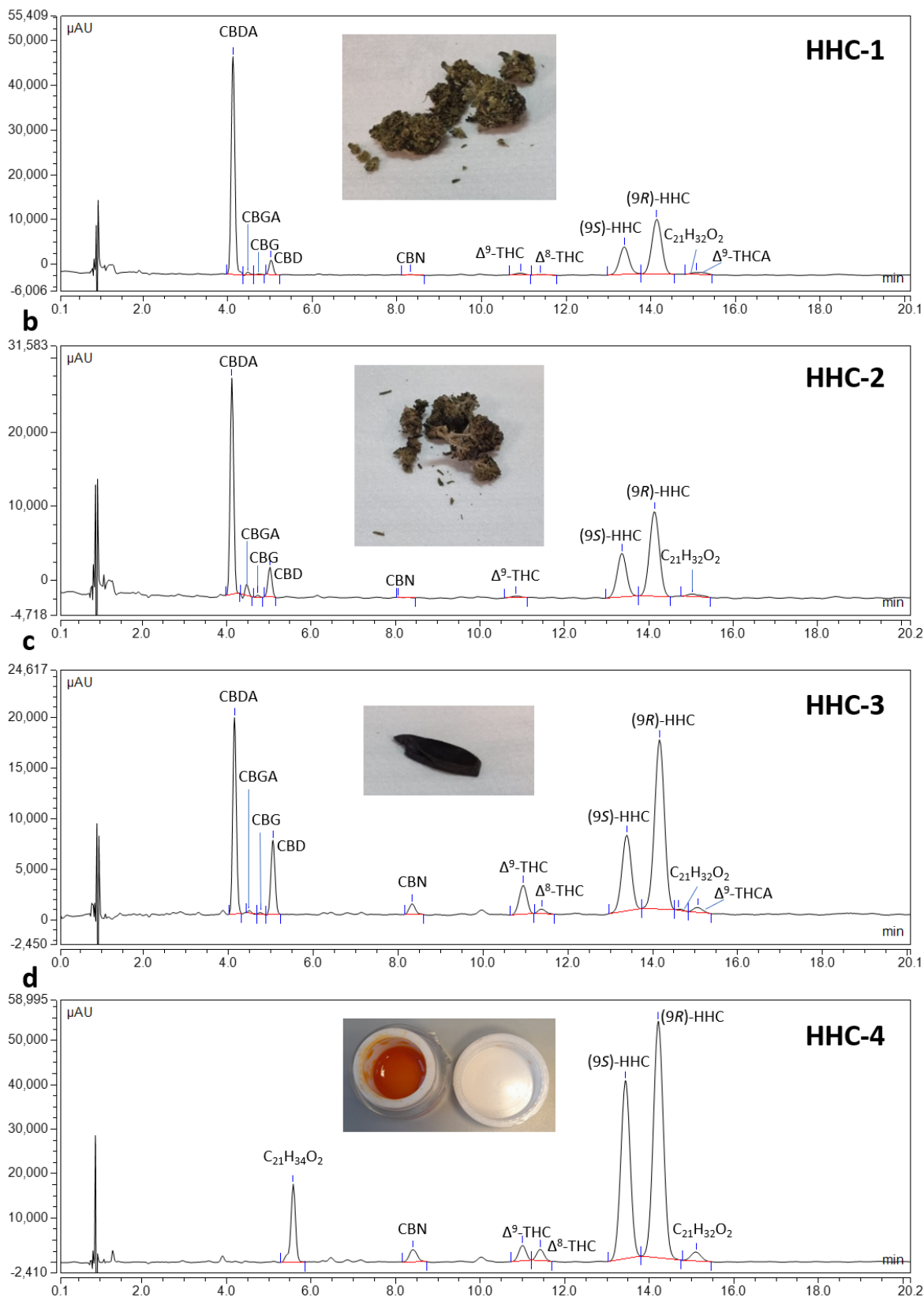


Figure S5. HPLC-UV chromatograms of the four samples: industrial hemp inflorescences (HHC-1 (a) and HHC-2 (b)), HHC hashish (HHC-3) (c) and pure HHC (HHC-4) (d). Picture of each sample is attached to the corresponding chromatogram.

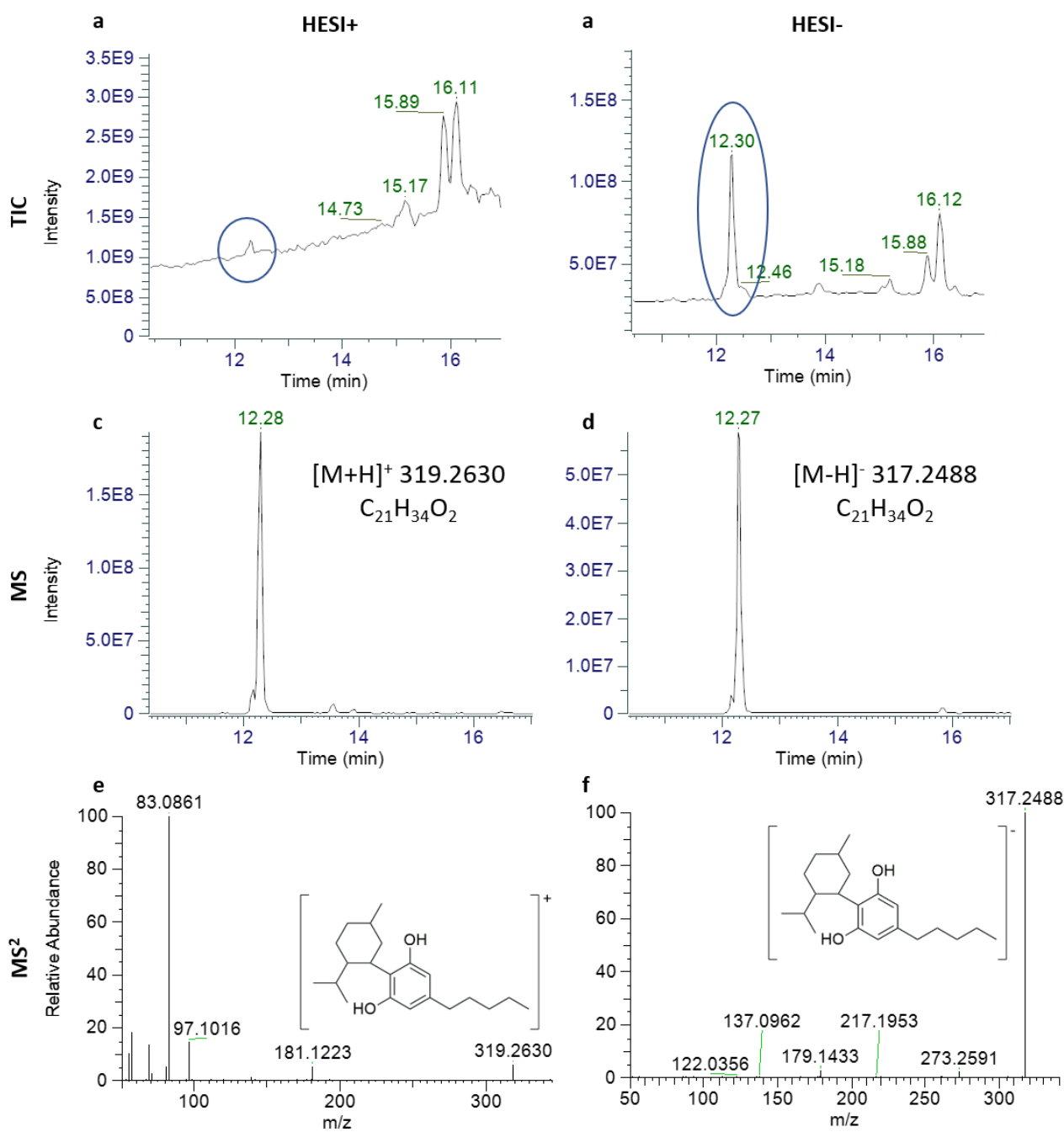


Figure S6. MS data of unknown impurity in sample HHC-4. Total ion current in HESI+ (a) and HESI- mode (b); extracted exact mass in HESI + (c) and HESI- mode (d); MS² spectrum in HESI+ and HESI- mode (f)

Table S4. UV Calibration parameters (linearity range and coefficient of determination R^2), retention time (R_T) and MS precursor ions in HESI+ and HESI- mode of the analytes.

Compound	R_T (min)	[M+H] ⁺	[M-H] ⁻	Linearity range ($\mu\text{g/mL}$)	R^2
CBDA	11.60	359.2217	357.2071	0.1-10.0	0.99791
CBGA	12.10	361.2373	359.2228	0.1-10.0	0.99833
CBG	12.30	317.2475	315.2330	0.1-10.0	0.99939
CBD	12.42	315.2319	313.2173	0.1-10.0	0.99813
CBN	14.60	311.2006	309.1864	0.1-10.0	0.99951
Δ^9 -THC	15.73	315.2319	313.2173	0.1-10.0	0.99938
Δ^8 -THC	15.95	315.2319	313.2173	0.1-10.0	0.99917
CBC	16.55	315.2319	313.2173	0.1-10.0	0.99810
(9S)-HHC	16.59	317.2475	315.2330	1.0-20.0	0.99959
(9R)-HHC	16.88	317.2475	315.2330	1.0-20.0	0.99959
Δ^9 -THCA	17.20	359.2217	357.2071	0.1-10.0	0.99874
CBCA	17.90	359.2217	357.2071	0.1-10.0	0.99746

SYNTHESIS AND GAS-CHROMATOGRAPHY COUPLED TO MASS SPECTROMETRY ANALYSIS OF HEXAHYDROCANNABIDIOL (H4-CBD)

INTRODUCTION

Unlike Δ^9 -Tetrahydrocannabinol (Δ^9 -THC), which is well known for its euphoric properties, cannabidiol (CBD) does not bind to the known CB1 cannabinoid receptors and hence does not show such activity but rather is reported to exert different pharmacological effects. Several studies show that CBD is a promising therapeutic agent for many diseases according to its numerous properties, including anticonvulsant, anxiolytic, antipsychotic, antiparkinsonian, antioxidant, neuroprotective, anti-inflammatory and analgesic effects.^{1,2} Therefore, CBD is largely employed and it is openly sold in shops and online as is free of risks of abuse or potential addiction. In the last few years, semi-synthetic derivatives of legal CBD have been found added to legal cannabis products to give effects similar to those given by Δ^9 -THC. Among these, the synthetic hydrogenated analogue of CBD, hexahydrocannabidiol (H4-CBD), has attracted the attention of scientists. H4-CBD is reported to be able to bind central cannabinoid receptor CB1 with a K_i of 145 ± 5 nM accounting for its psychoactive properties.³ Moreover, unlike CBD, H4-CBD does not present the double bond in positions 1 and 8 (Fig.1) and the hydrogenation of the double bond in position 1 leads to a possible formation of two diastereoisomers (1*R*,4*R*) and (1*S*,4*R*) (Fig.1).

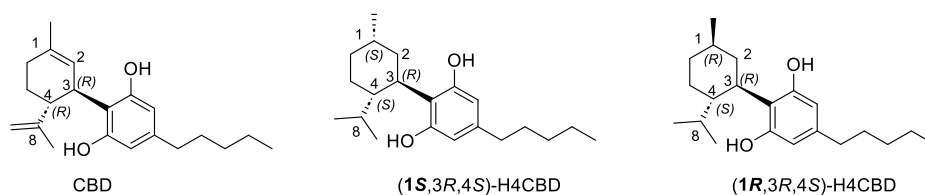


Fig.1 H4-CBD diastereoisomers

MATERIAL AND METHODS

The solvents and reagents used for the synthesis of the analytical standards were purchased from Merck (Darmstadt, Germania). Pure extracted CBD was kindly provided by the CBDepot company (Teplice, Czech Republic). The reactions were monitored by thin-layer chromatography (TLC) using 60F-254 silica gel plates (from Merck) and inspected with Vanillin/ H_2SO_4 2M stain. NMR spectra were recorded on a Bruker 700 (at 700 MHz for 1H and 175 MHz for ^{13}C) spectrometer. Chemical shifts (δ) are reported in parts per million (ppm) and referenced to the solvent residual peaks. Coupling

constants are reported in hertz (Hz) and the splitting pattern is reported as: singlet (s), doublet (d), triplet (t), quartet (q), double doublet (dd), quintet (quin), multiplet (m), broad signal (b).

Synthesis of hexahydrocannabinidiol (H4-CBD)

To a solution of pure extracted CBD (1g, 3.18 mmol) in ethanol (50 mL), Pt/C 10% (500 mg, 50% w/w) was added. The reaction was stirred in a sealed reaction bottle of the *Parr 3916 Shaker Reactor Hydrogenation* heated and connected to a hydrogen reservoir. Air was removed and replaced firstly with argon and then hydrogen atmosphere. The pressure system was set to 50 psi (3.5 bar). After 6 hours at room temperature, the suspension was filtered on celite and then the filtrate was concentrated to give H4-CBD as a 75:25 mixture of diastereoisomers (1 g, >99% yield).

^1H NMR (700 MHz, CDCl_3) δ 6.17 (s, 1H), 6.14 (s, 1H), 6.11 (s, 1H), 2.99 (td, $J = 11.7, 3.5$ Hz, 1H), 2.45 – 2.38 (m, 2H), 2.06 – 1.98 (m, 1H), 1.79 (dd, $J = 8.2, 4.4$ Hz, 1H), 1.75 – 1.68 (m, 1H), 1.66 – 1.51 (m, 6H), 1.35 – 1.27 (m, 4H), 0.89 (dt, $J = 7.0, 3.6$ Hz, 6H), 0.84 (d, $J = 7.0$ Hz, 3H), 0.70 (d, $J = 6.9$ Hz, 3H). ^{13}C NMR (176 MHz, CDCl_3) δ 155.53, 154.16, 141.93, 115.17, 109.07, 108.13, 44.65, 40.23, 38.17, 35.47, 35.30, 33.56, 31.62, 30.62, 28.65, 25.43, 22.56, 22.51, 21.71, 15.80, 14.05

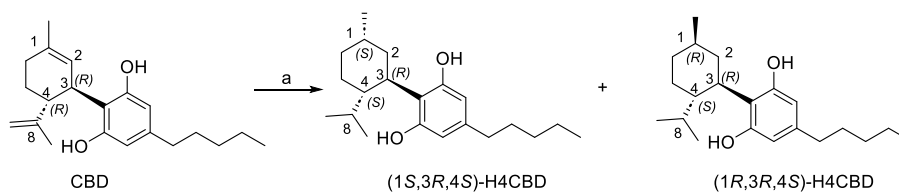
Gas chromatography-mass spectrometry qualitative analysis

The analyses were performed on an Agilent 6890 N (Agilent Technologies, Waldbronn, Germany) coupled with a 5973 Network mass spectrometer (Agilent Technologies). Separation was carried out on an Agilent HP-35 (30 m x 0.250 mm) column that incorporates a (35% -phenyl)-methyl polysiloxane phase (Agilent Technologies). Helium was used as a carrier gas (1.0 mL/min flow rate). The oven program started at a temperature of 70 °C and remained at this temperature for 1 minute. The temperature ramped at a rate of 10 °C/min up to 300°C. The post-run lasted 5 min. The total time was 30 min. The injector and ion-source temperatures were set at 250 °C. MS detection was performed with electron ionization (EI) at 70 eV, operating in the full-scan acquisition mode in the range 50-550 m/z . A solution of H4-CBD was prepared by diluting 1 mg of H4-CBD in 1 mL of ethanol.

RESULTS AND DISCUSSION

H4-CBD has been synthesized through the development of a quantitative hydrogenation reaction of CBD in the presence of H_2 and Pd/C. Considering that the removal of the double bond in position 1 generates a new stereogenic center, two epimers could be obtained (1*S*,3*R*,4*S* and 1*R*,3*R*,4*S*) (Scheme 1). Therefore, the product of the reaction was characterized through Nuclear Magnetic Resonance (NMR) and Gas Chromatography coupled with a Mass Spectrometer (GC-MS) analysis. GC-MS analysis showed the presence of two peaks corresponding to m/z 318. The former at the retention time

of 8.91 min and the second at 8.98 min (Fig.S1a). Moreover, the fragmentation spectra corresponding to each one are characterized by peculiar fragment ions at m/z 193, m/z 233, and m/z 262 (Fig.S1b-2c).⁴



Scheme 1. Synthesis of H4-CBD. a: Pd/C 10%, 1-3 bar, H₂, 25°C, 6 h.

It could be supposed that the two peaks correspond to the two H4-CBD epimers. This hypothesis was confirmed by NMR analysis. By comparison of ¹H-NMR of the single epimers reported in the literature⁴ and that of the product of the reaction, the percentages of (1R) and (1S) epimers in the sample were 75% and 25%, respectively. (Fig.S2-3)

CONCLUSION

A synthetic strategy was optimized to give a mixture of the two epimers of H4-CBD that were used as reference standard to develop a GC-MS method. The set reaction conditions mainly lead to a CBD conversion to the (1R) epimer. Therefore, this work provides an analytical method to apply to real samples, allowing the monitoring of H4-CBD, the CBD derivative with cannabimimetic activity.

REFERENCES

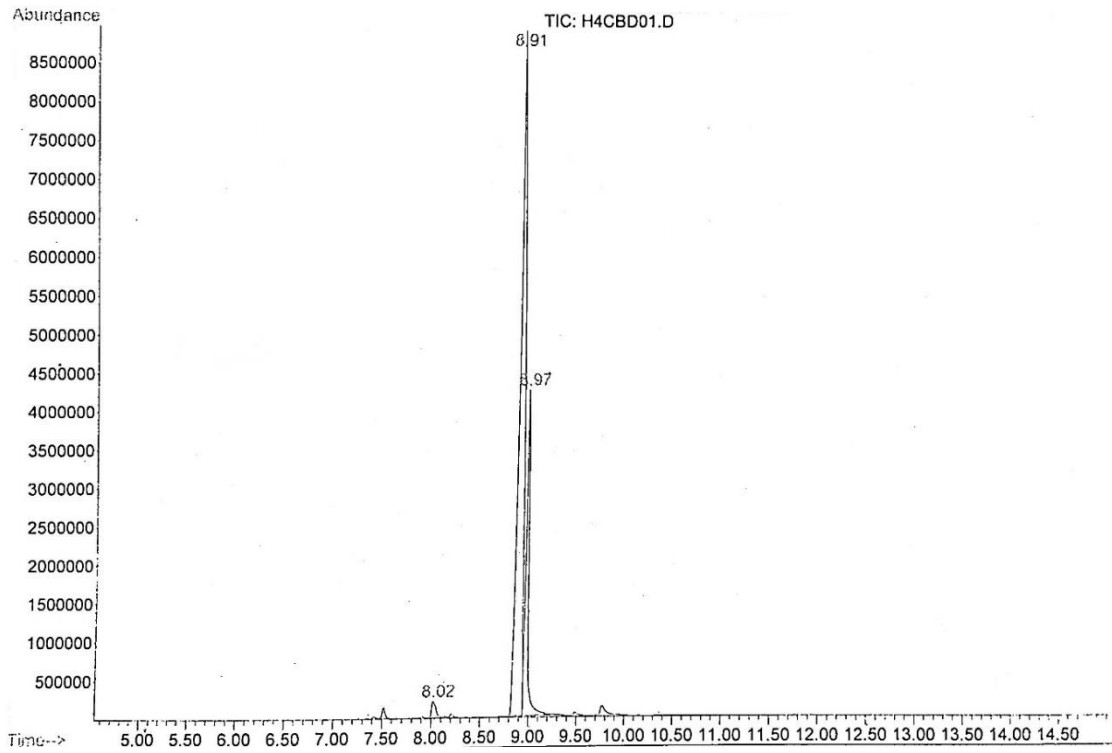
- (1) Pisanti, S.; Malfitano, A. M.; Ciaglia, E.; Lamberti, A.; Ranieri, R.; Cuomo, G.; Abate, M.; Faggiana, G.; Proto, M. C.; Fiore, D.; et al. Cannabidiol: State of the Art and New Challenges for Therapeutic Applications. *Pharmacol. Ther.* 2017, *175*, 133–150. <https://doi.org/10.1016/j.pharmthera.2017.02.041>.
- (2) Crippa, J. A.; Guimarães, F. S.; Campos, A. C.; Zuardi, A. W. Translational Investigation of the Therapeutic Potential of Cannabidiol (CBD): Toward a New Age. *Front. Immunol.* 2018, *9* (SEP), 1–16. <https://doi.org/10.3389/fimmu.2018.02009>.
- (3) Ben-Shabat, S.; Hanuš, L. O.; Katzavian, G.; Gallily, R. New Cannabidiol Derivatives: Synthesis, Binding to Cannabinoid Receptor, and Evaluation of Their Antiinflammatory Activity. *J. Med. Chem.* 2006, *49* (3), 1113–1117. <https://doi.org/10.1021/jm050709m>.(4) Collins, A.; Ramirez, G.; Tesfatsion, T.; Ray, K. P.; Caudill, S.; Cruces, W. Synthesis and Characterization of the Diastereomers of HHC and H4CBD. *Nat. Prod. Commun.* 2023, *18* (3), 1934578X2311589. <https://doi.org/10.1177/1934578X231158910>.

SUPPLEMENTARY MATERIAL
SYNTHESIS AND GAS-CHROMATOGRAPHY COUPLED TO MASS SPECTROMETRY
ANALYSIS OF HEXAHYDROCANNABIDIOL (H4-CBD)

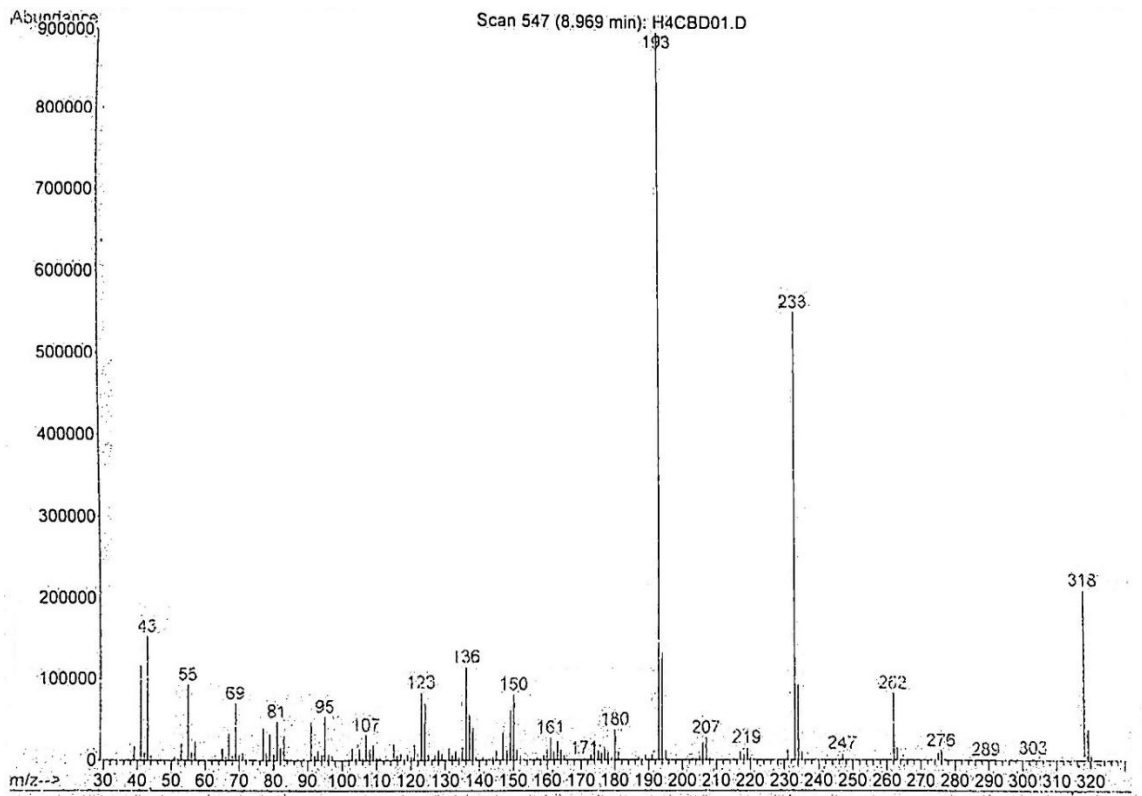
Table of content

GC-MS chromatogram of H4-CBD	S1a-c
¹H-NMR of H4CBD	S2
¹³C-NMR of H4CBD	S3

a



b



C

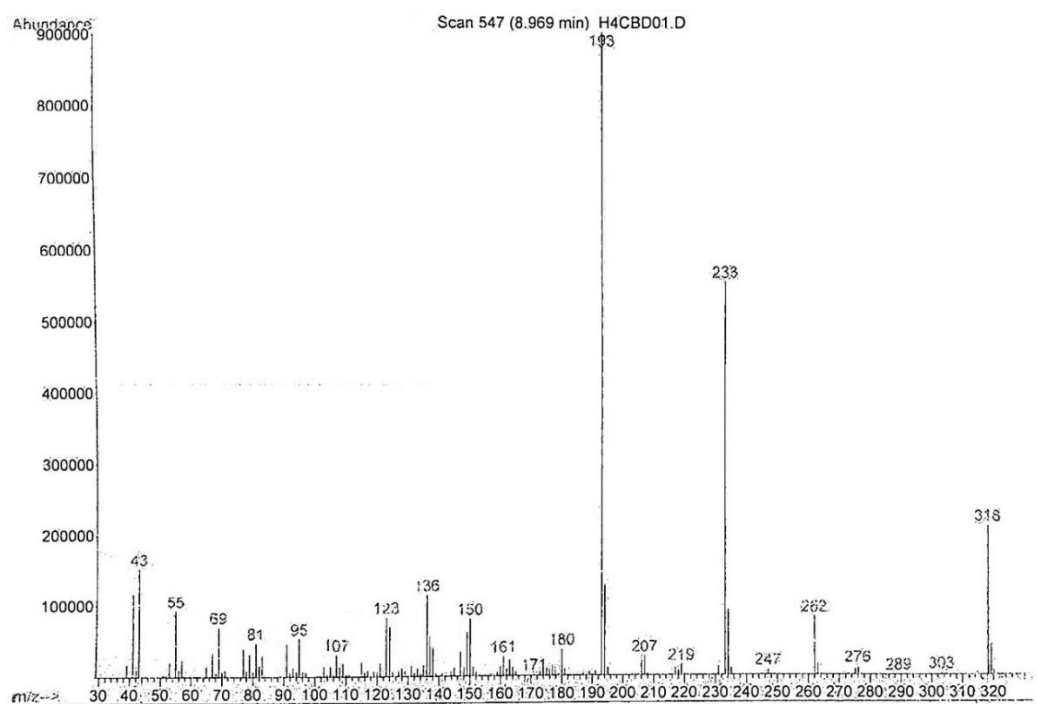


Figure S1. GC-MS chromatogram of H4-CBD sample. a) Total ion chromatogram, b)c) fragmentation spectra of the peaks eluting at 8.91 min ((1*R*)-H4CBD) and 8.97 min ((1*S*)-H4-CBD).

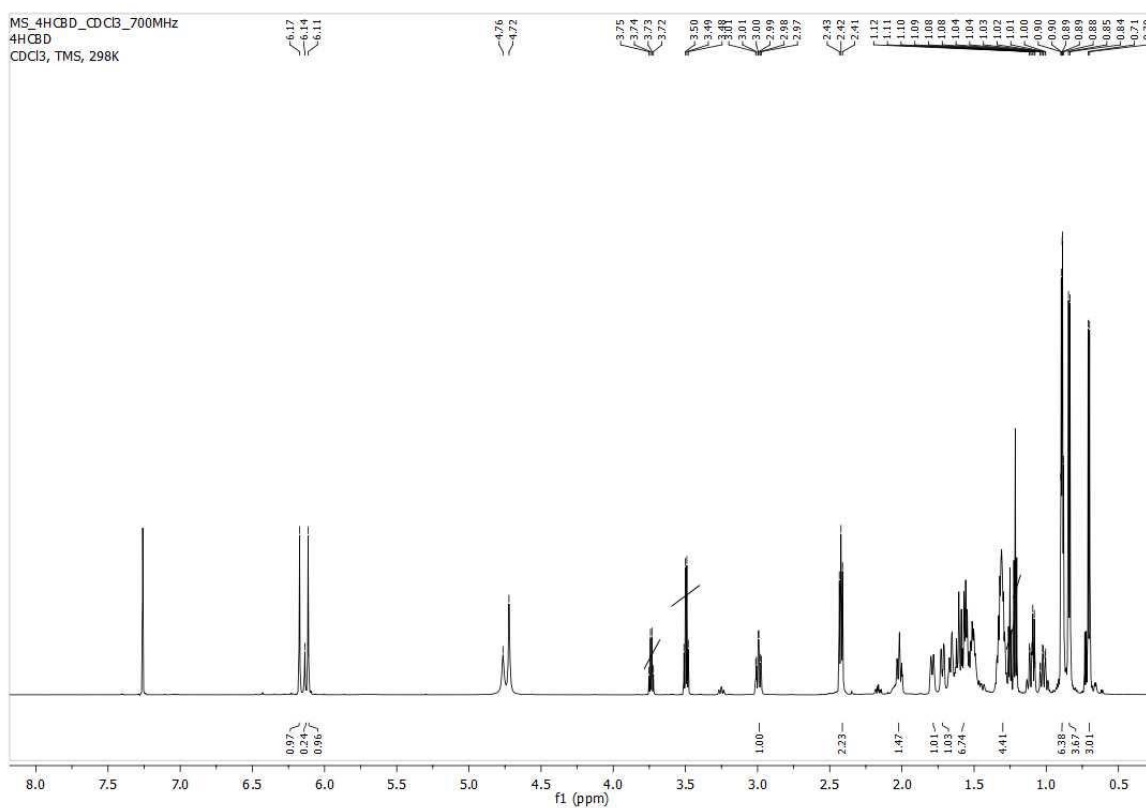


Fig.S2 ¹H NMR spectrum H4-CBD

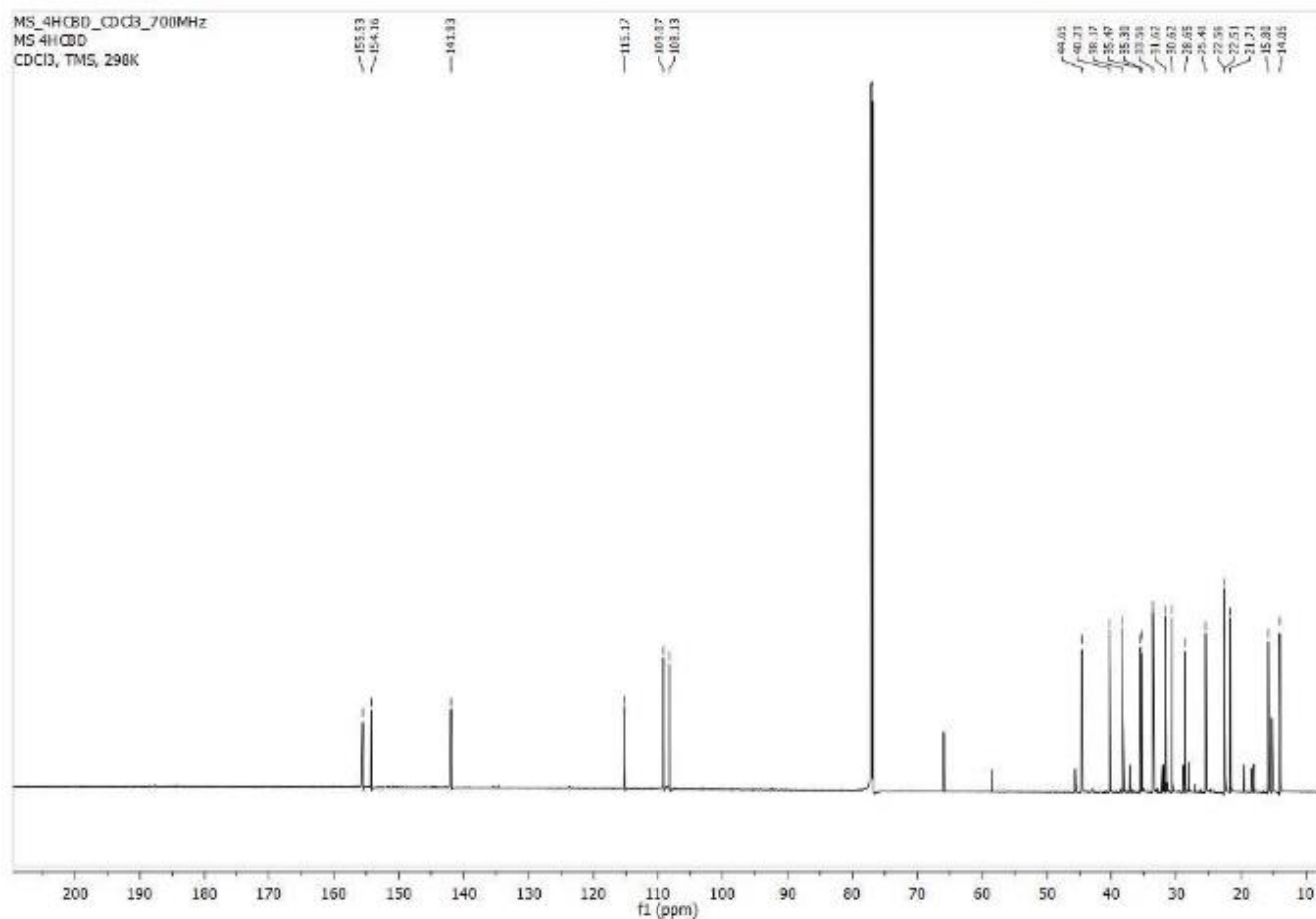


Fig.S3 ¹³CNMR spectrum H4-CBD

GENERAL CONCLUSION

The present PhD project focused on the identification of new phytocannabinoids and assessment of the stereoisomeric composition in order to provide a more comprehensive overview of the chemical composition of *Cannabis sativa* L. extracts. To this end, an analytical method based on high-performance liquid chromatography coupled with tandem high-resolution mass spectrometry (HPLC-HRMS/MS) was first developed in an *untargeted* metabolomics fashion. This approach has allowed for the putative identification of numerous carboxylated and decarboxylated phytocannabinoids present in different varieties of *Cannabis sativa* L.: CBDH (with antinociceptive activity in mice), Δ^9 -THCH, CBGB, *cis*- Δ^9 -THCA, Δ^9 -THCPA, CBDPA.^{1,2,3,4} Secondly, their identity was confirmed by their isolation from cannabis extract, their full characterization (mono- and bidimensional NMR, HRMS fragmentation, UV spectra, circular dichroism, optical rotatory power, and IR) and by comparison of such chemical and spectroscopic properties to those of the corresponding synthetic species obtained through the development of *ad hoc* synthetic strategies. Lastly, the pure synthetic compounds were also used as reference standards for the development of sensitive and selective HPLC-UV-HRMS methods under a *targeted* metabolomics approach to quantify such new phytocannabinoids in different cannabis varieties. Such new compounds were further subjected to *in vitro* and *in vivo* tests to assess their pharmacological profile.

In order to evaluate the stereometric composition of the main chiral phytocannabinoids present in cannabis extracts (Δ^9 -THCA, CBDA, CBCA, Δ^9 -THC, CBD, CBC), chiral HPLC methods coupled to a diode array detector (DAD) and to high-resolution mass spectrometry (HRMS) were developed and optimized. Afterward, such methods were coupled to the achiral HPLC-HRMS method through either an “offline”⁵ or a “heart-cut” bidimensional⁶ approach. Such methodology has resulted in the addition of new phytocannabinoids to the already long inventory, providing an increasingly comprehensive overview of the phytocannabinome. The project also provided sensitive and specific HPLC-UV-HRMS methods for the qualitative-quantitative and stereoisomeric evaluation of phytocannabinoids in *Cannabis sativa* L. extracts.

Lastly, the present project focused on the two CBD-derived NPS, HHC and H4-CBD, providing HPLC-HRMS and GC-MS methods for the qualitative and quantitative analysis in real samples of HHC and H4-CBD, respectively. It has also contributed to expanding the knowledge about the cannanomimetic activity of individual HHC epimers.

References (General introduction)

- (1) Dell, B.; McComb, A. J. Plant Resins—Their Formation, Secretion and Possible Functions; 1979; pp 277–316. [https://doi.org/10.1016/S0065-2296\(08\)60332-8](https://doi.org/10.1016/S0065-2296(08)60332-8).
- (2) Glas, J.; Schimmel, B.; Alba, J.; Escobar-Bravo, R.; Schuurink, R.; Kant, M. Plant Glandular Trichomes as Targets for Breeding or Engineering of Resistance to Herbivores. *Int. J. Mol. Sci.* **2012**, *13* (12), 17077–17103. <https://doi.org/10.3390/ijms131217077>.
- (3) Casano, S.; Grassi, G.; Martini, V.; Michelozzi, M. VARIATIONS IN TERPENE PROFILES OF DIFFERENT STRAINS OF CANNABIS SATIVA L. *Acta Hortic.* **2011**, No. 925, 115–121. <https://doi.org/10.17660/ActaHortic.2011.925.15>.
- (4) Russo, E. B. Taming THC: Potential Cannabis Synergy and Phytocannabinoid-terpenoid Entourage Effects. *Br. J. Pharmacol.* **2011**, *163* (7), 1344–1364. <https://doi.org/10.1111/j.1476-5381.2011.01238.x>.
- (5) Agus, H. H. Terpene Toxicity and Oxidative Stress. In *Toxicology*; Elsevier, 2021; pp 33–42. <https://doi.org/10.1016/B978-0-12-819092-0.00004-2>.
- (6) Booth, J. K.; Page, J. E.; Bohlmann, J. Terpene Synthases from Cannabis Sativa. *PLoS One* **2017**, *12* (3), e0173911. <https://doi.org/10.1371/journal.pone.0173911>.
- (7) Scurria, A.; Sciortino, M.; Presentato, A.; Lino, C.; Piacenza, E.; Albanese, L.; Zabini, F.; Meneguzzo, F.; Nuzzo, D.; Pagliaro, M.; et al. Volatile Compounds of Lemon and Grapefruit IntegroPectin. *Molecules* **2020**, *26* (1), 51. <https://doi.org/10.3390/molecules26010051>.
- (8) Marchini, M.; Charvoz, C.; Dujourdy, L.; Baldovini, N.; Filippi, J.-J. Multidimensional Analysis of Cannabis Volatile Constituents: Identification of 5,5-Dimethyl-1-Vinylbicyclo[2.1.1]Hexane as a Volatile Marker of Hashish, the Resin of Cannabis Sativa L. *J. Chromatogr. A* **2014**, *1370*, 200–215. <https://doi.org/10.1016/j.chroma.2014.10.045>.
- (9) Du, Z.-C.; Xia, Z.-S.; Zhang, M.-Z.; Wei, Y.-T.; Malhotra, N.; Saputra, F.; Audira, G.; Roldan, M. J. M.; Hsiao, C.-D.; Hao, E.-W.; et al. Sub-Lethal Camphor Exposure Triggers Oxidative Stress, Cardiotoxicity, and Cardiac Physiology Alterations in Zebrafish Embryos. *Cardiovasc. Toxicol.* **2021**, *21* (11), 901–913. <https://doi.org/10.1007/s12012-021-09682-x>.
- (10) Chueca, B.; Pagán, R.; García-Gonzalo, D. Oxygenated Monoterpenes Citral and Carvacrol Cause Oxidative Damage in Escherichia Coli without the Involvement of Tricarboxylic Acid Cycle and Fenton Reaction. *Int. J. Food Microbiol.* **2014**, *189*, 126–131. <https://doi.org/10.1016/j.ijfoodmicro.2014.08.008>.
- (11) Hanuš, L. O.; Meyer, S. M.; Muñoz, E.; Tagliatalata-Scafati, O.; Appendino, G. *Phytocannabinoids: A Unified Critical Inventory*; 2016; Vol. 33. <https://doi.org/10.1039/c6np00074f>.
- (12) Rosenthaler, S.; Pöhn, B.; Kolmanz, C.; Nguyen Huu, C.; Krewenka, C.; Huber, A.; Kranner, B.; Rausch, W.-D.; Moldzio, R. Differences in Receptor Binding Affinity of Several Phytocannabinoids Do Not Explain Their Effects on Neural Cell Cultures. *Neurotoxicol. Teratol.* **2014**, *46*, 49–56. <https://doi.org/10.1016/j.ntt.2014.09.003>.
- (13) Appendino, G.; Gibbons, S.; Giana, A.; Pagani, A.; Grassi, G.; Stavri, M.; Smith, E.; Rahman, M. M. Antibacterial Cannabinoids from Cannabis Sativa: A Structure-Activity Study. *J. Nat. Prod.* **2008**, *71* (8), 1427–1430. <https://doi.org/10.1021/np8002673>.
- (14) Bow, E. W.; Rimoldi, J. M. The Structure–Function Relationships of Classical Cannabinoids: CB1/CB2 Modulation. *Perspect. Medicin. Chem.* **2016**, *8*, PMC.S32171. <https://doi.org/10.4137/PMC.S32171>.
- (15) Berman, P.; Futoran, K.; Lewitus, G. M.; Mukha, D.; Benami, M.; Shlomi, T.; Meiri, D. A New ESI-LC/MS Approach for

- Comprehensive Metabolic Profiling of Phytocannabinoids in Cannabis. *Sci. Rep.* **2018**, *8* (1), 1–16. <https://doi.org/10.1038/s41598-018-32651-4>.
- (16) Moreno, T.; Dyer, P.; Tallon, S. Cannabinoid Decarboxylation: A Comparative Kinetic Study. *Ind. Eng. Chem. Res.* **2020**, *59* (46), 20307–20315. <https://doi.org/10.1021/acs.iecr.0c03791>.
- (17) Howlett, A. C. International Union of Pharmacology. XXVII. Classification of Cannabinoid Receptors. *Pharmacol. Rev.* **2002**, *54* (2), 161–202. <https://doi.org/10.1124/pr.54.2.161>.
- (18) Ramirez, S. H.; Haskó, J.; Skuba, A.; Fan, S.; Dykstra, H.; McCormick, R.; Reichenbach, N.; Krizbai, I.; Mahadevan, A.; Zhang, M.; et al. Activation of Cannabinoid Receptor 2 Attenuates Leukocyte–Endothelial Cell Interactions and Blood–Brain Barrier Dysfunction under Inflammatory Conditions. *J. Neurosci.* **2012**, *32* (12), 4004–4016. <https://doi.org/10.1523/JNEUROSCI.4628-11.2012>.
- (19) Walter, L.; Franklin, A.; Witting, A.; Wade, C.; Xie, Y.; Kunos, G.; Mackie, K.; Stella, N. Nonpsychotropic Cannabinoid Receptors Regulate Microglial Cell Migration. *J. Neurosci.* **2003**, *23* (4), 1398–1405. <https://doi.org/10.1523/JNEUROSCI.23-04-01398.2003>.
- (20) Alves, P.; Amaral, C.; Teixeira, N.; Correia-da-Silva, G. Cannabis Sativa: Much More beyond Δ^9 -Tetrahydrocannabinol. *Pharmacol. Res.* **2020**, *157*, 104822. <https://doi.org/10.1016/j.phrs.2020.104822>.
- (21) Pisanti, S.; Malfitano, A. M.; Ciaglia, E.; Lamberti, A.; Ranieri, R.; Cuomo, G.; Abate, M.; Faggiana, G.; Proto, M. C.; Fiore, D.; et al. Cannabidiol: State of the Art and New Challenges for Therapeutic Applications. *Pharmacol. Ther.* **2017**, *175*, 133–150. <https://doi.org/10.1016/j.pharmthera.2017.02.041>.
- (22) E.P., B. Comprehensive Review of Medicinal Marijuana, Cannabinoids, and Therapeutic Implications in Medicine and Headache: What a Long Strange Trip It's Been ... *Headache* **2015**, *55* (6), 885–916. <https://doi.org/10.1111/head.12570> LK - <http://sfx.library.uu.nl/utrecht?sid=EMBASE&issn=15264610&id=doi:10.1111%2Fhead.12570&atitle=Comprehensive+review+of+medicinal+marijuana%2C+cannabinoids%2C+and+therapeutic+implications+in+medicine+and+headache%3A+What+a+long+strange+trip+it%27s+been+...&stitle=Headache&title=Headache&volume=55&issue=6&spage=885&epage=916&auiast=Baron&aufirst=Eric+P.&aunit=E.P.&aufull=Baron+E.P.&coden=HEADA&isbn=&pages=885-916&date=2015&aunit1=E&aunitm=P>.
- (23) Romano, B.; Borrelli, F.; Fasolino, I.; Capasso, R.; Piscitelli, F.; Cascio, M.; Pertwee, R.; Coppola, D.; Vassallo, L.; Orlando, P.; et al. The Cannabinoid TRPA1 Agonist Cannabichromene Inhibits Nitric Oxide Production in Macrophages and Ameliorates Murine Colitis. *Br. J. Pharmacol.* **2013**, *169* (1), 213–229. <https://doi.org/10.1111/bph.12120>.
- (24) Anderson, L. L.; Ametovski, A.; Lin Luo, J.; Everett-Morgan, D.; McGregor, I. S.; Banister, S. D.; Arnold, J. C. Cannabichromene, Related Phytocannabinoids, and 5-Fluoro-Cannabichromene Have Anticonvulsant Properties in a Mouse Model of Dravet Syndrome. *ACS Chem. Neurosci.* **2021**, *12* (2), 330–339. <https://doi.org/10.1021/acschemneuro.0c00677>.
- (25) Anis, O.; Vinayaka, A. C.; Shalev, N.; Namdar, D.; Nadarajan, S.; Anil, S. M.; Cohen, O.; Belausov, E.; Ramon, J.; Mayzlish Gati, E.; et al. Cannabis-Derived Compounds Cannabichromene and Δ^9 -Tetrahydrocannabinol Interact and Exhibit Cytotoxic Activity against Urothelial Cell Carcinoma Correlated with Inhibition of Cell Migration and Cytoskeleton Organization. *Molecules* **2021**, *26* (2), 465. <https://doi.org/10.3390/molecules26020465>.
- (26) El-Alfy, A. T.; Ivey, K.; Robinson, K.; Ahmed, S.; Radwan, M.; Slade, D.; Khan, I.; ElSohly, M.; Ross, S. Antidepressant-like Effect of Δ^9 -Tetrahydrocannabinol and Other Cannabinoids Isolated from Cannabis Sativa L. *Pharmacol. Biochem. Behav.* **2010**, *95* (4), 434–442. <https://doi.org/10.1016/j.pbb.2010.03.004>.

- (27) Jastrzab, A.; Jarocka-Karpowicz, I.; Skrzydlewska, E. The Origin and Biomedical Relevance of Cannabigerol. *Int. J. Mol. Sci.* **2022**, *23* (14). <https://doi.org/10.3390/ijms23147929>.
- (28) Borrelli, F.; Fasolino, I.; Romano, B.; Capasso, R.; Maiello, F.; Coppola, D.; Orlando, P.; Battista, G.; Pagano, E.; Di Marzo, V.; et al. Beneficial Effect of the Non-Psychotropic Plant Cannabinoid Cannabigerol on Experimental Inflammatory Bowel Disease. *Biochem. Pharmacol.* **2013**, *85* (9), 1306–1316. <https://doi.org/10.1016/j.bcp.2013.01.017>.
- (29) Pagano, C.; Navarra, G.; Coppola, L.; Avilia, G.; Bifulco, M.; Laezza, C. Cannabinoids: Therapeutic Use in Clinical Practice. *Int. J. Mol. Sci.* **2022**, *23* (6), 1–20. <https://doi.org/10.3390/ijms23063344>.
- (30) Suzuki, S.; Fleig, A.; Penner, R. CBGA Ameliorates Inflammation and Fibrosis in Nephropathy. *Sci. Rep.* **2023**, *13* (1), 1–13. <https://doi.org/10.1038/s41598-023-33507-2>.
- (31) Martinenghi, L. D.; Jönsson, R.; Lund, T.; Jenssen, H. Isolation, Purification, and Antimicrobial Characterization of Cannabidiolic Acid and Cannabidiol from Cannabis Sativa L. *Biomolecules* **2020**, *10* (6), 900. <https://doi.org/10.3390/biom10060900>.
- (32) Formato, M.; Crescente, G.; Scognamiglio, M.; Fiorentino, A.; Pecoraro, M. T.; Piccolella, S.; Catauro, M.; Pacifico, S. (–)-Cannabidiolic Acid, a Still Overlooked Bioactive Compound: An Introductory Review and Preliminary Research. *Molecules* **2020**, *25* (11), 2638. <https://doi.org/10.3390/molecules25112638>.
- (33) Verhoeckx, K. C. M.; Korthout, H. A. A. J.; van Meeteren-Kreikamp, A. P.; Ehlert, K. A.; Wang, M.; van der Greef, J.; Rodenburg, R. J. T.; Witkamp, R. F. Unheated Cannabis Sativa Extracts and Its Major Compound THC-Acid Have Potential Immuno-Modulating Properties Not Mediated by CB1 and CB2 Receptor Coupled Pathways. *Int. Immunopharmacol.* **2006**, *6* (4), 656–665. <https://doi.org/10.1016/j.intimp.2005.10.002>.
- (34) Rock, E. M.; Sticht, M. A.; Parker, L. A. Effect of Phytocannabinoids on Nausea and Vomiting. In *Handbook of Cannabis*; Oxford University Press, 2014; pp 435–454. <https://doi.org/10.1093/acprof:oso/9780199662685.003.0023>.
- (35) Nadal, X.; del Río, C.; Casano, S.; Palomares, B.; Ferreira-Vera, C.; Navarrete, C.; Sánchez-Carnerero, C.; Cantarero, I.; Bellido, M. L.; Meyer, S.; et al. Tetrahydrocannabinolic Acid Is a Potent PPAR γ Agonist with Neuroprotective Activity. *Br. J. Pharmacol.* **2017**, *174* (23), 4263–4276. <https://doi.org/10.1111/bph.14019>.
- (36) Sulak, D.; Saneto, R.; Goldstein, B. The Current Status of Artisanal Cannabis for the Treatment of Epilepsy in the United States. *Epilepsy Behav.* **2017**, *70*, 328–333. <https://doi.org/10.1016/j.yebeh.2016.12.032>.
- (37) Galletta, M.; Reekie, T. A.; Nagalingam, G.; Bottomley, A. L.; Harry, E. J.; Kassiou, M.; Triccas, J. A. Rapid Antibacterial Activity of Cannabichromenic Acid against Methicillin-Resistant Staphylococcus Aureus. *Antibiotics* **2020**, *9* (8), 523. <https://doi.org/10.3390/antibiotics9080523>.
- (38) Battisti, U. M.; Citti, C.; Larini, M.; Ciccarella, G.; Stasiak, N.; Troisi, L.; Braghiroli, D.; Parenti, C.; Zoli, M.; Cannazza, G. “Heart-Cut” Bidimensional Achiral-Chiral Liquid Chromatography Applied to the Evaluation of Stereoselective Metabolism, in Vivo Biological Activity and Brain Response to Chiral Drug Candidates Targeting the Central Nervous System. *J. Chromatogr. A* **2016**, *1443*, 152–161. <https://doi.org/10.1016/j.chroma.2016.03.027>.
- (39) Battisti, U. M.; Citti, C.; Rastelli, G.; Pinzi, L.; Puja, G.; Ravazzini, F.; Ciccarella, G.; Braghiroli, D.; Cannazza, G. An Unexpected Reversal in the Pharmacological Stereoselectivity of Benzothiadiazine AMPA Positive Allosteric Modulators. *Medchemcomm* **2016**, *7* (12), 2410–2417. <https://doi.org/10.1039/C6MD00440G>.
- (40) González-Mariscal, I.; Carmona-Hidalgo, B.; Winkler, M.; Unciti-Broceta, J. D.; Escamilla, A.; Gómez-Cañas, M.; Fernández-Ruiz, J.; Fiebich, B. L.; Romero-Zerbo, S.-Y.; Bermúdez-Silva, F. J.; et al. (+)-Trans-Cannabidiol-2-Hydroxy Pentyl Is a Dual CB1R Antagonist/CB2R Agonist That Prevents Diabetic Nephropathy in Mice. *Pharmacol. Res.* **2021**, *169*,

105492. <https://doi.org/10.1016/j.phrs.2021.105492>.

- (41) Adams, R.; Hunt, M.; Clark, J. H. Structure of Cannabidiol, a Product Isolated from the Marijuana Extract of Minnesota Wild Hemp. *I. J. Am. Chem. Soc.* **1940**, *62* (1), 196–200. <https://doi.org/10.1021/ja01858a058>.
- (42) Casati, S.; Rota, P.; Bergamaschi, R. F.; Palmisano, E.; La Rocca, P.; Ravelli, A.; Angeli, I.; Minoli, M.; Roda, G.; Orioli, M. Hexahydrocannabinol on the Light Cannabis Market: The Latest “New” Entry. *Cannabis Cannabinoid Res.* **2022**. <https://doi.org/10.1089/can.2022.0253>.
- (43) EMCDDA. *European Drug Report 2022: Trends and Developments*; 2022.
- (44) Ben-Shabat, S.; Hanuš, L. O.; Katzavian, G.; Gallily, R. New Cannabidiol Derivatives: Synthesis, Binding to Cannabinoid Receptor, and Evaluation of Their Antiinflammatory Activity. *J. Med. Chem.* **2006**, *49* (3), 1113–1117. <https://doi.org/10.1021/jm050709m>.

References (General conclusion)

- (1) Linciano, P.; Citti, C.; Russo, F.; Tolomeo, F.; Laganà, A.; Capriotti, A. L.; Luongo, L.; Iannotta, M.; Belardo, C.; Maione, S.; et al. Identification of a New Cannabidiol N-Hexyl Homolog in a Medicinal Cannabis Variety with an Antinociceptive Activity in Mice: Cannabidihexol. *Sci. Rep.* **2020**, *10* (1), 1–11. <https://doi.org/10.1038/s41598-020-79042-2>.
- (2) Tolomeo, F.; Russo, F.; Vandelli, M. A.; Biagini, G.; Capriotti, A. L.; Laganà, A.; Carbone, L.; Gigli, G.; Cannazza, G.; Citti, C. HPLC-UV-HRMS Analysis of Cannabigerovarin and Cannabigerobutol, the Two Impurities of Cannabigerol Extracted from Hemp. *J. Pharm. Biomed. Anal.* **2021**, *203*, 114215. <https://doi.org/10.1016/j.jpba.2021.114215>.
- (3) Tolomeo, F.; Russo, F.; Kaczorova, D.; Vandelli, M. A.; Biagini, G.; Laganà, A.; Capriotti, A. L.; Paris, R.; Fulvio, F.; Carbone, L.; et al. Cis- Δ^9 -Tetrahydrocannabinolic Acid Occurrence in Cannabis Sativa L. *J. Pharm. Biomed. Anal.* **2022**, *219* (July). <https://doi.org/10.1016/j.jpba.2022.114958>.
- (4) Linciano, P.; Russo, F.; Citti, C.; Tolomeo, F.; Paris, R.; Fulvio, F.; Pecchioni, N.; Vandelli, M. A.; Laganà, A.; Capriotti, A. L.; et al. The Novel Heptyl Phorolic Acid Cannabinoids Content in Different Cannabis Sativa L. Accessions. *Talanta* **2021**, *235* (May). <https://doi.org/10.1016/j.talanta.2021.122704>.
- (5) Russo, F.; Tolomeo, F.; Angela Vandelli, M.; Biagini, G.; Laganà, A.; Capriotti, A. L.; Cerrato, A.; Carbone, L.; Perrone, E.; Cavazzini, A.; et al. Enantioseparation of Chiral Phytocannabinoids in Medicinal Cannabis. *J. Chromatogr. B Anal. Technol. Biomed. Life Sci.* **2023**, *1221* (January). <https://doi.org/10.1016/j.jchromb.2023.123682>.
- (6) Battisti, U. M.; Citti, C.; Larini, M.; Ciccarella, G.; Stasiak, N.; Troisi, L.; Braghiroli, D.; Parenti, C.; Zoli, M.; Cannazza, G. “Heart-Cut” Bidimensional Achiral-Chiral Liquid Chromatography Applied to the Evaluation of Stereoselective Metabolism, in Vivo Biological Activity and Brain Response to Chiral Drug Candidates Targeting the Central Nervous System. *J. Chromatogr. A* **2016**, *1443*, 152–161. <https://doi.org/10.1016/j.chroma.2016.03.027>.